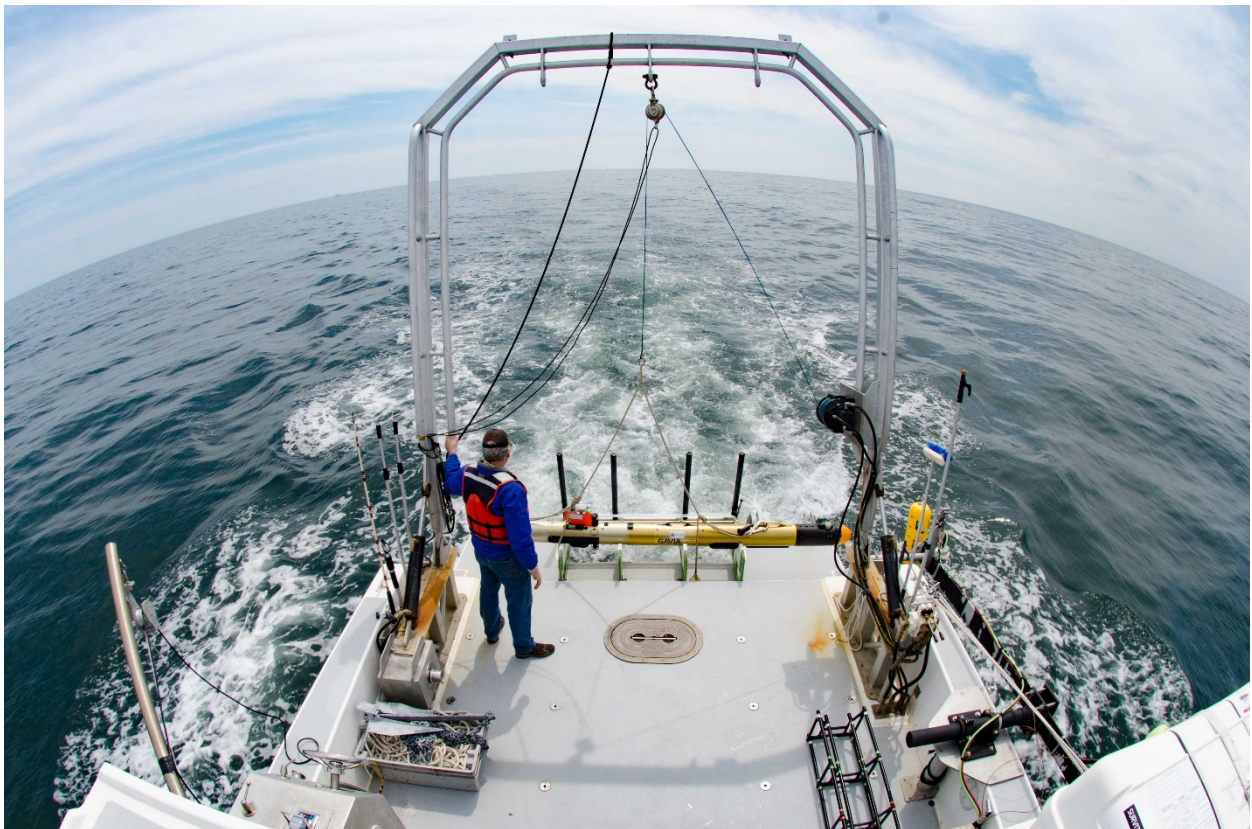


Munitions and Explosives of Concern Survey Methodology and In-field Testing for Wind Energy Areas on the Atlantic Outer Continental Shelf



Munitions and Explosives of Concern Survey Methodology and In-field Testing for Wind Energy Areas on the Atlantic Outer Continental Shelf

July 2017

Authors:

Geoffrey Carton¹, Carter DuVal², Art Trembanis², Margo Edwards³, Mark Rognstad³, Christian Briggs⁴,
Sonia Shjegstad⁴

Prepared under contract M16PC00001

By

¹CALIBRE Systems, Inc.
6345 Walker Lane
Metro Park, Suite 300
Alexandria, VA 22310-3252

With support from

²University of Delaware
255 Academy Street
109 Penny Hall
Newark, DE 19716

³Hawaii Institute of Geophysics and Planetology
School of Ocean and Earth Science and Technology
University of Hawaii
1680 East-West Road, POST 602
Honolulu, HI 96821

⁴Environet, Inc.
1286 Queen Emma Street
Honolulu, HI 96813

**US Department of the Interior
Bureau of Ocean Energy Management
Office of Renewable Energy Programs**

DISCLAIMER

Study concept, oversight, and funding were provided by the US Department of the Interior, Bureau of Ocean Energy Management (BOEM), Environmental Studies Program, Washington, DC, under Contract Number M16PC00001. This report has been technically reviewed by BOEM, and it has been approved for publication. The views and conclusions contained in this document are those of the authors and should not be interpreted as representing the opinions or policies of the US Government, nor does mention of trade names or commercial products constitute endorsement or recommendation for use.

REPORT AVAILABILITY

To download a PDF file of this report, go to the US Department of the Interior, Bureau of Ocean Energy Management website at <https://www.boem.gov/Renewable-Energy-Environmental-Studies/>. The report is also available at the National Technical Reports Library at <https://ntrl.ntis.gov/NTRL/>.

CITATION

Carton G, DuVal C, Trembanis A, Edwards M, Rognstad M, Briggs C, Shjegstad S. 2017. Munitions and Explosives of Concern Survey Methodology and In-field Testing for Wind Energy Areas on the Atlantic Outer Continental Shelf. US Department of Interior, Bureau of Ocean Energy Management. OCS Study 2017-xxx.

ABOUT THE COVER

Autonomous underwater vehicle on the University of Delaware R/V *Daiber* within the Delaware Wind Energy Area.

ACKNOWLEDGMENTS

Thank you to Jennifer Miller of the Bureau of Ocean Energy Management, Office of Renewable Energy Programs for her detailed reviews and technical input.

Page Intentionally Left Blank.

Table of Contents

| | |
|---|-----------|
| 1.0 INTRODUCTION..... | 1 |
| 1.1 PROJECT BACKGROUND | 1 |
| 1.2 PROJECT SCOPE AND OBJECTIVES | 2 |
| 2.0 PHYSICAL CONDITIONS AT THE ATLANTIC OCS WEAS..... | 5 |
| 3.0 MUNITIONS NEAR THE ATLANTIC OCS WEAS..... | 19 |
| 3.1 MEC RESEARCH FINDINGS | 19 |
| 3.2 MEC CONCLUSIONS..... | 20 |
| 4.0 TYPICAL OFFSHORE RENEWABLE ENERGY DEVELOPMENT ACTIVITIES | 57 |
| 4.1 OFFSHORE WIND ENERGY SYSTEMS | 57 |
| 4.1.1 <i>Meteorological Mast or LiDAR Buoy</i> | 57 |
| 4.1.2 <i>Wind Turbine</i> | 58 |
| 4.1.3 <i>Electrical Collection and Transmission Cables</i> | 58 |
| 4.1.4 <i>Substations</i> | 58 |
| 4.2 OFFSHORE WIND ENERGY DEVELOPMENT PRE-CONSTRUCTION ACTIVITIES | 58 |
| 4.2.1 <i>Characterization of Meteorological and Natural Resources</i> | 59 |
| 4.2.2 <i>Site and Cable Route Surveys</i> | 59 |
| 4.3 OFFSHORE WIND ENERGY DEVELOPMENT CONSTRUCTION ACTIVITIES | 59 |
| 4.3.1 <i>Electrical Collection and Transmission Cable Laying Operations</i> | 60 |
| 4.3.1.1 Pre-Lay Grapple Run | 60 |
| 4.3.1.2 Cable Ploughing..... | 60 |
| 4.3.1.3 ROV Cable Lay and Burial..... | 60 |
| 4.3.1.4 Cable Jetting | 61 |
| 4.3.1.5 Cable Trenching..... | 61 |
| 4.3.1.6 Deployment of Anchors..... | 61 |
| 4.3.1.7 Concrete Mattress Placement..... | 61 |
| 4.3.1.8 Rock Placement | 61 |
| 4.3.2 <i>Installation of Substructures and Foundations</i> | 62 |
| 4.3.2.1 Monopiles | 62 |
| 4.3.2.2 Jackets and Tripods..... | 62 |
| 4.3.2.3 Gravity Foundations..... | 62 |
| 4.3.2.4 Scour Protection Systems..... | 63 |
| 5.0 MEC RISK MANAGEMENT FRAMEWORK | 65 |
| 5.1 EVALUATING AND MANAGING MEC RISK..... | 65 |
| 5.2 MEC RISK MANAGEMENT FRAMEWORK COMPONENTS | 68 |
| 5.2.1 <i>MEC Hazard Assessment</i> | 69 |
| 5.2.2 <i>MEC Risk Assessment</i> | 70 |
| 5.2.3 <i>MEC Risk Validation</i> | 77 |
| 5.2.4 <i>MEC Risk Mitigation</i> | 77 |
| 6.0 TECHNOLOGIES, PLATFORMS, AND POSITIONING TECHNIQUES | 79 |
| 6.1 NAVIGATION AND POSITIONING | 79 |
| 6.1.1 <i>Global Navigation Satellite System</i> | 80 |
| 6.1.2 <i>Underwater Positioning Systems</i> | 80 |
| 6.1.2.1 Long Baseline | 81 |
| 6.1.2.2 Short and Ultra-Short Baseline | 81 |
| 6.1.2.3 Inertial Navigation Systems | 82 |
| 6.1.2.4 Buoy Systems | 83 |
| 6.1.2.5 Other Positioning Methods | 83 |
| 6.2 SENSORS | 87 |
| 6.2.1 <i>Acoustic Sensors</i> | 87 |

| | | |
|------------|---|------------|
| 6.2.1.1 | Sensors that Measure Sub-seafloor Impedance Changes | 87 |
| 6.2.1.2 | Sensors that Measure Seafloor Reflectivity | 88 |
| 6.2.1.2.1 | Side-scan sonar | 89 |
| 6.2.1.2.2 | Synthetic aperture sonar | 89 |
| 6.2.1.3 | Sensors that Measure Seafloor Shape | 92 |
| 6.2.1.3.1 | Echo-sounders | 92 |
| 6.2.1.3.2 | Multibeam echo-sounders..... | 93 |
| 6.2.1.4 | Phase Measuring Bathymetric Systems | 93 |
| 6.2.2 | <i>Magnetic Sensors</i> | 94 |
| 6.2.2.1 | Magnetometer | 95 |
| 6.2.2.2 | Gradiometers..... | 96 |
| 6.2.2.3 | Electromagnetic Induction | 97 |
| 6.2.3 | <i>Optical Sensors</i> | 97 |
| 6.3 | PLATFORMS..... | 103 |
| 6.3.1 | <i>Autonomous Underwater Vehicles</i> | 103 |
| 6.3.2 | <i>Remotely Operated Vehicles</i> | 104 |
| 6.3.2.1 | Standard Remotely Operated Vehicles..... | 104 |
| 6.3.2.2 | Remotely Operated Towed Vehicles..... | 105 |
| 6.3.3 | <i>Autonomous/Unmanned Surface Vehicles</i> | 106 |
| 6.3.4 | <i>Surface Vessels</i> | 107 |
| 6.3.4.1 | Small Boats | 108 |
| 6.3.4.2 | Survey Launches..... | 108 |
| 6.3.4.3 | Coastal/Regional Research or Commercial Vessels..... | 109 |
| 6.4 | CONSIDERATIONS FOR SURVEY DESIGN AND IMPLEMENTATION..... | 115 |
| 6.4.1 | <i>Sensor Configuration and Deployment</i> | 115 |
| 6.4.2 | <i>Quality Control</i> | 116 |
| 6.4.3 | <i>Considerations for Use of ROVs</i> | 117 |
| 6.5 | RECOMMENDED APPROACHES IN WEAS..... | 117 |
| 7.0 | DESCRIPTION OF IN-FIELD VERIFICATION STUDY AREA | 119 |
| 7.1 | STUDY AREA DESCRIPTION..... | 119 |
| 7.2 | PHYSICAL CHARACTERISTICS OF DELAWARE WEA..... | 119 |
| 7.2.1 | <i>Air Temperature</i> | 119 |
| 7.2.2 | <i>Bathymetry and Seafloor Geology</i> | 119 |
| 7.2.3 | <i>Currents and Tides</i> | 120 |
| 7.2.4 | <i>Water Column Profile</i> | 121 |
| 7.2.5 | <i>Storms</i> | 121 |
| 7.3 | AREA USE | 122 |
| 7.4 | BIOLOGICAL RESOURCES | 122 |
| 7.4.1 | <i>Coastal Habitats</i> | 122 |
| 7.4.2 | <i>Critical Marine Habitats and Resources</i> | 122 |
| 7.5 | ARCHAEOLOGICAL RESOURCES | 123 |
| 7.6 | MEC POTENTIALLY PRESENT IN THE DELAWARE WEA | 123 |
| 8.0 | APPLICATION OF MEC RISK ASSESSMENT TO DELAWARE WEA..... | 125 |
| 8.1 | IDENTIFICATION OF MEC POTENTIALLY PRESENT..... | 125 |
| 8.1.1 | <i>Naval Warfare</i> | 125 |
| 8.1.2 | <i>Coastal Defense</i> | 126 |
| 8.1.3 | <i>Training Ranges</i> | 126 |
| 8.1.4 | <i>Sea Disposal of Munitions</i> | 126 |
| 8.1.5 | <i>Summary of MEC Related Activities in Delaware WEA</i> | 126 |
| 8.1.6 | <i>Summary of MEC Potentially Present from Known Activities in the Delaware WEA</i> | 126 |
| 8.2 | MEC HAZARD ASSESSMENT FINDINGS..... | 128 |
| 8.3 | MEC RISK ASSESSMENT RESULTS FOR DELAWARE WEA..... | 128 |
| 8.3.1 | <i>Semi-quantitative Risk Assessment</i> | 128 |
| 8.3.2 | <i>MEC Risk Management and Mitigation</i> | 128 |

9.0 IN-FIELD VERIFICATION METHODS AND PROCEDURES..... 135

9.1 DESIGN OF THE IN-FIELD VERIFICATION STUDY.....135

 9.1.1 *Sensor Selection*.....135

 9.1.2 *Selected Platform for In-field Verification*.....135

 9.1.3 *Selected Positioning Techniques for In-field Verification*.....136

9.2 MOBILIZATION.....136

 9.2.1 *Equipment*.....137

 9.2.2 *Personnel*.....137

9.3 PREPARE STUDY AREA137

 9.3.1 *Instrument Verification Strip Survey*138

 9.3.2 *Blind Seeding*.....140

 9.3.3 *Seeded Area Blind Survey*.....141

 9.3.3.1 *Surface Vessel Wide Area Assessment*.....141

 9.3.3.2 *Monopile Network Survey*.....142

 9.3.3.3 *Cable and Pipeline Route Test Surveys*143

 9.3.3.4 *Targeted Optical Survey*143

9.4 NAVIGATION AND MAPPING SYSTEM.....144

9.5 COMBINED SURFACE VESSEL WIDE AREA ASSESSMENT AND TARGET INTERROGATION METHOD
ASSESSMENT144

9.6 DEMOBILIZATION.....144

10.0 IN-FIELD VERIFICATION RESULTS 145

10.1 DATA PROCESSING.....145

 10.1.1 *Initial Processing*.....145

 10.1.1.1 *Magnetometry*.....145

 10.1.1.2 *Side-scan Sonar*.....146

 10.1.1.3 *Imagery*.....146

 10.1.2 *Detection Team Target Identification*.....146

 10.1.2.1 *Magnetometry Anomaly Picking*.....148

 10.1.2.2 *Side-scan Sonar Target Selection*.....149

10.2 PERFORMANCE ANALYSIS.....150

 10.2.1 *Navigation*.....151

 10.2.2 *Node Mission Performance*152

 10.2.2.1 *Target Detection*154

 10.2.2.2 *Target Identification*.....155

 10.2.3 *Cable Route Mission Performance*156

 10.2.3.1 *Target Detection*157

 10.2.3.2 *Target Identification*.....159

 10.2.4 *Mission Variations*.....161

 10.2.4.1 *Simulated Burial*162

 10.2.4.2 *Variations in Transect Spacing and Altitude*.....162

 10.2.5 *Optical Survey*167

10.3 DISCUSSION168

 10.3.1 *Wide Area Assessment*168

 10.3.2 *AUV Platform and Sensor Suite Performance*.....169

 10.3.2.1 *IVS Metrics*.....169

 10.3.2.2 *Magnetometer*.....170

 10.3.2.3 *Side-scan Sonar*.....173

 10.3.3 *Node and Cable Mission Methodology Performance*.....174

 10.3.3.1 *Node Performance*174

 10.3.3.2 *Cable Route Performance*175

 10.3.4 *Multi-Platform Methodology Assessment*176

10.4 CONCLUSIONS AND RECOMMENDATIONS.....177

 10.4.1 *Environmental Interference and Compensation*177

 10.4.2 *Distinguishing ISOs*.....178

 10.4.3 *Evaluating ISO Identification*179

 10.4.4 *ISO Detectable Range*.....180

| | | |
|---|--|------------|
| 10.4.5 | <i>Cost and Coverage Rate</i> | 180 |
| 11.0 | POST-STORM SEASON ASSESSMENT | 181 |
| 11.1 | INTRODUCTION | 181 |
| 11.1.1 | <i>Background</i> | 181 |
| 11.1.2 | <i>Hydrodynamic Record</i> | 181 |
| 11.2 | FIELD EFFORT | 182 |
| 11.2.1 | WAA | 183 |
| 11.2.2 | IVS | 183 |
| 11.2.3 | <i>AUV Missions</i> | 184 |
| 11.3 | RESULTS | 185 |
| 11.3.1 | <i>Hydrodynamics and Projected Sediment Transport</i> | 186 |
| 11.3.2 | <i>WAA and Observed Morphological Modification</i> | 187 |
| 11.3.3 | <i>IVS and AUV Navigation</i> | 188 |
| 11.3.4 | <i>Surrogate Target Detection</i> | 189 |
| 11.3.4.1 | Node Missions | 190 |
| 11.3.4.2 | Cable Route Missions | 192 |
| 11.4 | DISCUSSION | 194 |
| 11.4.1 | <i>Sediment Transport and Morphodynamics</i> | 194 |
| 11.4.2 | <i>Fate of Surrogate MEC</i> | 195 |
| 11.4.2.1 | Exposed vs. Scour and Burial | 198 |
| 11.4.2.2 | Mobility | 199 |
| 11.4.3 | <i>Mission Design and IVS Performance Analysis</i> | 201 |
| 11.4.3.1 | IVS Mission and Design | 201 |
| 11.4.3.2 | Mission Design on Magnetometer Performance | 202 |
| 11.4.3.3 | Influence of Sediment Type and Bedforms on MEC Detection | 203 |
| 11.5 | CONCLUSION..... | 204 |
| 12.0 | REFERENCES | 207 |
| | | |
| APPENDIX A – IN-FIELD VERIFICATION TRIP REPORT | | 219 |
| APPENDIX B – SEED DESCRIPTIONS AND LOCATION | | 235 |
| APPENDIX C – TARGET SELECTION, POSITIONING AND SIZE ESTIMATION ... | | 237 |
| APPENDIX D – COMBINED MAGNETOMETER AND SIDE-SCAN REANALYSIS .. | | 243 |
| APPENDIX E – POST-STORM SEASON ASSESSMENT TRIP REPORT | | 247 |

List of Tables

| | |
|--|----|
| Table 2-1: Physical Characteristics: Cape WEA | 7 |
| Table 2-2: Physical Characteristics: Massachusetts WEA | 8 |
| Table 2-3: Physical Characteristics: Rhode Island WEA | 9 |
| Table 2-4: Physical Characteristics: New York WEA..... | 10 |
| Table 2-5: Physical Characteristics: New Jersey WEA..... | 11 |
| Table 2-6: Physical Characteristics: Delaware WEA | 12 |
| Table 2-7: Physical Characteristics: Maryland WEA..... | 13 |
| Table 2-8: Physical Characteristics: Virginia WEA | 14 |
| Table 2-9: Physical Characteristics: North Carolina Kitty Hawk WEA..... | 15 |
| Table 2-10: Physical Characteristics: North Carolina Wilmington West WEA..... | 16 |
| Table 2-11: Physical Characteristics: North Carolina Wilmington East WEA | 17 |
| | |
| Table 3-1: Historical Research Results: Cape WEA | 21 |
| Table 3-2: Historical Research Results: Massachusetts WEA | 22 |
| Table 3-3: Historical Research Results: Rhode Island/Massachusetts WEA | 24 |
| Table 3-4: Historical Research Results: New York WEA..... | 28 |
| Table 3-5: Historical Research Results: New Jersey WEA | 30 |
| Table 3-6: Historical Research Results: Delaware WEA | 32 |
| Table 3-7: Historical Research Results: Maryland WEA..... | 35 |
| Table 3-8: Historical Research Results: Virginia WEA | 38 |
| Table 3-9: Historical Research Results: North Carolina Kitty Hawk WEA..... | 41 |
| Table 3-10: Historical Research Results: North Carolina Wilmington East & West WEA..... | 42 |
| | |
| Table 5-1: MEC Encounter Probability Factor | 69 |
| Table 5-2: MEC Sensitivity Factor | 70 |
| Table 5-3: Development Activity Energy Factor..... | 71 |
| Table 5-4: Probability of Detonation Grade Matrix | 72 |
| Table 5-5: Severity of MEC Detonation Effects Factor | 73 |
| Table 5-6: Relation of Net Explosive Weight to Severity of Effects from Underwater Detonation on Vessels, on Board Personnel, and Equipment | 75 |
| Table 5-7: MEC Risk Assessment Matrix | 76 |

| | |
|---|-----|
| Table 6-1: Summary of Positioning Technologies | 85 |
| Table 6-2: Comparison of Commercial SAS and Three Side-Scan Sonars, Each with 5-centimeter Resolution | 91 |
| Table 6-3: Typical Maximum Magnetic Anomaly Strength of Common Objects | 95 |
| Table 6-4: Typical detection ranges for the Geometrics G-882 | 96 |
| Table 6-5: Summary of Environmental Characterization Technologies | 99 |
| Table 6-6: Summary of Underwater MEC Detection Technologies | 101 |
| Table 6-7: Summary of Platforms..... | 111 |
| Table 6-8: Effectiveness of Platforms and Technologies When Associated with Various Site Characteristics..... | 113 |
| | |
| Table 7-1: Delaware WEA Seasonal Description..... | 119 |
| Table 7-2: Sediment Description | 120 |
| Table 7-3: Bathymetric Description..... | 120 |
| Table 7-4: Potential MEC in or Near the Delaware WEA..... | 124 |
| | |
| Table 8-1: Description of MEC near Delaware WEA..... | 127 |
| Table 8-2: Probability of MEC near Delaware WEA..... | 129 |
| Table 8-3: Probability of Detonation Grades for Site Characterization Activities near Delaware WEA | 131 |
| Table 8-4: Risk Scores for Substructure and Foundation Activities near Delaware WEA | 132 |
| Table 8-5: Risk Scores for Cable Installation Activities near Delaware WEA | 133 |
| | |
| Table 9-1: Vessel Specifications – R/V <i>Joanne Daiber</i> | 136 |
| Table 9-2: Number and Size of Surrogates Placed at Each Seeding Site | 141 |
| | |
| Table 10-1: Typical Magnetometer Response for Surrogates by Size at 2 m Altitude | 147 |
| Table 10-2: Number and Size of Surrogates Relocated at Each Site by Seeding Team..... | 151 |
| Table 10-3: Number and Size of Surrogates Not Relocated by Seeding Team..... | 151 |
| Table 10-4: Target Detection by Surrogate Size for Node Missions using Magnetometry..... | 154 |
| Table 10-5: Target Detection by Surrogate Size for Node Missions using Side-scan Sonar Aided by Magnetometry | 155 |
| Table 10-6: Target Identification by Surrogate Size for Node Missions using Magnetometry. | 156 |
| Table 10-7: Target Identification by Surrogate Size for Node Missions using Side-scan Sonar Aided by Magnetometry | 156 |

| | |
|--|-----|
| Table 10-8: Target Detection by Surrogate Size for Cable Route Missions using Magnetometry | 158 |
| Table 10-9: Target Detection by Surrogate Size for Cable Route Missions using Side-scan Sonar Aided by Magnetometry | 159 |
| Table 10-10: Target Identification by Surrogate Size for Cable Route Missions using Magnetometry | 160 |
| Table 10-11: Target Identification by Surrogate Size for Cable Route Missions using Side-scan Sonar Aided by Magnetometry | 161 |
| Table 10-12: Target Detection and Identification by Surrogate Size for Simulated Burial Missions using Magnetometry | 163 |
| Table 10-13: Target Detection and Identification by Surrogate Size for Variable Transect Spacing and Altitude Missions using Magnetometry | 164 |
| Table 10-14: Target Detection and Identification by Surrogate Size for Variable Altitude Missions using Side-scan Sonar Aided Magnetometry | 165 |
| Table 10-15: Target Detection and Identification by Surrogate Size for Variable Transect Spacing using Side-scan Sonar Aided Magnetometry | 165 |
| | |
| Table 11-1: Node Mission Target Results from the 2017 Field Effort..... | 191 |
| Table 11-2: Cable Route Mission Target Results from the 2017 Field Effort..... | 192 |
| Table 11-3: Cable Route Mission Target Results from the 2017 Field Effort..... | 200 |
| Table 11-4: Total Number of Magnetometer Picks during All Node 3 Missions | 202 |
| | |
| Table B-1: Seed Sizes, and Locations..... | 235 |
| | |
| Table C-1: Target Identification Results by Mission and Mission Type for Magnetometer Data Along-track | 238 |
| Table C-2: Target Identification Results by Mission and Mission Type for Side-scan Sonar Data | 239 |
| Table C-3: Positioning and Size Estimate Results by Mission and Mission Type for Magnetometer Data Alone | 240 |
| Table C-4: Positioning and Size Estimate Results by Mission and Mission Type for Side-scan Sonar | 241 |
| | |
| Table D-1: Combined Magnetometer and Side-scan Reanalysis for Target Size Identification | 244 |
| Table D-2: Comparison of Results Between Side-scan Sonar, Magnetometry and Combined Reanalysis Target Size Estimation..... | 245 |

List of Figures

| | |
|--|-----|
| Figure 1-1: Atlantic OCS WEAs | 3 |
| Figure 1-2: Study Area..... | 4 |
| | |
| Figure 3-1: MEC Related Sites: Cape WEA..... | 43 |
| Figure 3-2: MEC Related Sites: Massachusetts WEA..... | 44 |
| Figure 3-3: MEC Related Sites: Rhode Island/Massachusetts WEA | 45 |
| Figure 3-4: MEC Related Sites: Rhode Island/Massachusetts WEA – Inset A..... | 46 |
| Figure 3-5: MEC Related Sites: Rhode Island/Massachusetts WEA – Inset B..... | 47 |
| Figure 3-6: MEC Related Sites: Rhode Island/Massachusetts WEA – Inset C..... | 48 |
| Figure 3-7: MEC Related Sites: New York WEA | 49 |
| Figure 3-8: MEC Related Sites: New Jersey WEA | 50 |
| Figure 3-9: MEC Related Sites: Delaware WEA | 51 |
| Figure 3-10: MEC Related Sites: Maryland WEA | 52 |
| Figure 3-11: MEC Related Sites: Virginia WEA | 53 |
| Figure 3-12: MEC Related Sites: Virginia WEA – Inset A..... | 54 |
| Figure 3-13: MEC Related Sites: North Carolina Kitty Hawk WEA..... | 55 |
| Figure 3-14: MEC Related Sites: North Carolina Wilmington East & West WEAs..... | 56 |
| | |
| Figure 5-1: MEC Risk Management Framework | 68 |
| | |
| Figure 6-1: Co-registration of Data Using a Tie-line..... | 84 |
| Figure 6-2: Synthesis of a Larger Array by Combining Multiple Pings..... | 90 |
| Figure 6-3: Image Showing Side-scan Sonar vs SAS..... | 92 |
| Figure 6-4: Geometric Limitation of Two-row Phase Measurement..... | 94 |
| Figure 6-5: EIVA ScanFish II ROTV | 105 |
| Figure 6-6: EIVA ScanFish Equipped with Four Magnetometers for High-resolution Magnetic Survey | 106 |
| Figure 6-7: Kraken Active Towfish, KATFISH-180 with a 180 cm SAS Array | 106 |
| Figure 6-8: R/V AHI, Survey Launch..... | 109 |
| | |
| Figure 7-1: MAB Cross-Shelf Currents..... | 121 |

Figure 9-1: Side-scan Sonar Coverage of Cable Route and 2 x 2 km Survey Box Collected 20 July 2016..... 138

Figure 9-2: IVS Configuration and AUV Mission Route..... 139

Figure 9-3: IVS Items and Location 140

Figure 9-4: IVS Items and Location 140

Figure 9-5: Munitions Surrogates and USBL Puck..... 141

Figure 10-1: Gavia AUV Mission Log Example Navigation Plot..... 145

Figure 10-2: Magnetometer Signal from IVS missions Over Duration of Field Effort..... 147

Figure 10-3: Magnetometer Anomalies Signal with Four Auto-detected Anomalies and Size Class..... 149

Figure 10-4: Contact with Length and Width Measured and Position, Site, and Size Estimate Cataloged 150

Figure 10-5: IVS Surrogate Positional Scatter Over Field Effort..... 152

Figure 10-6: Node Mission Overview 153

Figure 10-7: Cable Route Mission Overview 157

Figure 10-8: Section of Photomosaic from Node 3 Optical Survey 167

Figure 10-9: Overview of AUV Camera Missions Collected 28 July 2016..... 168

Figure 10-10: Illustration of Effects of Grazing Angles..... 169

Figure 10-11: Imagery Comparison of Previously Identified Targets..... 170

Figure 10-12: Magnetometry Signal to Noise Ratio for 6-inch Surrogate at Various Altitudes 172

Figure 10-13: Effect of Orientation on Acoustic Shadow of 6-inch Surrogate 173

Figure 10-14: Examples of Data that could Result in False-positive Identifications 176

Figure 11-1: Hydrodynamic Record for BOEM Study Area Derived from NOAA WaveWatch III..... 182

Figure 11-2: WAA conducted on April 10, 2017 183

Figure 11-3: Redesigned IVS..... 184

Figure 11-4: Location of 2017 IVS and Morphological Setting..... 184

Figure 11-5: Overview of BOEM In-field Verification 2016 Study Site and Surrogate Locations 185

Figure 11-6: Shields Parameter Estimates of Sediment Motion for Representative Sediment Types at the BOEM Study Area 186

Figure 11-7: Sediment Changes between 2016 and 2017 WAAs..... 187

Figure 11-8: IVS Magnetometer Results for the 2017 Field Effort..... 188

Figure 11-9: IVS Magnetometer Results for the 2017 Field Effort..... 189

Figure 11-10: Node Mission Target Results from the 2017 Field Effort 190

Figure 11-11: Side-scan Sonar Data showing 6-inch Surrogates Orthogonal to and In-line with
Dominant Ripple Crest Direction 191

Figure 11-12: Cable Route Mission Target Results from the 2017 Field Effort 193

Figure 11-13: Comparison of Position and Orientation of Cable Route 2 Mobile Surrogate ... 194

Figure 11-14: Scour and Burial Predictions for Surrogates at Shallow Sites by Sediment Type
..... 197

Figure 11-15: Scour and Burial Predictions for Surrogates at Deep Sites by Sediment Type .. 198

Figure 11-16: Raw Magnetometer Data at Node 3 by Altitude..... 203

Revisions

| Revision Number | Revision Date | Comment |
|-----------------|---------------|--------------------------------------|
| 0 | 7/21/2017 | Final |
| 1 | 7/28/2017 | Add BOEM information, replace covers |
| | | |
| | | |
| | | |
| | | |
| | | |

Acronyms and Abbreviations

| Acronym | Definition |
|--------------------|---|
| ° | degrees |
| °C | degrees Celsius |
| °F | degrees Fahrenheit |
| AMTB | anti-motor torpedo boat |
| AP | armor piercing |
| ASV | autonomous surface vehicle |
| AUV | autonomous underwater vehicle |
| BOEM | Bureau of Ocean Energy Management |
| CFR | Code of Federal Regulations |
| CIRIA | Construction Industry Research and Information Association |
| cm | centimeter(s) |
| cm s ⁻¹ | centimeters per second |
| CRM | Coastal Relief Model |
| CTD | conductivity-temperature-depth |
| DGPS | differential global positioning system |
| DoD | U.S. Department of Defense |
| Dp | dominant wave direction |
| DVL | Doppler velocity log |
| EM | electromagnetic |
| ESP | electric service platform |
| ESTCP | Environmental Security Technology Certification Program |
| FDEMI | Frequency Domain Electro Magnetic Induction |
| FUDS | Formerly Used Defense Site |
| GIS | geographic information system |
| GLONASS | GLObalnaya NAVigatsionnaya Sputnikovaya Sistema (English translation: global navigation satellite system) |
| GNSS | Global Navigation Satellite Systems |
| GPS | global positioning system |
| HE | high explosive |
| Hs | significant wave height |
| INS | inertial navigation system |
| ISO | industry standard object |
| IVS | instrument verification strip |

| Acronym | Definition |
|--------------------|--|
| kg | kilogram |
| kg m ⁻³ | kilogram per cubic meter |
| kHz | kilohertz |
| km | kilometer(s) |
| km ² | square kilometer(s) |
| lb | pound |
| LMCS | Littoral Mine Countermeasure SONAR |
| LBL | long baseline |
| LiDAR | Light Detection and Ranging |
| LLS | Laser line scan |
| m | meter |
| MAB | Middle Atlantic Bight |
| MBES | multibeam echo-sounder |
| MEC | munitions and explosives of concern |
| MHz | megahertz |
| MK | mark |
| mm | millimeter(s) |
| mph | miles per hour |
| NDBC | National Data Buoy Center |
| nmi | nautical mile |
| NOAA | National Oceanic and Atmospheric Administration |
| nT | nanoTesla |
| OCS | outer continental shelf |
| PLGR | pre-lay grapnel run |
| PMBS | phase-measuring bathymetric sonar |
| PPK | Post Processed Kinematic |
| R/V | research vessel |
| ROTV | remotely operated towed vehicle |
| ROV | remotely operated vehicle |
| RTK | Real Time Kinematic |
| SAS | synthetic aperture sonar |
| SBL | short baseline |
| SERDP | Strategic Environmental Research and Development Program |
| SNR | signal to noise ratio |

| Acronym | Definition |
|---------|---------------------------------------|
| TDEMI | time-domain electromagnetic induction |
| TNT | trinitrotoluene |
| Ub | near-bed wave orbital velocity |
| USBL | ultra-short baseline |
| USC | United States Code |
| USGS | U.S. Geological Survey |
| UXO | unexploded ordnance |
| WAAS | Wide Area Augmentation System |
| WEA | wind energy area |

1.0 Introduction

This report summarizes the in-field testing and methodology verification associated with Task 3 of the United States Department of the Interior, Bureau of Safety and Environmental Enforcement's Statement of Work, "*Unexploded Ordnance (UXO) Survey Methodology Investigation*" under contract M16PC00001. CALIBRE and its subcontractors (University of Delaware, University of Hawaii, and Environet, Inc.) met the goal of the study by investigating, verifying, and recommending methodologies to identify munitions and explosives of concern (MEC), including UXO, specific to conditions found in renewable energy lease and planning areas along the Atlantic Outer Continental Shelf (OCS). Regional expectations of type, size, and likelihood of presence for UXO and MEC along the Atlantic OCS were identified through desktop review. The overarching goal of this project is to develop an approach for identifying technologies and methodologies to be used in the ocean to determine routes free from significant obstacles to enable the safe construction and operation of wind turbines, power cables, and similar offshore energy projects. Based on this research, the Bureau of Ocean Energy Management (BOEM) may develop guidance for lessees on surveying for MEC on the Atlantic OCS.

In-field testing was performed within the Delaware Wind Energy Area (WEA), an approximately 391 square kilometer (km²) area offshore of Delaware (Figure 1-1). The closest point to shore is approximately 18 kilometers (km) due east from Rehoboth Beach, Delaware. A 4.5 km² area within the Delaware WEA was designated as the study area and was investigated between July 18 and 29, 2016 (Figure 1-2).

1.1 Project Background

Munitions are present in U.S. waters as a result of live-fire testing and training (both ongoing and past); combat operations (acts of war through World War II); sea disposal (conducted through 1970); accidents (periodic); and disposal (e.g., jettisoning) during emergencies.

The Outer Continental Shelf Lands Act of 1953 and its subsequent amendments require the Secretary of the Interior to balance the nation's energy needs with the protection of the human, marine, and coastal environments, while ensuring that the concerns of coastal states and competing users are taken into account. BOEM, a bureau within the Department of the Interior, has jurisdiction over all mineral resources on the federal OCS, and is charged with conducting OCS lease sales as well as monitoring and mitigating unwelcome impacts that might be associated with resource development.

In 2005, the Energy Policy Act amended Section 388 of the Outer Continental Shelf Lands Act, giving the Secretary of the Interior discretionary authority to issue leases, easements, or rights-of-way for renewable energy projects on the OCS. Under this new authority, BOEM may issue leases on the OCS for potential renewable energy projects including, but not limited to, wind energy, wave energy, ocean current energy, solar energy, and hydrogen production. BOEM recognizes that new and future uses of the OCS, including renewable energy development, should be managed in a deliberate and responsible manner, keeping the nation's energy needs, concerns for the marine environment, and human safety in mind. To comply with the National Environmental Policy Act and other relevant laws, BOEM's renewable energy regulations require a lessee to identify man-made hazards, such as MEC. Areas of the seabed that will be disturbed during installation of renewable energy facilities should be cleared of MEC

prior to installation activities to the extent necessary for both human safety and environmental protection. There is little detailed guidance on the selection and application of methodologies capable of identifying surficial, partially buried, and fully buried MEC (to a depth of 10 meters [m]) likely to be encountered on the Atlantic OCS.

1.2 Project Scope and Objectives

The scope of this project is to address methodology development, in-field testing, and methodology verification. Several critical components were developed for this project:

- ▶ Development of a list of anticipated MEC based on a review of historical documentation;
- ▶ Preparation of a summary of relevant environmental conditions (e.g., sediment type, water depth, bottom current strength, stratification) that could affect the ability of a selected technology to complete the survey objectives;
- ▶ Evaluation of currently-available technologies/methodologies; and
- ▶ Preparation of a risk assessment to determine the relative risks associated with the survey and installation of marine cables based on the munitions in the Delaware WEA, and that potentially pose a risk to renewable energy development and need to be identified.

The overarching project objective is to develop an approach for identifying technologies and optimizing methodologies to determine a route along the seabed for the safe construction and operation of wind turbines and associated power cables. This research may be used by BOEM in developing guidance for renewable energy development off the Atlantic Coast of the United States, in an area where MEC may be present on or beneath the seabed. This project provides an approach that is consistent with federal regulations and that provides viable methodologies for optimizing MEC surveys. The project goal is to describe an approach that can be translated into non-technology-specific guidance. Specifically, the objectives of the project are as follows:

- ▶ Determine regional expectations for MEC in the Atlantic OCS based on historical research,
- ▶ Develop an approach to select MEC detection and identification technologies and methods appropriate for the Atlantic OCS WEAs and compatibility with expected MEC, and
- ▶ Verify an approach to optimize the selected technologies/methodologies with an offshore field effort to identify surficial, buried, and partially buried objects that match the size and signature of MEC anticipated in the WEA.

In order to select a threshold for MEC detection, a MEC risk management framework is presented. The MEC risk assessment approach must be considered preliminary and requires testing and validation before it can be relied upon. The design and implementation of MEC risk mitigation measures is beyond the scope of the current study.

Because the presence of MEC at the area selected for the in-field verification could not be assured, the field approach and optimization were verified by placing and locating objects (e.g., industry standard objects [ISO]) of similar size and shape to the anticipated MEC in the study area. The capability to detect MEC partially buried, and buried at a depth of 2 m beneath the seabed was demonstrated by varying the height of the sensors above the seabed rather than by burying the ISO.

Figure 1-1: Atlantic OCS WEAs

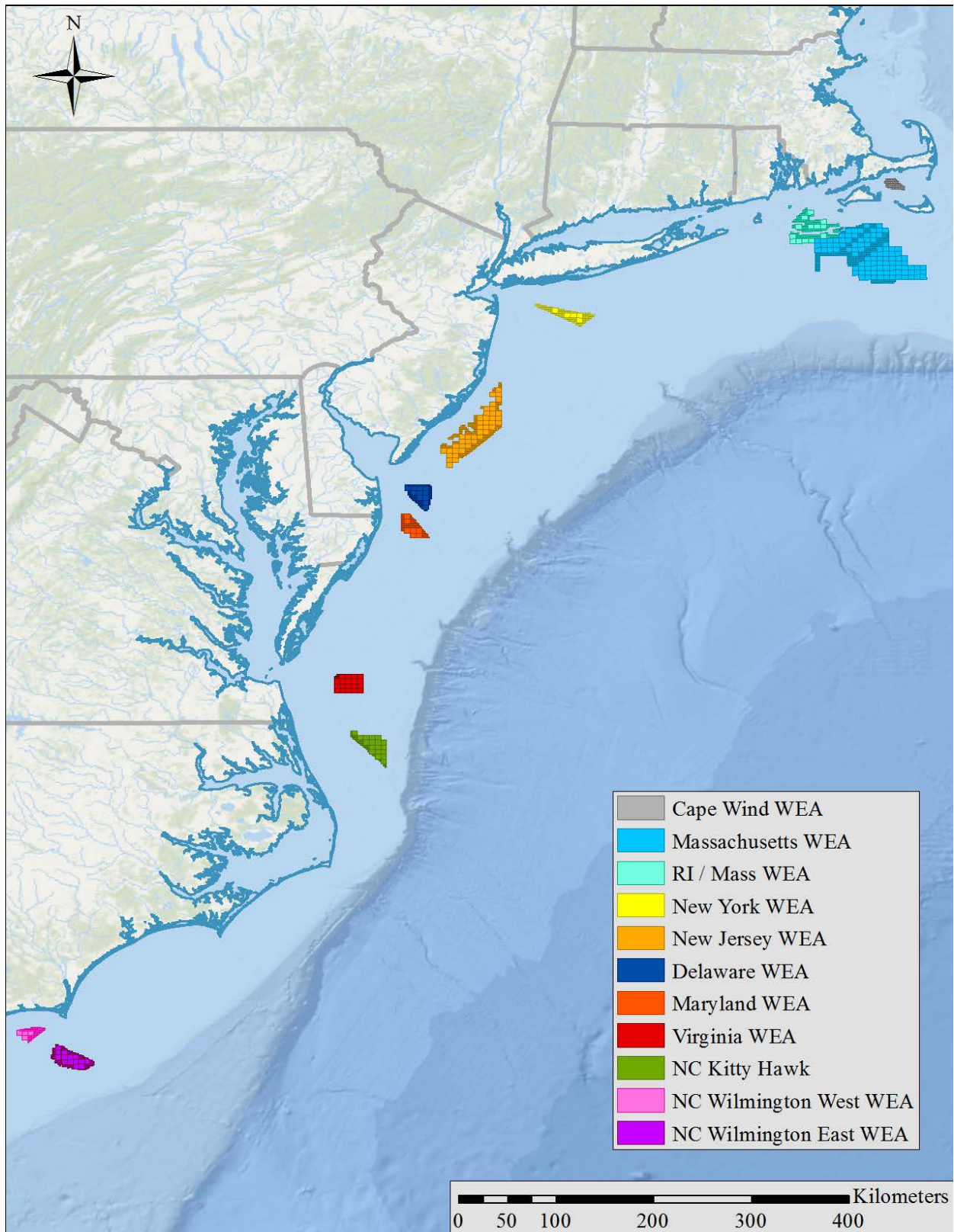
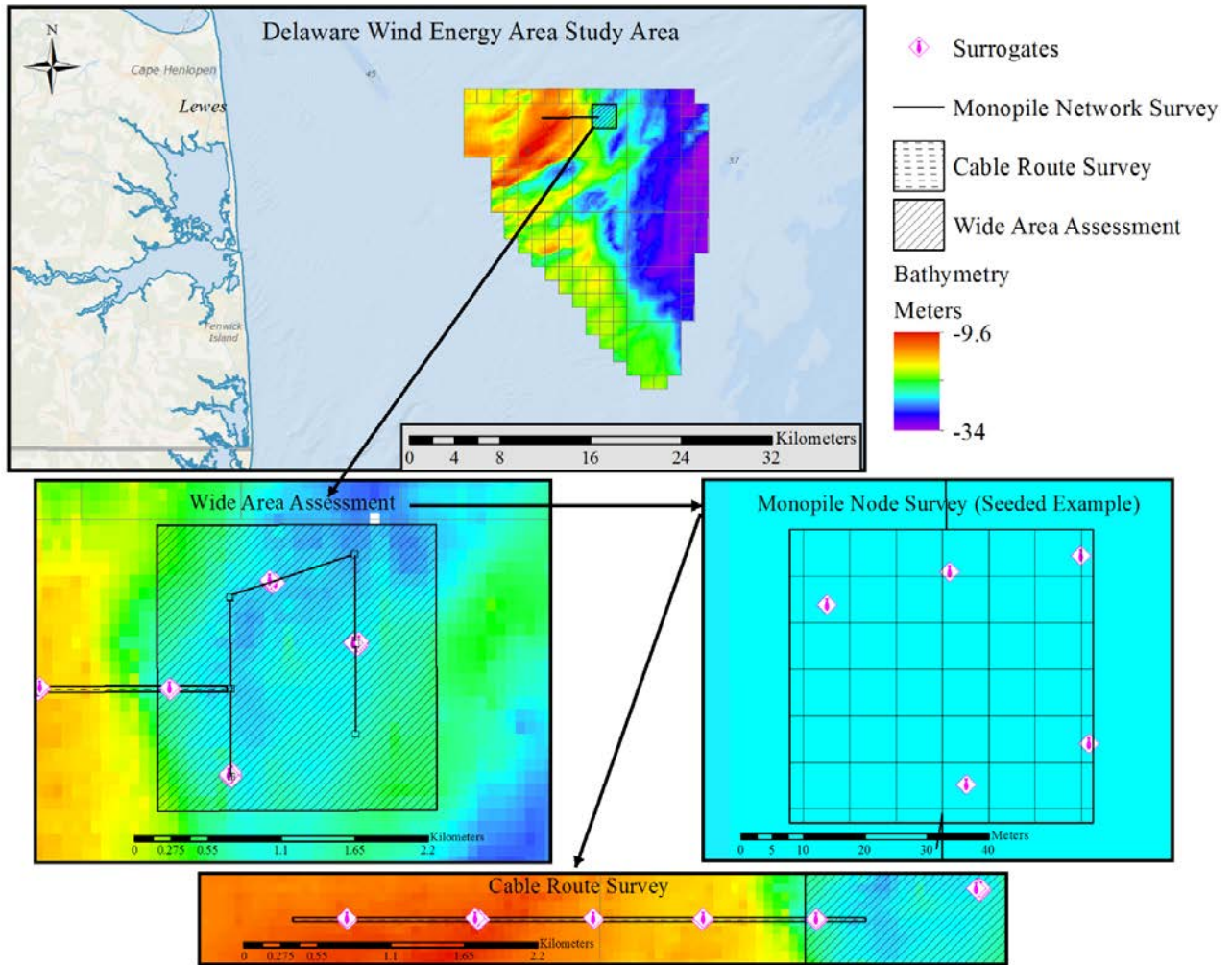


Figure 1-2: Study Area



2.0 Physical Conditions at the Atlantic OCS WEAs

In preparation for the in-field verification efforts for BOEM's UXO Survey Methodology Investigation, pertinent geophysical and oceanographic data, regarding BOEM's existing WEAs, Planned WEAs, and Lease Areas, was compiled. This data supported literature review efforts for Task 2 – Methodology Development.

The data collected represents existing sources of information available to public and private interests. Sources, which are cited with the data in the tables below, include the National Oceanographic and Atmospheric Administration's (NOAA) [National Data Buoy Center \(NDBC\)](#) (National Oceanic and Atmospheric Administration 2016c) and [Coastal Relief Model \(CRM\)](#) (National Oceanic and Atmospheric Administration 2016d), the U.S. Geological Survey's (USGS) [usSEABED sediment database](#) (U.S. Geological Survey and University of Colorado 2005), the Nature Conservancy (2016), and BOEM. In specific cases, such as the Maryland WEA, geophysical and geotechnical data has been made available. Collated data has been cataloged and a Geographic Information System (GIS) database has been created for relevant geospatial data.

The data summarized includes site:

- ▶ **General Description:** site total area and total number of lease blocks;
- ▶ **Sediment Description:** seabed sediment classification and distribution;
- ▶ **Bathymetric Description:** depth range, distribution and bathymetric relief general characterization;
- ▶ **Seasonal Description:** average sea surface temperature and density stratification in the water column (presented as difference between densities at the surface versus the bottom); and
- ▶ **Wave Climate Description:** monthly averages for wave height, period, and directions calculated from NOAA NDBC historical data.

The data described are pertinent when considering the appropriate timing, conditions, and technology for detailed seafloor surveying and MEC detection. Sediment distributions described in Wentworth Sediment size classes, will generally indicate the acoustic properties of the seafloor (e.g., coarser sediments trends more acoustically reflective), and when paired with wave climate, may indicate the behavior of MEC on the seabed (i.e., scour or burial in higher wave energy in non-cohesive sands and gravels). Bathymetric descriptions indicate the depth range and complexity of seafloor topography, which must be taken into account when deciding whether surface, towed, or autonomous platforms are best suited for the surveying task. Seasonal descriptions, specifically stratification, is important when considering surface-based acoustic surveying, as more stratified water (greater than 1 kilogram [kg] per cubic m [m³] difference in density) may affect acoustic sensor performance, and with bathymetric sonars, must be accounted for with water column measurements (i.e., sound speed profiles). Wave climate descriptions indicate the most suitable times for vessel based surveying; relative higher monthly average wave heights and period indicate a greater chance for poor surface conditions or seasonal storm events, and dominant wave direction should be accounted when designing and executing surface vessel surveys.

More data are available from the sources listed than is summarized here. Additional site characteristics can and may be referenced or calculated from these databases.

The tables below summarize the geophysical and oceanographic characteristics for the following BOEM WEAs, Planned Areas, or Leases: Cape (Table 2-1), Massachusetts (Table 2-2), Rhode Island (Table 2-3), New York (Table 2-4), New Jersey (Table 2-5), Delaware (Table 2-6), Maryland (Table 2-7), Virginia (Table 2-8), North Carolina Kitty Hawk (Table 2-9), North Carolina Wilmington West (Table 2-10), and North Carolina Wilmington East (Table 2-11). Distinctions between sites were based on state association and nearest historical NOAA buoy data. Each table is accompanied by a brief description of the WEA and assessment of potential issues to survey technology and methods posed by seafloor topography or oceanographic characteristics.

Table 2-1: Physical Characteristics: Cape WEA

| Cape Wind Energy Area | | | | | | | | | | | | | | |
|---|--|------------|-----------|-----------|-------------|-----------------------|-----------|-----------|-----------|-----------|---|--|--|--|
| General Description | | | | | | | | | | | Data Source(s) | | | |
| Area (sq. km) | | | | | | 119.14 | | | | | | Bureau of Ocean Energy Management 2016 | | |
| Lease Blocks | | | | | | 84 | | | | | | | | |
| Sediment Description | | | | | | | | | | | See U.S. Geological Survey and University of Colorado 2005, ATL_PRS: usSEABED PaRSed data for point sediment sample data; The Nature Conservancy 2016 | | | |
| Wentworth (1922) Scale | Silts | Sandy Silt | Fine Sand | Med Sand | Coarse Sand | Coarse Sand w/ Gravel | | | | | | | | |
| Sediment Distribution (% area) | 0.00 | 0.00 | 10.00 | 48.79 | 1.07 | 40.13 | | | | | | | | |
| Bathymetric Description | | | | | | | | | | | National Oceanic and Atmospheric Administration 2016d | | | |
| Bathymetric Relief | Shoal in W section w/ ridge along shoal, Slope central, Shoal Ridge SE | | | | | | | | | | | | | |
| Depth Range | 0.5 -33 m | | | | | | | | | | | | | |
| Depth Distribution (%) | 0 - 5 m | 5 - 10 m | 10 - 15 m | 15 - 20 m | 20 - 25 m | 25 - 30 m | 30 - 35 m | 35 - 40 m | 40 - 45 m | 45 - 50 m | 50 - 55m | > 55m | Interpreted from: Coastal Relief Model - National Oceanic and Atmospheric Administration 2016d | |
| | | 10.329 | 47.516 | 37.214 | 3.086 | 1.027 | 0.741 | 0.086 | 0.000 | 0.000 | 0.000 | 0.000 | | |
| Seasonal Description | | | | | | | | | | | The Nature Conservancy 2016 | | | |
| Season | Winter | | | Spring | | | Summer | | | Fall | | | | |
| Avg. Sea Surface Temperature (°C) | 4.47 | | | 6.06 | | | 11.14 | | | 10.30 | | | | |
| Stratification (kg/m ³) (Difference in density from surface to depth) | 0.03 | | | 0.24 | | | 0.53 | | | 0.05 | | | | |
| Wave Climate Description | | | | | | | | | | | | | | |
| Month | January | February | March | April | May | June | July | August | September | October | November | December | National Oceanic and Atmospheric Administration 2016c (Station 44020) | |
| Avg. Significant Wave Height (m) | 0.62 | 0.62 | 0.62 | 0.53 | 0.45 | 0.43 | 0.39 | 0.39 | 0.46 | 0.60 | 0.65 | 0.66 | | |
| Avg. Wave Period (s) | 4.19 | 4.25 | 4.40 | 4.44 | 4.35 | 4.25 | 4.01 | 4.43 | 4.39 | 4.22 | 4.29 | 4.40 | | |
| Avg. Wave Direction (° from North) | 215.16 | 208.00 | 177.62 | 169.91 | 168.67 | 165.98 | 193.62 | 186.71 | 161.21 | 181.72 | 183.34 | 196.98 | | |

The Cape WEA covers 119.14 km² and is characterized by very shallow bathymetry, with a shoal in the western section approaching depths of less than one m. The shallow topography poses an issue for a surface vessel survey, becoming too shallow for any craft of significant draft, and also poses issues for terrain following submersible vehicles or towed sensors. Because the area is dominated by medium-to-coarse non-cohesive sediments, seabed objects will tend to scour and bury in events with significant energy. However, the wave climate is generally calm, being sheltered by Cape Cod, Nantucket Island and Martha’s Vineyard. Coarse sediments will be more acoustically reflective, and tend to form ripple bedforms, both of which may obscure the signature of small munitions. Low water column stratification suggests the area is fairly well mixed and should not significantly affect the performance of surface-based sonars.

Table 2-2: Physical Characteristics: Massachusetts WEA

| Massachusetts Wind Energy Area | | | | | | | | | | | | | | | |
|---|---|------------|-----------|-----------|-------------|-----------------------|-----------|-----------|-----------|-----------|----------|--|--|---|--|
| General Description | | | | | | | | | | | | Data Source(s) | | | |
| Area (sq. km) | | | | | | 3007.84 | | | | | | Bureau of Ocean Energy Management 2016 | | | |
| Lease Blocks | | | | | | 603 | | | | | | | | | |
| Sediment Description | | | | | | | | | | | | | | | |
| Wentworth (1922) Scale | Silts | Sandy Silt | Fine Sand | Med Sand | Coarse Sand | Coarse Sand w/ Gravel | | | | | | | | See U.S. Geological Survey and University of Colorado 2005, ATL_PRS: usSEABED PaRSed data for point sediment sample data; The Nature Conservancy 2016 | |
| Sediment Distribution (% area) | 4.37 | 32.14 | 53.29 | 8.51 | 0.02 | 1.68 | | | | | | | | | |
| Bathymetric Description | | | | | | | | | | | | | | | |
| Bathymetric Relief | Shoal NE, slopes to SW, Slight Ridge and Swale NW | | | | | | | | | | | | National Oceanic and Atmospheric Administration 2016d | | |
| Depth Range | 28 - 64 m | | | | | | | | | | | | | | |
| Depth Distribution (%) | 0 - 5 m | 5 - 10 m | 10 - 15 m | 15 - 20 m | 20 - 25 m | 25 - 30 m | 30 - 35 m | 35 - 40 m | 40 - 45 m | 45 - 50 m | 50 - 55m | > 55m | Interpreted from: Coastal Relief Model - National Oceanic and Atmospheric Administration 2016d | | |
| | 0.000 | 0.000 | 0.000 | 0.000 | 0.000 | 0.000 | 0.197 | 4.381 | 18.577 | 24.501 | 30.466 | 21.877 | | | |
| Seasonal Description | | | | | | | | | | | | | | | |
| Season | Winter | | | Spring | | | Summer | | | Fall | | | The Nature Conservancy 2016 | | |
| Avg. Sea Surface Temperature (°C) | 5.54 | | | 7.85 | | | 12.64 | | | 11.96 | | | | | |
| Stratification (kg/m ³) (Difference in density from surface to depth) | 0.04 | | | 0.73 | | | 1.97 | | | 0.22 | | | | | |
| Wave Climate Description | | | | | | | | | | | | | | | |
| Month | January | February | March | April | May | June | July | August | September | October | November | December | National Oceanic and Atmospheric Administration 2016c (Station 44097) | | |
| Avg. Significant Wave Height (m) | 1.85 | 1.78 | 1.56 | 1.42 | 1.18 | 1.04 | 1.02 | 0.99 | 1.19 | 1.53 | 1.82 | 1.81 | | | |
| Avg. Wave Period (s) | 7.25 | 7.51 | 7.94 | 8.19 | 7.76 | 7.18 | 7.05 | 7.82 | 8.18 | 7.55 | 7.76 | 7.60 | | | |
| Avg. Wave Direction (° from North) | 216.72 | 200.40 | 188.68 | 180.94 | 177.78 | 177.82 | 193.44 | 177.38 | 172.37 | 192.02 | 189.58 | 197.74 | | | |

The Massachusetts WEA covers over 3,008 km², posing logistical issues for comprehensive surveys. Overall, this WEA trends deeper than others in the region, sloping deeper from Northeast-Southwest with slight ridge and swale topography in the northwest region. The sediment is largely characterized by fine sands and silts, which are acoustically absorbent in contrast to metallic objects such as munitions, which are acoustically reflective materials. In a region dominated by nor'easters, surveying may be subject to poor conditions from October – April, during which there are historically higher wave heights. The calmest season, summer, also proves to have the highest water column stratification, which must be accounted for in surface-based acoustic surveys through water column measurements (e.g., sound speed profiles).

Table 2-3: Physical Characteristics: Rhode Island WEA

| Rhode Island / Massachusetts Wind Energy Area(s) | | | | | | | | | | | | | | |
|---|---|------------|-----------|-----------|-------------|-----------------------|-----------|-----------|-----------|-----------|----------|---|---|--|
| General Description | | | | | | | | | | | | Data Source(s) | | |
| Area (sq. km) | | | | | | 666.75 | | | | | | Bureau of Ocean Energy Management 2016 | | |
| Lease Blocks | | | | | | 268 | | | | | | | | |
| Sediment Description | | | | | | | | | | | | | | |
| Wentworth (1922) Scale | Silts | Sandy Silt | Fine Sand | Med Sand | Coarse Sand | Coarse Sand w/ Gravel | | | | | | | See U.S. Geological Survey and University of Colorado 2005, ATL_PRS: usSEABED PaRSed data for point sediment sample data; The Nature Conservancy 2016 | |
| Sediment Distribution (% area) | 0.00 | 0.96 | 33.39 | 4.69 | 8.50 | 52.47 | | | | | | | | |
| Bathymetric Description | | | | | | | | | | | | | | |
| Bathymetric Relief | Shoals in North, Slopes deeper to South | | | | | | | | | | | National Oceanic and Atmospheric Administration 2016d | | |
| Depth Range | 7-54 m | | | | | | | | | | | | | |
| Depth Distribution (%) | 0 - 5 m | 5 - 10 m | 10 - 15 m | 15 - 20 m | 20 - 25 m | 25 - 30 m | 30 - 35 m | 35 - 40 m | 40 - 45 m | 45 - 50 m | 50 - 55m | > 55m | Interpreted from: Coastal Relief Model - National Oceanic and Atmospheric Administration 2016d | |
| | 0.000 | 0.001 | 0.000 | 0.000 | 0.002 | 0.931 | 25.027 | 27.206 | 16.273 | 20.043 | 10.518 | 0.000 | | |
| Seasonal Description | | | | | | | | | | | | | | |
| Season | Winter | | | Spring | | | Summer | | | Fall | | | The Nature Conservancy 2016 | |
| Avg. Sea Surface Temperature (°C) | 5.06 | | | 8.32 | | | 14.46 | | | 12.74 | | | | |
| Stratification (kg/m ³) (Difference in density from surface to depth) | 0.09 | | | 1.00 | | | 2.01 | | | 0.27 | | | | |
| Wave Climate Description | | | | | | | | | | | | | | |
| Month | January | February | March | April | May | June | July | August | September | October | November | December | National Oceanic and Atmospheric Administration 2016c (Station 44097) | |
| Avg. Significant Wave Height (m) | 1.85 | 1.78 | 1.56 | 1.42 | 1.18 | 1.04 | 1.02 | 0.99 | 1.19 | 1.53 | 1.82 | 1.81 | | |
| Avg. Wave Period (s) | 7.25 | 7.51 | 7.94 | 8.19 | 7.76 | 7.18 | 7.05 | 7.82 | 8.18 | 7.55 | 7.76 | 7.60 | | |
| Avg. Wave Direction (° from North) | 216.72 | 200.40 | 188.68 | 180.94 | 177.78 | 177.82 | 193.44 | 177.38 | 172.37 | 192.02 | 189.58 | 197.74 | | |

The Rhode Island / Massachusetts WEA consists of a 667 km² area. This WEA abuts the Massachusetts WEA, but is overall shallower, approaching depths of 7 m on a shoal in the northern section. The majority of the site falls much deeper than this (from 30-50 m), but the topography is variable in the northern lease blocks, which may present issues with towed instruments. The sediment skews coarser, which may lead to object scour and burial, or obscuring in bedforms that typically form in coarse sediments. Local historic wave climate data is from the same source as the Massachusetts WEA, which shows seasonal increases in wave height from October – April. Strong water column stratification is also apparent during the summer, which must be taken into account with surface-based acoustic surveys.

Table 2-4: Physical Characteristics: New York WEA

| New York Wind Energy Area | | | | | | | | | | | | | | | |
|---|-------------------------------|------------|-----------|-----------|-------------|-----------------------|-----------|---|-----------|-----------|----------------|---|--|-----------------------------|-------|
| General Description | | | | | | | | | | | Data Source(s) | | | | |
| Area (sq. km) | | | | | | 328.42 | | | | | | Bureau of Ocean Energy Management 2016 | | | |
| Lease Blocks | | | | | | 153 | | | | | | | | | |
| Sediment Description | | | | | | | | | | | | | | | |
| Wentworth (1922) Scale | Silts | Sandy Silt | Fine Sand | Med Sand | Coarse Sand | Coarse Sand w/ Gravel | | See U.S. Geological Survey and University of Colorado 2005, ATL_PRS: usSEABED PaRSed data for point sediment sample data; The Nature Conservancy 2016 | | | | | | | |
| Sediment Distribution (% area) | 0.00 | 0.23 | 21.84 | 15.69 | 33.29 | | 28.95 | | | | | | | | |
| Bathymetric Description | | | | | | | | | | | | | | | |
| Bathymetric Relief | Shallow Sloping from NW to SE | | | | | | | | | | | National Oceanic and Atmospheric Administration 2016d | | | |
| Depth Range | 18 - 42 m | | | | | | | | | | | | | | |
| Depth Distribution (%) | 0 - 5 m | 5 - 10 m | 10 - 15 m | 15 - 20 m | 20 - 25 m | 25 - 30 m | 30 - 35 m | 35 - 40 m | 40 - 45 m | 45 - 50 m | 50 - 55m | > 55m | Interpreted from: Coastal Relief Model - National Oceanic and Atmospheric Administration 2016d | | |
| | | 0.000 | 0.000 | 0.000 | 0.190 | 5.874 | 11.346 | 29.238 | 44.775 | 8.577 | 0.000 | 0.000 | | | 0.000 |
| Seasonal Descriptions | | | | | | | | | | | | | | | |
| Season | Winter | | | Spring | | | Summer | | | Fall | | | | The Nature Conservancy 2016 | |
| Avg. Sea Surface Temperature (°C) | 5.72 | | | 8.52 | | | 12.74 | | | 13.17 | | | | | |
| Stratification (kg/m ³) (Difference in density from surface to depth) | 0.20 | | | 1.93 | | | 3.24 | | | 0.30 | | | | | |
| Wave Climate Description | | | | | | | | | | | | | | | |
| Month | January | February | March | April | May | June | July | August | September | October | November | December | National Oceanic and Atmospheric Administration 2016c (Station 44065) | | |
| Avg. Significant Wave Height (m) | 1.02 | 1.11 | 1.13 | 1.07 | 0.98 | 0.86 | 0.82 | 0.83 | 1.01 | 1.13 | 1.16 | 1.20 | | | |
| Avg. Wave Period (s) | 6.61 | 6.91 | 8.11 | 7.84 | 7.60 | 7.12 | 7.15 | 7.69 | 8.16 | 7.70 | 8.02 | 8.02 | | | |
| Avg. Wave Direction (° from North) | 194.80 | 185.42 | 155.52 | 153.48 | 148.27 | 144.59 | 153.17 | 144.95 | 138.16 | 157.92 | 160.23 | 165.05 | | | |

The New York WEA consists of a 328 km² area extending Northwest-Southeast. Bathymetry follows this trend, sloping from 18 m in the northwest to 42 m in the southeast, with slight ridge and swale features in the center. Sediment distribution skews coarser, which may lead to object scour, burial or obscuring in bedforms. As with other northeastern WEAs, seasonal storm activity leads to historically rougher surface conditions from October – April. Stratification is very strong in the spring and summer seasons, which may cause issues with surface-based acoustic surveys. This should be accounted for with water column profiling. The gentle topography favors near-bed surveying by towed instrument or autonomous underwater vehicles (AUV).

Table 2-5: Physical Characteristics: New Jersey WEA

| New Jersey Wind Energy Area | | | | | | | | | | | | | | |
|---|----------------------------|------------|-----------|-----------|-------------|-----------------------|-----------|--|-----------|-----------|----------|--|--|--|
| General Description | | | | | | | | | | | | Data Source(s) | | |
| Area (sq. km) | | | | | | 1391.97 | | | | | | Bureau of Ocean Energy Management 2016 | | |
| Lease Blocks | | | | | | 343 | | | | | | | | |
| Sediment Description | | | | | | | | | | | | | | |
| Wentworth (1922) Scale | Silts | Sandy Silt | Fine Sand | Med Sand | Coarse Sand | Coarse Sand w/ Gravel | | See U.S. Geological Survey and University of Colorado 2005, ATL_PRS: usSEABED PaR.Sed data for point sediment sample data; The Nature Conservency 2016 | | | | | | |
| Sediment Distribution (% area) | 0.00 | 4.42 | 22.35 | 17.38 | 22.06 | 33.80 | | | | | | | | |
| Bathymetric Description | | | | | | | | | | | | | | |
| Bathymetric Relief | Ridge and Swale Topography | | | | | | | | | | | | National Oceanic and Atmospheric Administration 2016d | |
| Depth Range | 5-40 m | | | | | | | | | | | | | |
| Depth Distribution (%) | 0 - 5 m | 5 - 10 m | 10 - 15 m | 15 - 20 m | 20 - 25 m | 25 - 30 m | 30 - 35 m | 35 - 40 m | 40 - 45 m | 45 - 50 m | 50 - 55m | > 55m | Interpreted from: Coastal Relief Model - National Oceanic and Atmospheric Administration 2016d | |
| | | 0.000 | 0.000 | 0.058 | 8.819 | 43.073 | 37.824 | 9.828 | 0.396 | 0.000 | 0.000 | 0.000 | | |
| Seasonal Description | | | | | | | | | | | | | | |
| Season | Winter | | | Spring | | | Summer | | | Fall | | | The Nature Conservency 2016 | |
| Avg. Sea Surface Temperature (°C) | 5.90 | | | 9.62 | | | 13.34 | | | 13.45 | | | | |
| Stratification (kg/m ³) (Difference in density from surface to depth) | 0.25 | | | 1.44 | | | 2.41 | | | 0.12 | | | | |
| Wave Climate Description* | | | | | | | | | | | | | | |
| Month | January | February | March | April | May | June | July | August | September | October | November | December | *only 2014-2015 | |
| Avg. Significant Wave Height (m) | 1.53 | 1.71 | 1.10 | 1.30 | 0.93 | 1.14 | 0.92 | 0.86 | 1.24 | 1.69 | 1.24 | 1.26 | National Oceanic and Atmospheric Administration 2016c (Station 44091) | |
| Avg. Wave Period (s) | 7.34 | 8.15 | 7.07 | 7.68 | 6.27 | 7.03 | 7.61 | 8.81 | 8.52 | 8.20 | 7.86 | 7.53 | | |
| Avg. Wave Direction (° from North) | 169.84 | 159.69 | 159.13 | 139.27 | 170.02 | 136.50 | 148.17 | 119.51 | 125.96 | 132.27 | 128.03 | 153.36 | | |

The New Jersey WEA is a 1,392 km² area extending Southwest – Northeast with highly variable topography. The region is dominated by ridge and swale topography extending Northwest-Southeast, alternately shoaling to depths as little as 5 or as deep as 40 m. This may prove troublesome for towed instrument surveying. The sediment is characterized by both fine sands, as well as coarse sands with gravel, often juxtaposed locally in sorted bedforms. Wave climate shows strong seasonal patterns, with wave averages increasing from September – April, although local historical wave data is only available from 2014 – present. Water column stratification is strong during the spring and summer seasons, and may cause issues with surface-based acoustic surveys.

Table 2-6: Physical Characteristics: Delaware WEA

| Delaware Wind Energy Area | | | | | | | | | | | | | | |
|---|-----------------------------------|----------|------------|-----------|-----------|-----------|-----------|-----------|-------------|-----------|-----------------------|--|---|--|
| General Description | | | | | | | | | | | | Data Source(s) | | |
| Area (sq. km) | | | | | | 390.54 | | | | | | Bureau of Ocean Energy Management 2016 | | |
| Lease Blocks | | | | | | 106 | | | | | | | | |
| Sediment Description | | | | | | | | | | | | | | |
| Wentworth (1922) Scale | Silts | | Sandy Silt | | Fine Sand | | Med Sand | | Coarse Sand | | Coarse Sand w/ Gravel | | See U.S. Geological Survey and University of Colorado 2005, ATL_PRS: usSEABED PaRSed data for point sediment sample data; The Nature Conservancy 2016 | |
| Sediment Distribution (% area) | 0.00 | | 0.00 | | 5.15 | | 15.96 | | 13.03 | | 65.03 | | | |
| Bathymetric Description | | | | | | | | | | | | | | |
| Bathymetric Relief | W Ridge and Swale, E Gentle Slope | | | | | | | | | | | | National Oceanic and Atmospheric Administration 2016d | |
| Depth Range | 9 - 34m | | | | | | | | | | | | | |
| Depth Distribution (%) | 0 - 5 m | 5 - 10 m | 10 - 15 m | 15 - 20 m | 20 - 25 m | 25 - 30 m | 30 - 35 m | 35 - 40 m | 40 - 45 m | 45 - 50 m | 50 - 55m | > 55m | Interpreted from: Coastal Relief Model - National Oceanic and Atmospheric Administration 2016d | |
| | 0.000 | 0.003 | 5.583 | 26.084 | 28.550 | 30.133 | 9.644 | 0.000 | 0.000 | 0.000 | 0.000 | 0.000 | | |
| Seasonal Description | | | | | | | | | | | | | | |
| Season | Winter | | | Spring | | | Summer | | | Fall | | | The Nature Conservancy 2016 | |
| Avg. Sea Surface Temperature (°C) | 6.84 | | | 9.26 | | | 11.95 | | | 12.86 | | | | |
| Stratification (kg/m ³) (Difference in density from surface to depth) | 0.37 | | | 1.45 | | | 2.26 | | | 0.20 | | | | |
| Wave Climate Description | | | | | | | | | | | | | | |
| Month | January | February | March | April | May | June | July | August | September | October | November | December | National Oceanic and Atmospheric Administration 2016c (Station 44009) | |
| Avg. Significant Wave Height (m) | 1.38 | 1.34 | 1.38 | 1.27 | 1.12 | 0.92 | 0.87 | 0.96 | 1.19 | 1.31 | 1.37 | 1.30 | | |
| Avg. Wave Period (s) | 7.17 | 7.28 | 7.95 | 7.85 | 7.75 | 7.21 | 7.07 | 7.67 | 8.20 | 7.62 | 7.30 | 7.01 | | |
| Avg. Wave Direction (° from North) | 162.95 | 151.06 | 141.06 | 133.89 | 128.47 | 129.44 | 140.61 | 121.75 | 124.25 | 138.21 | 158.81 | 167.47 | | |

The Delaware WEA is a 391 km² area characterized by ridge and swale topography in the western blocks, with gentle slopes in the eastern blocks. The difference in topography within the WEA may require a suite of different approaches for wide area surveying: surface-based surveying in the shallower, ridge and swale areas, or towed instrument or AUV surveying in the deeper, less variable areas. The sediment is characterized by both fine sands, as well as coarse sands with gravel, often juxtaposed locally in sorted bedforms. Wave climate shows strong seasonal patterns, with wave averages increasing from October - April. The region is often buffeted by nor'easter, with occasional hurricane activity historically. Water column stratification is high during the spring and summer seasons, and may cause issues with surface-based acoustic surveys.

Table 2-7: Physical Characteristics: Maryland WEA

| Maryland Wind Energy Area | | | | | | | | | | | | | | | |
|---|-------------------------------------|------------|-----------|-----------|-------------|-----------------------|-----------|-----------|-----------|-----------|----------|--|--|---|-------|
| General Description | | | | | | | | | | | | Data Source(s) | | | |
| Area (sq. km) | | | | | | 322.81 | | | | | | Bureau of Ocean Energy Management 2016 | | | |
| Lease Blocks | | | | | | 119 | | | | | | | | | |
| Sediment Description | | | | | | | | | | | | | | | |
| Wentworth (1922) Scale | Silts | Sandy Silt | Fine Sand | Med Sand | Coarse Sand | Coarse Sand w/ Gravel | | | | | | | | See U.S. Geological Survey and University of Colorado 2005, ATL_PRS: usSEABED PaRSed data for point sediment sample data; The Nature Conservency 2016 | |
| Sediment Distribution (% area) | 0.00 | 0.32 | 10.23 | 12.10 | 23.26 | 54.09 | | | | | | | | | |
| Bathymetric Description | | | | | | | | | | | | | | | |
| Bathymetric Relief | W Shallow Ridge, SE Ridge and Swale | | | | | | | | | | | | National Oceanic and Atmospheric Administration 2016d | | |
| Depth Range | 12-42 m | | | | | | | | | | | | | | |
| Depth Distribution (%) | 0 - 5 m | 5 - 10 m | 10 - 15 m | 15 - 20 m | 20 - 25 m | 25 - 30 m | 30 - 35 m | 35 - 40 m | 40 - 45 m | 45 - 50 m | 50 - 55m | > 55m | Interpreted from: Coastal Relief Model - National Oceanic and Atmospheric Administration 2016d | | |
| | | 0.002 | 0.000 | 0.461 | 14.782 | 25.622 | 44.792 | 11.763 | 2.121 | 0.456 | 0.000 | 0.000 | | | 0.000 |
| Seasonal Description | | | | | | | | | | | | | | | |
| Season | Winter | | | Spring | | | Summer | | | Fall | | | The Nature Conservency 2016 | | |
| Avg. Sea Surface Temperature (°C) | 7.37 | | | 9.25 | | | 11.41 | | | 12.87 | | | | | |
| Stratification (kg/m ³) (Difference in density from surface to depth) | 0.39 | | | 1.56 | | | 2.25 | | | 0.19 | | | | | |
| Wave Climate Description | | | | | | | | | | | | | | | |
| Month | January | February | March | April | May | June | July | August | September | October | November | December | National Oceanic and Atmospheric Administration 2016c (Station 44009) | | |
| Avg. Significant Wave Height (m) | 1.38 | 1.34 | 1.38 | 1.27 | 1.12 | 0.92 | 0.87 | 0.96 | 1.19 | 1.31 | 1.37 | 1.30 | | | |
| Avg. Wave Period (s) | 7.17 | 7.28 | 7.95 | 7.85 | 7.75 | 7.21 | 7.07 | 7.67 | 8.20 | 7.62 | 7.30 | 7.01 | | | |
| Avg. Wave Direction (° from North) | 162.95 | 151.06 | 141.06 | 133.89 | 128.47 | 129.44 | 140.61 | 121.75 | 124.25 | 138.21 | 158.81 | 167.47 | | | |

The Maryland WEA is a 323 km² area. The Maryland WEA lies near the Delaware WEA, is characterized by a shallow ridge in the west, and ridge and swale topography in the central and southeast blocks. Depths range from 12 to 42 m. Sediment distributions are coarse, which may lead to seabed objects scour or burial. As discussed above, the coarse sediments will be more acoustically reflective and form ripple bedforms, both of which may obscure the signature of small munitions. As with other sites in the region, historic wave climate shows seasonal increases in wave height during the October – April months, with strong water column stratification occurring during the spring and summer seasons, which may cause issues with surface-based acoustic surveys.

Table 2-8: Physical Characteristics: Virginia WEA

| Virginia Wind Energy Area | | | | | | | | | | | | | | |
|---|---|------------|-----------|-----------|-------------|-----------------------|-----------|-----------|-----------|-----------|----------|---|--|--|
| General Description | | | | | | | | | | | | Data Source(s) | | |
| Area (sq. km) | | | | | | 456.83 | | | | | | Bureau of Ocean Energy Management 2016 | | |
| Lease Blocks | | | | | | 32 | | | | | | | | |
| Sediment Description | | | | | | | | | | | | | | |
| Wentworth (1922) Scale | Silts | Sandy Silt | Fine Sand | Med Sand | Coarse Sand | Coarse Sand w/ Gravel | | | | | | See U.S. Geological Survey and University of Colorado 2005, ATL_PRS: usSEABED PaRSed data for point sediment sample data; The Nature Conservancy 2016 | | |
| Sediment Distribution (% area) | 1.42 | 6.13 | 8.12 | 8.09 | 0.89 | 75.34 | | | | | | | | |
| Bathymetric Description | | | | | | | | | | | | | | |
| Bathymetric Relief | Ridge and Swale in SW, Gentle Slopes NE | | | | | | | | | | | National Oceanic and Atmospheric Administration 2016d | | |
| Depth Range | 18 - 40 m | | | | | | | | | | | | | |
| Depth Distribution (%) | 0 - 5 m | 5 - 10 m | 10 - 15 m | 15 - 20 m | 20 - 25 m | 25 - 30 m | 30 - 35 m | 35 - 40 m | 40 - 45 m | 45 - 50 m | 50 - 55m | > 55m | Interpreted from: Coastal Relief Model - National Oceanic and Atmospheric Administration 2016d | |
| | 0.000 | 0.000 | 0.000 | 0.080 | 11.318 | 57.099 | 28.959 | 2.543 | 0.000 | 0.000 | 0.000 | 0.000 | | |
| Seasonal Description | | | | | | | | | | | | | | |
| Season | Winter | | | Spring | | | Summer | | | Fall | | | The Nature Conservancy 2016 | |
| Avg. Sea Surface Temperature (°C) | 7.89 | | | 9.00 | | | 10.57 | | | 12.44 | | | | |
| Stratification (kg/m ³) (Difference in density from surface to depth) | 0.30 | | | 2.11 | | | 2.74 | | | 0.37 | | | | |
| Wave Climate Description* | | | | | | | | | | | | | | |
| Month | January | February | March | April | May | June | July | August | September | October | November | December | *from Buoy 44099 only | |
| Avg. Significant Wave Height (m) | 1.00 | 1.04 | 1.13 | 1.00 | 0.93 | 0.80 | 0.79 | 0.82 | 1.12 | 1.12 | 1.21 | 1.07 | | |
| Avg. Wave Period (s) | 7.10 | 7.70 | 8.58 | 7.87 | 7.75 | 7.63 | 8.01 | 8.47 | 8.96 | 8.05 | 7.98 | 8.20 | National Oceanic and Atmospheric Administration 2016c (Station(s) 44093, 44099) | |
| Avg. Wave Direction (° from North) | 125.34 | 120.70 | 102.00 | 111.09 | 112.96 | 112.17 | 118.93 | 109.12 | 99.71 | 111.92 | 107.42 | 114.41 | | |

The Virginia WEA consists of nearly 457 km². The bathymetry, which ranges from 18 to 40 m, is largely variable with ridge and swale topography in the western blocks, shifting to gentle slopes on the eastern blocks. Sediment is dominated by coarse sands with gravels, which may pose issues with object detection in acoustic surveys due to high acoustic reflectivity. Although with slightly lower historical wave height, the strong seasonal pattern remains, with higher wave heights recorded from September – March. Further south, hurricanes and extra-tropical storms are the dominant large-wave events, and the shift earlier for periods of higher wave height reflects the timing of hurricane season (August – November). The water column again becomes highly stratified during the spring and summer seasons, which must be taken into account with surface-based acoustic surveys.

Table 2-9: Physical Characteristics: North Carolina Kitty Hawk WEA

| North Carolina Kitty Hawk Wind Energy Area | | | | | | | | | | | | | | |
|---|-----------------------------------|------------|-----------|-----------|-------------|-----------------------|---|-----------|-----------|-----------|----------------|---|--|--|
| General Description | | | | | | | | | | | Data Source(s) | | | |
| Area (sq. km) | | | | | | 500.08 | | | | | | Bureau of Ocean Energy Management 2016 | | |
| Lease Blocks | | | | | | 77 | | | | | | | | |
| Sediment Description | | | | | | | | | | | | | | |
| Wentworth (1922) Scale | Silts | Sandy Silt | Fine Sand | Med Sand | Coarse Sand | Coarse Sand w/ Gravel | See U.S. Geological Survey and University of Colorado 2005, ATL_PRS: usSEABED PaRSed data for point sediment sample data; The Nature Conservency 2016 | | | | | | | |
| Sediment Distribution (% area) | 0.00 | 11.58 | 20.32 | 59.05 | 6.33 | 2.72 | | | | | | | | |
| Bathymetric Description | | | | | | | | | | | | | | |
| Bathymetric Relief | Gentle Slope W, Ridge and Swale E | | | | | | | | | | | National Oceanic and Atmospheric Administration 2016d | | |
| Depth Range | 11 - 48 m | | | | | | | | | | | | | |
| Depth Distribution (%) | 0 - 5 m | 5 - 10 m | 10 - 15 m | 15 - 20 m | 20 - 25 m | 25 - 30 m | 30 - 35 m | 35 - 40 m | 40 - 45 m | 45 - 50 m | 50 - 55m | > 55m | Interpreted from: Coastal Relief Model - National Oceanic and Atmospheric Administration 2016d | |
| | 0.000 | 0.000 | 0.001 | 0.008 | 0.036 | 9.895 | 35.902 | 39.882 | 14.009 | 0.266 | 0.000 | 0.000 | | |
| Seasonal Description | | | | | | | | | | | | | | |
| Season | Winter | | | Spring | | | Summer | | | Fall | | | The Nature Conservency 2016 | |
| Avg. Sea Surface Temperature (°C) | 8.82 | | | 8.80 | | | 10.27 | | | 12.24 | | | | |
| Stratification (kg/m ³) (Difference in density from surface to depth) | 0.25 | | | 1.74 | | | 3.04 | | | 0.39 | | | | |
| Wave Climate Description | | | | | | | | | | | | | | |
| Month | January | February | March | April | May | June | July | August | September | October | November | December | National Oceanic and Atmospheric Administration 2016c (Station 44100) | |
| Avg. Significant Wave Height (m) | 1.22 | 1.33 | 1.52 | 1.19 | 1.04 | 0.84 | 0.82 | 0.89 | 1.36 | 1.29 | 1.49 | 1.34 | | |
| Avg. Wave Period (s) | 7.86 | 8.16 | 9.22 | 8.54 | 7.88 | 8.08 | 8.22 | 8.35 | 8.98 | 8.28 | 8.27 | 8.75 | | |
| Avg. Wave Direction (° from North) | 99.96 | 96.02 | 85.09 | 102.67 | 105.56 | 106.36 | 115.22 | 104.20 | 90.90 | 96.90 | 87.06 | 87.85 | | |

The North Carolina Kitty Hawk WEA is a 500 km² area. It is characterized by gentle sloping topography in the in the west, giving way to ridge and swale topography the in the deeper eastern lease blocks. The sediment is largely fine to medium non-cohesive sands. As with the Virginia WEA, wave height increases during the September – March period, with strong stratification during the spring and summer seasons. Stratification must be addressed when conducting surface-based acoustic surveys, usually through water column sound speed profiles. Hurricanes and extra-tropical storms are experienced in this region from August – November.

Table 2-10: Physical Characteristics: North Carolina Wilmington West WEA

| North Carolina Wilmington West Wind Energy Area | | | | | | | | | | | | | | |
|---|--------------------------------------|------------|-----------|-----------|-------------|-----------------------|-----------|-----------|-----------|-----------|----------|---|--|--|
| General Description | | | | | | | | | | | | Data Source(s) | | |
| Area (sq. km) | | | | | | 208.95 | | | | | | Bureau of Ocean Energy Management 2016 | | |
| Lease Blocks | | | | | | 85 | | | | | | | | |
| Sediment Description | | | | | | | | | | | | | | |
| Wentworth (1922) Scale | Silts | Sandy Silt | Fine Sand | Med Sand | Coarse Sand | Coarse Sand w/ Gravel | | | | | | | See U.S. Geological Survey and University of Colorado 2005, ATL_PRS: usSEABED PaRSed data for point sediment sample data | |
| Sediment Distribution (% area) | N/A | N/A | N/A | N/A | N/A | N/A | | | | | | | | |
| Bathymetric Description | | | | | | | | | | | | | | |
| Bathymetric Relief | Shoaler in N and E, Depression in SW | | | | | | | | | | | National Oceanic and Atmospheric Administration 2016d | | |
| Depth Range | 13 - 21 m | | | | | | | | | | | | | |
| Depth Distribution (%) | 0 - 5 m | 5 - 10 m | 10 - 15 m | 15 - 20 m | 20 - 25 m | 25 - 30 m | 30 - 35 m | 35 - 40 m | 40 - 45 m | 45 - 50 m | 50 - 55m | > 55m | Interpreted from: Coastal Relief Model - National Oceanic and Atmospheric Administration 2016d | |
| | | 0.000 | 0.000 | 6.231 | 93.287 | 0.483 | 0.000 | 0.000 | 0.000 | 0.000 | 0.000 | 0.000 | | |
| Seasonal Description | | | | | | | | | | | | | | |
| Season | Winter | | | Spring | | | Summer | | | Fall | | | The Nature Conservancy 2016 | |
| Avg. Sea Surface Temperature (°C) | 17.19 | | | 20.93 | | | 27.27 | | | 22.39 | | | | |
| Stratification (kg/m ³) (Difference in density from surface to depth) | 0.08 | | | 0.30 | | | 0.23 | | | 0.11 | | | | |
| Wave Climate Description* | | | | | | | | | | | | | | |
| Month | January | February | March | April | May | June | July | August | September | October | November | December | *only 2013-2015 | |
| Avg. Significant Wave Height (m) | 1.11 | 1.13 | 1.04 | 1.04 | 1.01 | 1.08 | 1.01 | 0.88 | 0.91 | 0.88 | 1.03 | 0.97 | National Oceanic and Atmospheric Administration 2016c (Station 41108) | |
| Avg. Wave Period (s) | 6.99 | 7.35 | 7.29 | 6.76 | 6.82 | 6.20 | 6.23 | 6.68 | 6.77 | 7.66 | 7.17 | 7.95 | | |
| Avg. Wave Direction (° from North) | 166.58 | 154.04 | 159.64 | 142.39 | 152.10 | 170.75 | 168.83 | 151.10 | 132.55 | 145.24 | 140.43 | 144.63 | | |

The North Carolina Wilmington West WEA is a smaller, shallower WEA, encompassing only 209 km² and ranging from 13 to 21 m deep. The northern blocks are shallower, with a slight depression in the southern blocks. Sediment distribution data is not available for this region, although point sediment sample data is available through the USGS (Table 2-10). Wave climate, although only available locally from 2013 – present, suggests fairly calm wave conditions year round. However, this region does experience hurricane and extra-tropical storm events from August – November. The area does not experience strong seasonal stratification, and combined with the shallow bathymetry, is well suited for surface-based acoustic surveying.

Table 2-11: Physical Characteristics: North Carolina Wilmington East WEA

| North Carolina Wilmington East Wind Energy Area | | | | | | | | | | | | | |
|---|--|------------|-----------|-----------|-------------|-----------------------|-----------|-----------|-----------|-----------|----------------|---|--|
| General Description | | | | | | | | | | | Data Source(s) | | |
| Area (sq. km) | | | | | | 540.63 | | | | | | Bureau of Ocean Energy Management 2016 | |
| Lease Blocks | | | | | | 165 | | | | | | | |
| Sediment Description | | | | | | | | | | | | | |
| Wentworth (1922) Scale | Silts | Sandy Silt | Fine Sand | Med Sand | Coarse Sand | Coarse Sand w/ Gravel | | | | | | | See U.S. Geological Survey and University of Colorado 2005, ATL_PRS: usSEABED PaRSed data for point sediment sample data |
| Sediment Distribution (% area) | N/A | N/A | N/A | N/A | N/A | N/A | | | | | | | |
| Bathymetric Description | | | | | | | | | | | | | |
| Bathymetric Relief | Shallow Ridge and Swale NW, Gentle Slope to SE | | | | | | | | | | | National Oceanic and Atmospheric Administration 2016d | |
| Depth Range | 8-31 m | | | | | | | | | | | | |
| Depth Distribution (%) | 0 - 5 m | 5 - 10 m | 10 - 15 m | 15 - 20 m | 20 - 25 m | 25 - 30 m | 30 - 35 m | 35 - 40 m | 40 - 45 m | 45 - 50 m | 50 - 55m | > 55m | Interpreted from: Coastal Relief Model - National Oceanic and Atmospheric Administration 2016d |
| | | 0.000 | 0.001 | 0.003 | 2.582 | 25.221 | 66.939 | 5.254 | 0.000 | 0.000 | 0.000 | 0.000 | |
| Seasonal Description | | | | | | | | | | | | | |
| Season | Winter | | | Spring | | | Summer | | | Fall | | | The Nature Conservancy 2016 |
| Avg. Sea Surface Temperature (°C) | 18.08 | | | 15.99 | | | 26.88 | | | 22.92 | | | |
| Stratification (kg/m ³) (Difference in density from surface to depth) | 0.10 | | | 0.41 | | | 0.59 | | | 0.20 | | | |
| Wave Climate Description | | | | | | | | | | | | | |
| Month | January | February | March | April | May | June | July | August | September | October | November | December | National Oceanic and Atmospheric Administration 2016c (Station 41013) |
| Avg. Significant Wave Height (m) | 1.44 | 1.49 | 1.51 | 1.38 | 1.26 | 1.06 | 1.07 | 1.02 | 1.40 | 1.34 | 1.51 | 1.50 | |
| Avg. Wave Period (s) | 7.19 | 7.35 | 7.82 | 7.48 | 7.28 | 6.76 | 6.87 | 7.37 | 8.62 | 7.75 | 7.82 | 7.84 | |
| Avg. Wave Direction (° from North) | 152.61 | 147.00 | 136.94 | 137.23 | 134.85 | 153.65 | 151.40 | 139.39 | 115.96 | 124.34 | 124.63 | 137.83 | |

The North Carolina Wilmington East WEA is larger and deeper than the North Carolina Wilmington West WEA, encompassing over 540 km² and ranging from 8 to 31 m deep. The NW blocks are shallower, with ridge and swale topography, while the remaining blocks slope to the SE. Sediment distribution data is also not available for this region, although point sediment sample data is available through the USGS (Table 2-11). Wave climate shows a seasonal pattern of higher wave heights during September – April, with this region experiencing hurricane and extra-tropical storm events from August – November. This area does not experience strong seasonal stratification.

Page Intentionally Left Blank.

3.0 Munitions near the Atlantic OCS WEAs

In support of BOEM's UXO Survey Methodology Investigation, CALIBRE conducted historical research and mapping relating to MEC potentially present in the Atlantic OCS WEAs. This section presents a summary of the findings from the historical research.

Existing sources of information provide a wealth of relevant data that aid in planning investigation activities. CALIBRE reviewed documents available from the National Archives and Records Administration, Department of Defense (DoD), and various other Government sources relating to ranges, coastal defense, sea disposals, and known MEC discoveries on or close to the Atlantic OCS WEAs to identify other areas of potential concern. Additional resources utilized include the U.S. Army Corps of Engineers Formerly Used Defense Sites (FUDS) [website](#) (U.S. Army Corps of Engineers 2013a), NOAA Historical Map and Chart Collection [website](#) (National Oceanic and Atmospheric Administration 2016a), and the FortWiki Harbor Defense [Portal](#) (Harbor Defense Portal 2015).

To the extent practical, MEC related information relevant to the Atlantic OCS WEAs was mapped. This included newly identified sea disposal and MEC activities, range fans for FUDS, and coastal defense sites within a 10-nautical mile radius of each Atlantic OCS WEA and between the OCS WEA and the nearest shore (e.g., Massachusetts WEA export cable is assumed to make landfall to the north of the site at Martha's Vineyard or Nantucket). A significant amount of the documentation reviewed concerning MEC related activities does not include coordinates and reports such information without an exact location. When no location information was available, the munitions were not included in the tables.

As expected, a variety of munitions may be present in each of the WEAs. However, the exact type and quantity of munitions present as reported in this report is likely to be incomplete. The data provided should be considered a starting point for further research that would be required prior to development of the WEAs.

3.1 MEC Research Findings

Table 3-1 through Table 3-10 summarize the findings relating to each Atlantic OCS WEA identified through historical research that are within a 10-nautical mile radius of each Atlantic OCS WEA and between the OCS WEA and shore. Figure 3-1 through Figure 3-14 show the Atlantic OCS WEAs and the MEC related sites identified in the vicinity. Information on FUDS was somewhat difficult to obtain but further details would be available through a Freedom of Information Act request to the U.S. Army Corps of Engineers on specific FUDS properties. Information on MEC related to FUDS near the Delaware WEA, the site for the in-field verification, is complete. Locations of the WEAs and related MEC findings are summarized in the figures that follow.

Although information on combat operations along the Atlantic Coast is available, little was found that identified coordinates where munitions may be present. Thus, anti-submarine munitions, mines, and torpedoes may be present due to combat but documentation is not readily reviewable and therefore it is possible that these munitions may be present in the WEAs.

3.2 MEC Conclusions

CALIBRE conducted intensive historical research, including reviewing documents and resources from the National Archives and Records Administration, DoD, U.S. Army Corps of Engineers FUDS data, NOAA historical maps and charts, and public resources such as the FortWiki Harbor Defense Portal (Harbor Defense Portal 2015). Findings from this research effort indicate that a variety of MEC are potentially present at the WEAs. Additionally, naval warfare activities were conducted in the vicinity of the Atlantic OCS WEAs during both World War I and World War II, including German U-boat attacks and anti-submarine activities (such as the deployment of depth charges, depth bombs, and mines). Given the limited number of mines deployed by German U-boats in the areas near the WEAs between 1918 and 1942, knowledge of their activities and minesweeping activities, it is likely that these mines have been recovered or destroyed. In addition, it is believed that all of the controlled-mine-system mines (mines controlled from shore through cables) associated with harbor defense were removed following the World Wars. However, anti-submarine operations may have resulted in the presence of a variety of munitions. It is highly unlikely that all munitions related activities surrounding the Atlantic Ocean WEAs have been identified; additional munitions are likely to be present in the vicinity.

Table 3-1: Historical Research Results: Cape WEA

| Location | MEC | Description | Source |
|--|-------------------------------|---|---|
| Cape – Sites Near WEA | | | |
| MA-WEA-01 Nantucket Sound/Horseshoe Shoal, MA Polygon Coordinates: Latitude: 41°31'12"N Longitude: 71°22'58"W Latitude: 41°31'12"N Longitude: 70°21'38"W Latitude: 41°30'12"N Longitude: 70°22'58"W Latitude: 41°30'12"N Longitude: 70°22'38"W Center of Area: Latitude: 41°30'42"N Longitude: 70°22'18"W | Unknown (assumed to be bombs) | Naval bombing target area in Nantucket Sound, Horseshoe Shoal area. Area is one square mile. | (U.S. Navy 1948) |
| Cape – Sites Between WEA and Shore | | | |
| MA-WEA-02 Nantucket Sound/Bass River, MA Area is a circle with 2-mile radius centered at: Latitude: 41°38'18"N Longitude: 70°10'18"W | Unknown (assumed to be bombs) | Masthead bombing near Bass River/Nantucket Sound areas. Bombing target on breakwater. | (U.S. Navy 1946c) (U.S. Navy 1947a) |
| FUDS# D01MA0450 Mashpee, MA Latitude: 41°33'15"N Longitude: 70°30'32"W | Unknown (assumed to be bombs) | Practice bombing target area at Great Neck for the U.S. Naval Air Station at Quonset Point, RI. | (U.S. Navy 1944a) (U.S. Army Corps of Engineers 2013a) |

Table 3-2: Historical Research Results: Massachusetts WEA

| Location | MEC | Description | Source |
|---|---|---|---|
| Massachusetts - Sites Near WEA | | | |
| MA-03 Polygon Coordinates: Latitude: 40°40'N Longitude: 70°45'W Latitude: 40°40° Longitude: 71°00'W Latitude: 40°50'N Longitude: 70°45'W Latitude: 40°50'N Longitude: 71°00'W | Unexploded bombs may exist, other munitions are possible | Area 13A/Emergency Bomb Jettisoning. Established in 1946 as an emergency bomb jettisoning area. 1952 Fleet Guide identifies as a "General Dumping Area, formerly an Explosives Dumping Area". Site is annotated as disused in 1959 NRC Report suggesting its use for radioactive disposal area. No confirmation of civilian use. Nautical Charts 13003 and 12300 list as "Dumping Area Caution". | (National Research Council 1959) (National Oceanic and Atmospheric Administration 2016f) (National Oceanic and Atmospheric Administration 2016e) (U.S. Coast Guard 1946) |
| MA-07 Polygon Coordinates: Latitude: 40°43.5'N Longitude: 71°00.0'W Latitude: 40°43.5'N Longitude: 70°55.5'W Latitude: 40°40'N Longitude: 71°00.0'W Latitude: 40°40'N Longitude: 70°55.5'W | Unknown | Narragansett Bay dumping area for "sinkable objects". Note that "sinkable objects" is not defined, but is thought to consist of debris. | (U.S. Navy 1953) |
| Massachusetts – Sites Between WEA and Shore | | | |
| MA-WEA-03 No Man's Land Island, MA Area is a circle with 3-mile radius centered at: Latitude: 41°14'N Longitude: 70°49'W Also described as Latitude: 41°16'00"N Longitude: 70°47'30"W Latitude: 41°12'30"N Longitude: 70°47'30"W Latitude: 41°12'00"N Longitude: 70°50'30"W Latitude: 41°16'00"N Longitude: 70°50'30"W | Explosives: 500 pound (lb.) General purpose bombs 5"/38 Projectiles 20 mm Ammunition Small Arms: 50 Caliber ball Pyrotechnic: Parachute flares Other: Miniature practice bombs Water/sand-filled bombs 5-inch Rockets, inert | Rocket projectile, strafing, and dive-bomb activity around No Man's Land Island. | (U.S. Navy 1946c) (Secretary of War 1944) (U.S. Navy 1976) |

| Location | MEC | Description | Source |
|--|---|---|---|
| Massachusetts – Sites Between WEA and Shore (Continued) | | | |
| <p>FUDS# D01MA0453 West Tisbury, MA</p> <p>Area is a circle with 2-mile radius centered at: Latitude: 41°20'48"N Longitude: 70°39'06"W</p> | <p>Munitions practice ordnance potentially used include:</p> <p>Small Arms: 0.30 and 0.50 caliber</p> <p>Other: Miniature Practice Bombs, AN-MK5 Mod 1; AN-MK23; AN-MK43; General Purpose Practice Bombs (100-500 lb), MK5, MK15, MK21</p> | <p>Practice dive bombing and strafing range at Tisbury Great Pond Munitions Response Area. This range was in use between 1943 and 1947.</p> | <p>(U.S. Navy 1946c)</p> <p>(U.S. Army Corps of Engineers 2015d)</p> <p>(U.S. Army Corps of Engineers 2013a)</p> |
| <p>FUDS# D01MA0486</p> <p>Latitude: 41°17'40"N Longitude: 70°31'09"W</p> | <p>Pyrotechnic: Flare, aircraft, parachute, M26 & AN-M26</p> <p>Other: Miniature practice bombs, AN-MK5 Mod 1, AN-MK23, AN-MK43 100-pound practice bombs, AN-MK15; Signal practice bombs, AN-MK4 Mods 3 & 4; AN-MK6 Mod 0</p> | <p>Moving target machine gun range and rocket targets at the South Beach Gunnery Training Facility during World War II.</p> | <p>(U.S. Army Corps of Engineers 2014b)</p> <p>(U.S. Army Corps of Engineers 2015c)</p> <p>(U.S. Army Corps of Engineers 2013a)</p> |
| <p>FUDS# D01MA0455 Nantucket, MA</p> | <p>Unknown</p> | <p>Sheep Pond bombing area used was between 1944 and 1946. The Navy acquired the site to use as a bombing range in conjunction with the adjacent Hummock Pond Bombing area.</p> | <p>(U.S. Army Corps of Engineers 2013a)</p> |
| <p>FUDS# D01MA0456 Nantucket, MA</p> | <p>Rockets: 5-inch high velocity aircraft rockets (HVARs) 3.5-inch forward firing aircraft rockets (FFARs) 2.25-inch subcaliber aircraft rockets (SCARs)</p> | <p>U.S. Navy conducted air-to-ground military training exercises with aerial rockets at the former Nantucket Beach range during WWII.</p> | <p>(U.S. Army Corps of Engineers 2014a)</p> <p>(U.S. Army Corps of Engineers 2015a)</p> <p>(U.S. Army Corps of Engineers 2013a)</p> |
| <p>RI-WEA-07</p> <p>Latitude: 41°05'26"N Longitude: 70°51'56"W</p> | <p>Reported UXO, Unknown</p> | <p>Explosives dumping ground</p> | <p>(National Oceanic and Atmospheric Administration 2016b)</p> |

Table 3-3: Historical Research Results: Rhode Island/Massachusetts WEA

| Location | MEC | Description | Source |
|---|----------------------------------|--------------------------------------|---|
| Rhode Island/Massachusetts – Sites Near WEA | | | |
| RI-WEA-01 Latitude: 41°13'48"N Longitude: 71°19'08"W Position approximate | Unexploded Depth Charge, Unknown | Explosives dumping ground | (National Oceanic and Atmospheric Administration 2016b) |
| RI-WEA-02 Latitude: 41°17'02"N Longitude: 71°04'W | Unexploded Depth Charge, Unknown | Explosives dumping ground | (National Oceanic and Atmospheric Administration 2016b) |
| RI-WEA-03 Latitude: 41°14'12"N Longitude: 71°12'35"W | Unexploded Depth Charge, Unknown | Explosives dumping ground | (National Oceanic and Atmospheric Administration 2016b) |
| RI-WEA-04 Latitude: 41°14'06"N Longitude: 71°24'59"W | Unexploded Depth Charge, Unknown | Explosives dumping ground | (National Oceanic and Atmospheric Administration 2016b) |
| RI-WEA-05 Latitude: 41°06'59"N Longitude: 71°17'57"W | Unexploded Bombs, Unknown | Explosives dumping ground | (National Oceanic and Atmospheric Administration 2016b) |
| RI-WEA-06 Polygon Coordinates: Latitude: 41°12'N Longitude: 71°05'58"W Latitude: 41°12'N Longitude: 71°03'31"W Latitude: 41°10'N Longitude: 71°05'58"W Latitude: 41°10'N Longitude: 71°03'31"W | UXO, Unknown | Explosives dumping ground | (National Oceanic and Atmospheric Administration 2016b) |
| RI-WEA-07 Latitude: 41°05'26"N Longitude: 70°51'56"W | Reported UXO, Unknown | Explosives dumping ground | (National Oceanic and Atmospheric Administration 2016b) |
| RI-WEA-08 Narragansett Bay, RI Polygon coordinates: Latitude: 41°27'N Longitude: 71°23'W Latitude: 41°27'N Longitude: 71°25'W Latitude: 41°17'N Longitude: 71°23'W Latitude: 41°17'N Longitude: 71°25'W | Torpedoes | Narragansett Bay Outer Torpedo range | (U.S. Navy 1946c) (U.S. Navy 1947a) |

| Location | MEC | Description | Source |
|--|--|--|---|
| Rhode Island/Massachusetts – Sites Near WEA (Continued) | | | |
| FUDS# C02NY0024 Suffolk County, NY | Large Caliber: 16-inch Rifle 6-inch Rifle | Camp Hero. Coastal defense site for Long Island Sound area. Deactivated as coastal fort in 1949. | (U.S. Army 1945b) (U.S. Army Corps of Engineers 2013a) (Berhow 2015, 208) |
| FUDS# D01RI0333 Narragansett, RI | Small Arms: .50 caliber and smaller Large Caliber: 16-inch Rifle 6-inch, AP (Shot), M1911 1.457-inch, TP, subcaliber 155 mm, HE, MKI | Fort Nathaniel Greene. Coastal defense site for Narragansett Bay area. Deactivated as coastal fort in 1948. | (U.S. Army 1945c) (U.S. Army Corps of Engineers 2013a) (Berhow 2015, 207) |
| RI-01 Latitude: 41°12'N Longitude: 71°12'W | Fuzes | Site appears to be a single use. | (U.S. Naval Air Station 1945) |
| Rhode Island/Massachusetts – Sites Between WEA and Shore | | | |
| RI-WEA-09 Jamestown, RI | Large Caliber: 16-inch Rifle 6-inch Rifle 3-inch Rifle | Fort Burnside. Coastal defense site for Narragansett Bay area. Deactivated as coastal fort in 1948. | (U.S. Army 1945c) (Berhow 2015, 207) |
| FUDS# D01RI0041 Newport, RI Area covered by the segment between the bearings of 135° and 215° true, of a circle of 10,000 yards radius centered in: Latitude: 41°28'24"N Longitude: 71°14'48"W | Unknown | Restricted area established over the field of fire of a gunnery range near Sachuest Point, south of Newport, RI. | (U.S. Navy 1945a) (U.S. Army Corps of Engineers 2013a) |
| MA-WEA-03 No Man's Land Island, MA Area is a circle with 3-mile radius centered at: Latitude: 41°14'N Longitude: 70°49'W | Explosives: 500 lb. General purpose bombs 5"/38 Projectiles 20 mm Ammunition Small Arms: .50 Caliber ball Pyrotechnic: Parachute flares Other: Miniature practice bombs Water/sand-filled bombs 5-inch Rockets, inert | Rocket projectile, strafing, and dive-bomb activity around No Man's Land Island. | (U.S. Navy 1946c) (U.S. Navy 1947b) (U.S. Navy 1976) (National Oceanic and Atmospheric Administration 2016e) |

| Location | MEC | Description | Source |
|---|---|---|--|
| Rhode Island/Massachusetts – Sites Between WEA and Shore (Continued) | | | |
| FUDS# D01MA0569 Gull Island, MA Area is a circle with 2-mile radius centered at: Latitude: 41°26'48"N Longitude: 70°54'24"W | Unknown | Dive & high altitude bombing activities at Gull Island near Gull Island. 1947 reference describes as a practice bombing water target, rock at northern end of small sand spit. | (U.S. Navy 1946c) (U.S. Navy 1947a) (U.S. Army Corps of Engineers 2013a) |
| FUDS# D01MA0544 Dukes County, MA | Unknown (Commonly 90 mm Rifle) | Anti-motor torpedo boat | (U.S. Army Corps of Engineers 2013a) |
| FUDS# D01MA0507 Dartmouth, MA | 90 mm Rifle | Barneys Joy Battery | (U.S. Army Corps of Engineers 2013a) (Coast Defense Study Group 2013) |
| FUDS# C02NY0024 Suffolk County, NY | Large Caliber: 16-inch Rifle 6-inch Rifle | Camp Hero. Coastal defense site for Long Island Sound area. Deactivated as coastal fort in 1949. | (U.S. Army 1945b) (U.S. Army Corps of Engineers 2013a) |
| FUDS# D01RI0044 Newport, RI Price's Neck Restricted Area Location: Area covered by the segment between the bearings of 130° and 180° true, of a circle of 15,000 yards radius centered in: Latitude: 41°27'N Longitude: 71°20'15"W | Large Caliber: 12-inch Mortar 10-inch Rifle 8-inch Rifle 6-inch Rifle 4.7-inch Rifle 3-inch Rifle 90 mm Rifle | Fort Adams. Coastal defense site for Narragansett Bay area. Deactivated as coastal fort in 1943. Included a restricted area established over the field of fire of a gunnery range near Price's Neck, south of Newport, RI. | (U.S. Army 1945c) (U.S. Navy 1945a) (U.S. Army Corps of Engineers 2013a) (Berhow 2015, 207) |
| FUDS# D01RI0331 Little Compton, RI | Large Caliber: 16-inch Rifle 8-inch Rifle 6-inch Rifle 155 mm | Fort Church. Coastal defense site for Narragansett Bay area. Deactivated as coastal fort in 1948. | (U.S. Army 1945c) (U.S. Army Corps of Engineers 2013a) (Berhow 2015, 206) |
| FUDS# D01RI0333 Narragansett, RI | Large Caliber: 16-inch Rifle 6-inch Rifle | Fort Nathaniel Greene. Coastal defense site for Narragansett Bay area. Deactivated as coastal fort in 1948. | (U.S. Army 1945c) (U.S. Army Corps of Engineers 2013a) |
| FUDS# D01MA0513 New Bedford, MA | Large Caliber: 12-inch Rifle 8-inch Rifle 6-inch Rifle 5-inch Rifle 3-inch Rifle 155 mm 90 mm Rifle | Fort Rodman | (U.S. Army Corps of Engineers 2013a) (Harbor Defense Portal 2015) (Berhow 2015, 206) |

| Location | MEC | Description | Source |
|---|--|---|---|
| Rhode Island/Massachusetts – Sites Between WEA and Shore (Continued) | | | |
| FUDS# D01RI0335 Narragansett, RI | Large Caliber: 6-inch Rifle 3-inch Rifle 90 mm Rifle | Fort Varnum. Coastal defense site for Narragansett Bay area. Deactivated as coastal fort in 1947. | (U.S. Army 1945c) (U.S. Army Corps of Engineers 2013a) (Berhow 2015, 207) |

Table 3-4: Historical Research Results: New York WEA

| Location | MEC | Description | Source |
|--|--|--|--|
| New York – Sites Near WEA | | | |
| AC-02 | Chemical munitions: 75 mm Projectiles Other: Bulk Chemical Agent (bulk containers) | Loaded in Baltimore, MD and disposed of at sea from the <i>U.S.S. Elinor</i> . Newspaper reports indicate disposal of 2,100 tons including 200,000 75 mm mustard projectiles. Government records indicate 75 mm shells, gas drums, phosgene drums, mustard projectiles. <i>U.S.S. Elinor</i> completed disposal of mustard-filled projectiles in this vicinity. Refer to map for projected track for disposal. | (U.S. Navy 1919) (Carton, Cioffi and Overfield 2009) |
| NJ-X02 Dumping ground for explosives described as 15 to 25 nautical miles (nmi) SE of Scotland Lightship (40°26'30"N, 73°55'15"W) | Unknown | Established in 1926, but several disposals are reported to have occurred earlier. Anecdotal report that grenades were recovered in this general area. | (Robins 1926) Location of Lightship from (National Oceanic and Atmospheric Administration 1926) |
| NY-WEA-01 Corners at: 40°36'00"N, 73°15'00"W 40°49'00"N, 72°30'00"W 40°00'00"N, 72°30'00"W 40°00'00"N, 73°15'00"W | Unknown | AS3D Air-to-Air gunnery and bombing area. | (U.S. Navy 1947a) |
| FUDS# C02NY0016 Rockaway, NY | Large Caliber: 16-inch Rifle 12-inch Rifle 6-inch Rifle 3-inch Rifle 90 mm Rifle | Fort Tilden. Coastal defense site for Southern New York area. Deactivated as coastal fort in 1948. | (U.S. Army 1944) (U.S. Army Corps of Engineers 2013a) (Berhow 2015, 209) |

| Location | MEC | Description | Source |
|--|--|--|--|
| New York – Sites Between WEA and Shore | | | |
| AC-02 | Chemical munitions: 75 mm Projectiles Other: Bulk Chemical Agent (bulk containers) | Loaded in Baltimore, MD and disposed of at sea from the <i>U.S.S. Elinor</i> . Newspaper reports indicate disposal of 2,100 tons including 200,000 75 mm mustard projectiles. Government records indicate 75 mm shells, gas drums, phosgene drums, mustard projectiles. <i>U.S.S. Elinor</i> completed disposal of mustard-filled projectiles in this vicinity. Refer to map for projected track for disposal. | (U.S. Navy 1919) (Carton, Ciolfi and Overfield 2009) |
| NJ-X02 Dumping ground for explosives described as 15 to 25 nmi SE of Scotland Lightship (40°26'30"N, 73°55'15"W) | Unknown | Established in 1926, but several disposals are reported to have occurred earlier. Anecdotal report that grenades were recovered in this general area. | (Robins 1926) Location of Lightship from (National Oceanic and Atmospheric Administration 1926) |
| NY-WEA-01 Corners at: 40°36'00"N, 73°15'00"W 40°49'00"N, 72°30'00"W 40°00'00"N, 72°30'00"W 40°00'00"N, 73°15'00"W | Unknown | AS3D Air-to-Air gunnery and bombing area. | (U.S. Navy 1947a) |
| NY-WEA-02 | Unknown | Explosive Jettisoned 1952 | (National Oceanic and Atmospheric Administration 2016h) |
| FUDS# C02NY0016 Rockaway, NY | Large Caliber: 16-inch Rifle 12-inch Rifle 6-inch Rifle 3-inch Rifle 90 mm Rifle | Fort Tilden. Coastal defense site for Southern New York area. Deactivated as coastal fort in 1948. | (U.S. Army 1944) (U.S. Army Corps of Engineers 2013a) (Berhow 2015, 209) |

Table 3-5: Historical Research Results: New Jersey WEA

| Location | MEC | Description | Source |
|---|---------|--|--|
| New Jersey – Sites Near WEA | | | |
| DE-001 Polygon Coordinates: Latitude: 39°0.8'N Longitude: 74°7.8'W Latitude: 38°50.5'N Longitude: 74°7.8'W Latitude: 38°50.5'N Longitude: 74°20.4'W Latitude: 39°0.8'N Longitude: 74°20.4'W | Unknown | Delaware Bay dumping area for “sinkable objects”. Note that “sinkable objects” is not defined, but is thought to consist of debris. | (U.S. Navy 1953) |
| NJ-WEA-01 Firing Danger Area | Unknown | Firing Danger Area | (National Oceanic and Atmospheric Administration 2016e) |
| NJ-WEA-02 Offshore Gunnery Area Corners at: 39°38'00"N 74°11'00"W 39°00'30"N 73°09'00"W 38°30'00"N 73°39'00"W 38°30'00"N 74°50'30"W 38°47'30"N 74°44'00"W 38°51'00"N 74°43'00"W 39°10'00"N 74°22'00"W 39°17'00"N 74°34'00"W | Unknown | Air-to-air gunnery and bombing area. | (U.S. Navy 1947a) |
| New Jersey – Sites Between WEA and Shore | | | |
| FUDS# C02NJ1011 Absecon, NJ Area is a circle with 3-mile radius centered at: Latitude: 39°26'48"N Longitude: 74°24'00"W | Bombs | Black Point Target served as a target area for bombing practice runs for Navy planes between 1944 and 1952. Identified as skip bombing. | (U.S. Navy 1946b) (U.S. Navy 1947a) (U.S. Army Corps of Engineers 2013a) |
| FUDS# C02NJ0993 Seaside Heights, NJ Area 10 miles seaward from: Latitude: 39°46'N Longitude: 74°06'W North along shoreline to: Latitude: 39°55'N Longitude: 74°04'30"W | Rockets | Island Beach Test Site used between 1944 and 1946 for development of propulsion system for jet-powered, anti-aircraft missiles which included use of five-inch rocket motors as boosters for the missiles. | (U.S. Navy 1945b) (U.S. Army Corps of Engineers 2013a) |

| Location | MEC | Description | Source |
|---|---------|--------------------------------------|-------------------|
| New Jersey – Sites Between WEA and Shore (Continued) | | | |
| NJ-WEA-02 Offshore Gunnery Area Corners at: 39°38'00"N 74°11'00"W 39°00'30"N 73°09'00"W 38°30'00"N 73°39'00"W 38°30'00"N 74°50'30"W 38°47'30"N 74°44'00"W 38°51'00"N 74°43'00"W 39°10'00"N 74°22'00"W 39°17'00"N 74°34'00"W | Unknown | Air-to-air gunnery and bombing area. | (U.S. Navy 1947a) |

Table 3-6: Historical Research Results: Delaware WEA

| Location | MEC | Description | Source |
|---|---|---|---|
| Delaware – Sites Near WEA | | | |
| DE-X01 Latitude: 38°30'N Longitude: 74°23'W | Large Caliber: 155 mm Shells, MK (MK number illegible, 500 units) | Dumped overboard at sea outside the three-mile limit on May 24, 1920. Location estimated based on hand plotting measurements. | (War Department 1920) |
| FUDS# C03DE0064 Bethany Beach, DE Polygon Coordinates: Latitude: 38°40'56"N Longitude: 74°50'26"W Latitude: 38°36'26"N Longitude: 74°45'3"W Latitude: 38°20'33"N Longitude: 74°48'59"W Latitude: 38°30'15"N Longitude: 75°02'60"W | Explosives: 40 mm, HE & HEI, MKII Small Arms: General Other: 3.25-inch Target Rocket, Practice, MK1 | Delaware Target Areas (1 of 2) | (U.S. Army Corps of Engineers 2010) (U.S. Army Corps of Engineers 2013a) |
| FUDS# C03DE0064 Bethany Beach, DE Polygon Coordinates: Latitude: 38°45'19"N Longitude: 75°01'19"W Latitude: 38°43'06"N Longitude: 74°57'26"W Latitude: 38°39'08"N Longitude: 74°55'25"W Latitude: 38°36'36"N Longitude: 74°57'19"W Latitude: 38°39'23"N Longitude: 75°03'52"W | Explosives: 120 mm, HE, M73 90 mm, HE, M71 and HE-T, M71A1 40 mm, HE & HEI, MKII 37 mm, HE (recovered during dredging) Small Arms: General .50 Caliber Machine Gun Other: 40 mm, Practice, M382 3.25-inch Target Rocket, Practice, MK1 | Delaware Target Areas (2 of 2) | (U.S. Army Corps of Engineers 2010) (U.S. Army Corps of Engineers 2013a) |
| NJ-WEA-02 Offshore Gunnery Area Corners at: 39°38'00"N 74°11'00"W 39°00'30"N 73°09'00"W 38°30'00"N 73°39'00"W 38°30'00"N 74°50'30"W 38°47'30"N 74°44'00"W 38°51'00"N 74°43'00"W 39°10'00"N 74°22'00"W 39°17'00"N 74°34'00"W | Unknown | Air-to-air gunnery and bombing area. | (U.S. Navy 1947a) |

| Location | MEC | Description | Source |
|---|---|--|--|
| Delaware – Sites Near WEA (Continued) | | | |
| FUDS# C03DE0063 Lewes, DE Range Fan Latitude: 38°47'10"N Longitude: 75°05'17"W | Explosives: 3-inch HE and Practice, M42 40 mm, AP-T M81 40 mm, HE-T, MKII 6-inch Complete Round 90 mm, HE, M71 155 mm Complete Round 8-inch, AP, MK19 12-inch AP, MK15 16-inch AP, MK5 Small Arms: General Other: 3.5-inch Rocket, Practice, M36 and M29A2 2.36-inch Rocket, Practice, M7 | Fort Miles. Coastal defense site for Delaware area. Deactivated as coastal fort in 1948. Range fans are for 6-inch guns. | (U.S. Army Corps of Engineers 2006) (U.S. Army Corps of Engineers 1997) (U.S. Army Corps of Engineers 2013a) (Berhow 2015, 211) |
| Delaware – Sites Between WEA and Shore | | | |
| FUDS# C03DE0064 Bethany Beach, DE Polygon Coordinates: Latitude: 38°40'56"N Longitude: 74°50'26"W Latitude: 38°36'26"N Longitude: 74°45'03"W Latitude: 38°20'33"N Longitude: 74°48'59"W Latitude: 38°30'15"N Longitude: 75°02'60"W | Explosives: 40 mm, HE & HEI, MKII Small Arms: General Other: 3.25-inch Target Rocket, Practice, MK1 | Delaware Target Areas (1 of 2) | (U.S. Army Corps of Engineers 2010) (U.S. Army Corps of Engineers 2013a) |
| FUDS# C03DE0064 Bethany Beach, DE Polygon Coordinates: Latitude: 38°45'19"N Longitude: 75°01'19"W Latitude: 38°43'06"N Longitude: 74°57'26"W Latitude: 38°39'08"N Longitude: 74°55'25"W Latitude: 38°36'36"N Longitude: 74°57'19"W Latitude: 38°39'23"N Longitude: 75°03'52"W | Explosives: 120 mm, HE, M73 90 mm, HE, M71 and HE-T, M71A1 40 mm, HE & HEI, MKII 37 mm, HE (recovered during dredging) Small Arms: General .50 Caliber Machine Gun Other: 40 mm, Practice, M382 3.25-inch Target Rocket, Practice, MK1 | Delaware Target Areas (2 of 2) | (U.S. Army Corps of Engineers 2010) (U.S. Army Corps of Engineers 2013a) |

| Location | MEC | Description | Source |
|--|---|---|---|
| Delaware – Sites Between WEA and Shore (Continued) | | | |
| <p>FUDS# C03DE0063 Lewes, DE</p> <p>Range Fan Latitude: 38°47'10"N Longitude: 75°05'17"W</p> | <p>Explosives: 3-inch HE and Practice, M42 40 mm, AP-T M81 40 mm, HE-T, MKII 6-inch Complete Round 90 mm, HE, M71 155 mm Complete Round 8-inch, AP, MK19 12-inch AP, MK15 16-inch AP, MK5 M4 Submarine Mine</p> <p>Small Arms: General</p> <p>Other: 3.5-inch Rocket, Practice, M36 and M29A2 2.36-inch Rocket, Practice, M7</p> | <p>Fort Miles. Coastal defense site for Delaware area. Deactivated as coastal fort in 1948. Range fans are for 6-inch guns.</p> | <p>(U.S. Army Corps of Engineers 2006)</p> <p>(U.S. Army Corps of Engineers 1997)</p> <p>(U.S. Army Corps of Engineers 2013a)</p> <p>(Berhow 2015, 211)</p> |
| <p>FUDS# C02NJ0776 Cape May County, NJ</p> <p>Latitude: 38°55'53"N Longitude: 74°57'20"W</p> | <p>Large Caliber: 6-inch Rifle 90 mm Rifle 155 mm Rifle</p> | <p>Cape May Military Reservation. Coastal defense site for Delaware area. Deactivated as coastal fort in 1947.</p> | <p>(U.S. Army 1945a)</p> <p>(U.S. Army Corps of Engineers 2013a)</p> <p>(Berhow 2015, 211)</p> |

Table 3-7: Historical Research Results: Maryland WEA

| Location | MEC | Description | Source |
|---|---|---|---|
| Maryland – Sites Near WEA | | | |
| MD-WEA-01 Polygon Coordinates: Latitude: 38°7.5'N Longitude: 74°35.7'W Latitude: 37°59'N Longitude: 74°28.2'W Latitude: 37°53.4'N Longitude: 74°39.2'W Latitude: 38°1.9'N Longitude: 74°46'W | Unknown | Delaware Bay dumping area for “sinkable objects”. Note that “sinkable objects” is not defined, but is thought to consist of debris. | (U.S. Navy 1953) |
| FUDS# C03DE0064 Bethany Beach, DE Polygon Coordinates: Latitude: 38°40'56"N Longitude: 74°50'26"W Latitude: 38°36'26"N Longitude: 74°45'03"W Latitude: 38°20'33"N Longitude: 74°48'59"W Latitude: 38°30'15"N Longitude: 75°02'60"W | Explosives: 40 mm, HE & HEI, MKII Small Arms: General Other: 3.25-inch Target Rocket, Practice, MK1 | Delaware Target Areas (1 of 2) | (U.S. Army Corps of Engineers 2010) (U.S. Army Corps of Engineers 2013a) |
| FUDS# C03DE0064 Bethany Beach, DE Polygon Coordinates: Latitude: 38°45'19"N Longitude: 75°01'19"W Latitude: 38°43'06"N Longitude: 74°57'26"W Latitude: 38°39'08"N Longitude: 74°55'25"W Latitude: 38°36'36"N Longitude: 74°57'19"W Latitude: 38°39'23"N Longitude: 75°03'52"W | Explosives: 40 mm, HE & HEI, MKII 90 mm, HE, M71 and HE-T, M71A1 120 mm, HE, M73 37 mm, HE (recovered during dredging) Small Arms: General .50 Caliber Machine Gun Other: 40 mm, Practice, M382 3.25-inch Target Rocket, Practice, MK1 | Delaware Target Areas (2 of 2) | (U.S. Army Corps of Engineers 2010) (U.S. Army Corps of Engineers 2013a) |

| Location | MEC | Description | Source |
|---|---|--------------------------------------|---|
| Maryland – Sites Near WEA (Continued) | | | |
| NJ-WEA-02 Offshore Gunnery Area Corners at: 39°38'00"N 74°11'00"W 39°00'30"N 73°09'00"W 38°30'00"N 73°39'00"W 38°30'00"N 74°50'30"W 38°47'30"N 74°44'00"W 38°51'00"N 74°43'00"W 39°10'00"N 74°22'00"W 39°17'00"N 74°34'00"W | Unknown | Air-to-air gunnery and bombing area. | (U.S. Navy 1947a) |
| Maryland – Sites Between WEA and Shore | | | |
| FUDS# C03DE0064 Bethany Beach, DE Polygon Coordinates: Latitude: 38°40'56"N Longitude: 74°50'26"W Latitude: 38°36'26"N Longitude: 74°45'03"W Latitude: 38°20'33"N Longitude: 74°48'59"W Latitude: 38°30'15"N Longitude: 75°02'60"W | Explosives: 40 mm, HE & HEI, MKII Small Arms: General Other: 3.25-inch Target Rocket, Practice, MK1 | Delaware Target Areas (1 of 2) | (U.S. Army Corps of Engineers 2010) (U.S. Army Corps of Engineers 2013a) |
| FUDS# C03DE0064 Bethany Beach, DE Polygon Coordinates: Latitude: 38°45'19"N Longitude: 75°01'19"W Latitude: 38°43'06"N Longitude: 74°57'26"W Latitude: 38°39'08"N Longitude: 74°55'25"W Latitude: 38°36'36"N Longitude: 74°57'19"W Latitude: 38°39'23"N Longitude: 75°03'52"W | Explosives: 120 mm, HE, M73 90 mm, HE, M71 and HE-T, M71A1 40 mm, HE & HEI, MKII 37 mm, HE (recovered during dredging) Small Arms: General .50 Caliber Machine Gun Other: 40 mm, Practice, M382 3.25-inch Target Rocket, Practice, MK1 | Delaware Target Areas (2 of 2) | (U.S. Army Corps of Engineers 2010) (U.S. Army Corps of Engineers 2013a) |

| Location | MEC | Description | Source |
|--|--|---|--|
| Maryland – Sites Between WEA and Shore (Continued) | | | |
| <p>FUDS# C03MD0930 Worcester County, MD</p> <p>Area is a circle with 3-mile radius centered at: Latitude: 38°06'42"N Longitude: 75°11'15"W</p> | <p>Explosive: 20 mm projectile, HE-I, MK1, M96 & M97</p> <p>Other: 20 mm projectile, AP-T, M75 & M95 3-lb practice bomb, AN-MK23 4.5-lb practice bomb, AN-MK43 25-lb practice bomb, AN-MK76 2.25-inch rocket, practice, SCAR 3.25-inch rocket, target, M2, M2A1, M2A2 3.5-inch rocket practice, AR 5-inch Rocket, practice, HVAR</p> | <p>Fifth Naval District test site #32. Rocket range at Assateague Island.</p> | <p>(U.S. Navy 1945c)</p> <p>(U.S. Navy 1946c)</p> <p>(U.S. Army Corps of Engineers 1994)</p> <p>(U.S. Army Corps of Engineers 2013a)</p> |
| <p>FUDS# C03MD0930 Worcester County, MD</p> <p>Area is a circle with 3-mile radius centered at: Latitude: 38°12'42"N Longitude: 75°09'00"W</p> | <p>Explosive: 20 mm projectile, HE-I, MK1, M96 & M97</p> <p>Other: 20 mm projectile, AP-T, M75 & M95 3-lb practice bomb, AN-MK23 4.5-lb practice bomb, AN-MK43 25-lb practice bomb, AN-MK76 2.25-inch rocket, practice, SCAR 3.25-inch rocket, target, M2, M2A1, M2A2 3.5-inch rocket practice, AR 5-inch Rocket, practice, HVAR</p> | <p>Fifth Naval District test site #33. Rocket range at Assateague Island.</p> | <p>(U.S. Navy 1945c)</p> <p>(U.S. Navy 1946c)</p> <p>(U.S. Army Corps of Engineers 1994)</p> <p>(U.S. Army Corps of Engineers 2013a)</p> |

Table 3-8: Historical Research Results: Virginia WEA

| Location | MEC | Description | Source |
|--|--|--|---|
| Virginia – Sites Near WEA | | | |
| AC-02 | Chemical munitions: 75 mm Projectiles Other: Bulk Chemical Agent (bulk containers) | Loaded in Baltimore, MD and disposed of at sea from the <i>U.S.S. Elinor</i> . Newspaper reports indicate disposal of 2,100 tons including 200,000 75 mm mustard projectiles. Government records indicate 75 mm shells, gas drums, phosgene drums, mustard projectiles. Refer to map for projected track for disposal. | (U.S. Navy 1919) (Carton, Ciolfi and Overfield 2009) |
| VA-WEA-01 Chesapeake Bay, VA Approximate Coordinates at Time of Disposals: Latitude: 36°51.7'N Longitude: 75°24.8'W Latitude: 36°50.1'N Longitude: 75°21'W | Mines: Case Mine, HBX-1 Loaded, Mark 36-2 (4 units) Case Mine, HBX-1 Loaded, Mark 39-0 (2 units) Case Mine, TNT Loaded, Mark 51-2 (1 unit) | Three mines found in the vicinity of the Chesapeake Bay entrance. Ammunition was disposed of by the <i>U.S.S. Calhoun County</i> . Known mines are believed to have been recovered. Reports indicate that further disposals likely occurred; however, this is uncertain. | (U.S. Navy 1957) |
| VA-WEA-12 Latitude: 37°09.0'N Longitude: 75°17.2'W | Unknown | UXO reported | (National Oceanic and Atmospheric Administration 2016f) |
| VA-WEA-13 Latitude: 37°07.75'N Longitude: 75°22.0'W | Unknown | UXO reported | (National Oceanic and Atmospheric Administration 2016f) |
| Virginia – Sites Between WEA and Shore | | | |
| VA-WEA-02 Myrtle Island, VA Polygon Coordinates: Latitude: 37°12'18"N Longitude: 75°46'00"W Latitude: 37°08'21"N Longitude: 75°50'00"W Latitude: 37°11'16"N Longitude: 75°49'29"W Latitude: 37°10'14"N Longitude: 75°52'57"W Latitude: 37°14'30"N Longitude: 75°48'32"W Latitude: 37°13'38"N Longitude: 75°46'18"W | Bombs Rockets Projectiles | Air Force practice bombing, rocket firing, and gunnery range danger zone. | (U.S. Department of Commerce 1961, 44) (U.S. Government Printing Office 2016c) |

| Location | MEC | Description | Source |
|---|---------|---|--|
| Virginia – Sites Between WEA and Shore (Continued) | | | |
| VA-WEA-03 Cape Henry, VA Polygon Coordinates: Latitude: 36°53'N Longitude: 75°55'W Latitude: 36°53N Longitude: 76°00'W Latitude: 36°59'N Longitude: 75°55'WW Latitude: 36°59'N Longitude: 76°00'W | Unknown | Cape Henry test field facility established by Navy's Bureau of Ordnance. | (U.S. Navy 1947b) (National Oceanic and Atmospheric Administration 2016g) |
| VA-WEA-04 Dam Neck, VA Area extends seaward for a distance of 15 miles from: Latitude: 36°46.8'N Longitude: 75°57.4'W | Unknown | Danger zone for firing range at Dam Neck, VA. | (U.S. Department of Commerce 1947, 94-95) |
| VA-WEA-05 Dam Neck, VA Latitude: 36°46'24"N Longitude: 75°55'22"W | Unknown | First of five unlighted targets anchored off Dam Neck, approximately 40 feet in length by 15 feet in height. | (U.S. Department of Commerce 1947, 95) |
| VA-WEA-06 Dam Neck, VA Latitude: 36°46'46"N Longitude: 75°56'03"W | Unknown | Second of five unlighted targets anchored off Dam Neck, approximately 40 feet in length by 15 feet in height. | (U.S. Department of Commerce 1947, 95) |
| VA-WEA-07 Dam Neck, VA Latitude: 36°46'07"N Longitude: 75°55'41"W | Unknown | Third of five unlighted targets anchored off Dam Neck, approximately 40 feet in length by 15 feet in height. | (U.S. Department of Commerce 1947, 95) |
| VA-WEA-08 Dam Neck, VA Latitude: 36°46'08"N Longitude: 75°56'03"W | Unknown | Fourth of five unlighted targets anchored off Dam Neck, approximately 40 feet in length by 15 feet in height. | (U.S. Department of Commerce 1947, 95) |
| VA-WEA-09 Dam Neck, VA Longitude: 36°46'31"N Latitude: 75°56'42"W | Unknown | Fifth of five unlighted targets anchored off Dam Neck, approximately 40 feet in length by 15 feet in height. | (U.S. Department of Commerce 1947, 95) |

| Location | MEC | Description | Source |
|--|----------------|--|--|
| Virginia – Sites Between WEA and Shore (Continued) | | | |
| <p>VA-WEA-10</p> <p>Latitude: 36°51'00"N Longitude: 75°56'00"W Latitude: 35°50'00"N Longitude: 75°56'00"W Latitude: 36°50'00"N Longitude: 75°40'00"W Latitude: 37°01'00"N Longitude: 75°40'00"W Latitude: 37°01'00"N Longitude: 75°50'00"W Latitude: 37°04'30"N Longitude: 75°52'57"W Latitude: 37°03'05"N Longitude: 75°54'15"W Latitude: 36°51'00"N Longitude: 75°54'15"W</p> | <p>Unknown</p> | <p>Firing Danger Area</p> | <p>(National Oceanic and Atmospheric Administration 2016g)</p> |
| <p>VA-WEA-11</p> <p>Firing Danger Areas</p> <p>Extending seaward 7,500 yards between 35° and 92° true, from a point on shore at latitude 36° 47'33" N, longitude 75° 58'23" W.</p> <p>Extending seaward 12,000 yards between 30° and 83° true, from a point on shore at latitude 36°46'48" N, longitude 75°57'24" W; and an adjacent sector extending seaward for 15 nautical miles between 83° and 150° true, respectively, from the same shore position.</p> | <p>Unknown</p> | <p>Firing Danger Areas Dam Neck, Virginia; naval firing range.</p> | <p>(National Oceanic and Atmospheric Administration 2016g)</p> <p>(U.S. Government Printing Office 2016a)</p> <p>(U.S. Government Printing Office 2016b)</p> |

Table 3-9: Historical Research Results: North Carolina Kitty Hawk WEA

| Location | MEC | Description | Source |
|--|--|---|--|
| North Carolina Kitty Hawk – Sites Near WEA | | | |
| NC-WEA-01 Area is a circle with 3-mile radius centered at: Latitude: 36°35'00"N Longitude: 75°27'00"W | Unknown | Radar target area (#30) | (U.S. Navy 1946c) |
| North Carolina Kitty Hawk – Sites Between WEA and Shore | | | |
| FUDS# I04NC1071 Corolla, NC | Bombs Rockets Projectiles 20 mm projectiles | Corolla Naval Target was used between 1944 and 1965 as a combination bombing, strafing, and rocket target. | (U.S. Army Corps of Engineers 2013a) |
| FUDS# I04NC0984 Duck, NC | Other: Miniature practice bombs, MK5, MK23, MK43 25-lb practice bomb, MK76 50-lb practice bomb, MK89 100-lb practice bomb, MK15, Mod 2 250-lb practice bomb, MK86 2.75-inch rocket, practice, MK2, MK3, MK4, MK5, MK6, MK7 3.5-inch rocket, practice, Aircraft, MK3 5-inch rocket, practice, MK28, MK32, MK34, MK35 11.75-inch rocket, practice, MK4 | Duck Target Facility only known to have used practice munitions. Navy bombing and rocket range from 1941 to 1965. | (U.S. Army Corps of Engineers 2015b) (U.S. Army Corps of Engineers 2013a) |
| FUDS# I04NC1072 Nags Head, NC | Unknown | Bodie Island was a target area for the U.S. Navy. Reportedly, no ammunition was used. | (U.S. Navy 1945c) (U.S. Navy 1946a) (U.S. Army Corps of Engineers 2013a) |
| FUDS# I04NC1076 Nags Head, NC | Unknown | Jockey's Ridge was a target area for the U.S. Navy from the early 1940s until 1945. | (U.S. Army Corps of Engineers 2013a) |
| FUDS# I04NC1085 Southern Shores, NC | Unknown | Southern Shores was a target area for the U.S. Navy from the early 1940s until 1945. | (U.S. Army Corps of Engineers 2013a) |

Table 3-10: Historical Research Results: North Carolina Wilmington East & West WEA

| Location | MEC | Description | Source |
|--|--|---|--------------------|
| North Carolina Wilmington East & West – Sites Between WEA and Shore | | | |
| NC-WEA-02 Oak Island, NC Latitude: 33°53'28"N Longitude: 78°01'36"W | Large Caliber: 12-inch Mortar 12-inch Rifle 8-inch Rifle 6-inch Rifle 5-inch Rifle 4.7-inch Rifle 3-inch Rifle 155 mm | Fort Caswell. Coastal defense site defending Cape Fear River area. Deactivated as coastal fort in 1925. | (Berhow 2015, 213) |

Figure 3-1: MEC Related Sites: Cape WEA

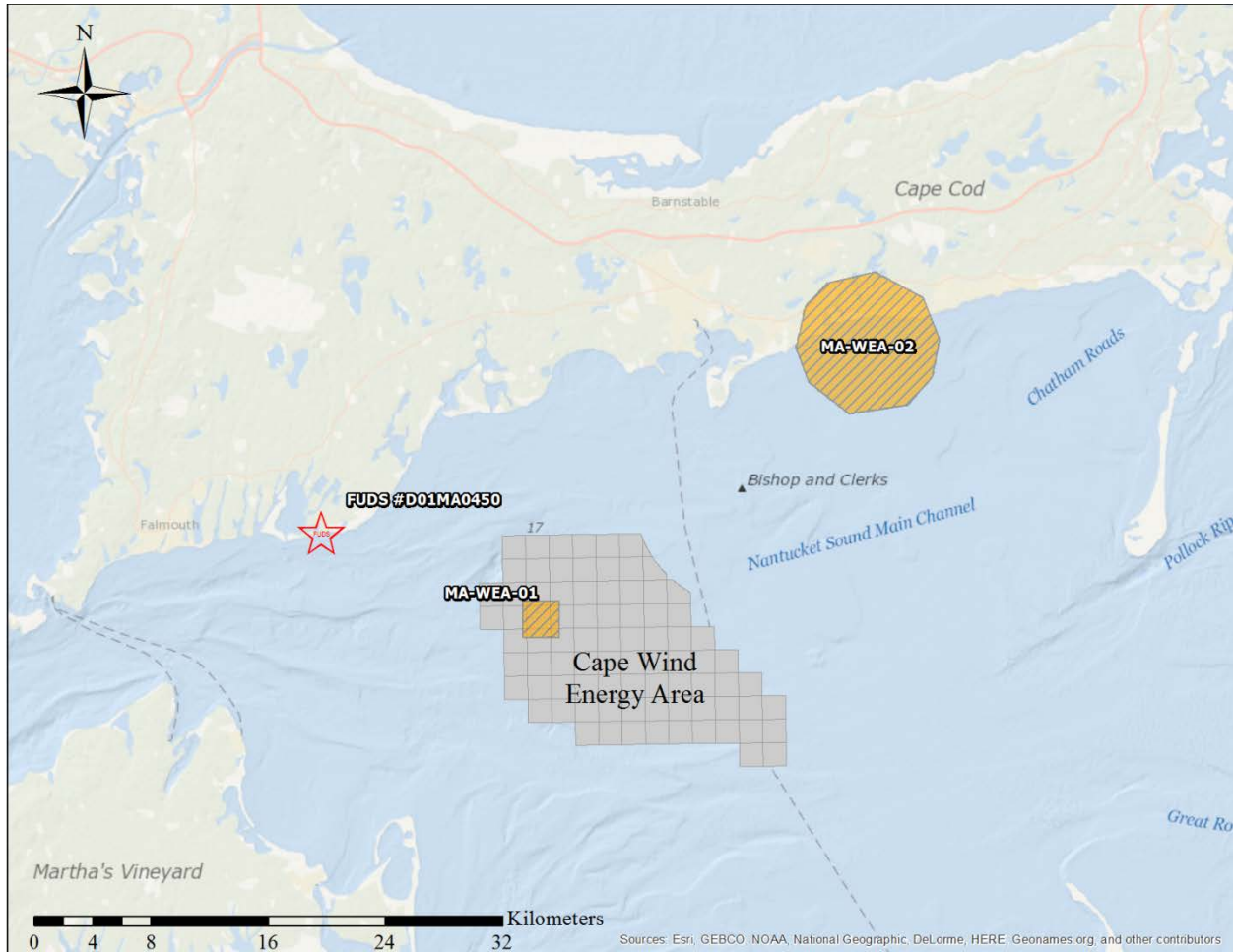


Figure 3-2: MEC Related Sites: Massachusetts WEA

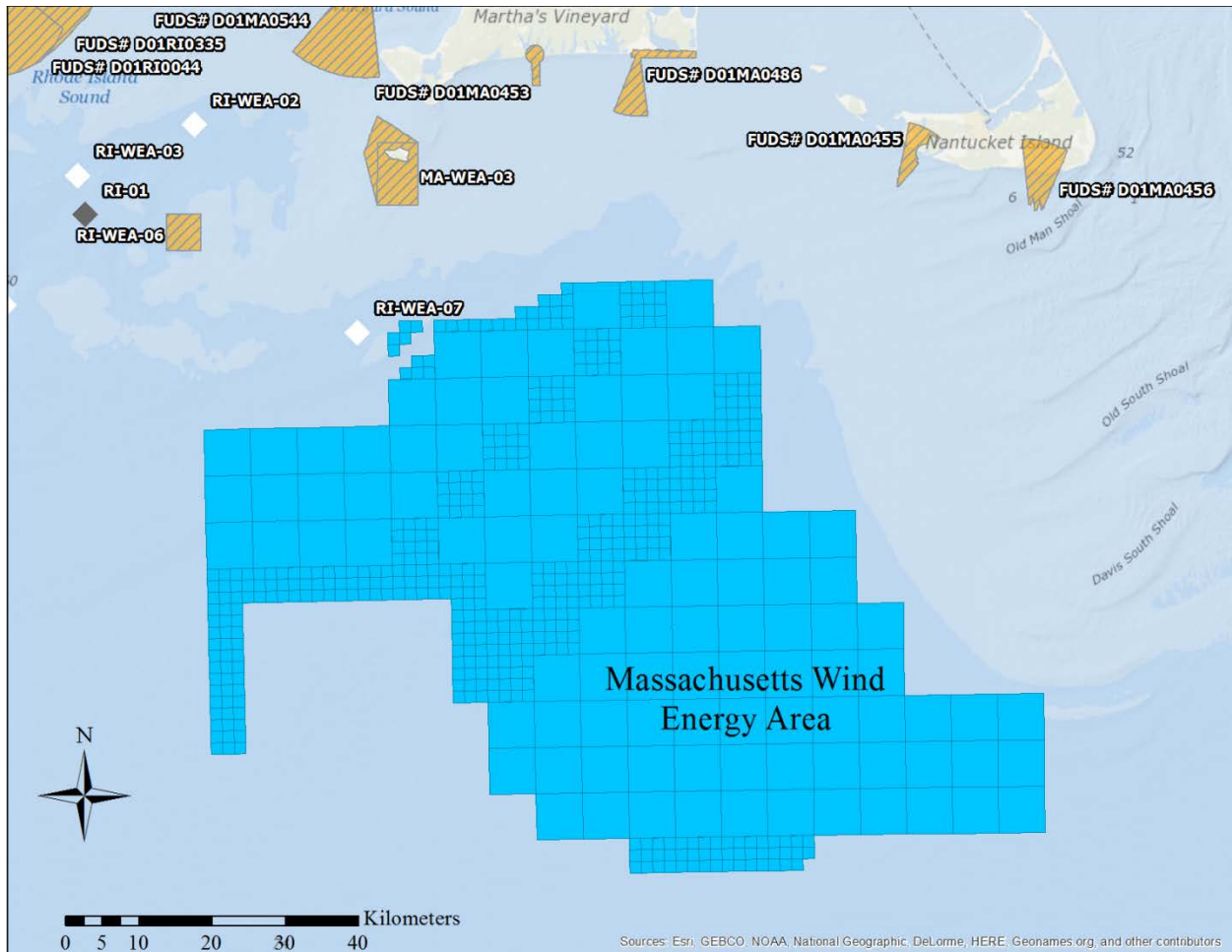
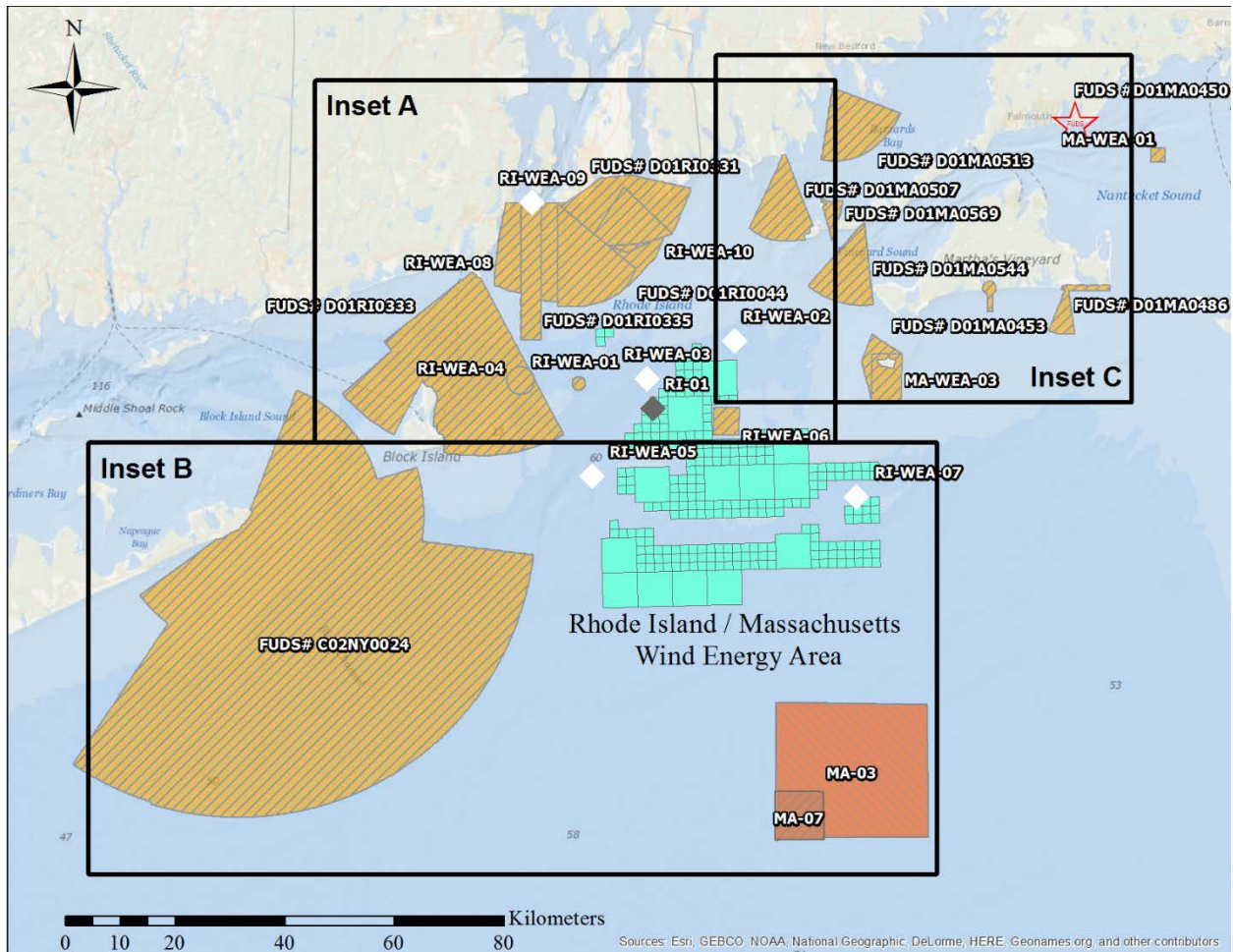


Figure 3-3: MEC Related Sites: Rhode Island/Massachusetts WEA



Note: Map Insets A (Figure 3-4), B (Figure 3-5), and C (Figure 3-6) provide details.

Figure 3-4: MEC Related Sites: Rhode Island/Massachusetts WEA – Inset A

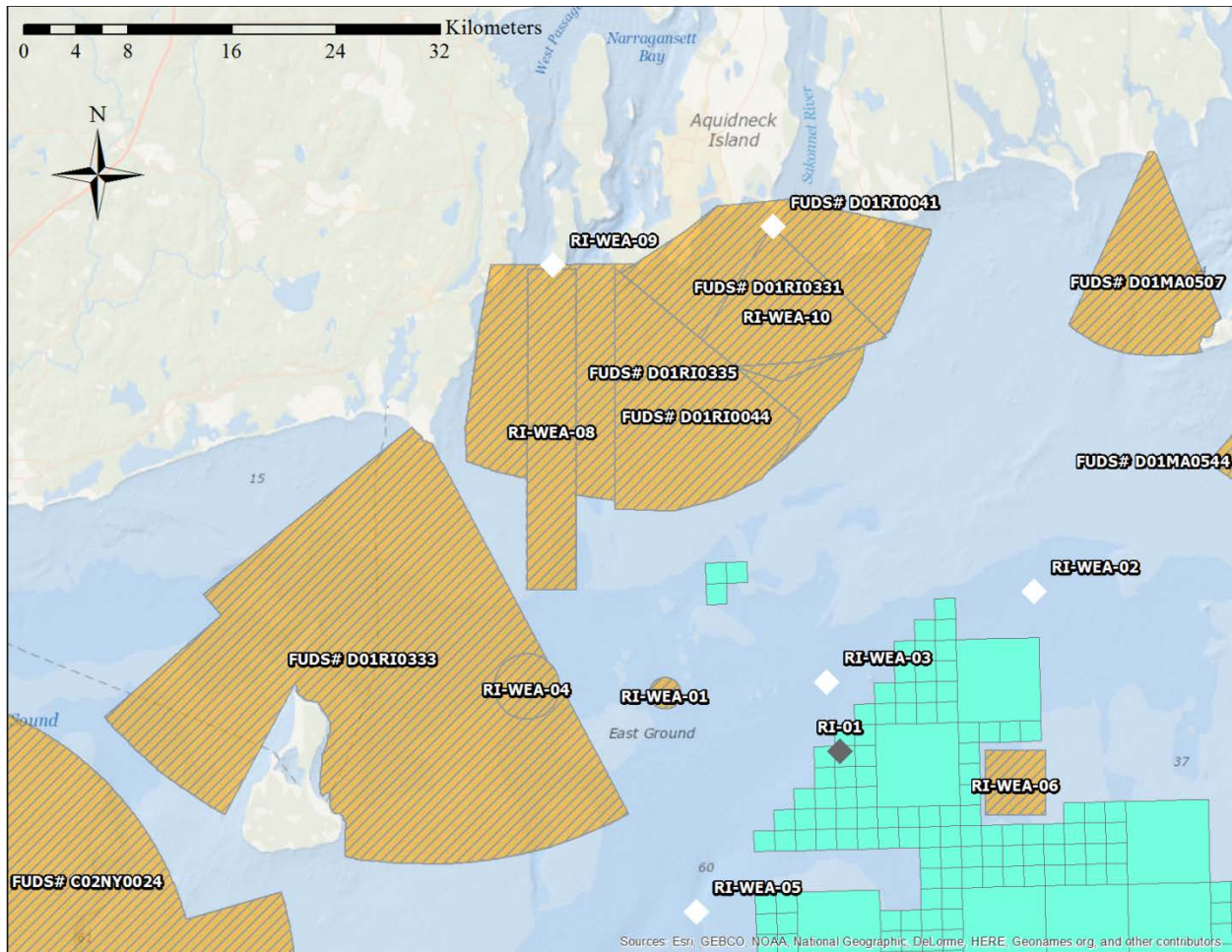


Figure 3-5: MEC Related Sites: Rhode Island/Massachusetts WEA – Inset B

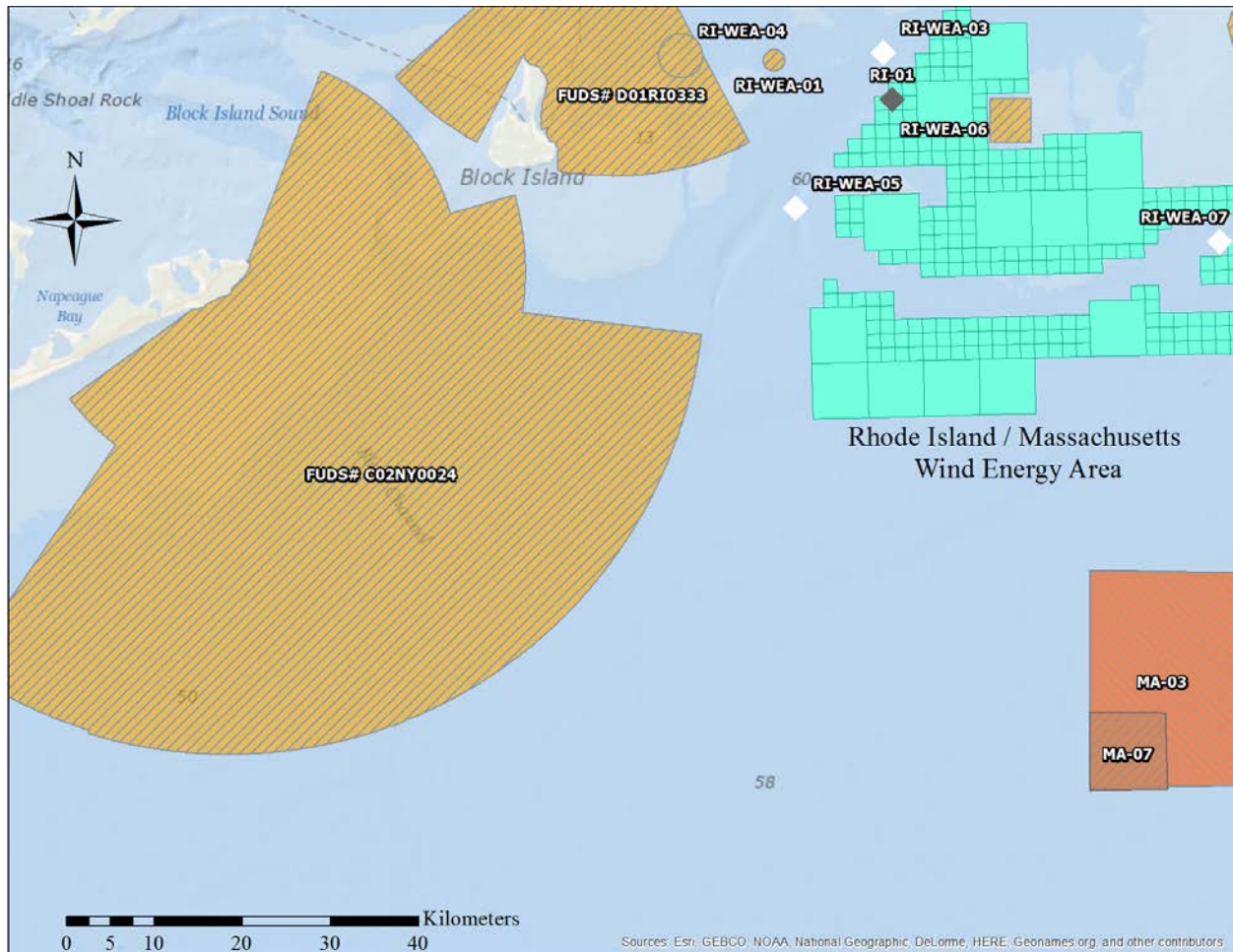


Figure 3-6: MEC Related Sites: Rhode Island/Massachusetts WEA – Inset C

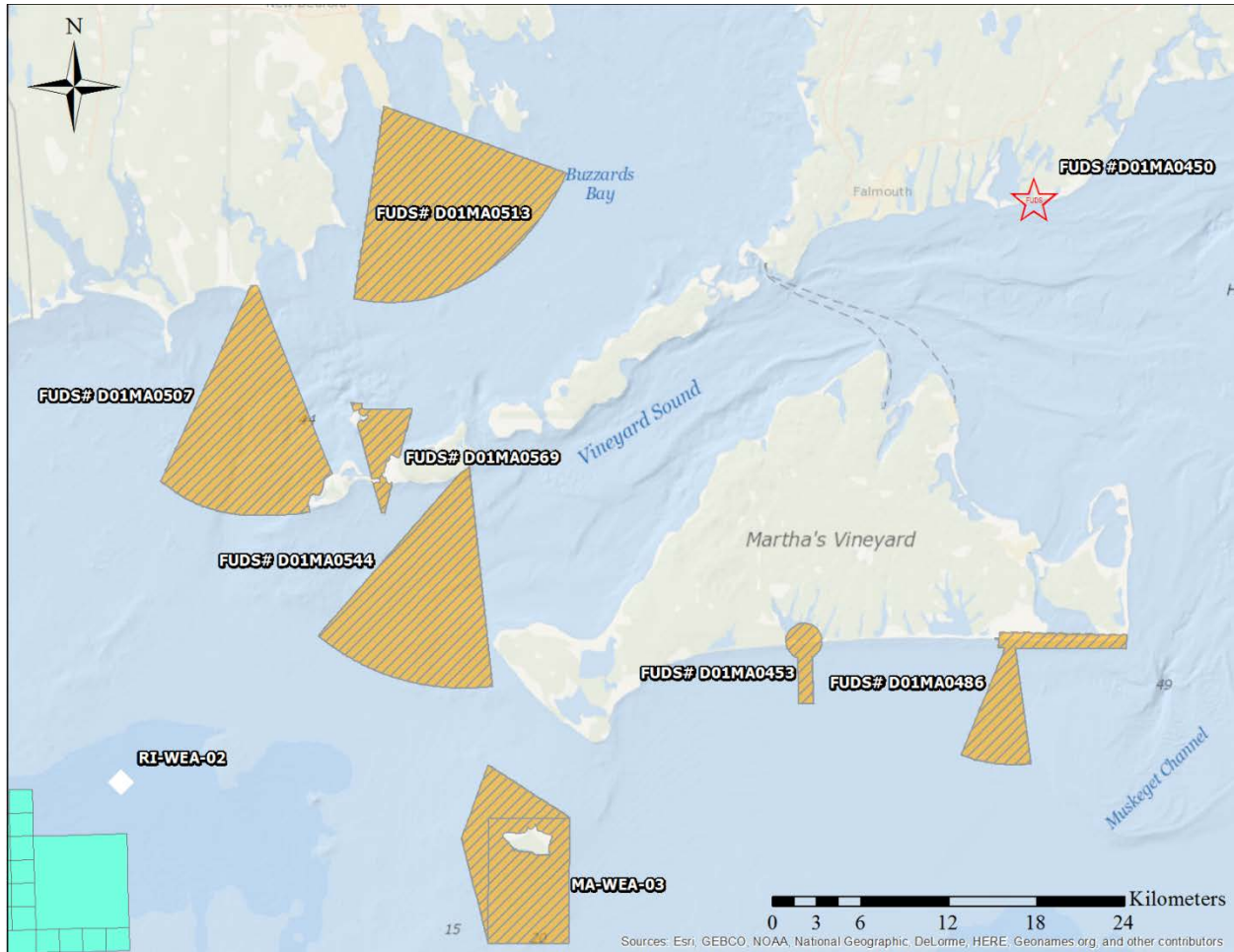


Figure 3-7: MEC Related Sites: New York WEA

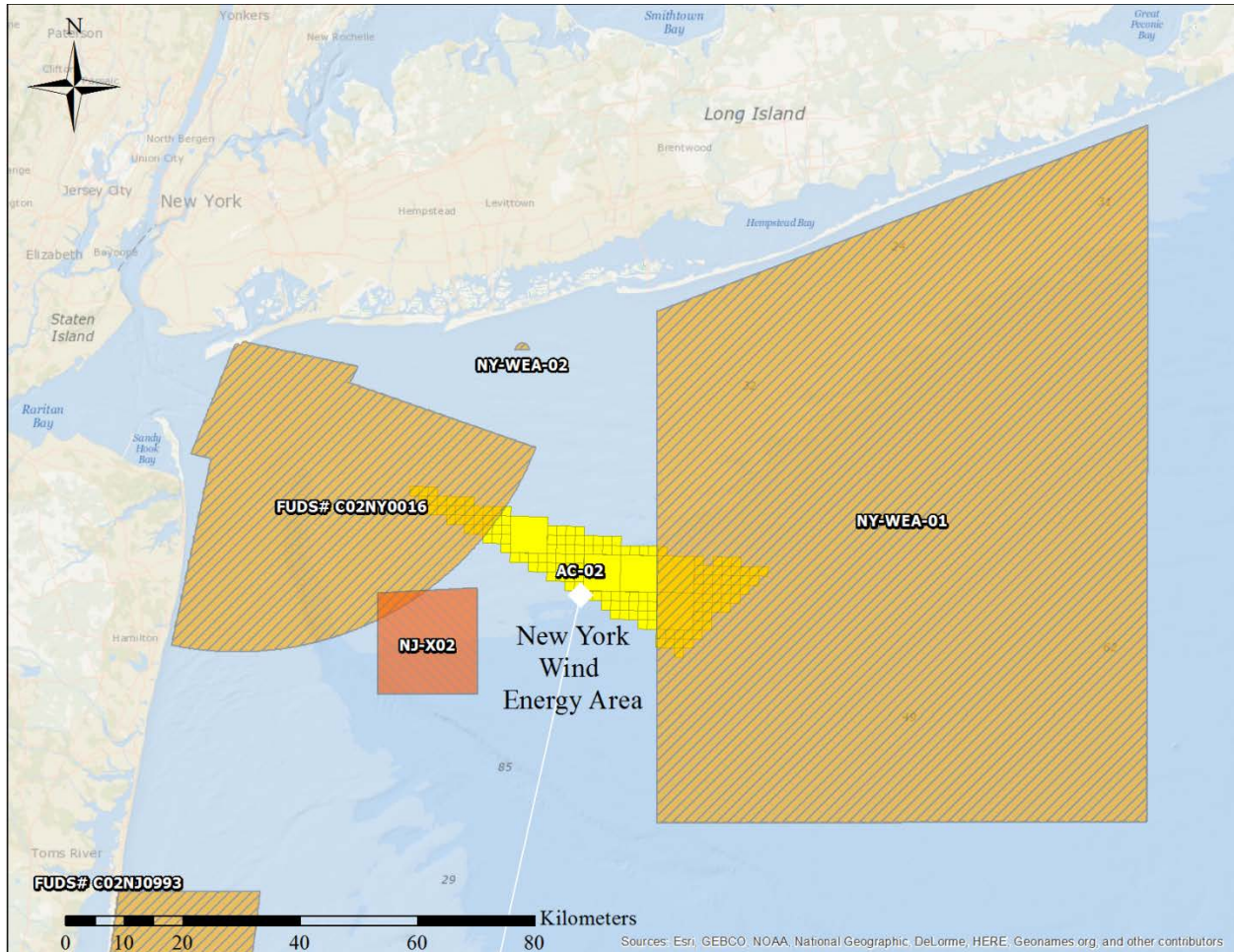


Figure 3-8: MEC Related Sites: New Jersey WEA

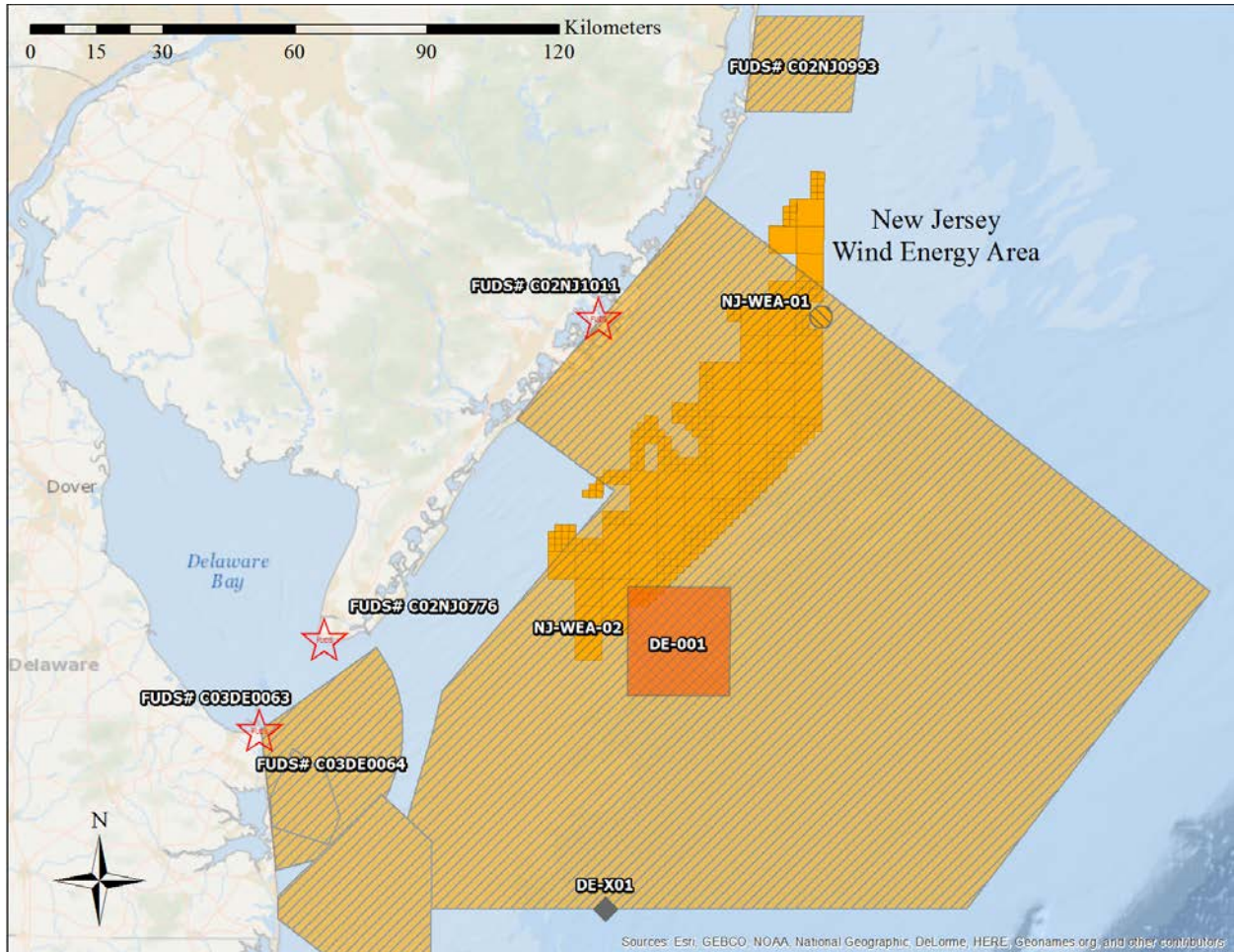


Figure 3-9: MEC Related Sites: Delaware WEA

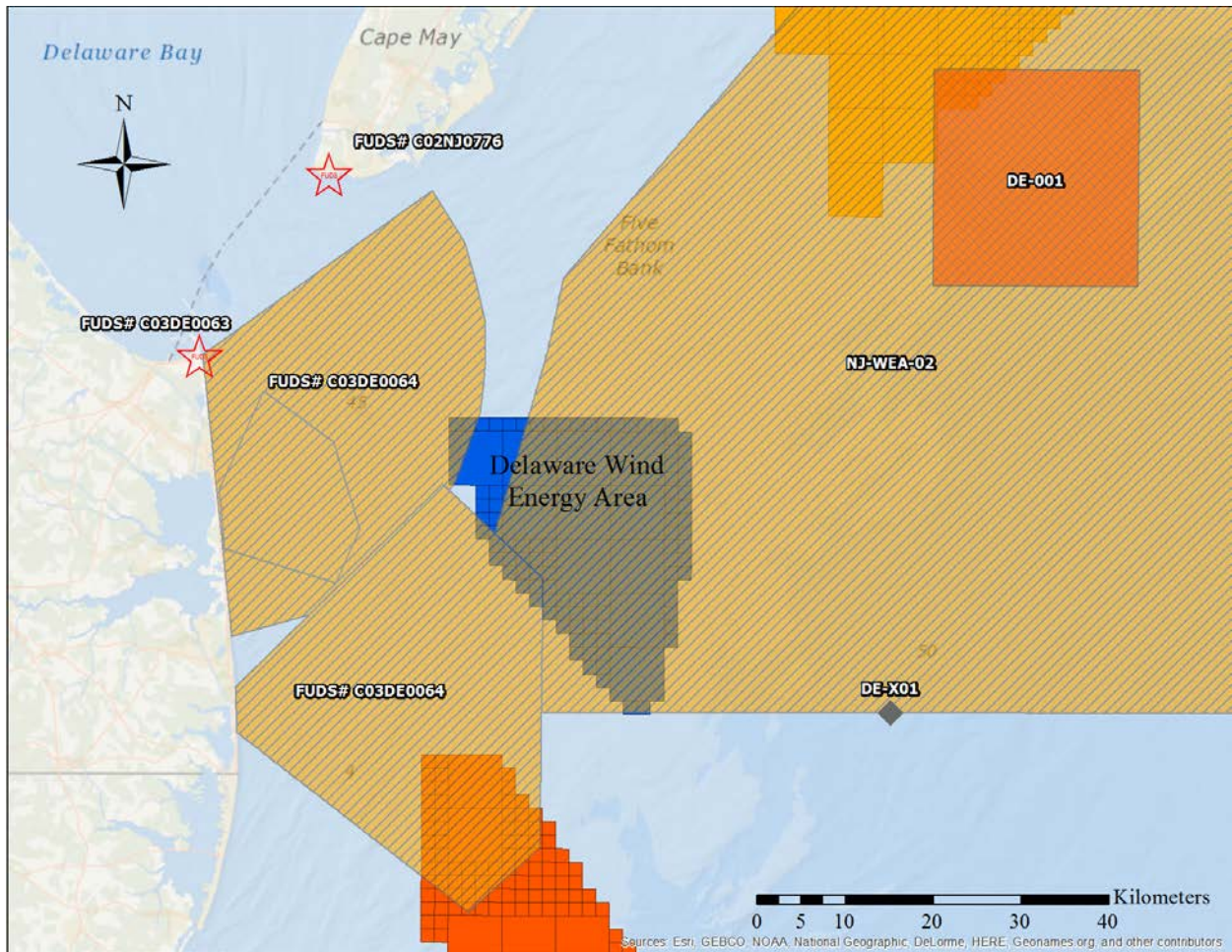


Figure 3-10: MEC Related Sites: Maryland WEA

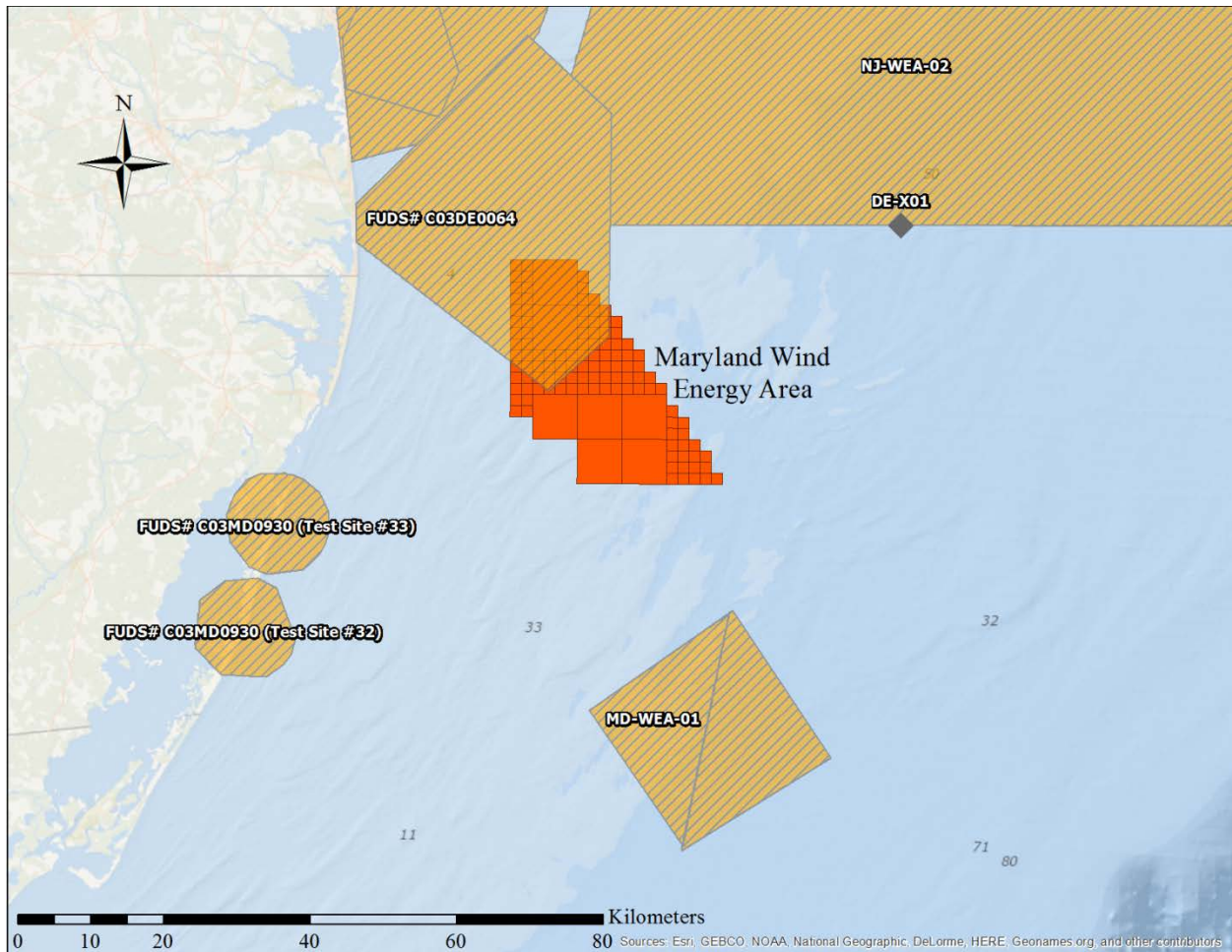
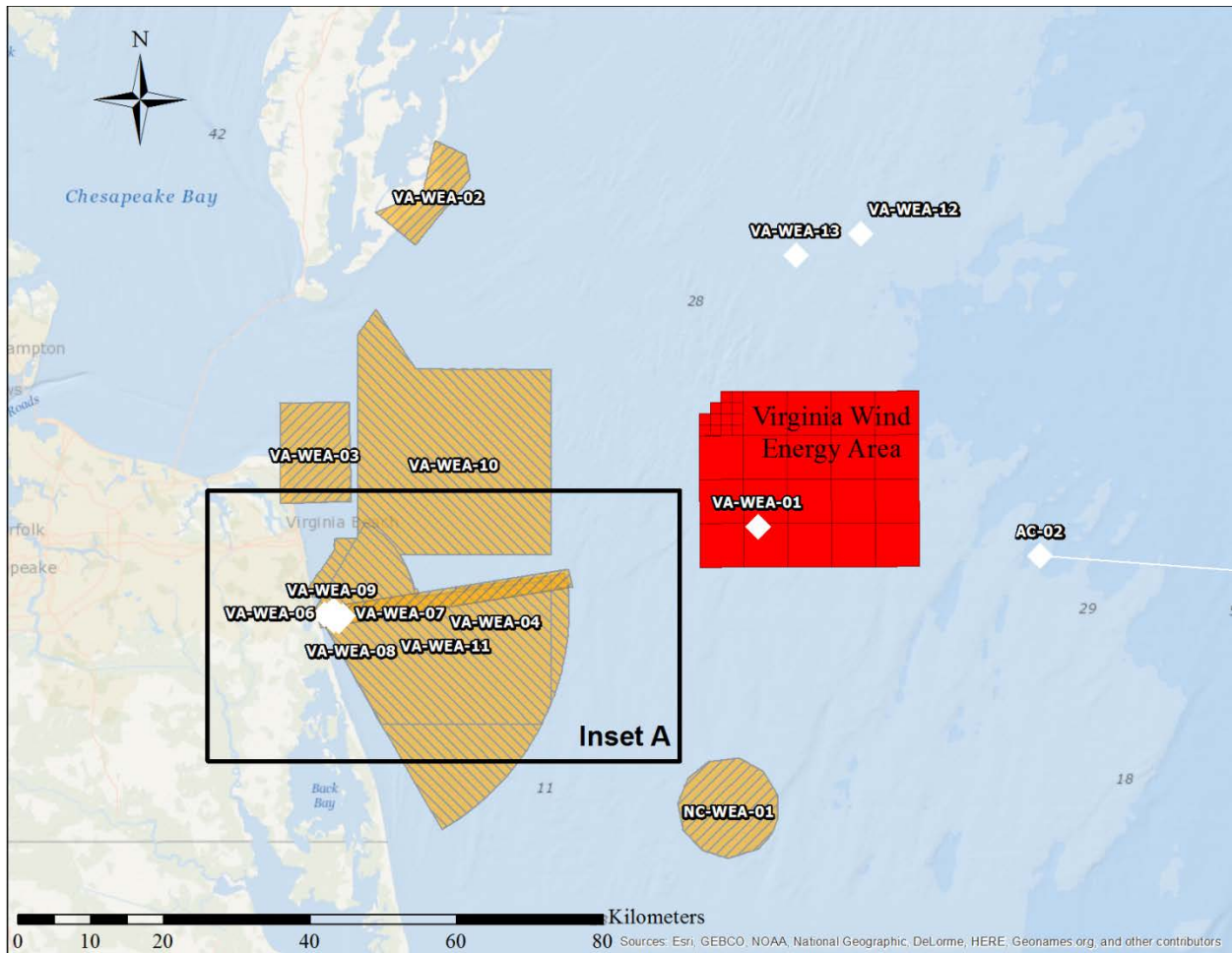


Figure 3-11: MEC Related Sites: Virginia WEA



Note: Map Inset A (Figure 3-12) provides more detail.

Figure 3-12: MEC Related Sites: Virginia WEA – Inset A

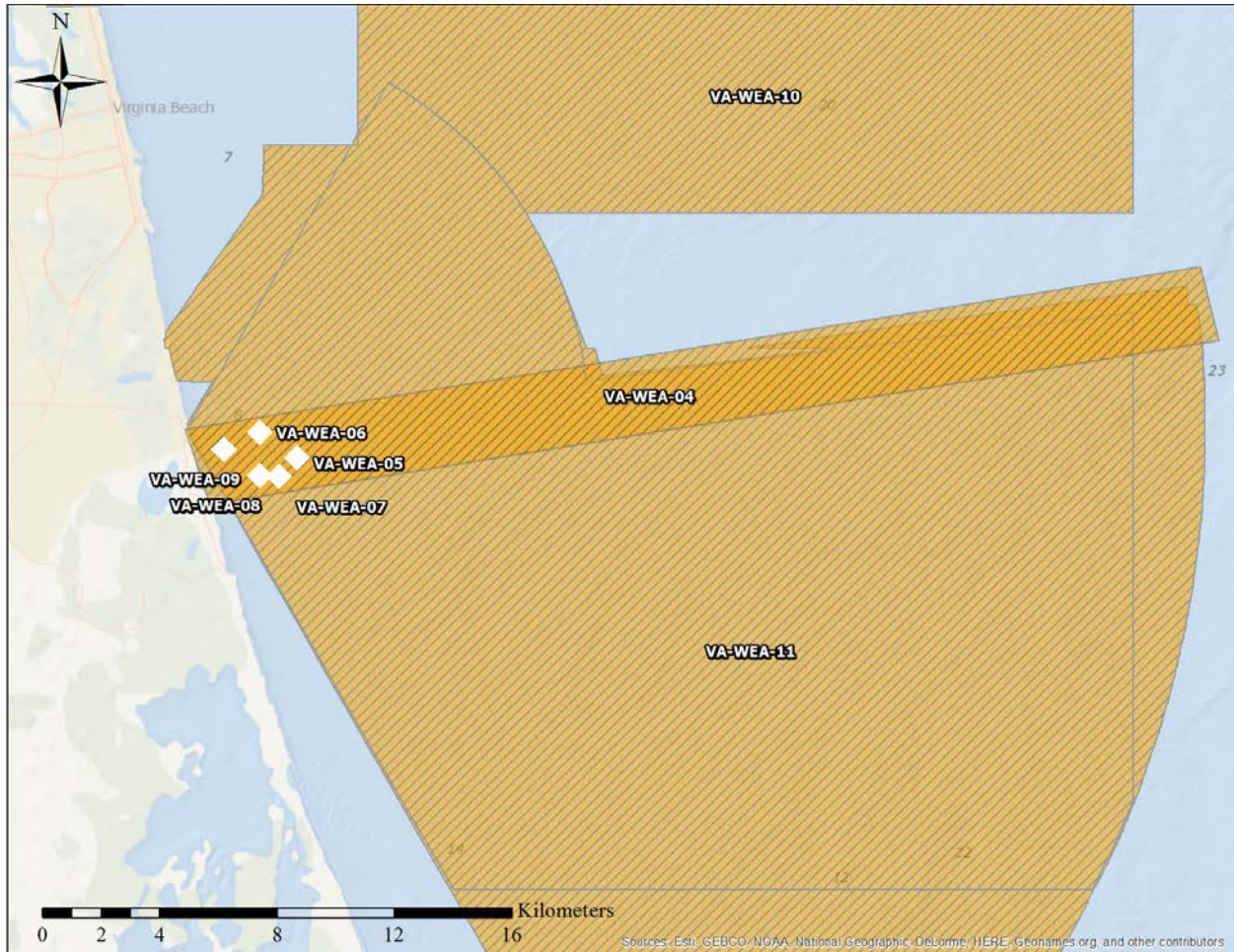


Figure 3-13: MEC Related Sites: North Carolina Kitty Hawk WEA

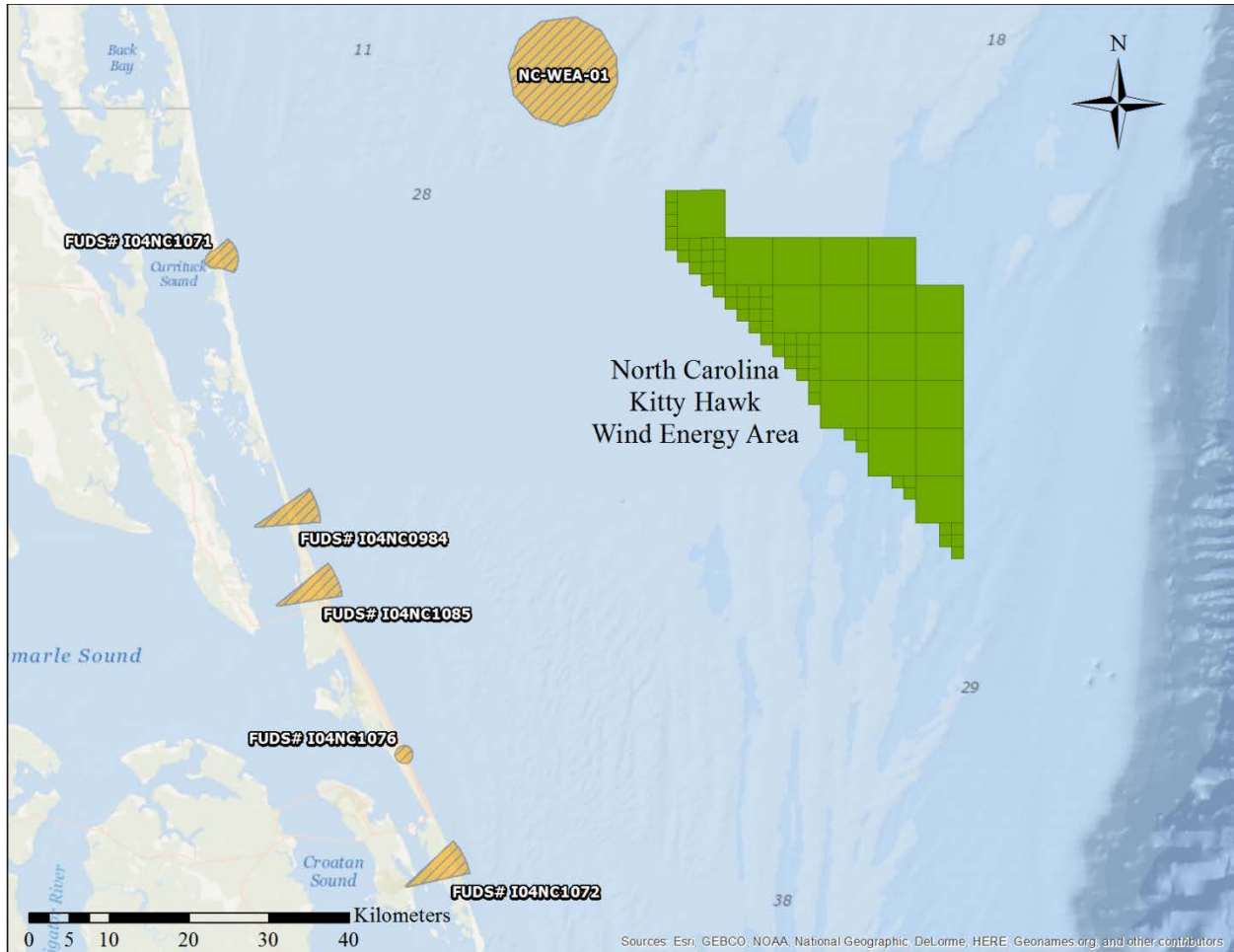
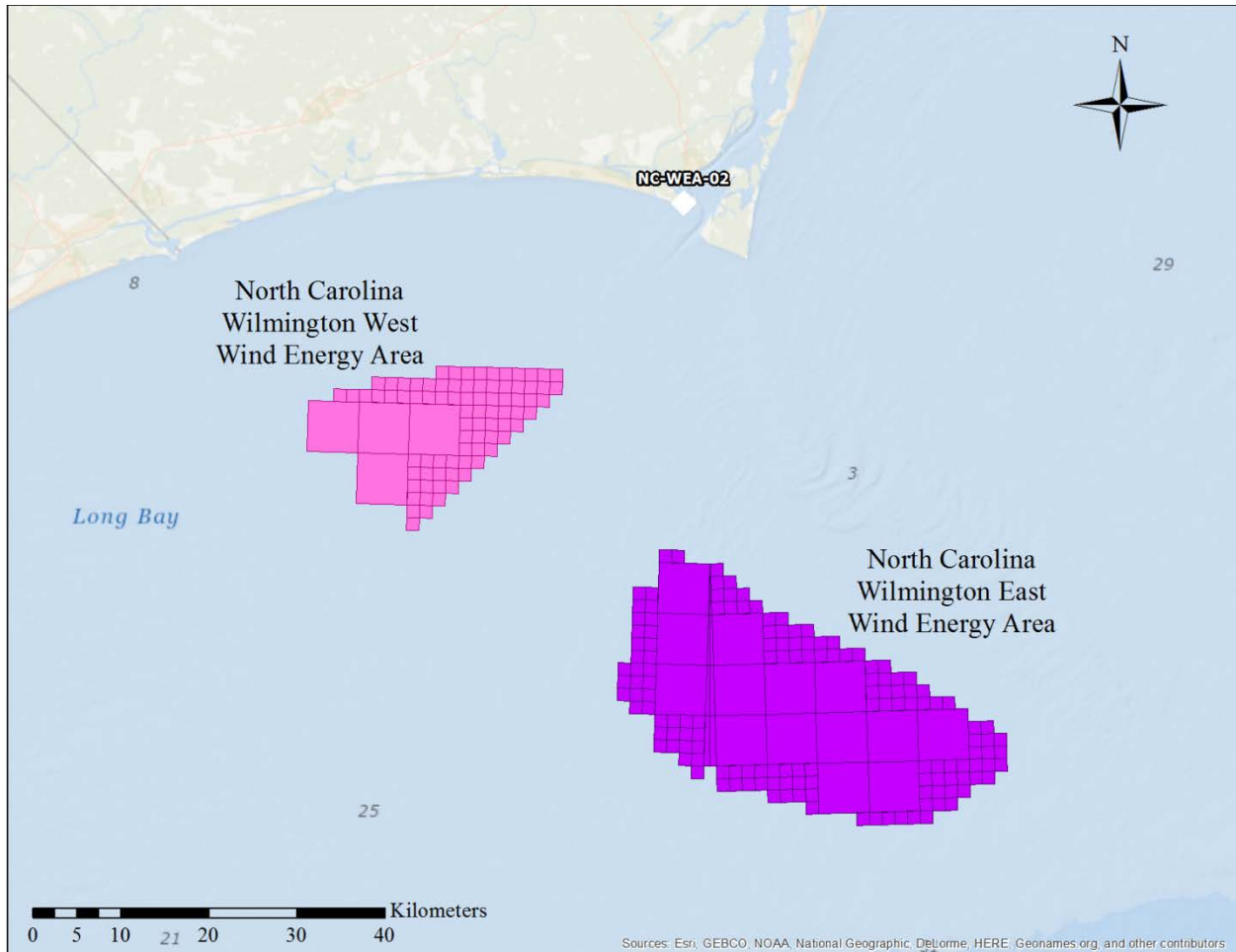


Figure 3-14: MEC Related Sites: North Carolina Wilmington East & West WEAs



4.0 Typical Offshore Renewable Energy Development Activities

Offshore renewable energy developments (e.g., wind farms, tidal facilities) consist of an array of energy harvesting equipment (e.g., wind turbines, solar panels) that are typically on foundations, secured to the seafloor. Electricity from the energy harvesting equipment is transmitted to shore through a series of cables and substations. BOEM is currently supporting the development of offshore wind by making available leases for suitable development areas on the U.S. OCS. Thus, the discussion below is focused on offshore wind energy development but other renewable energy projects will have similar requirements. The general description of offshore renewable energy development activities presented here is largely based on descriptions of wind energy development from Mineral Management Service (2007) and Kaiser and Snyder (2011).

Offshore renewable energy development technologies that are ready or nearly ready for commercial operation include offshore wind, wave, and ocean energy capture. Of these technologies, offshore wind is the most developed for operation in the Atlantic OCS and is the focus of the following descriptions. Once a developer obtains a lease, they must undertake a number of activities and balance a variety of competing factors and impacts.

4.1 Offshore Wind Energy Systems

Offshore wind energy systems are composed of a number of connected components. The major components include:

- ▶ Meteorological mast or Light Detection and Ranging (LiDAR) buoy,
- ▶ Wind turbine,
- ▶ Electrical collection and transmission cables,
 - Inter-array cables,
 - Export cables,
- ▶ Substations.

4.1.1 Meteorological Mast or LiDAR Buoy

Monitoring meteorological conditions is necessary for proper planning of offshore energy systems. A meteorological mast or LiDAR buoy is typically the first structure installed during the initial planning stages of a WEA development. This equipment collects meteorological and natural resource data to aid in estimating the profitability of a proposed development.

A meteorological mast consists of a foundation, platform for boat loading, meteorological and other instrumentation, navigational lights and marking, and related equipment. The support system consists of the foundation, transition piece, and scour protection. A transition piece attaches to the foundation and simplifies tower attachment. Scour protection helps shield the foundation and support system from environmental conditions (e.g., erosion of sediment).

A LiDAR buoy is of modest size and is installed with an anchor and chain sweep. This makes it easy to install, recover and relocate. The buoys are capable of measuring wind speed and direction at various heights and other sensors measure oceanographic parameters such as waves and current profiles.

4.1.2 Wind Turbine

Principal components of an offshore wind turbine generator include the: foundation, tower, rotor (consisting of blades and blade hub connected through a drivetrain to the turbine), and nacelle (housing the turbine assembly). The rotors and turbine harness kinetic energy from the wind to produce electricity. The tower is attached to the foundation with a transition piece, and the nacelle is attached to the tower, followed by the rotor. There are several different options for installation of the foundation that often requires scour protection.

Within a wind farm, foundations are tailored to the site-specific water depth and soil type. Four basic types of foundations are used in offshore wind farms: monopiles, jackets and tripods, gravity, and floating foundations. It is anticipated that monopiles will be the preferred choice in shallow water and jackets or tripods will be the preferred choice in deeper water (Kaiser and Snyder 2011). There are indications that gravity and floating foundations may be used to address conditions at specific sites.

4.1.3 Electrical Collection and Transmission Cables

The electrical collection and transmission cables include inter-array cables to carry power from the rows of turbines to an offshore substation, an export cable to carry power from the offshore substation to landfall and the onshore substation and infrastructure. The export cable is larger than the array cables.

Inner-array cables connect to the turbine transformer and exit the foundation near the seafloor. The cables are buried 1 to 2 m below the seafloor and connect to the next turbine in the string. The power carried by cables increases as more turbines are connected and the cable voltage may increase to handle the increased load. The amount of cabling required depends on the layout of the farm, the distance between turbines, and the number of turbines.

Export cables connect the wind farm (usually at the electric service platform [ESP]) to the onshore transmission system. Export cables are composed of three insulated conductors protected by galvanized steel wire. Medium voltage cables are used when no offshore substation (ESP) is installed and high voltage cables are used with offshore substations. Export cables are buried, and in some places, export cables may require scour protection. At the landfall, cables may be spliced to a similar cable and/or connected to an onshore substation. Water depths along the cable route, soil type, coastline types, and many other factors determine the cable route. At the onshore substation, energy from the offshore wind farm is delivered to the electrical grid.

4.1.4 Substations

A wind energy facility often has an ESP housing an offshore substation and providing for interconnectivity of the turbines. The need for offshore substations depends upon the power generated and the distance to shore. Use of an offshore substation minimizes transmission losses by transforming electricity generated at the wind turbine to a higher voltage suitable for transmission to shore and bringing the generated electricity into phase. Substations are sited within the wind farm to minimize the length of export and inner-array cables (Kaiser and Snyder 2011, Mineral Management Service 2007).

4.2 Offshore Wind Energy Development Pre-Construction Activities

Site characterization activities involve the collection of meteorological, geological, geotechnical, and geophysical data to aid in siting the renewable energy infrastructure in an appropriate

location and to inform the engineering and design process. The meteorological study generally includes erection of a mast or LiDAR buoy to monitor weather for a year or more to verify conditions. Installation of a meteorological mast results in disturbance of the seafloor from pile-driving activities. The geological, geotechnical, and geophysical characterization of the WEA development area and cable routes employs intrusive and non-intrusive surveys (Mineral Management Service 2007).

4.2.1 Characterization of Meteorological and Natural Resources

This characterization involves the installation of the meteorological mast or LiDAR buoy during the planning stages. A meteorological mast is installed in a manner similar to a monopile foundation or jacket structure, but the diameter is smaller and weight is considerably less. The support system refers to the foundation, transition piece, and scour protection. A description of potential meteorological mast foundation and substructure construction activities is provided in Section 4.3.2, Installation of Substructures and Foundations.

Installation of a LiDAR buoy is similar to anchoring of a vessel with a single anchor and chain sweep. The dropping of anchors impart a moderate amount of energy on the seafloor on impact but the area of impact is quite small. An area of seafloor can be disturbed by the chain sweep throughout the buoy deployment but the amount of energy involved is low.

4.2.2 Site and Cable Route Surveys

A site survey is performed to identify appropriate locations for the energy generation infrastructure (e.g., wind turbines, substation) and safe routes for cables. A cable route survey identifies an optimal route for cables by taking into consideration factors such as bathymetry, bottom type, distances, and presence of obstacles and potential hazards. A desktop study identifies potential sites for the infrastructure and cable routes and a site survey confirms the assumptions and field conditions. The site and cable route surveys employ similar techniques and are discussed together.

Both intrusive and non-intrusive surveys of the cable route and renewable energy development area are typically conducted. Non-intrusive surveys include geophysical surveys such as bathymetry, sonar, sub-bottom profiling, and magnetometry to gain an understanding of the seafloor conditions. The energy transmitted by typical non-intrusive survey methods and equipment is very low.

Intrusive surveys include geotechnical and some environmental investigations. Marine geotechnical investigations include grab sampling, drilling, and cone penetrometer testing. The kinetic energy generated during geotechnical investigations can be sufficient to initiate a MEC detonation, particularly if the equipment directly impacts the MEC. Jack up platforms or a dynamically positioned vessels are often employed for geotechnical investigations. The deployment of legs or anchors to the seafloor may generate significant, short-duration, kinetic energy.

4.3 Offshore Wind Energy Development Construction Activities

The engineering and design of offshore wind facilities depends on site-specific conditions, particularly water depth, geology of the seafloor, and wave loading. The largest MEC risks from wind energy construction activities are associated with installation of the wind turbine and ESP foundations and the electrical collection and transmission cables.

4.3.1 Electrical Collection and Transmission Cable Laying Operations

Virtually all offshore renewable energy developments will generate electricity that requires installation of cables to transmit the electricity to shore. The cables used for offshore renewable energy projects are typically buried beneath the seafloor, where they are safe from damage caused by anchors or fishing gear and to reduce their exposure to the marine environment. Cables are most often buried using a cable plough towed from a barge, or purpose-built large dynamic positioning vessel. Other methods for cable burial include simultaneously lay and bury using tracked remotely operated vehicles (ROVs), and pre-excavating a trench. In keeping with the United Nations Convention on the Law of the Sea, cable installation vessels usually establish a one nautical mile safety zone around the area when installing or handling cables. This also provides a safety buffer should MEC be encountered during operations.

In water depths of the U.S. Atlantic OCS, the target cable burial depth is likely to be approximately 2 m. Cables are often buried in a narrow (less than 1 m wide) trench cut by plough or water jet. The majority of cable burial operations are in deeper waters and are done using cable ploughs, ROVs, or the bottom is jetted or trenched. Cable burial may be carried out by divers in shallow water or horizontal directional drilling can route the cable under the beach and offshore to deeper waters. If the water is too shallow for the main lay vessel to approach safely, a smaller shallow drafted vessel may be used to lay the shore end. Activities associated with the installation of marine cables have the potential for interacting with MEC. Typical marine cable construction includes installation operations and equipment that are described in the following paragraphs.

4.3.1.1 Pre-Lay Grapnel Run

A Pre-Lay Grapnel Run (PLGR) is carried out if the developer plans to use a plough to bury the cable. The PLGR is done following the cable route survey and usually a few weeks before the main laying. The PLGR is performed to ensure that the route is clear of obstructions such as discarded cables or debris, abandoned fishing equipment, and cables. Removal of debris ensures a clear route for the cable lay to proceed so that burial can be efficient. Because it involves towing a plough or heavy grapnels along the planned cable route, it may encounter MEC that is either just beneath or proud to the bottom. A typical PLGR is not selective and is not a considered an appropriate method for addressing MEC because it involves a high probability of encountering MEC due to the area disturbed and the potential for a detonation.

4.3.1.2 Cable Ploughing

The most efficient cable burial method is by cable plough which is towed on the seafloor behind the cable ship. The cable passes through the plough and is buried into the seafloor. The plough lifts a wedge of sediment so that the cable can be inserted below, thus minimizing seafloor disturbance to a very narrow corridor. The cable is laid to conform to the contours of the seafloor thus avoiding suspension of the cable above the seafloor.

Ploughs typically weigh from 10 to 30 metric tons for shallow cable burial and can generate significant forces during deployed to the seafloor and operations and therefore have potential to detonate encountered MEC located both on and below the seafloor.

4.3.1.3 ROV Cable Lay and Burial

Simultaneous cable lay and burial using a tracked ROV is similar to installation using a cable plough but uses an ROV instead of a plough. Use of tracked ROVs is typically limited to inner-

array cable due to the size and quantity of cable the ROV can carry. The forces are sufficient to detonate sensitive MEC that the tracked ROV encounters directly.

Connecting the inner-array cable to the wind turbines usually requires divers or an ROV.

4.3.1.4 Cable Jetting

Cable jetting is often employed to install inter-array cables, especially where the sediment is mobile or is relatively soft and does not require a plough for cable burial. In addition, following plough burial, a post lay burial and inspection is normally conducted in areas where the plough is unable to bury the cable, such as at cable and pipeline crossings, and where the plough may have been recovered for repairs. This burial is typically carried out by ROVs (AUVs are also being developed that perform the burial), which buries the cable to the same target depth as the main lay plough but through use of a water jet. The conduct of water jetting with an ROV minimizes seafloor disturbance, is a less aggressive installation methodology (compared with cable ploughing), and is less likely to inadvertently cause MEC to detonate. Although some cable ploughs use water jets, the plough, rather than the water jet is the main source of concern in relation to MEC.

4.3.1.5 Cable Trenching

Cable trenching proceeds by pre-excavating a trench using a backhoe dredge, laying cable in the trench using a cable laying vessel and filling the trench with the dredge. The cable must be buried and trenching tools such as rock saws or chain saws can cut a cable trench when use of a cable plough or jetting is not effective because the seafloor is too hard. It is possible to concurrently cut the trench and lay the cable. The forces generated during cable trenching are sufficient to cause MEC to detonate.

4.3.1.6 Deployment of Anchors

Where the water is less than 10 m in depth, cable ploughs may be deployed from a moored vessels. Anchors are required to stabilize the vessel and to give it sufficient counter-force to plough in the cable. The anchors facilitate this and the anchors are generally positioned using a tugboat. There is a risk that anchors dropped directly on MEC could cause a detonation. However, the deployment and tensioning of the anchor cables are less likely to cause MEC to detonate.

4.3.1.7 Concrete Mattress Placement

When conditions prevent cable burial, concrete mattresses are often placed over the cables for protection. This is typically done by carefully lowering the mattress using a crane with divers or ROVs guiding the final emplacement. Although concrete mattress placement is not a very aggressive installation technique (when compared with foundation and/or cable installation) it is possible that the kinetic energy involved is sufficient to result in an MEC detonation. The consequences of such a detonation are a significant concern if divers are present.

4.3.1.8 Rock Placement

Where seafloor conditions prevent cable burial or deployment of concrete mattresses, rock can be used for cable burial. When pipelines proud of the seafloor are crossed by cables, the cable and pipeline can be protected by a post cable lay rock placement. The protective layer of rock is designed to minimize impacts from fishing gear. Rock emplacement involves a sufficient amount of kinetic energy that could cause the detonation of MEC.

4.3.2 Installation of Substructures and Foundations

Construction of meteorological masts, wind turbines, and ESPs for offshore substations involves the installation of substructures and foundations. The installation methods for the various foundation types are similar. It is expected that monopiles or jacket foundations will be used for most U.S. construction. Typically, piled jacket foundations are installed using a specialty vessel and involves significant force to drive the piles into the seafloor. In addition, the vessels typically place legs or spuds on the seafloor to maintain position and stability. Placement of the legs can generate enough kinetic energy to cause MEC to detonate.

4.3.2.1 Monopiles

Monopiles are driven into the seafloor to depths of 80 to 100 feet below the sediment surface, ensuring structural stability. A transition protruding above the waterline provides a level surface to which the tower is attached. At shallow sites with a solid seafloor, gravity-based systems can be used, eliminating the need to use a large pile-driving hammer. Monopiles can be installed in several ways.

Installation of monopiles and jackets is commonly done using purpose designed jack up vessels. After arrival on site, the pile is turned so that its base sits on the seafloor. A hydraulic hammer drives the pile into the seabed. A drill inserted through the pile is used to reach the target depth when rocky subsurface conditions preclude pile-driving operations. Regardless of the foundation installation method used, the key factor concerning MEC risk is the kinetic energy employed during the installation, which could be sufficient to cause MEC to detonate.

4.3.2.2 Jackets and Tripods

Jackets and tripods are raised into place by heavy-lift vessels. The piles used to secure jackets and tripods to the seafloor are significantly smaller in diameter and length than monopile foundations. Piles are either driven through sleeves at each corner of the jacket or the jacket may be placed over pre-driven piles. A transition piece is pre-attached to save a lifting operation. Scour protection is less critical for jackets and tripods than for monopiles. Similar to the installation of monopiles, the forces from pile installation are sufficient to cause MEC to detonate.

4.3.2.3 Gravity Foundations

Gravity foundations are concrete structures that use their weight (including ballast) to resist wind and wave loading and remain upright. Gravity foundations are most likely to be used where piles cannot be driven as they rest upon on the seafloor. Gravity foundations require subsurface preparation and the use of heavy-lift vessels.

The site on the seafloor on which a gravity foundation is placed is prepared to produce a flat solid base. This preparation may include removal of sediment using an excavator on a barge or a dredge and placement of stone to create a weight-bearing layer. Depending upon the method used to prepare the seafloor (e.g., clamshell bucket) for the foundation it is possible the MEC could be brought to the surface.

Gravity foundations are either floated and towed to the site and sunk, or are transported on a vessel, lifted and placed in position. Once in their final position, the foundations are sunk by filling them with sand, gravel or concrete. The sinking process is gradual allowing the foundation to be placed precisely on the prepared area. After placement of the foundation, scour

protection is installed. Although gravity foundation installation is not an especially aggressive installation methodology (when compared to pile-driving) it is possible that the operation could cause MEC to detonate.

4.3.2.4 Scour Protection Systems

Structures placed in a current where the seabed is erodible are subject to scour that may lead to structural instability. Scour is the removal of sediment from around an object on the seafloor. Wind turbines, offshore substations, and meteorological mast foundations are likely to require scour protection. Common measures for scour protection include dumping rock of differing sizes and placing concrete mattresses around the foundation. Monopiles, gravity foundations, and tripods require significant scour protection, while piled jackets require little or no scour protection (Kaiser and Snyder 2011).

Rock is usually installed by side dumping barges or other vessels following completion of the inter-array cabling to guard against erosion. Scour protection may also be laid before piling operations commence. The placement of rock or scour protection systems, may generate enough kinetic energy to cause MEC to detonate.

Page Intentionally Left Blank.

5.0 MEC Risk Management Framework

BOEM plans to develop guidance for renewable energy developers (e.g., offshore wind, wave, and ocean energy capture) on identification and site clearance methodologies specific to MEC as required in a Construction and Operations Plan. This guidance will aid the developers in identifying and addressing concerns for human safety and environmental protection relating to MEC. Currently, offshore renewable energy project contractors do not have guidance to aid them in collecting desktop data concerning the possible presence of MEC, where they can expect to encounter MEC or the technologies available to detect these hazards. It is recommended that offshore wind developers consider an approach for integrating risk assessment information into the process of evaluating their site. An essential part of the risk assessment is the development of a framework for assessing sites that may vary greatly in terms of complexity, physical and chemical characteristics and in the risk that they may pose to human health and the environment.

In order to assist BOEM in taking an informed approach to developing guidance for addressing the concerns for human safety and environmental protection during offshore renewable energy development, CALIBRE collected and mapped historical data relating to MEC potentially present in each of the Atlantic OCS WEAs and is using this to evaluate a technology and methodology selection process. The data collected is a sampling of what is available and is not comprehensive. The information presented here does not meet the appropriate inquiry baseline that should be undertaken for each site to determine MEC hazards.

The MEC hazard and risk assessments presented in this chapter are based on methods described in the Construction Industry Research and Information Association (CIRIA 2015) risk management framework but differ in some significant ways. For example, the model proposed here incorporates the probability of an MEC encounter, the MEC sensitivity, and the energy from a specific activity in developing a probability of detonation in a structured fashion for incorporation into the risk assessment. The MEC hazard and risk assessment methods presented in this chapter are based on a solid approach but the model requires testing before being applied by BOEM. Therefore, the approach presented here must be considered preliminary until it is fully tested. In addition, the approach as presented here addresses only a detonation on the seafloor and does not address the hazard to workers in the water (e.g., divers) at the time of detonation or the detonation of MEC at the surface of the sea (e.g., on deck).

5.1 Evaluating and Managing MEC Risk

The presence of a valid risk, defined as a measure of the potential for a particular MEC hazard to have an adverse effect on an identified receptor, is based on several factors. These include the presence of MEC, receptors, and an activity that can allow the MEC to affect the receptors, often referred to as an exposure pathway. A complete, or potentially complete, exposure pathway is necessary to consider when evaluating risk. Clearly, if MEC or receptors are not present in an area, then harm cannot occur. Likewise, MEC that has remained undisturbed is unlikely to detonate without some outside influence (e.g., impact, shock).

MEC is a term that distinguishes specific categories of military munitions that may pose unique explosives safety risks. MEC includes:

- ▶ UXO¹, as defined in 10 U.S. Code (USC) 2710 (e) (9);
- ▶ Discarded military munitions², as defined in 10 USC 2710 (e) (2), or
- ▶ Munitions constituents³ (e.g., trinitrotoluene [TNT], RDX) present in high enough concentrations to pose an explosive hazard. (10 USC 2710 (e) (3)).

Initiation of an MEC item during renewable energy development could adversely affect a number of receptors. Typical receptors include:

- ▶ Personnel (e.g., construction workers),
- ▶ Equipment /Infrastructure (e.g., work vessels, pipelines),
- ▶ Natural Resources (e.g., marine mammals, fish), and
- ▶ Cultural resources (e.g., ship wrecks).

An underwater MEC detonation presents several main hazards: cutting, blast, fragmentation, bubble jet, and shockwave. These may directly or indirectly affect the receptor. A discussion of the various effects can be found in CIRIA (2015, 45-47).

Activities with the potential to affect MEC and impact these receptors must be identified and the impacts evaluated. Typical offshore renewable energy development activities are described in the previous section and include:

- ▶ Site characterization,
- ▶ Construction,
 - Cable laying, and
 - Installation of substructures and foundations.

A hazard is a condition with the potential to cause injury, illness, or death of personnel; adverse impacts to the environment; damage to or loss of equipment or property; or that affects operations. Therefore, a hazard can have several possible negative outcomes or losses (e.g., death, adverse environmental impacts, increased cost, schedule slippage, adverse public relations).

Risk is determined after hazards are identified and analyzed and is presented as a combined expression of loss probability and severity. The four principles of risk management are:

1. Integrate risk management into all phases of missions and operations.
2. Make risk decisions at the appropriate level.

¹ Unexploded Ordnance (UXO). Military munitions that have been primed, fuzed, armed, or otherwise prepared for action; have been fired, dropped, launched, projected, or placed in such a manner as to constitute a hazard to operations, installations, personnel, or material; and remain unexploded whether by malfunction, design, or any other cause.

² Discarded Military Munitions. Generally, military munitions that have been abandoned without proper disposal or removed from storage in a military magazine or other storage area for the purpose of disposal.

³ Munitions Constituent. Generally, any materials originating from UXO, discarded military munitions, or other military munitions, including explosive and nonexplosive materials, and emission, degradation, or breakdown elements of such ordnance or munitions.

3. Accept no unnecessary risk.
4. Apply risk management cyclically and continuously (U.S. Army 2014).

Addressing the hazards posed by MEC is just one part of the risk management strategy necessary during renewable energy development activities.

Risk management is the primary process for assisting organizations and individuals in making informed risk decisions in order to reduce or mitigate risk, increasing the probability of successfully completing not only a given activity, but the development project as a whole. Risk management is a systematic, cyclical process consisting of identifying and assessing hazards, and controlling associated risks and making decisions that balance risk costs with benefits. Although not considered MEC, a good example of a risk management decision based on a cost benefit analysis involves the risk posed by small arms ammunition. The severity of an incident involving small arms ammunition is negligible while the cost of detecting and addressing the risk *in situ* would be exorbitant. Thus, responsible decision makers are likely to find the risk tolerable given that there is only a negligible risk to start with, and there is likely to be little reduction in risk by implementing mitigation measures while costs would be quite high.

It is the responsibility of all members of the development team, from the developer's staff to their consultants and subcontractors, to integrate risk management into planning and operations. The risk assessment provides for enhanced situational awareness that builds confidence and allows the implementation of timely, efficient, and effective protective control measures.

CIRIA recently published essential risk management guidelines in their report entitled, *Assessment and management of unexploded ordnance (UXO) risk in the marine environment* (CIRIA 2015). In the report, CIRIA provides a four-stage risk management plan to deal with munitions hazards in construction. The approach presented here is an adaptation of the CIRIA guidelines and is iterative because the steps build upon previous work completed. The MEC risk framework consists of the following steps:

- ▶ MEC Hazard Assessment
- ▶ MEC Risk Assessment
- ▶ MEC Risk Validation
- ▶ MEC Risk Mitigation

For this project, the focus is on MEC risk assessment in the Delaware WEA. The completion of the second step of the risk management process relies on data collected during the MEC hazard assessment. The MEC hazard assessment identifies the hazards (i.e., MEC) that may be encountered in a specific development area and the sensitivity of those items. The MEC risk assessment determines the potential impact of each hazard on specific development activities. The third step includes a management review to determine which of the identified theoretical MEC risks are partially tolerable or intolerable and to validate those to allow for their mitigation.

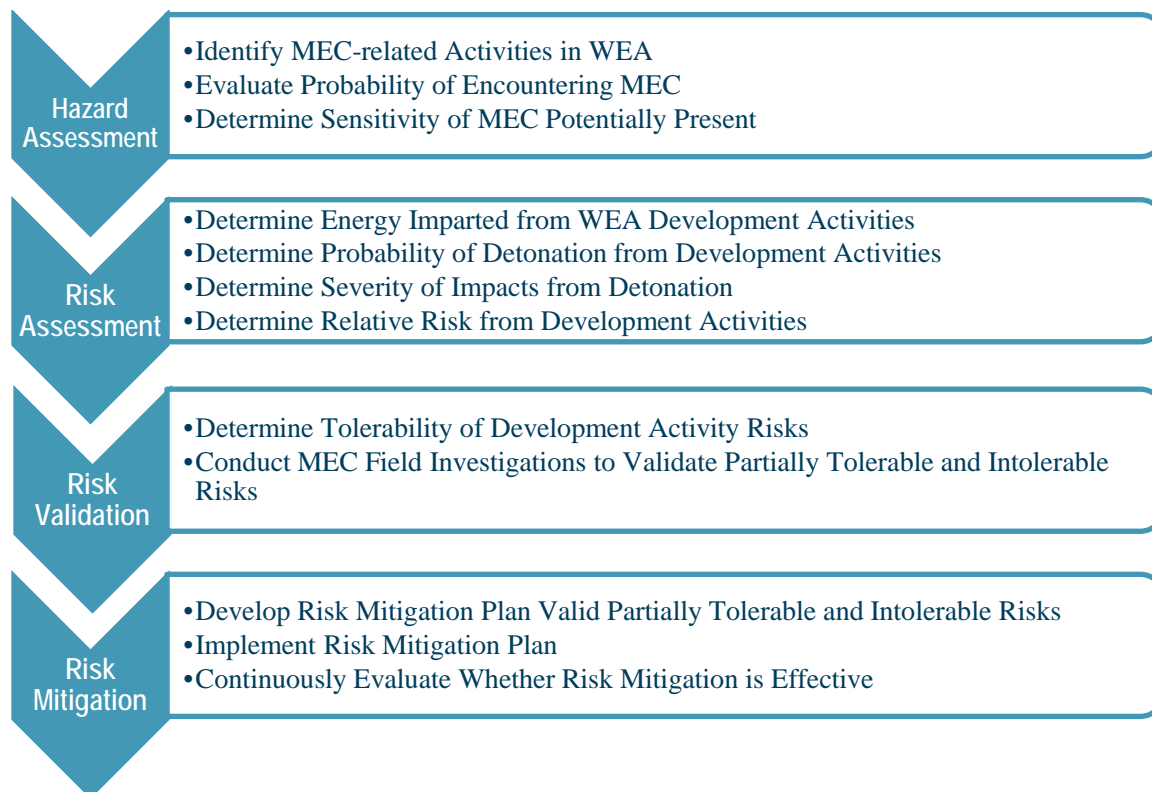
The purpose of this document is to explain a method for determining the risk for survey and installation of the marine cables, substructures and foundations for offshore renewable energy development using the munitions we have identified in the Delaware WEA. The MEC risk assessment in this document was done as a demonstration of one of way to evaluate MEC risk but the methodology is still conceptual at this time and should not be considered fully developed or verified.

5.2 MEC Risk Management Framework Components

The MEC risk management framework (Figure 5-1) consists of four components.

1. **MEC Hazard Assessment.** Identify risks associated with MEC found in the renewable energy development area. The initial step is an analysis of current and historical activities involving munitions, as described in Section 5.2.1 MEC Hazard Assessment.
2. **MEC Risk Assessment.** Review each risk in terms of the probability and severity of impact of occurring as described in Section 5.2.2 MEC Risk Assessment. Based on the probability and magnitude of the impact, prioritize the risks and determine how to validate them, if necessary.
3. **MEC Risk Validation.** Based on the prioritization and type of risk, validate the partially tolerable and intolerable risks through fieldwork (in this case, identify those munitions that need to be detected), as described in Section 5.2.3 MEC Risk Validation.
4. **MEC Risk Mitigation.** Once the risk scores are determined, decision makers review the partially tolerable and intolerable risks and identify risk mitigation measures as described in Section 5.2.4 MEC Risk Mitigation. The identified risk mitigation measures are then implemented, and are continuously evaluated for effectiveness.

Figure 5-1: MEC Risk Management Framework



5.2.1 MEC Hazard Assessment

The MEC hazard assessment is largely a desktop exercise that identifies potential sources of danger related to MEC. The MEC hazard assessment consists of the collection of information to establish the types of activities that occurred or are currently occurring in the renewable energy development area and the anticipated types, location, and distribution of MEC involved. The MEC hazard assessment is based on obtaining and reviewing information that is publicly available, obtainable from its source within reasonable time and cost constraints, and practically reviewable. The MEC hazard assessment assigns a probability grade concerning the likelihood of an encounter with MEC present in the renewable energy development area.

Given the complexity and cost of renewable energy development, this research should include review of records at a variety of repositories such as those at the National Archives and Record Administration and available from the DoD. If research determines that MEC is potentially present, the probability of encountering MEC is evaluated and is assigned a grade. A probability grade between 1 (unlikely) and 5 (probable) is assigned (Table 5-1) based on the history of the area (e.g., training area used for decades) and likely distribution of MEC (e.g., low intensity anti-submarine activity). The likelihood of encountering MEC is based upon site history (e.g., UXO type and distribution) and physical environment factors (e.g., site bathymetry sediment accumulation rate). As the MEC risk evaluation framework is further developed, it may be desirable to also consider the area that a given renewable energy development activity will interact with (i.e., an activity that disturbs a km² of the seafloor is more likely to encounter MEC than an activity that only disturbs one m²).

Table 5-1: MEC Encounter Probability Factor

| Probability Factor | Descriptor | Definition |
|--------------------|-------------|---|
| 1 | Unlikely | Possible encounters but improbable |
| 2 | Possible | Infrequent encounters |
| 3 | Likely | Sporadic or intermittent encounters |
| 4 | Very Likely | Several or numerous encounters |
| 5 | Probable | Regular or almost inevitable encounters |

Once the MEC potentially present is identified an explosive safety specialist evaluates the events leading to its possible deposition in the study area (e.g., disposal, combat, training), explosive train status (e.g., incomplete, fuzed and fired), sensitivity of the munitions (e.g., sensitive fuzing, armor piercing), and sensitivity of the filling (e.g., insensitive explosive, shock sensitive explosive). Based upon the explosive safety specialist's professional judgment, the MEC is assigned a sensitivity factor of 1 (insensitive) to 5 (high) (Table 5-2).

Table 5-2: MEC Sensitivity Factor

| Sensitivity Factor | Descriptor | Examples |
|--------------------|-------------|---|
| 1 | Insensitive | Armor piercing munitions Pyrotechnics Bulk propellants and explosives |
| 2 | Low | Munitions with incomplete explosive trains such as sea-disposed military munitions |
| 3 | Moderate | UXO Fuzed sensitive disposed military munitions |
| 4 | High | Fuzed sensitive munitions such as a sea mine with chemical horns Sensitive fillings such as picric acid filled munitions |

If this research determines that MEC are potentially present in the renewable energy development area, the probability and sensitivity grades can be used when undertaking an MEC risk assessment.

5.2.2 MEC Risk Assessment

The MEC risk assessment is also a desktop study that measures the potential for anticipated MEC hazards to have an adverse effect on an identified receptor, based on the MEC hazard assessment, and planned renewable energy area development activities. The MEC risk assessment is based on the MEC hazard assessment (probability of encountering and sensitivity of the specific MEC), the energy imparted during the planned renewable energy area development activities and the severity of the consequences should the MEC detonate. Semi-quantitative grades are assigned to the probability of detonation and severity of a given scenario, which are used to determine an overall risk. The results of the risk assessment are used to prioritize risks based on their probabilities and impact. A number of factors come into play when applying professional judgment to the probability and consequences of a detonation. These include:

- ▶ Age and condition of the MEC
 - Explosive properties may change with extended exposure to seawater (Pfeiffer 2012)
 - Mechanical aspects of the explosive train may be disrupted (e.g., corrosion may fuse mechanical parts)
- ▶ Type of explosive, power and sensitivity
- ▶ Net explosive weight (i.e., TNT equivalent weight)
- ▶ Location relative to seafloor (e.g., floating above, on surface, partially or fully buried)
- ▶ Proximity to sensitive receptors (e.g., diver at the site of detonation)
- ▶ Design and construction of vessels, equipment or structures at the site of a detonation
- ▶ Vertical and lateral offset (e.g., depth, distance) of detonation from receptor

The likelihood of an MEC detonation is based on the sensitivity of the item and the energy imparted to the item during the planned renewable energy area development activities. A relative energy factor between 1 (very low) and 5 (very high) is assigned to each activity (Table 5-3).

Table 5-3: Development Activity Energy Factor

| Activity Energy Factor | Descriptor | Examples |
|------------------------|------------|--|
| 1 | Very Low | Non-intrusive, non-contact geophysical survey |
| 2 | Low | Geotechnical survey |
| 3 | Moderate | PLGR operation Placement of jack up barge legs Anchor deployment Cable jetting Concrete mattress placement |
| 4 | High | Cable ploughing Cable trenching Scour protection Armoring with rock |
| 5 | Very High | Driving of monopiles |

The probability of detonation grade determination is based on a combination of factors including the probability of an encounter with an MEC type, sensitivity of the MEC, and the energy transmitted (Table 5-4).

A severity grade is assigned based on the type of receptor and the likely impact to that receptor from an MEC incident (Table 5-5). The severity of the effects from a detonation is based on a number of factors. The primary factor is the net explosive weight of the MEC. However, these effects may be mitigated by the water column and burial in sediments. Other factors include distance from the receptor (e.g., individual, vessel, equipment) and the robustness of the receptor (e.g., double-steel-hull vessel, marine mammal).

Table 5-6 equates the severity of the effects of a detonation on vessels, personnel on the vessel, and equipment based on the net explosive weight⁴. When considering the severity of effects on equipment, important considerations are the distance from the detonation and the nature of the equipment (e.g., setback for a cable plough may be sufficient that a detonation will have little effect on the vessel and onboard equipment but may have catastrophic effects on the plough). Additional tables can be prepared to equate the effects on other receptors to the net explosive weight. For example, the net explosive weight that would cause a catastrophic effect on a diver in the water would be much less.

Severity grades are not appropriate for evaluating risk associated with chemical warfare materiel.

⁴ Net explosive weight - The total weight of all explosives substances (i.e., high explosive, propellant weight, and pyrotechnic weight), usually expressed as pounds of a TNT equivalent.

Table 5-4: Probability of Detonation Grade Matrix

| Activity Energy Factor (Table 5-2) | MEC Sensitivity Factor (Table 5-2) | MEC Encounter Probability Factor (Table 5-1) | | | | |
|------------------------------------|------------------------------------|--|----------|--------|-------------|----------|
| | | Unlikely | Possible | Likely | Very Likely | Probable |
| 1 - Very Low | 1 - Insensitive | 1 | 2 | 3 | 4 | 5 |
| | 2 - Low | 2 | 4 | 6 | 8 | 10 |
| | 3 - Moderate | 3 | 6 | 9 | 12 | 15 |
| | 4 - High | 4 | 8 | 12 | 16 | 20 |
| 2 - Low | 1 - Insensitive | 2 | 4 | 6 | 8 | 10 |
| | 2 - Low | 4 | 8 | 12 | 16 | 20 |
| | 3 - Moderate | 6 | 12 | 18 | 24 | 30 |
| | 4 - High | 8 | 16 | 24 | 32 | 40 |
| 3 - Moderate | 1 - Insensitive | 3 | 6 | 9 | 12 | 15 |
| | 2 - Low | 6 | 12 | 18 | 24 | 30 |
| | 3 - Moderate | 9 | 18 | 27 | 36 | 45 |
| | 4 - High | 12 | 24 | 36 | 48 | 60 |
| 4 - High | 1 - Insensitive | 4 | 8 | 12 | 16 | 20 |
| | 2 - Low | 8 | 16 | 24 | 32 | 40 |
| | 3 - Moderate | 12 | 24 | 36 | 48 | 60 |
| | 4 - High | 16 | 32 | 48 | 64 | 80 |
| 5 - Very High | 1 - Insensitive | 5 | 10 | 15 | 20 | 25 |
| | 2 - Low | 10 | 20 | 30 | 40 | 50 |
| | 3 - Moderate | 15 | 30 | 45 | 60 | 75 |
| | 4 - High | 20 | 40 | 60 | 80 | 100 |

Table 5-5: Severity of MEC Detonation Effects Factor

| Severity Factor | Description | Definition | Summary |
|-----------------|--------------|---|---|
| 1 | Negligible | <p><u>Personnel</u> – Occurrence (e.g., startling sound) causing minor disruption of activity</p> <p><u>Equipment/Infrastructure</u> – Damage that does not affect usability (e.g., cosmetic) or is similar to normal wear and tear that is readily repaired by onsite personnel (e.g., replace shear pin)</p> <p><u>Natural Resources</u> – Temporary minor disturbance (e.g., sound causing feeding birds to take flight) or other <i>de minimus</i> impacts (e.g., disturbance of sediments impacting a small area)</p> <p><u>Cultural Resources</u> – <i>De minimus</i> impacts to a cultural resource (e.g., similar to typical aging processes)</p> | No injury or loss, with <i>de minimus</i> damage or impact to activities |
| 2 | Minor | <p><u>Personnel</u> – One or more injuries requiring no more than onsite first aid (e.g., cut, bruise), outpatient medical care and may result in restricted work or transfer to another job (29 CFR 1907.4(b)(4))</p> <p><u>Equipment/Infrastructure</u> – Relatively minor damage that may affect usability and requires repair</p> <p><u>Natural Resources</u> – Temporary disturbance (e.g., sound causing minor injury to marine mammals, fish or birds) or other minor impacts with no significant long term impacts (e.g., loss of a small number of individuals of a common species)</p> <p><u>Cultural Resources</u> – Minor impacts to a cultural resource (e.g., similar to typical aging processes)</p> | Minimal injury, loss, or damage; little or no impact to activities |
| 3 | Moderate | <p><u>Personnel</u> – Lost time accident (29 CFR 1904.7(b)(3)) to one or two individuals</p> <p><u>Equipment/Infrastructure</u> – Significant damage limited to a small area</p> <p><u>Natural Resources</u> – Significant temporary disturbance/impact to marine animals (e.g., injure a small number of protected marine animals, injure or kill a modest number of common fish or birds)</p> <p><u>Cultural Resources</u> – Significant impacts but no greater than might be expected from a large natural event (e.g., storm)</p> | Minor injury, illness, loss, or damage; degraded ability to complete activities |
| 4 | Severe | <p><u>Personnel</u> – Injuries to three or more individuals requiring hospitalization or resulting in one or more permanent partial disabilities</p> <p><u>Equipment/Infrastructure</u> – Significant damage to a major item that hinders operations and requires a shore-based repair</p> <p><u>Natural Resources</u> – Significant disturbance/impact to marine animals (e.g., kill a protected marine animal, injure or kill a significant number of common fish or birds)</p> <p><u>Cultural Resources</u> – Impacts greater than might be expected from a large natural event (e.g., storm)</p> | Severe injury, illness, loss, or damage; significantly degraded ability to complete activities |
| 5 | Catastrophic | <p><u>Personnel</u> – Injuries to one or more individuals resulting in permanent total disabilities or one or more fatalities</p> <p><u>Equipment/Infrastructure</u> – Significant damage to a major item requiring major rebuilding or repair, threatens the seaworthiness of a vessel or causes damage to nearby infrastructure (e.g., ruptures a pipeline)</p> <p><u>Natural Resources</u> – Kill more than one protected marine animal, or kill or injure a large number of common fish or birds</p> <p><u>Cultural Resources</u> – Loss of the resource (e.g., demolition of shipwreck)</p> | Death, unacceptable loss or damage, mission failure, or ability to complete activities eliminated |

Notes: Table based on CIRIA (2015) and U.S. Army (2014).

Page Intentionally Left Blank.

Table 5-6: Relation of Net Explosive Weight to Severity of Effects from Underwater Detonation on Vessels, on Board Personnel, and Equipment

| Severity Grade | Descriptor | Net Explosive Weight | | Examples |
|----------------|--------------|----------------------|-------------|------------------------------------|
| | | kg | lb | |
| 1 | Negligible | <5 | <11 | Anti-aircraft artillery projectile |
| 2 | Minor | >5 to 15 | >11 to 33 | Artillery projectile |
| 3 | Moderate | >15 to 50 | >33 to 110 | Hedgehog |
| 4 | Severe | >50 to 250 | >110 to 550 | Depth charges, torpedoes, bombs |
| 5 | Catastrophic | >250 | >550 | Sea mine, torpedoes |

Note: This table is to be used for a detonation on the seafloor when no personnel are in the water (e.g., no divers). The same net explosive weight may have differing severity grades depending on the situation (e.g., detonation in the water near divers, recovery of MEC and subsequent detonation on deck).

The risk matrix uses the probability of a MEC detonation from a specific renewable energy development activity and the severity of the consequences should that occur, to determine the relative risk (Table 5-7). The developer must make a determination as to whether the risk is tolerable or if mitigation measures are necessary. The advantage of using a risk matrix as the risk assessment tool is that it enables MEC hazards to be quickly assessed and provides a comparison of relative risk levels between MEC hazards. This allows insignificant MEC hazards to be screened out and focuses risk management activities on the more significant MEC hazards.

All renewable energy area development activities involve some level of risk. The conduct of a semi-quantitative evaluation allows decision makers to understand the risks associated with the development activities and to identify when it is necessary to take action to mitigate the risks. The MEC risk assessment step considers the MEC identified in the hazard assessment as potentially present in the area of operations, the probability of a detonation and the consequences should a detonation occur and is used by the developer’s management team to determine the tolerability of the theoretical MEC risks. Those risks that the management team determines may require mitigation are typically investigated through fieldwork during the MEC risk validation step.

Table 5-7: MEC Risk Assessment Matrix

| | | | | | | |
|--|-----------|--|---------------|---------------|------------------|------------------|
| Probability of Detonation Grade (Table 5-4) | 81 to 100 | Low | Medium | High | Very High | Very High |
| | 61 to 80 | Low | Medium | High | Very High | Very High |
| | 41 to 60 | Low | Medium | Medium | High | Very High |
| | 21 to 40 | Low | Low | Medium | High | High |
| | 1 to 20 | Low | Low | Medium | Medium | High |
| | | Negligible | Minor | Moderate | Severe | Catastrophic |
| | | 1 | 2 | 3 | 4 | 5 |
| | | Severity of Detonation Effects Factor (Table 5-6) | | | | |

5.2.3 MEC Risk Validation

Effective MEC risk management reduces the probability or impact of adverse events involving MEC throughout the life of the development. MEC risk management involves making decisions concerning the tolerability of the risks identified and developing a strategy to avoid (e.g., reroute cables to avoid MEC) or mitigate MEC risks to tolerable levels. The risk assessment identifies the MEC that may pose unacceptable risks during specific renewable energy area development activities. As part of MEC risk validation, investigative surveys are performed to determine the presence of MEC so that a plan for mitigating the MEC presenting an unacceptable risk can be developed prior to any potentially hazardous investigative or installation activities (e.g., removal of a sea mine prior to cable burial activities). Establishing effective lines of communication is essential to project safety and success.

5.2.4 MEC Risk Mitigation

During the MEC risk validation step, the developer's management team determines the conditions requiring MEC risk mitigation. MEC risk mitigation measures are developed and implemented to reduce the probability and impact of the identified MEC risks. The mitigation measures depend on the nature of the risk and how that interacts with the renewable energy area development activities. In general, the measures can be categorized as proactive and reactive. Proactive mitigation measures vary from geophysical MEC surveys to identify the MEC, allowing simple avoidance of the MEC during development and operations to elimination of the hazard (e.g., removal, detonation). Reactive mitigation measures include the preparation of emergency response procedures and staffing UXO-qualified personnel onboard during site activities. Once the MEC risk mitigation measures are identified, monitoring their implementation and effectiveness is necessary as well as periodically determining if new risks requiring mitigation are present. The design and implementation of MEC risk mitigation measures is beyond the scope of the current study.

Page Intentionally Left Blank.

6.0 Technologies, Platforms, and Positioning Techniques

This section summarizes research on available technologies for understanding MEC in areas that are designated for offshore renewable energy development on the Atlantic OCS. MEC are potentially present in renewable energy lease and planning areas managed by BOEM along the Atlantic OCS. Assessing the risk posed by MEC is critical in the early stages of renewable energy development. This chapter presents a market survey summary to provide a broad overview of available technologies. It is not a comprehensive database of all available technologies, but it provides a broad overview of the technologies available.

This section was developed based on a literature review of both peer-reviewed journals and other sources (e.g., trade journals, manufacturer's specifications) to identify technologies that may be applicable to the detection of MEC in the Atlantic OCS WEAs. The market survey consisted of a review of technical literature, marketing materials from vendors, and follow up discussions with vendors to address questions or ambiguities.

Technology selection and deployment is a step-wise process, requiring multiple data inputs and a series of screening processes. Primary data inputs are the environmental conditions of the study area, the MEC types expected, and how deeply they might be buried below the sediment surface. The process may also be multi-phased with initial phases oriented to general characterization of the physical conditions at a site (e.g., relief), concentrations of metallic items and other potential hazards. Later phases may focus more closely on smaller areas, identifying locations for foundations and cable routes that are relatively free of potential hazards.

A nested series of surveys, with increasing resolution at each successive step, is a typical approach for surveying due to the differing capabilities, platforms and resolution of datasets necessary to characterize a site. Developing an approach involves estimating the vessel size and amount of ship time needed for a certain area and type of coverage. As with all survey work, navigation precision and accuracy are important considerations. Detection and discrimination performance, availability, coverage rates and cost are additional criteria in identifying a preferred approach and in developing a survey methodology.

A variety of technologies are available for detecting and locating MEC in a given area, and an effective survey often requires using multiple techniques. Detection technologies fall into three categories: optical, acoustic or electromagnetic. Successful detection may involve a combination of sensors and the operation of multiple platforms. Commonly used platforms from which sensors are deployed include surface vessels, towed systems, and remotely controlled or autonomous vehicles. This section provides a summary of the methodologies and technologies reviewed, and it identifies those that are most promising for detection of MEC in the Atlantic OCS WEAs. The various platforms and technologies and their applicability to various site conditions is summarized in Table 6-8 at the end of this Section.

6.1 Navigation and Positioning

The goal of any underwater investigation is to use the most accurate and cost-effective positioning systems available, though care must be taken in selecting how positioning systems used for mapping and later reacquisition, for detailed investigation or recovery purposes, relate to one another. A number of common navigation and positioning systems can be combined with underwater platforms and technologies to provide positional accuracy on the order of a meter (or sub-meter).

The objective for surveying a WEA is to determine the locations of MEC presenting potential threats to operations therefore accurate positioning of the sensor is a critical component of underwater MEC detection and mapping. Detecting and discriminating individual anomalies and targets is more difficult if they cannot be accurately positioned for analysis alongside other vital datasets (e.g., bathymetry, side-scan sonar, and sub-bottom profiler data) or to support follow-on activities, such as a more detailed investigation at higher resolution or intrusive investigations to reacquire the same target of interest. If the location of a target of interest is not accurate, it may be necessary to investigate multiple locations to ensure the target of interest is evaluated, leading to a reduction in productivity.

Producing accurate geospatial maps of the detected anomalies is a standard starting point for their close examination. This initial step helps determine if the anomalies are indeed MEC and not false positives. In order to carry out that determination, the object position must be measured with sufficient accuracy. The horizontal navigation uncertainty should be no more than ± 2 m, and if possible ± 1 m (CIRIA 2015).

Information on the various positioning technologies is provided in Table 6-1.

6.1.1 Global Navigation Satellite System

Global Navigation Satellite Systems (GNSS) provide positioning information using radio signals from a constellation of orbiting satellites. The original GNSS system is the United States' Global Positioning System (GPS), which was followed by the Russian GLObalnaya NAVigatsionnaya Sputnikovaya Sistema (GLONASS); other global satellite navigation systems under development include the European Union's Galileo and China's BeiDou. Receivers available today are capable of using GPS and GLONASS, as well as Galileo and BeiDou as they become available. GNSS receivers using GPS or GLONASS individually have positional accuracy of 5-10 m; receivers combining both systems improve accuracy to ± 2 m.

Further improvements in positional accuracy involve correcting for small changes in properties of the atmosphere, known as augmentation. The correction signals may be broadcast by satellite or by terrestrial transmitters. In the United States, the satellite-based augmentation system is Wide Area Augmentation System (WAAS), which typically provides a positional accuracy of ± 1 m. Use of ground-based augmentation, such as Differential GPS (DGPS), can reduce errors further, depending on the distance from the differential transmitter. Carrier-phase augmentation can reduce the error to a centimeter, and can be applied in real time (known as Real Time Kinematic, or RTK) or corrected during post processing of the position data (known as Post Processed Kinematic, or PPK).

GNSS has wide usage in underwater surveying; the particular version used will depend on the required accuracy for positions and the proximity to terrestrial or space based correction sources. GNSS receivers are often mounted to fixed points (e.g., survey vessel, foundation, shore) to provide an accurate surface position. When installed on a survey vessel, positional data can be obtained for other sensors affixed to the survey vessel by calculating offset or layback (U.S. Air Force 2014).

6.1.2 Underwater Positioning Systems

Unfortunately, the radio frequencies used by GNSS are strongly absorbed by water, so different solutions are required for determining position underwater. Sound waves can travel long

distances in water and form the basis for standard underwater positioning systems. The speed of sound in water is to first order constant, so by measuring the travel time between two points a distance can be calculated. There are three common acoustic underwater positioning systems: long baseline (LBL), short baseline (SBL), and ultra-short baseline (USBL). These systems work with surface GPS to provide an underwater position in relation to a surface GPS coordinate. Water temperature, salinity, and pressure affect sound velocity by up to several percent in the ocean, and so if those characteristics are measured the distance calculation can be made more accurately.

6.1.2.1 Long Baseline

The LBL positioning system relies on multiple acoustic transponders positioned on the seafloor that are interrogated by an acoustic signal from the platform; each transponder replies with a unique acoustic signal. The vehicle position is calculated based on the known positions of the transponders and the 2-way travel time to each. Errors are typically about 0.1 percent (%) of the range between transponders and vehicle.

The LBL system supplied with the Hydroid Remus 100, typical for work in water depths less than 100 m, has a maximum range of 2000 m. In setting up a survey, transponders are typically deployed on the seafloor 1000-1500 m apart (Hartsfield 2005). For a typical lease block on the OCS of 4,800 x 4,800 m, a 4 x 4 array of transponders, spaced 1200 m apart, would support a survey of one block with positioning errors of roughly 1 m throughout. However, deploying and recovering the transponders is time consuming; after a transponder is placed on the seafloor its position must be surveyed by piloting the vessel in a circle around the nominal transponder position while recording ranges and vessel positions. Placing and surveying 16 transponders in waters depths of ~100 m would take at least 8 hours; recovering them a similar amount of time. It would be possible to use transponders in a leapfrog fashion, placing a subset of transponders in the next area where navigation is needed while the MEC surveying occurs in the first area, then recovering and repositioning the first transponders after the survey begins in the new area.

Advantages of LBL systems include excellent positional accuracy (decimeter accuracy) independent of water depth (National Oceanic and Atmospheric Administration 2001), redundancy, and wide area coverage. Disadvantages include long deployment, recovery and calibration times, and system complexity that requires experienced operators (Christ and Wernli 2007). LBL system performance may also be reduced by local topographic variations or the presence of large reflectors on the seafloor.

6.1.2.2 Short and Ultra-Short Baseline

SBL and USBL underwater positioning systems rely on transponders mounted on the surface vessel rather than on the seafloor. For SBL systems, three to four transponders are mounted to the vessel as far apart as possible, and ranging is done between those transponders and a responder on the undersea platform. This data is combined with the GNSS positions of the transponders on the vessel to calculate the position of the platform. If the undersea platform requires its position for self-navigation, a telemetry system must be used to transmit the positioning data from the surface. The advantages of SBL systems include redundancy and the ability to be deployed aboard a survey vessel. Disadvantages include lower accuracy when deployed from small vessels potentially necessitating deployment of the system from additional support vessels (Christ and Wernli 2007). Accuracy is increased when utilizing larger vessels

(e.g., coastal research vessels [R/V], which are usually >50 m in length) that allow SBL systems to attain 0.5 to 1 m accuracy (National Oceanic and Atmospheric Administration 2001). For these reasons, USBL systems are used much more frequently.

USBL systems use multiple transducers built into a single transceiver mounted on the support vessel. A USBL system determines a range to the underwater transponder through travel time, but then makes use of an array of hydrophones to measure the direction of arrival for the acoustic response. This is accomplished by measuring the phase difference between the hydrophones and calculating the azimuth and elevation angles. The positional error depends upon range; a 0.1° error in angle will lead to a 17 centimeter (cm) error at 100 m range, or 1.7 m at a range of 1000 m. As range increases, spreading losses and attenuation in the water reduce the strength of the acoustic signal, leading to the greater errors in the phase measurement. Typical USBL systems have errors of 0.5 to 0.2% of slant range (Thomson 2005).

The advantages of the USBL system include ease of operation, generally good accuracy (1 to 2 m accuracy (HDR 2013)), and the ability to deploy from small vessels. Disadvantages include the need for a detailed calibration of the transceiver, that positional accuracy is dependent on the accuracy of the surface DGPS system, and that there are minimal redundancies (Christ and Wernli 2007). Positional accuracy is a function of the distance between the vessel transceiver and the responder, with positional accuracy decreasing as distance increases. Global Acoustic Positioning Systems combines USBL with GNSS and an Inertial Navigation System (INS) to achieve a higher level of accuracy.

6.1.2.3 Inertial Navigation Systems

INS, in combination with a Doppler Velocity Log (DVL) and depth sensor and integrated with GNSS, is commonly used for AUV positioning. AUVs typically carry a GNSS receiver, but since these signals are absorbed by water, the GNSS receiver only functions when the platform is at the surface. Once the platform submerges, the DVL bounces sound off the seafloor both along and across the track of the platform, and by measuring the Doppler shift of those reflected beams, can measure the platform velocity over the seafloor. The INS measures accelerations, rotation, and sometimes magnetic field for magnetic heading determination; more expensive and sensitive INS systems can measure the rotation of the Earth to determine true heading.

By combining the last GNSS position obtained before submerging with that of the INS and depth sensor, a position in three dimensions can be calculated for the platform. Error in the accuracy of the measurements accumulates over distance traveled after submerging, typically at a rate of 0.1% of distance (iXBlue Inc. 2014). For a typical survey speed of 2.5 knots, the platform travels 1000 m in 13 minutes, at which time the error increases by 1 m. Byrne, Schmidt, and Hengrenæs (2015) describe controlling the error accumulation by surfacing the platform periodically to obtain GNSS fixes. Another approach is to run survey lines with reciprocal headings, since some DVL errors will cancel. Byrne, Schmidt, and Hengrenæs (2015) describe a survey consisting of nine lines lasting 90 minutes, with GNSS fixes at the start and finish, and navigation data post processed using Kongsberg Maritime NavLab software to keep errors within 6 m, which is the International Hydrographic Office allowable horizontal navigation uncertainty for the survey depth.

An important consideration in this navigation technique is that the AUV's DVL must maintain bottom lock while the platform is underway, surfacing to obtain the GNSS fix, and returning to

survey altitude. Many smaller AUV's such as the Remus 600 and Gavia utilize the RD Instruments Workhorse Navigator 1200 kilohertz (kHz) DVL, which has a maximum altitude of 30 m for acceptable performance (Teledyne 2013). All of the WEAs under consideration for this report have areas deeper than 30 m. The Kearfott T-24 Ring Laser Gyro INS, incorporated into several AUVs, has specifications that give a positional accuracy of ± 1 nautical mile after 8 hours with aid from a speed log alone (Kearfott Corp. n.d.); the iXBlue PHINS Fiber Optic Gyro INS specifies positional accuracy of 3 m after 2 minutes and 20 m after 5 minutes without aiding (iXBlue Inc. 2014).

INS systems are initially highly accurate, but they tend to lose accuracy due to the inherent drift in inertial heading sensors as distance and time increase from the last GNSS coordinate (HDR 2014). The use of INS systems requires the platform to surface regularly to maintain accurate positioning information, which will increase the amount of time necessary to complete a survey.

6.1.2.4 Buoy Systems

GNSS devices can also be attached to surface buoys for tracking underwater platforms (e.g., AUVs) and technologies (e.g., magnetometers). GNSS devices are typically deployed as a multi-buoy acoustic system or as a single buoy fixed-line system.

The multi-buoy acoustic system (e.g., a GPS Intelligent Buoy) operates by deploying several surface buoys equipped with GNSS receivers linked through network. These buoys receive acoustic signals from pingers mounted on underwater platforms and technologies, and transmit their positions together with these signals to determine an underwater position (Alcocer, Oliveria and Pascoa 2006). Survey areas are limited to an area defined by the placement of the GNSS-equipped buoys and provide an accuracy of 1 to 3 m (U.S. Air Force 2014).

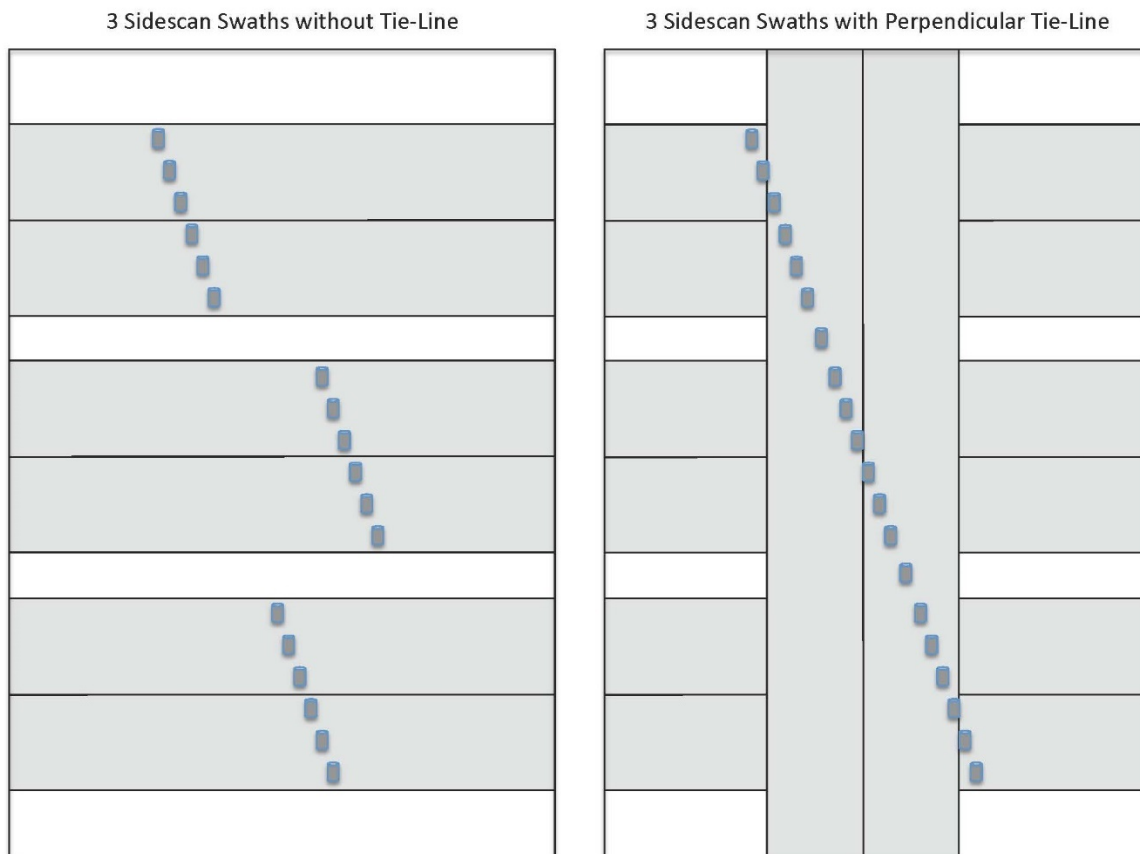
Single buoy fixed-line systems consist of a GNSS mounted on a surface buoy attached to a submerged platform or technology. This system can achieve a 1 m level accuracy in shallow water (<25 m) with limited currents and small wave heights. The accuracy of these systems rapidly degrades with increasing depth, currents, and wave heights (HDR 2013).

6.1.2.5 Other Positioning Methods

Another positioning technique allows side-scan sonar data recorded by an AUV or other platform with overlapping, adjacent lines to be used to correct navigation data during post processing. If a single feature, fixed on the seafloor, appears in the sonar data from different vehicle positions, the positions can be adjusted so the different views of the feature co-register. While there may be some error overall, the relative positions within the survey will be as accurate as the side-scan sonar's resolution (Keller, Hamilton and Hird 2015). This adjustment of navigation requires that there be sufficient features in the side-scan data that can be recognized in the adjacent swaths, so flat, uniform seafloor or regions with dynamic sediment movement are poor settings for this approach. Although less accurate in terms of geo-locating objects in latitude and longitude, the co-registration approach has value, for example, when there are gaps in navigational data, or even when positioning systems fail completely during a field program. In the latter case, collecting a single tie-line that crosses the entire survey can provide the basis for co-registering the entire dataset with very good relative positional accuracy (Figure 6-1). Subsequent surveys would allow the data to be shifted to improve real-world accuracy. Another method involves comparing the anomalies identified in multiple datasets, including those with only relative positioning, to confirm the positional accuracy of each dataset. Survey

data can be aligned by co-registering similar targets across multiple datasets; for example, large targets identified in side-scan data may also have multibeam echo-sounders (MBES) signatures that can be used to confirm co-registration among sonar datasets. Similarly, sonar targets can be co-registered with anomalies detected and positioned by non-sonar sensors such as magnetometers or in optical data. This method allows data collected from multiple surveys to be aligned to the most accurate survey.

Figure 6-1: Co-registration of Data Using a Tie-line



Another navigation technique uses multiple AUVs equipped with LBL transponders (Matsuda, et al. 2013). In each survey area, one AUV lands on the seafloor and provides a navigation reference to the other AUVs. The process leapfrogs when the survey within range of the stationary AUV is complete; another AUV lands on the seafloor at the edge of the survey to become the new reference, and the first AUV becomes mobile and begins the next survey. This technique is still under development.

Table 6-1: Summary of Positioning Technologies

| Positioning System | Description | Considerations | Relative Level of Accuracy |
|---------------------------|--|---|---|
| Surface GNSS | Typically fixed DGPS/RTK-GPS used for obtaining a position above water. Paired with a subsea positioning technology. | Does not provide an underwater position, so it must be paired with an underwater positioning technology or used in conjunction with offset or layback calculations to achieve an underwater position. | High |
| Multi-buoy | A field of GNSS-equipped surface buoys linked to an underwater pinger. | The system requires a field of GNSS-equipped surface buoys, limiting use to a small pre-defined area. | Moderate |
| Single Buoy | GNSS attached by line to a UXO diver. | An inexpensive method for tracking divers. Not suitable for tasks requiring accurate positioning or large area coverage. Diver safety is a concern, | Low/moderate initially, rapidly losing accuracy as depth |
| LBL | A field of transducers underwater with a transducer mounted to a vessel and a transponder mounted on the platform. | LBL systems require a field of transducers installed on the bottom, thus is best suited to investigations in small areas. | High |
| SBL | Multiple transducers mounted on a vessel or vessels with a transponder/responder mounted on a survey platform. | SBL transducers generally need to be installed on larger vessels (or vessels) to achieve a high degree of accuracy, which may increase project costs. | High |
| USBL | A single surface-based transceiver and a transponder/responder mounted on a survey platform. | USBL systems are a good tradeoff between accuracy, ease of use and mobility during underwater activities. | Moderate initially, slowly losing accuracy as range increases. |
| INS/DVL | A GNSS, INS and DVL positioning system mounted on the platform in combination with other data provides a current position in relation to the last GNSS coordinate. | The system requires regular surfacing to maintain accuracy, thus is best suited to underwater activities in specific areas that do not require extended submersion. | High initially, slowly losing accuracy as distance and time increase. |
| Other Positioning Methods | Distinctive features seen in multiple datasets are used to correct for positional errors. | Must be determined during post processing, requiring additional time; features may not appear in some datasets. | Can be as high as best datasets used |

Based on U.S. Air Force (2014)

Page Intentionally Left Blank.

6.2 Sensors

There are several general categories of sensors that can be mounted on mobile platforms and used to detect MEC in WEAs: acoustic, electromagnetic (EM) and optical. Acoustic systems measure the response of objects to sound waves; they are useful for area characterization, and for identifying individual targets in areas with a low density of bottom debris and low background levels of acoustic reflectivity. EM sensors measure the electromagnetic field of objects relative to the surrounding environment and optical sensors record objects in response to light, including laser beams.

Table 6-5 and Table 6-6 present a general overview of common and emerging environmental characterization and MEC detection technologies.

6.2.1 Acoustic Sensors

A fundamental complication when working in underwater environments is that light does not penetrate very far into the water column due to scattering or absorption caused by particles and organisms in the water column. Most of the visible light spectrum is absorbed within 10 m of the ocean surface, and even in very clear water environments light penetration over 100 m is rare. In contrast, sound waves of sufficiently long wavelengths can penetrate to the deepest part of the ocean and even provide information regarding sediment layers and buried objects in the sub-seafloor. Any investigation intending to locate MEC in regions greater than a few tens of meters deep will thus require the use of acoustic sensors, which can provide three basic types of information: seafloor shape; seafloor reflectivity; and impedance changes in the sub-seafloor. Seafloor shape, typically referred to as bathymetry or more generally topography, depicts changes in underwater elevation that provides information ranging from where low-lying areas might accumulate debris to whether safe operations can be conducted in locations with highly variable relief. Seafloor reflectivity provides information about the texture of the seafloor, such as whether it is smooth or rough, and is particularly useful for finding objects on or buried just below the seafloor surface that have high acoustic contrast relative to the surrounding environment. Acoustic impedance contrasts in the subsurface can either indicate changes in the vertical stratigraphy of the seafloor or detect buried objects with different acoustic properties than the materials in which they are embedded. All three types of acoustic data are produced by sensors mounted on platforms that, in combination, are referred to as sonar systems.

6.2.1.1 Sensors that Measure Sub-seafloor Impedance Changes

Bottom-penetrating, or sub-bottom, sonars use low frequency sound (hundreds to about 20,000 hertz) that can penetrate the seafloor to map sediment conditions with depth. These sound waves are reflected by changes in acoustic impedance caused by different types of sediment, rock, or man-made objects. Fine-grained silt or mud has acoustic impedance close to the impedance of water and does not scatter sound well, allowing the sound to penetrate deeper. Coarse sand or fine gravel scatter sound better, providing a stronger reflection but allowing less sound to penetrate to deeper layers. Very low frequency sounds, tens to hundreds of hertz, together with very powerful sound sources like explosives and extensive hydrophone arrays, can penetrate many km but have wavelengths of tens to hundreds of m and cannot resolve m scale and smaller objects. For MEC surveys, higher frequency systems operating at hundreds of hertz to tens of kHz are used, in order to resolve objects of decimeter to centimeter scale. Penetration of higher frequencies into the seabed is on the scale of m, but can be increased by increasing the transmitted sound pressure level. This is limited by cavitation, especially in shallow water. Another way to increase penetration is to

transmit a longer pulse of sound, although this reduces spatial resolution. By sweeping over a range of frequencies, a technique known as “chirp,” a long pulse is transmitted that combines penetration with higher resolution. The use of sub-bottom sonar for MEC detection represents an emerging technology, with recent Strategic Environmental Research and Development Program (SERDP) studies suggesting it may be an effective detection solution (Strategic Environmental Research and Development Program 2013).

For surveying cable routes in Atlantic OCS WEAs, the maximum burial depth to consider is the 2-m depth that cables may be entrenched, so the best sub-bottom systems are those that operate at higher frequencies, such as the Falmouth Scientific HMS-622 Chirpceiver at 8-23 kHz or the EdgeTech 3100 at 0.5 – 24 kHz. In parts of a survey area where sediments are more coarse grained, systems with lower frequency sound will be desirable.

Another consideration with sub-bottom is the directivity, or beam width. The sound projected towards the seafloor is shaped like a cone; anything within the cone will reflect and can be detected, but the position within that cone is not known. The HMS-622 has a cone angle of 27°, so at a distance of 2 m, the cone is almost 1 m in diameter. If the altitude were 20 m, the cone covers 10 m. To obtain good positioning information, the sub-bottom sonar must be near the seafloor. However, difficulties in maintaining a constant altitude above the seafloor, while simultaneously reducing the positioning error of a submerged, towed sub-bottom profiler, limits the applicability of sub-bottom profilers for MEC detection in the relatively shallow and variable topography found in the Mid-Atlantic WEAs.

6.2.1.2 Sensors that Measure Seafloor Reflectivity

Side-scan sonar data are used to characterize swaths of the bottom by measuring acoustic reflectivity. Several factors contribute to the ability of side-scan sonars to detect targets on the seafloor. For example, as the operating frequencies of side-scan sonars increase, the size of objects that can be detected by the sonar becomes smaller. Thus, a 20 kHz system might detect a 3-10-m shipwreck, while a 200 kHz system would depict both the same wreck and parts of its exposed infrastructure. Seafloor substrate character also contributes to the ability of side-scan sonars to detect MEC. For example, in Hawaii, sea-disposed munitions that are obvious on a featureless sandy seafloor but are exceedingly difficult to detect in adjacent areas that are composed of reflective drowned coral reefs (Edwards, et al. 2012). Additionally, the position of targets relative to the side-scan sonar affects performance. Objects within 5-10° of sonar nadir, which is located directly under the vehicle, are difficult to detect because of interference from acoustic signals arriving from both sides of the sonar and because of how the sonar pulses interact with the bottom. In contrast, low relief objects located at high incidence angles from the sonar may cast acoustic shadows that render them easier to see.

Bottom characterization provided by seafloor reflectivity data is a useful tool to inventory and characterize each target (or clusters of targets). This information is initially collected to:

- ▶ Identify targets or clusters of targets requiring further evaluation;
- ▶ Avoid objects during subsequent investigations, and;
- ▶ Quantify the density of various types of debris on the bottom to support an assessment of the general condition of the bottom for use in future investigations.

6.2.1.2.1 Side-scan sonar

Side-scan sonars project fan-shaped beams of sound to each side, covering from directly beneath the projector, known as the nadir, to close to the horizon. The projectors transmit a short burst of sound called a ping, and then hydrophones record the reflected sound wave. Over a flat bottom, the nearest point will be at nadir, and the first reflection will be from there; over time, reflections from greater ranges will arrive. Parts of the seafloor or objects on it will reflect sound differently, giving variances in the strength of the returned hydrophone signal. These changes result in a strip of pixels, collected from nadir out to the side; then the sonar is moved forward and pings again, building up a two dimensional image of seafloor reflectivity.

The size of the projector array that creates the sound determines the shape of the beam of sound emitted. An array that is long parallel to the sonar track will create a beam that is narrow in angle along the track. The size of this angle sets the size of the patch on the bottom that reflects that sound back to the receiving array. A beam angle of 1° will cover a patch 1.75 m wide at a range of 100 m. A useful approximation for calculating beam width in degrees is 3000 divided by the product of sonar frequency in kilohertz and array length in inches (EdgeTech 2005). For example, a 100 kHz sonar would need an array 30 inches long to produce a 1° beam width. Increasing the frequency will reduce the beam width and increase along-track resolution at the expense of reduced range because of higher attenuation. Cross-track resolution depends on transmitted pulse length, or for coded pulses, the bandwidth of the transmitted pulse. Narrow pulses provide better resolution but carry less energy and so have reduced range. Currently-available sonars operating at frequencies near 1 megahertz (MHz) have high enough resolution for MEC identification.

6.2.1.2.2 Synthetic aperture sonar

Synthetic aperture sonar (SAS) is an emerging technology for providing high-resolution swath imagery of the bottom, with signal and processing algorithms potentially increasing detection effectiveness in cluttered environments (Strategic Environmental Research and Development Program 2013, Strategic Environmental Research and Development Program 2013), and the ability to discriminate MEC detected by the sensor by comparison of the objects' "fingerprints" to known values for MEC. SAS systems are similar to side-scan sonars in that they project a beam of sound to each side of the platform, but the principle of SAS is to combine successive acoustic pings coherently along a known track in order to increase the apparent azimuth (along-track) resolution, with the potential to produce high-resolution images down to cm scale over hundreds of m in range (Hansen 2011). In SAS, a much wider sound beam is transmitted to insure that any point on the seafloor reflects sound from many pings as the sonar moves through the water. By combining the signals received along this path, it is as though the signals were received by a hydrophone array as long as the distance the sonar traveled (Figure 6-2). In this way, a large array can be synthesized and resolution greatly increased (Hoggarth and Kenny 2015). The challenge in implementing this technique is that if the array does not travel in a straight line, parallel with the long axis of the array, the offsets must be measured and compensation introduced for each ping. Variations in motion of the SAS system must be minimized, and require active control of the host vehicle attitude. For this reason SAS systems cannot currently be mounted on a surface vessel; it is towed behind a survey vessel or mounted to an AUV.

Increasing the apparent length of the sonar transducers creates a beam of sound with a smaller angular width, making possible very high-resolution data, especially at the outer parts of the swath. As the beam width is reduced, the area covered by the beam is reduced, and so the speed at which the sonar can advance must be reduced if gaps in survey coverage are to be avoided. For example,

a sonar with an along-track beam width of 1° will cover 1.75 m at a slant range of 100 m, and the sound will take 0.133 seconds to travel out and back. Sampling with 50% overlap means the sonar should not advance more than 0.875 m between pings, limiting speed to 6.57 m/second, or almost 13 knots – not a significant limitation. However, if the resolution desired was just 5 cm at 100 m range, the sonar array would need to be 35 times as long, and the speed would be limited to just over one-third of a knot. This would leave gaps between samples in the swath closer to the sonar, where the beam covers a smaller area; to avoid these gaps the survey speed would have to be reduced even further.

Figure 6-2: Synthesis of a Larger Array by Combining Multiple Pings

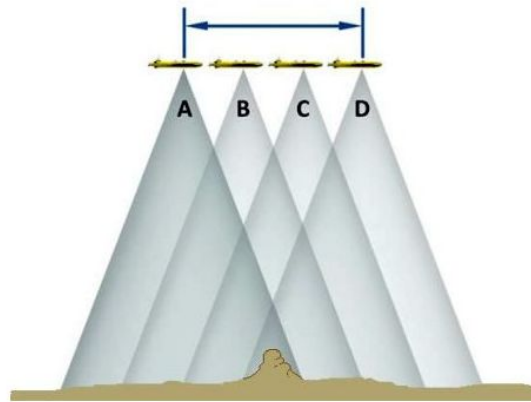


Image from Hoggarth & Kenny (2015)

The Kraken Sonar Inc. Aquapix SAS systems come in several different configurations, but a typical system suitable for mounting on an AUV or ROV is their MINSAS 120. It can survey at 3 knots, mapping a backscatter swath of 480 m, all at 3-cm resolution. It has two rows of hydrophones to measure phase difference, and so calculates bathymetry over the same swath, with a lower resolution of 25-cm horizontal and 10-cm vertical.

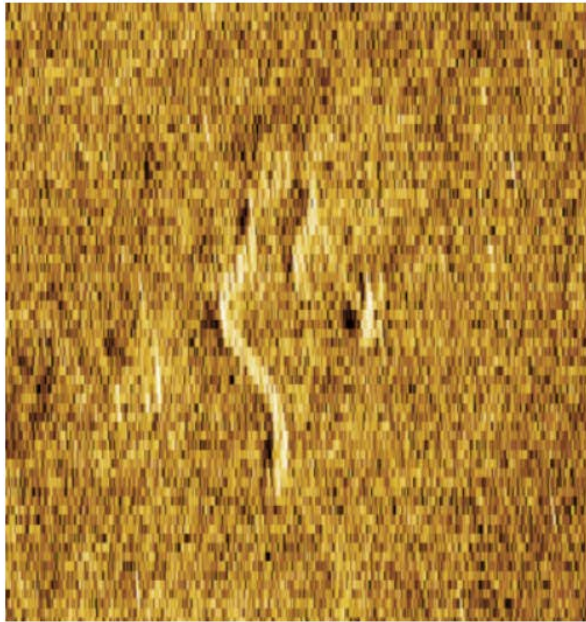
As shown in Table 6-2, coverage rate for the Kraken system is an order of magnitude greater than conventional side-scan sonars (e.g., Figure 6-3). This gives it an enormous advantage in reducing survey time and expense. However, the acquisition cost of these systems is high; the MINSAS 120 costs about \$300,000, and a complete system with sonar, their KATFISH active tow vehicle, plus a launch and recovery system would cost about \$1.5 million. If the survey area has a hard bottom with all MEC proud of the seafloor, the reduction of ship time for a large survey could justify the investment. However, if MEC could be buried beneath the seafloor, a magnetometer must be used, with survey line spacing of 1 – 10 m. A conventional side-scan sonar survey, carried out at the same time as the magnetometer survey, would provide resolution nearly equal to the SAS system.

Table 6-2: Comparison of Commercial SAS and Three Side-Scan Sonars, Each with 5-centimeter Resolution

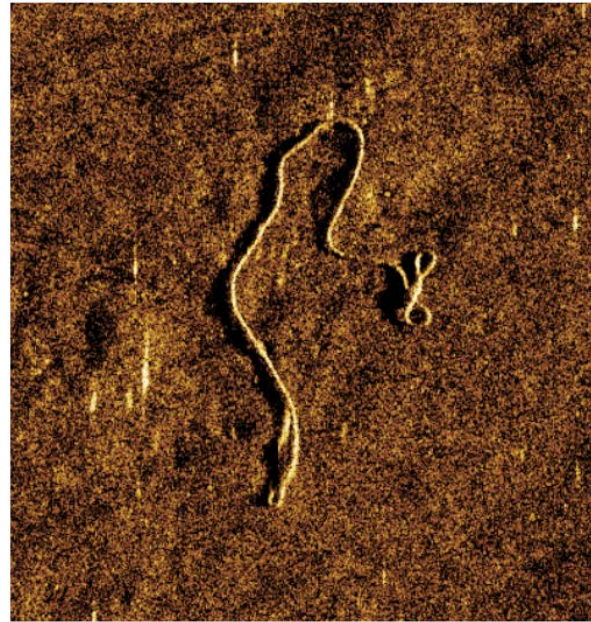
| Manufacturer | Kraken Sonar Systems | Edgetech | Sonardyne | L3 |
|--------------------------------------|--|---|-------------------------------------|---|
| Model | MINSAS 120 | Littoral Mine Countermeasure SONAR (LMCS) | Solstice | 5900 |
| Type | SAS | Side-scan | Side-scan | Side-scan |
| Frequency | 300 kHz | 600/1600 kHz CHIRP | 750 kHz | 600 kHz |
| Max Range | 240 m | 35 / 125 m | 100 m | 150 m |
| Max Swath | 480 m | 70 / 250 m | 200 m | 300 m |
| Survey Speed | 3-6 knots | 2-6 / 12-14 knots | 3-3.2 knots | 2-14 knots |
| Resolution | 3 cm @ 240 m | <6 cm to <17 m 7 cm @ 20 m 8 cm @ 25 m 9 cm @ 30 m 10.5 cm @ 35 m | 5-20 cm @ 100 m | 6.2 cm @ 50 m 9.3 cm @ 75 m 15.5 cm @ 125 m |
| Area Coverage Rate (5 cm resolution) | 2.0 km ² /hr | 0.2 km ² /hr | 0.8 km ² /hr | 0.3 km ² /hr |
| Bathymetry – Range | Yes – 240 m | No Bathymetry | Yes – 100 m | Yes – 125 m |
| Detect/Classify | In-stride Detection, Classification and Localization | Requires Target Revisit To Classify | Requires Target Revisit To Classify | Requires Target Revisit To Classify |
| Operational Depth Rating | 1000 m | 300 m | 200 m | 750 m |

References: (EdgeTech n.d., Balloch 2010, Sonardyne 2010, Klein Associates, Inc. 2015, Kraken Sonar Systems, Inc. 2012, Kraken Sonar Systems, Inc. 2015b)

Figure 6-3: Image Showing Side-scan Sonar vs SAS



Conventional Sonar



Kraken AquaPix® SAS

Backscatter image of a tow rope at a range of 50 m. (Kraken Sonar Systems, Inc. 2015b)

6.2.1.3 Sensors that Measure Seafloor Shape

Bathymetry is acoustic data that represents seafloor shape. Accurate bathymetry is useful in mission planning (e.g., areas where towed systems cannot be used effectively; determining transect orientation, identifying collision or entanglement hazards). Geo-referenced bathymetric maps can serve as a GIS base map for the survey teams and can be co-registered with other data to improve positional accuracy. This helps to ensure that sonar anomalies selected as targets for reacquisition possess an appropriate acoustic signature correlated to the size of the object and to the MEC item of concern present at the site. Displaying current ROV positioning information on top of the bathymetry in real time allows an ROV operator to navigate directly to a target for verification (Schultz, et al. 2011). There are two primary systems for acquiring bathymetric data: narrow track echo-sounders and wide-track multibeam swath systems.

6.2.1.3.1 Echo-sounders

Conventional echo-sounder systems consist of a single transducer pointed straight down, either hull- or pole-mounted, that acts as both an acoustic transmitter and a receiver (transceiver). These systems produce an acoustic pulse with a vertical resolution that depends on the pulse width; for systems operating at frequencies of several hundred kHz the resolution is on a cm scale. Overall, the quality of narrow track echo-sounder surveys does not compare well with wide-track multibeam surveys, and echo-sounder surveys take significantly longer to conduct, but they have the advantage of being less expensive, and some useful results can be obtained (Nautical Archaeology Society 2009).

Echo-sounder systems allow development of a digital terrain model of the survey area. Geo-referenced acoustic data are processed and analyzed, with detailed bathymetric results used for:

- ▶ Developing a digital terrain model for planning subsequent deployment of high-resolution acoustic, magnetic or optical sensors;
- ▶ Identifying large debris for avoidance;
- ▶ Characterizing of the bottom including slope, roughness and scour features to support ROV deployment, and;
- ▶ Determining water depth to plan for efficient operations, and guide development of all future phases of a project.

A digital terrain model is useful for co-registering other datasets, which allows for improved positional accuracy.

6.2.1.3.2 Multibeam echo-sounders

MBES use the same fan-shaped beams of sound as side-scan sonars, but use an array of hydrophones having dozens or even hundreds of elements to receive the reflected signals. Signals from the individual elements are combined to form beams pointing in many directions across the track, and the travel time for a reflection from the bottom gives a range for that beam. In this way the position of the seafloor is measured to produce topographic maps, also known as bathymetry. The aperture of the receive array – the width of the array of elements – determines how small each individual beam can be. Most multibeam sonars can also produce backscatter imagery of the seafloor but at lower resolution than side-scan sonars.

MBES surveys are typically undertaken from surface vessels, but they may also be conducted from ROVs and AUVs. MBES data collection using an ROV is generally more expensive due to reduced production rates caused by the slower speed of most ROVs. MBES swath bathymetry is a standard survey tool for both high-resolution site work and for coverage of wide areas (Nautical Archaeology Society 2009).

6.2.1.4 Phase Measuring Bathymetric Systems

Some acoustic systems are capable of measuring both seafloor shape and texture. Most multibeam sonars can also produce reflectivity data for the seafloor, although it is often at lower resolution than side-scan sonars produce. The simplest side-scan/bathymetry sonars use a pair of receiving hydrophone arrays listening to the backscattered sound. Because the receivers are separated by a small distance, sound arriving from different directions reach each receiver at a slightly different time. The time differences are expressed as the fraction of the wavelength of the transmitted sound, known as phase. By measuring the phase difference between the two receivers (transducers), the angle from which that sound arrived can be calculated. The amplitude of the reflected sound provides a backscatter image, and the phase difference provides bathymetry. These systems are often referred to as interferometric sonars, however, a true interferometric sonar produces imagery with interference fringes where the signals from the two receivers combine destructively (Robinson and Bjorkheim 1989). A more accurate term for this type of system is a phase-measuring bathymetric sonar (PMBS).

A simple system with two transducers depends on having just a single reflected signal arriving at any one time. Over seafloor with low relief this is often the case, but in some situations as in Figure 6-4 a phase difference cannot be measured. This difficulty also arises when surveying areas

where the maximum sonar range is greater than water depth; sound reflecting from the bottom can bounce off the sea surface and be received by the sonar, with the corresponding arrival angle. These echoes are known as “multiples.” By using more than two transducers on a side it is possible to resolve signals arriving from different directions at the same time and eliminate erroneous signals from multiples or noise sources (Kraeutner and Bird 1999). This enables great precision in the measurement of arrival angles, allowing modern phase bathymetry sonars like the EdgeTech 6205 to map a bathymetric swath eight times the sonar altitude, while simultaneously acquiring high-resolution backscatter imagery.

Figure 6-4: Geometric Limitation of Two-row Phase Measurement

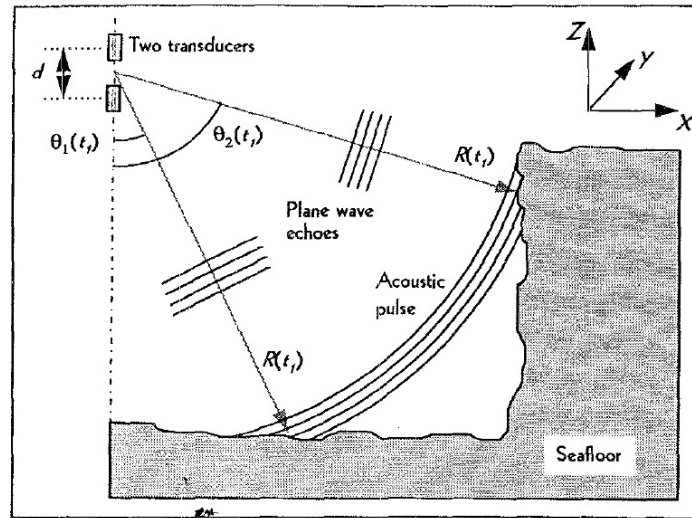


Image from Kraeutner & Bird (1997)

6.2.2 Magnetic Sensors

All MEC interacts with EM fields in the surrounding environment. The majority of MEC have housings made largely of ferromagnetic materials (e.g., steel) that exert local effects on the Earth’s magnetic field. Precise measurements of the magnetic field will reveal local effects from metallic objects such as MEC as anomalies. The effect is given by Breiner (1999) as proportional to the magnetic moment of a round object and inversely proportional to the distance cubed. The magnetic moment depends on the amount of ferrous metal in the object. A long object such as a steel pipeline can be considered as a long line of round objects, all adding together, which makes the effect diminish more slowly, as the distance squared. Table 6-3 (Breiner 1999), gives typical anomaly strengths in nanoteslas (nT) for a number of common objects at various distances.

EM sensors used for mapping electromagnetic fields fall into two broad categories: magnetometers and electromagnetic induction systems. Passive magnetometers (e.g. fluxgate, cesium vapor) detect ferrous metal, while active sensors, such as electromagnetic induction, detect ferrous and non-ferrous metals. Passive magnetometers detect irregularities in the Earth’s magnetic field caused by the ferromagnetic materials such as those in munitions. Passive magnetometers typically perform better for large, deep, ferrous objects. They may also detect small ferrous objects at or near the surface better than electromagnetic sensors with large sensor coils. Electromagnetic induction systems induce an electromagnetic field and measure the response of objects near the sensor. Electromagnetic induction systems measure the secondary magnetic field induced in metal objects either in the time-domain or frequency domain. Time-domain electromagnetic

induction (TDEMI) is most commonly used in underwater MEC detection. Both types of sensors can be used to map surface and buried metallic anomalies and can be useful for detecting MEC (Butler 2004). Magnetic sensor platforms generally consist of a vessel, a tow system, and a sensor or an array of sensors equipped with a positioning system. The effect of the platform (e.g., power supply, metal content) on the performance of the sensor is an important consideration in selection and deployment of the system.

Table 6-3: Typical Maximum Magnetic Anomaly Strength of Common Objects

| Object | Nearby | | Far | |
|-----------------------------|--------------|---------------|--------------|---------------|
| | Distance (m) | Strength (nT) | Distance (m) | Strength (nT) |
| Automobile (908 kg) | 9.1 | 40 | 30.5 | 1 |
| Ship (907,000 kg) | 30.5 | 300 to 700 | 305 | 0.3 to 0.7 |
| Light Aircraft | 6.1 | 10 to 30 | 15.2 | 0.5 to 2 |
| File (25 cm) | 1.5 | 50 to 100 | 3.0 | 5 to 10 |
| Screwdriver (13 cm) | 1.5 | 5 to 10 | 3.0 | 0.5 to 1 |
| Rifle | 1.5 | 10 to 50 | 3.0 | 2 to 10 |
| Ball Bearing (2 mm) | 0.1 | 4 | 0.2 | 0.5 |
| Pipeline (30.5 cm) | 7.6 | 50 to 200 | 15.2 | 12 to 50 |
| Magnet (1.3 X 7.6 cm) | 3.0 | 20 | 6.1 | 2 |
| Well Casing and Wellhead | 15.2 | 200 to 500 | 152 | 2 to 5 |

Note: Anomaly strengths are only representative and may vary by a factor of 5 to 10 for a number of reasons.
Table after Breiner (1999).

6.2.2.1 Magnetometer

Magnetometry is a proven technology for detecting ferrous material and has been widely used for detection of MEC (Schultz, et al. 2011). Magnetometers have the ability to detect ferrous material buried under sediment to greater depths than can be achieved by TDEMI systems, and magnetometers can identify small anomalies because the instruments have high levels of sensitivity. However, this sensitivity means that magnetometers are affected by ferrous minerals, which can impact the detection probability by creating false positives and masking signals from MEC. This limits their utility in volcanic and, basaltic terrain and in other areas where the bottom has high ferrous content.

There are three types of magnetometers used for detection of magnetic anomalies in the field: proton precession, Overhauser, and alkali metal vapor (principally cesium). Proton precession magnetometers (such as the JW Fishers Proton 4) have a higher noise level of about 1 nT, and a slower sample rate of 0.5 to 0.25 hertz. A 100-kilogram steel object would likely be detected at a range of up to 10 m, but many MEC are smaller. A 5-kg object would need to pass within 0.5 m to produce a detectable signal. The fairly low sample rate would also limit survey speed for small

objects. At a 2-knot survey speed, the sensor moves a meter per second, so at the slower sample rate of 0.5 to 0.25 hertz there would be 2 to 4 m between samples acquired.

Overhauser and cesium vapor magnetometers have considerably less noise and have higher sample rates; the Overhauser magnetometers like the Marine Magnetics SeaSpy2 can sample at up to 4 hertz and the cesium magnetometers such as the Geometrics G-882 can sample at up to 40 hertz. Sampling at lower rates averages a number of measurements, which results in reduced noise. Geometrics specifies sensitivity for the G-882 as “typically 0.02 nT P-P at a 0.1 second sample rate or 0.002 nT at 1 second sample rate” (Geomatrics n.d.), while the SeaSpy2 specification is for 0.01 nT at 4 hertz (Marine Magnetics 2016). The cesium vapor design is sensitive to orientation of the Earth’s magnetic field; survey lines must be aligned at an angle greater than 60° from the sensor's equator and greater than 60° away from the sensor's long axis, so surveys must be planned carefully; the Overhauser devices are scalar sensors and do not depend on orientation.

Table 6-4 shows that the smallest items would barely be detectable by a Geometrics G-882 if they were buried 2 m below the seafloor and magnetometer survey lines would need to be spaced no more than a meter apart. The MEC of concern in WEAs under consideration have a minimum size close to 100 pounds of steel, giving a detection range of 7 to 8 m. Survey lines could be spaced approximately 10 m apart and still have some overlap, as long as those lines were accurately located.

Table 6-4: Typical detection ranges for the Geometrics G-882

| Object | Distance | | Anomaly strength |
|-----------------------|----------|----|------------------|
| | ft | m | nT |
| 1000-pound bomb | 100 | 30 | 1-5 |
| 500-pound bomb | 50 | 16 | 0.5-5 |
| 100-kilograms of iron | 50 | 15 | 1-2 |
| 100 pounds of iron | 30 | 9 | 0.5-1 |
| 10 pounds of iron | 20 | 6 | 0.5-1 |
| 1 pound of iron | 10 | 3 | 0.5-1 |
| Grenade | 10 | 3 | 0.5-2 |

6.2.2.2 Gradiometers

A gradiometer uses two or more magnetometers with fixed spacing to make simultaneous measurements and determine the change, or gradient, of magnetic field over distance. The separation distance is determined by the scale of magnetic anomalies of interest. Searching for magnetic ore bodies that may be buried hundreds of meters deep would typically use a pair of magnetometers towed in line separated by up to 1000 m or more, but searching for smaller objects like MEC might use a spacing of a few meters. The gradient signal can provide information about location and size of detected objects. Magnetic anomalies depend on mass of ferrous metal and separation from the sensor, so a single measurement could indicate either a small object nearby or a larger one farther away. Since the magnetic anomaly for round objects is inversely proportional to the distance cubed, the gradient for the small object would be larger. Gradiometers with magnetometers spaced across-track provide the significant advantage of mapping a wider track and requiring fewer track lines, provided the objects of interest have detection ranges on the order of magnetometer spacing.

6.2.2.3 Electromagnetic Induction

Electromagnetic induction sensors, commonly known as “metal detectors,” create an oscillating magnetic field with a loop electromagnet. This induces eddy currents in conductors within the field, and the magnetic field generated by those eddy currents is detected by a receiving loop. These sensors can detect non-ferrous metals. Unfortunately, seawater is conductive and so these electromagnetic induction sensors have limited range in the ocean. The JW Fishers Pulse 12 Boat Towed Metal Detector gives a range of 4 feet for detecting a 1-gallon can and 9 feet for detecting an automobile in salt water (JW Fishers Mfg Inc n.d.). The most common underwater electromagnetic induction devices are hand-held instruments used by divers (Frequency Domain Electro Magnetic Induction, or FDEMI sensors). Unless there was a need to detect large MEC without ferrous metal content, a magnetometer or gradiometer is a better tool than an electromagnetic induction sensor.

6.2.3 Optical Sensors

Optical systems require that the objects be exposed on the sediment surface for them to be visible. Two main factors affect collection of optical images: light and turbidity. As light decreases and turbidity increases, the effective field of view is reduced. Poor visibility can be mitigated by coupling underwater lighting with the optical system and configuring the combination to provide adequate illumination.

Optical sensors include still image and video camera equipment used to photograph the seafloor. These sensors may be off-the-shelf cameras adapted for use underwater, or specifically designed for low-light or high-backscatter conditions that may be encountered in the marine environment. They are usually accompanied by an artificial light source. Typically, optical sensors are mounted on tow-bodies, ROVs, or AUVs, which are operated within a few meters of the seafloor. While useful for visual confirmation or identification of a target, the field of view of visual sensors can be very limited in turbid underwater environments. Given this case, visual sensors are often used in tandem with other sensors, most often acoustic sensors, such as side-scan or sector-scanning sonars.

Laser line scanners (LLS) use lasers to illuminate and record detailed video over 3- to 65-m wide areas of the bottom, and can cover an area up to five times larger than conventional underwater cameras while retaining fine detail (if visibility is good, it is possible to see details less than 3 cm in size). Laser pulses generate line scan images on the bottom that are captured by a high-speed camera, providing one-dimensional energy distribution images at the laser’s target. This energy distribution profile helps identify the target’s position. Triangulation between the target, the laser scanner, and the camera is used to develop bathymetric data. Testing of LLS as a detection and characterization technology for MEC exposed on the sediment surface found that for the blind testing element, Tier I classification success (target correctly identified as UXO simulator or dummy object) was 89% for targets surveyed. Tier II classification success (specific target identification correctly identified) was 78%. The probability of false alarm (Type I error; dummy objects falsely identified as UXO simulators) and the probability of false negative (Type II error; UXO simulators falsely identified as dummy objects) were both 0%. These results suggest that the technology is capable of providing accurate target discrimination for objects proud of the seafloor (Environmental Security Technology Certification Program 2012).

Although optical technologies (e.g., LLS, video) can be used to conduct surveys, their primary use is in the identification of material that has been located underwater by other sensors (e.g., magnetometers). In shallow depths, they can be used to limit the amount of time MEC-qualified

divers or ROVs spend on the bottom investigating anomalies. A simple underwater drop camera can be used to select material for further investigation. ROVs built with optical systems add the capability of remote control and movement to assist in positioning camera systems, insuring an adequate picture for the viewer.

LLS systems can be towed behind a vessel on a sled or mounted on an AUV. In addition to collecting imagery of the bottom, LLS systems can be configured to provide bathymetric maps. The system was specifically designed to identify semi-submerged mines in coastal waters. As the LLS moves over the bottom, it builds a bathymetric map by taking consecutive images.

Table 6-5: Summary of Environmental Characterization Technologies

| Technology | General Use | Description | Effectiveness | Implementability | Cost |
|----------------------------------|---|--|---|---|---|
| Towed/AUV Technologies | | | | | |
| Side-scan sonar | Side-scan sonar is most effective as an environmental characterization technology, but can be used for MEC detection and characterization for larger MEC in areas of low clutter or for detecting clusters of MEC. Side-scan sonar with operating frequencies > ~100 kHz have a demonstrated ability to detect small (<1-m diameter) metal objects in low reflectivity backgrounds at altitudes of <100 m above the seabed. | Side-scan sonar surveys typically involve towing a sensor behind a survey vessel, but side-scan sonar can also be deployed on an AUV. The sensor pings at a designated frequency and collects time and intensity information related to these pings as they return after bouncing off objects on the bottom. The typical product is a 2-dimensional map showing strong responses from reflective objects and weak responses from features that absorb sound. | Side-scan sonar is most effective for creating images of large areas of the bottom for environmental characterization. For MEC detection, MEC must be fully or partially exposed and uncluttered by nearby environmental factors such as coral, rocks, and vegetation (Schwartz and Brandenburg 2009). In certain conditions, side-scan sonar images can be helpful for detecting individual MEC (particularly large MEC) items or clusters of MEC items. False negative rates for MEC detection are not yet fully characterized; however, it is known that false negative rates are greater than zero. Images from side-scan sonar are also useful for characterizing the physical setting of a site. | Side-scan sonar sensors are readily available and have been used for survey work. | Side-scan sonar costs are moderate, but deployment and collection costs are low due to its rapid areal coverage. |
| Sub-bottom profiler | Sub-bottom profilers are most effective as an environmental characterization technology. | Sub-bottom profilers generate low frequency sound pulses that penetrate into soft seafloor substrates such as sand and mud. The pulses reflect off of objects or differentiate layers of the sub-bottom. | Sub-bottom profilers are useful in characterizing sediment and sub-bottom conditions for determining the burial depth of MEC and for planning intrusive investigations. Sediment cores can be used to ground-truth and refine analysis of sub-bottom profiler data. | Sub-bottom profilers are readily available and have been used for survey work. | Sub-bottom profilers costs are moderate, but deployment and collection costs are low due to its rapid areal coverage. |
| Synthetic Aperture Sonar (SAS) | SAS is an environmental characterization technology. Recent SERDP studies indicate low frequency sonar may be an emerging MEC detection and characterization technology (Strategic Environmental Research and Development Program 2013). | The principle of SAS is to combine successive acoustic pings coherently along a known track in order to increase the azimuth (along-track) resolution, with the potential to produce high-resolution images down to centimeter resolution over areas that are up to hundreds of m in size (Hansen 2011). | SAS is capable of generating high-resolution images of swaths of the bottom. This technology is used to perform environmental characterizations. Low frequency sonar techniques may also be suitable for detecting buried MEC and MEC at the sediment/water interface (Strategic Environmental Research and Development Program 2013). This approach works best in uncluttered environmental conditions, though signal and processing algorithms may increase discrimination effectiveness in cluttered environments. | SAS systems are readily available for environmental characterization, and represent an emerging technology for MEC detection. | SAS costs are generally high, but deployment and collection costs are low due to its rapid areal coverage. |
| Hull-Mounted Technologies | | | | | |
| Echo-sounders | Echo-sounders are most effective for environmental characterization, and under certain conditions may be used for MEC detection. | MBES, like other sonar systems, transmit sound energy and analyze the return signal that has bounced off the bottom or other objects. MBES are typically pole or hull-mounted on a ship and emit sound waves to produce fan-shaped coverage of the seafloor. These systems measure and record the time for the acoustic signal to travel from the transmitter (transducer) to the seafloor (or object) and back to the receiver. MBES produce a “swath” of soundings (i.e., depths) to ensure full coverage of an area. The coverage area on the bottom is dependent on the swath width and water depth, typically two to four times the water depth. Many MBES systems are capable of recording acoustic backscatter data that can be processed to create low-resolution imagery. Backscatter data co-registered with bathymetry facilitates data interpretation and post processing (National Oceanic and Atmospheric Administration 2016i). | MBES is most effective for environmental characterization and these data are best suited to developing detailed bathymetric maps of an area to guide follow-on activities. For detection, MEC must be fully or partially exposed on the bottom. False negative rates for MEC detection are not yet fully characterized; however, it is known that false negative rates are greater than zero. If used to detect MEC, MBES works best in uncluttered environmental conditions such as those free from coral, rocks, and vegetation (Schwartz and Brandenburg 2009). | Echo-sounders are readily available and have been used for survey work. | Echo-sounder costs are high, but deployment and collection costs are low due to its rapid areal coverage. |

| Technology | General Use | Description | Effectiveness | Implementability | Cost |
|---|--|--|---|--|---|
| Phase-Measuring Bathymetric Sonars (PMBS) | PMBS are most effective for high-resolution environmental characterization and are capable of measuring both seafloor shape and texture. They may be able to detect MEC in combination with high-resolution inertial motion units. | PMBS can be hull-mounted, deployed over the side of the vessel on a pole, or configured for ROV or AUV deployment. | PMBS are capable of rapidly generating high-resolution images of swaths of the bottom. This technology is used to perform environmental characterizations and detecting targets on or very near the seafloor surface. | PMBS are readily available and have been used for survey work. | PMBS costs are moderate to high, but deployment and collection costs are low due to its rapid areal coverage. |

Table 6-6: Summary of Underwater MEC Detection Technologies

| Technology | General Use | Description | Effectiveness | Implementability | Cost |
|-----------------|---|---|---|--|--|
| Optical Sensors | Optical technologies can be used for environmental characterization, situational awareness, and as an MEC detection technology. | Optical technologies include camera systems that provide still and video images of the bottom. LLS systems can create swath imagery of the bottom similar to black-and-white photography. | Optical technologies provide photographic and video records for activities performed by ROVs, and can be a component of AUV systems. The data from these systems are effective as a qualitative quality control measure, and to assist in the identification of MEC exposed on the bottom. | Optical technologies are readily available and have been deployed regularly at MEC sites. LLS is commercially available and has application at underwater sites to create high-resolution swath imagery of the bottom. | Optical technologies are an inexpensive item for divers, and are generally a built in cost for ROVs. LLS system costs are generally high, but deployment and collection costs are low due to its rapid areal coverage. |
| Magnetometers | Magnetometers are a MEC detection and characterization technology. | Magnetometers detect ferrous metal and are generally used to perform mapping of areas containing MEC. Although magnetometers can be deployed underwater on AUVs, ROVs and divers for MEC detection, they are most commonly and effectively submerged and towed by a vessel. Magnetometers most commonly used for underwater mapping are the cesium vapor, fluxgate systems, and Overhauser systems. Magnetometers can be configured as total field sensors or as gradiometers (horizontal or vertical). When used for underwater mapping, consideration needs to be given to selecting a system with the capability to detect the smallest munitions of concern and to the system with the best positional accuracy. Magnetometers may also be deployed from airborne platforms for use in shallow water. | Magnetometer arrays are typically reliable and rugged. These systems can detect small and large ferrous items (Schwartz and Brandenburg 2009). Effectiveness increases with larger arrays capable of surveying a larger footprint per transect, and through accurate positioning allowing follow-on reacquisition of targeted anomalies in ferrous-dense environments. EM mapping conducted from an airborne platform is best suited to large and very shallow sites. The detection range of the typical sensors coupled with the sizes of the munitions items at the site generally limit the effectiveness of EM mapping conducted from an airborne platform to waters less than 2 m deep. Areas with substantial non-MEC related ferrous debris and/or ferrous rock are detrimental to the effectiveness of EM sensors. | Towed magnetometer arrays are readily available and have been deployed for underwater MEC surveys. Airborne magnetometer arrays (i.e., HeliMag) are readily available and have been deployed for underwater MEC surveys. The altitude of operation (30 m) limits detection to MEC larger than 1000-pound bombs. | Sensor costs are generally high, with additional costs associated with deployment platforms and positioning capabilities, which vary with more robust and accurate systems costing more. Airborne platforms for EM mapping are relatively expensive compared to other underwater EM mapping technologies, but are economically feasible for large shallow areas where MEC are physically large. |
| TDEMI | TDEMI sensors are a MEC detection and characterization technology. | TDEMI sensors generate a magnetic field from the sensor transmitter coil, which in turn measures a secondary magnetic field on the sensor receiver coil emanating from nearby conductive objects energized by the transmitted signal. TDEMI sensors are used to perform EM mapping of ferrous and non-ferrous metallic objects. TDEMI systems are generally towed behind vessels, but can be mounted on inspection-class or larger ROVs and deployed by UXO divers. When used for underwater EM mapping, consideration needs to be given to selecting a system with the capability to detect the smallest munitions of concern and to the system with the best positional accuracy. | Typical off-the-shelf TDEMI systems are well suited for use in shallow environments. Array platforms may be hard to control. Detection depth can be increased minimally by increasing the system power output. TDEMI systems can detect small and large metal items (Schwartz and Brandenburg 2009). TDEMI systems have increased detection and classification capabilities compared to magnetometer systems, but lack the detection range of a magnetometer system, and are thus better suited to flatter sites and sites with low bottom debris density obstructing the operation of the sensor. Areas with substantial non-MEC related metallic debris or ferrous rock are detrimental to the effectiveness of TDEMI systems. | Towed TDEMI arrays are available and have been deployed for underwater MEC surveys. | Sensor costs are generally high, with additional costs associated with deployment platforms and positioning capabilities, which vary with more robust and accurate systems costing more. |

Page Intentionally Left Blank.

6.3 Platforms

In the context of survey Atlantic OCS WEA, platforms are the vehicles on which sensors and supporting technologies are mounted to conduct MEC detection surveys. Major categories of platforms include AUVs, remotely operated towed vehicles, ROVs and surface vessels. Surface vessels can serve as a platform for pole or hull-mounted sensors or may be used to deploy towed systems. Platform selection for a survey is based on the ability to operate effectively and efficiently in the area being studied. For example, a survey of a portion of a WEA may be conducted by a single AUV or surface vessels. As the size of a WEA survey expands, cost reductions and productivity gains can be achieved by deploying multiple AUVs and/or surface vessels capable of housing additional sensors. Some platforms are capable of deploying multiple technologies simultaneously.

Table 6-7 presents a general overview of common and emerging platforms for use during underwater MEC investigations. It also provides an overview of how each platform may be used.

6.3.1 Autonomous Underwater Vehicles

AUVs range in size from small, cylindrical objects able to be deployed and recovered by a single person to vehicles many meters in length, weighing several tons, and requiring large ships to accommodate their launch and recovery systems. AUVs components include an energy storage device (usually a rechargeable battery), a propulsion system, a command-and-control system, a navigational system, a payload (i.e., sensors), and very often an acoustic telemetry system. The acoustic telemetry system has limited bandwidth and range, and as a result cannot transmit large amounts of data to the surface or over distances of more than a few km. Typically, position and command-and-control system parameters are transmitted continuously; subsampled sensor data may be transmitted as well.

AUVs are available in various sizes and are capable of carrying payloads with one or more acoustic, optical or EM sensors such as optical imaging, sonar, and metal detectors (Nautical Archaeology Society 2009). AUVs are well suited for wide area assessment and can be programmed to autonomously carry out a survey. Some surveys initially use an AUV to map the area of interest and identify anomalies, then use ROVs launched from the same vessel to investigate the anomalies while an AUV survey is underway at another site. This allows near-real time refinements to the survey (Camelli, et al. 2009).

AUVs are able to operate in bottom-following mode and have ranges of 2 km or greater. Some systems are capable of operating continuously for more than 25 hours. Their autonomy allows AUVs to transmit sensor data via wireless signal or by downloading the data after the AUV has completed its mission.

As a multi-sensor autonomous platform, AUVs provide unique benefits in the detection and discrimination stages of investigations (Strategic Environmental Research and Development Program 2009). The sensors carried by an AUV must be balanced against payload size, power requirements and the impact to mission duration. The autonomous sensing capability may provide a significant improvement over the mapping accuracy and efficiency available on towed EM systems and ROVs.

Water temperature, depth, and sea state generally do not affect the operational effectiveness of AUVs. Water conditions such as surge, currents and tides can affect the productivity of an AUV by increasing the power necessary to maintain a steady heading and speed and reducing the power

supply. Sea state also affects the ability to launch and recover the AUV. Low visibility may be a concern for AUV equipped with optical sensors, because an operator cannot adjust camera and lighting operations in real time, as is possible with an ROV. Debris can obstruct the ability to carry out low-altitude, bottom-following transect surveys or create an entanglement. Vessel traffic through the survey area is generally not a factor, unless the AUV is operating in shallow water areas (Strategic Environmental Research and Development Program 2009).

6.3.2 Remotely Operated Vehicles

Two types of ROVs are used in surveys, a standard ROV that is equipped with its own thrusters for maneuvering and remotely operated towed vehicles. Standard ROVs are best suited to work in smaller, well-defined areas (e.g., reacquisition and investigation of an anomaly) or for surveying a narrow defined area (e.g., a cable route). Remotely operated towed vehicles are capable of covering larger areas and incorporate controls so the vehicle itself can adjust its altitude and path.

Connecting an ROV with its sensor package to the surface by cable has two advantages. First, power can be supplied over the cable to the platform and sensor, so the survey does not need to be interrupted to replenish batteries. Second, the nearly unlimited bandwidth offered by such cables allows data from the sensor to be monitored, recorded and processed in real time. ROVs are connected to a surface vessel via a tether/cable that transmits sensor data, and are operated by an ROV pilot.

Motion of the surface vessel, caused by wind, seas and swell can perturb the motion of a vehicle connected to the surface from the desired path. The most common technique for minimizing this perturbation is using a depressor weight in combination with a neutrally buoyant vehicle as a two-body towed system, which attenuates undesired motion of the vessel.

6.3.2.1 Standard Remotely Operated Vehicles

ROV depth is controlled by amount of towing cable deployed and by ship's speed. Standard ROVs are divided by size and function into three categories: 1) Working-class (approximately the size of a small forklift); 2) Inspection-class (approximately the size of a suitcase); and 3) Mini-ROVs (approximately the size of a 5-gallon bucket or smaller). Working-class ROVs are larger in order to support hydraulic systems, tooling, manipulators, etc.

Mini-ROVs are small enough to be lifted by a single person. Inspection-class ROVs vary in size, with smaller models able to be lifted by a single person and larger models requiring a team to move. Both mini- and inspection-class ROVs have very small operational footprints, allowing for multiple launch and recovery options, high maneuverability and station keeping capabilities, and integrated sensor packages. Both types of ROVs are capable of being equipped with low-light video, lighting systems, altimeters, imaging sonars, and various positioning systems. Mini-ROVs generally do not have the capability to carry a payload beyond optical sensors, sonar and a positioning system. Inspection-class ROVs can be configured to deploy attachments developed to increase the functionality of an ROV (such as sediment sample collection devices).

Mini-ROVs and inspection-class ROVs are deployable from shorelines and small vessels with little support. However, relatively low thruster power and a shorter tether (compared to working-class ROVs) limits the maximum range from the initial deployment location and the ability to function effectively in areas with strong currents.

Working-class ROVs require additional support equipment, a larger crew (up to five people, more if 24-hour operations are required), and a large staging area. Mini-ROVs and inspection-class

ROVs are smaller and supported primarily by electrical systems and tooling. They are deployable from much smaller vessels and do not require as large an operational/maintenance crew to support modest project goals.

ROVs are multi-use platforms for underwater MEC activities when the proper form factors (e.g., platform shape) and payloads are utilized. Recent advances in technology have increased the ability of inspection-class ROVs to deploy with sonar, metal detecting, and environmental manipulation equipment such as hydraulic suckers and blowers, gripping appendages, etc. They are able to survey underwater for extended periods and are able to provide a 100% video record of underwater activities.

The payloads for ROVs are similar to that for AUVs except that size and power requirement concerns are not as great, and data can be telemetered to the surface in real time. ROV quality control generally consists of sensor function tests and verification of positional accuracy. This is performed in a fashion similar to that described for AUVs.

6.3.2.2 Remotely Operated Towed Vehicles

Figure 6-5: EIVA ScanFish II ROTV



Image courtesy of EIVA.

A recent development for towed vehicles is the addition of hydrodynamic surfaces and control systems so the vehicle itself can adjust its path. One example of a remotely operated towed vehicle (ROTV) is the EIVA ScanFish (Figure 6-5), which has sensors for depth, attitude and altitude and can be towed at speeds of 4-10 knots. It can be set to maintain a constant depth or altitude, with an accuracy of 0.2 m; the constant altitude function handles slopes of 20° during routine surveying. The Scanfish has an anti-collision mode that will initiate ascent at 3 m/second when towed at a speed of 6 knots, clearing a slope of 45° (EIVA n.d.). This vehicle can be equipped with four magnetometers as seen in Figure 6-6; when surveying for

small objects with a maximum detection range of just a few meters, this quadruples the survey coverage.

Other remotely operated towed vehicles include the Kraken Sonar's KATFISH (Figure 6-7), which includes automatic depth or altitude tracking for an integrated SAS system. This combination has a substantial acquisition cost of roughly \$1.5 million but can be towed continuously from a surface vessel with co-registered bathymetric and backscatter data available in real time (Kraken Sonar Systems, Inc. 2015a).

Figure 6-6: EIVA ScanFish Equipped with Four Magnetometers for High-resolution Magnetic Survey

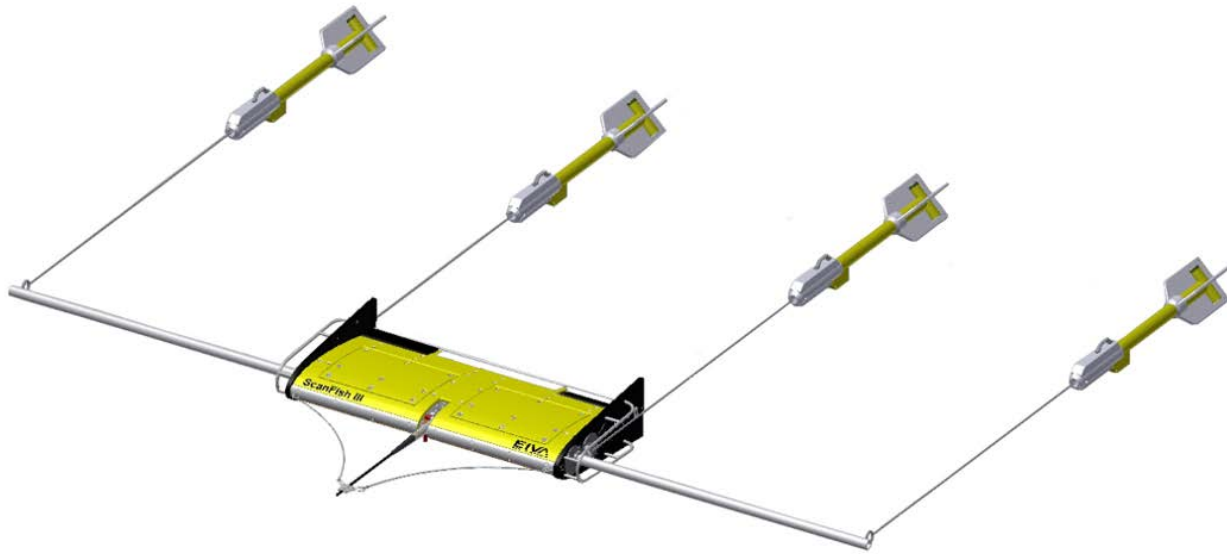


Image courtesy of EIVA.

Figure 6-7: Kraken Active Towfish, KATFISH-180 with a 180 cm SAS Array

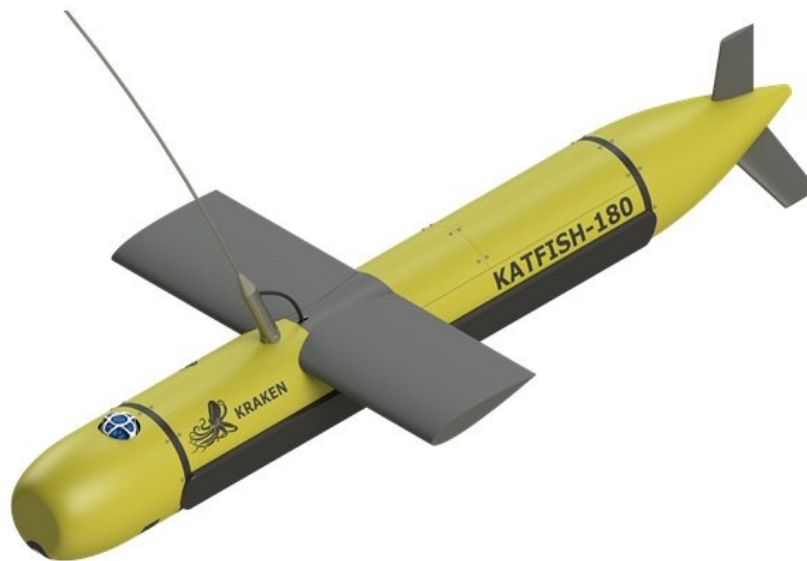


Photo courtesy of Kraken Sonar.

6.3.3 Autonomous/Unmanned Surface Vehicles

Autonomous surface vehicles (ASV - sometimes called unmanned surface vehicles) are the surface equivalent to AUV. They are surface vessels that are operated remotely and/or follow the commands programmed into their control systems. Many are like AUVs in that they have rechargeable batteries as a form of stored energy, but some take advantage of the air surrounding them to combust fuel to provide high energy density. Others harvest energy from the sun with photovoltaic panels or by capturing wave energy. ASVs have another advantage in that they can take advantage of GNSS for navigation. Finally, they can use radio frequency telemetry to

communicate with an operator some distance away and provide all sensor readings in real time if desired.

Most ASVs on the market presently are small, roughly 2 m in length, with survey speeds around 4 knots. They are able to operate for 3 to 8 hours using onboard batteries. Typically they are equipped with small MBES or side-scan sonars, and use Wi-Fi for communication and data transfer, limiting their maximum telemetry range to 1 or 2 km. ASVs can be launched by hand from the shore or at sea from a small boat, and they are especially well suited for surveying shallow water where conventional boats may not be able to operate safely. One example is the Teledyne Oceanscience Z-boat, a 1.8-m-long vehicle that can survey at up to 5 km per hour and has a maximum Wi-Fi range in excess of one km (Martin, McDonald and Munday 2015). Another is the Deep Ocean Engineering H-1750, a 1.75 m ASV, with a Wi-Fi telemetry range of 2 km and a high-definition 720p video feed from the vehicle. Depending on speed, the H-1750 has battery capacity to operate for as long as eight hours duration (Cecchetti 2015).

Some more recent ASVs are larger; ASV Global makes several models that are 4 to 11 m in length, with endurance of many days and speeds of 6 to 9 knots (ASV Global 2016). Their C-Worker 6 has a length of 6 m and is capable of operating for 30 days. One application that has been developed is the ability to monitor positions of transponder-equipped subsea vehicles, with the integration of the Sonardyne Ranger 2 Gyro USBL system. This produces improved positioning information for AUVs that are too far away to be monitored from their mother ship, allowing for a greater number of AUVs to be deployed at one time (Sonardyne 2014). ASV Global's C-Enduro vehicle can lower a small conductivity-temperature-depth (CTD) sensor for measuring properties of the water column, and is developing a capability for towing a larger ROTV. Kraken Sonar Systems Inc. announced that their KATFISH ROTV, equipped with their SAS, and its associated launch and recovery system, was to be integrated with Elbit Systems' Seagull ASV, a vessel 40 feet in length. This combination is intended for mine countermeasure operations (Kraken Sonar Systems, Inc. 2016).

As ASVs get larger and their speed and endurance increase, telemetry systems for control and monitoring that are limited by line-of-sight, such as Wi-Fi, become a serious limitation. In order to use an ASV over the horizon, a satellite communication system is necessary. Not only must this system transmit sensor data back to the control station, but laws governing the prevention of collisions at sea require the vessel have someone standing watch, so a video link would also be required. Satellite data links cost on the order of a dollar per megabyte, and a video stream, even digitally compressed, can require 10 megabytes per minute, which could add up to roughly \$14,000 per day. Operation at night or in poor visibility would require the ASV to be equipped with radar, with the data transmitted to the remote watchstander. Carrying out a survey controlled from shore using ASVs towing acoustic and magnetic sensors near the seafloor will soon be possible, but will not be cost-effective for commercial use for some time.

6.3.4 Surface Vessels

MEC surveys require the use of watercraft to tow or deploy sonar and metal detecting arrays, and to deploy and recover ROVs and AUVs. The cost to mobilize and demobilize a vessel to for a project can be significant. Therefore, it is common to select a "vessel of opportunity" near the project site capable of performing the desired operations.

The selection of vessels of opportunity to support MEC surveys must be based on adequate deck space for equipment, berths for the survey team, the ability to remain at sea as required for the

MEC investigation, and cost. The requirements of the various platforms and technologies to be deployed from the vessel of opportunity affect the type, size and layout of the vessel. The support vessels must include infrastructure to hoist and lower heavy equipment from the deck into the water (e.g., A-frames, overboard sheaves, winches) or attach transducers or MBES to pole mounts, and they must have sufficient space to set up computers to collect and monitor data. A small AUV or mini-ROV may be able to accomplish project objectives from a small vessel, while the deployment of a work-class ROV necessitates a vessel large enough to house the ROV and the associated control center, including operational and engineering personnel. Many working-class ROVs have a dedicated launch and recovery system, in which case suitable deck space and power must be available on the vessel; other ROVs are deployed and recovered using a ship's crane. Costs for vessels of opportunity can range significantly based on the number and size of vessels used.

6.3.4.1 Small Boats

Small boats are open boats, typically 5 to 7 m in length, with very limited resources for carrying out surveys. They are often found as tenders aboard coastal and larger R/Vs and frequently used to deploy and recover smaller AUVs and other equipment. They are very inexpensive but do not have shelter for electronic equipment and crew and are steered by hand, making accurate survey lines difficult to achieve.

6.3.4.2 Survey Launches

Survey launches are larger than small boats, ranging from 8 to 14 m in length. They have an enclosed, air-conditioned wheelhouse with room for survey electronics and personnel. Instruments such as MBES or phase bathymetry/backscatter sonars, as well as attitude and position sensors can be mounted on survey launches. The vessel may also be equipped with an autopilot system.

The specific example described below, the R/V *AHI* (Figure 6-8), is capable of deploying a CTD sensor to measure water column properties. It has no berthing and so is used during daylight only. With a planing hull, it can transit at speeds of up to 21 knots, but surveying is typically done at speeds of 6 to 10 knots. The draft, including a MBES, is 1 m (National Oceanic and Atmospheric Administration 2005). It can accommodate launching and recovering a small AUV.

Figure 6-8: R/V AHI, Survey Launch



The R/V AHI, an example of a survey launch. Photo courtesy of NOAA.

6.3.4.3 Coastal/Regional Research or Commercial Vessels

Coastal/regional research or commercial vessels are capable of operating hundreds of miles offshore, for periods of several weeks or more. Operating 24 hours a day, they require a crew of eight to ten people, and can accommodate survey parties of ten to twenty. Typical sizes of these vessels are 30 to 45 m (100 to 150 feet) in length, and cost per day of use runs from \$10,000-15,000. One example is the University of Delaware's *R/V Hugh R. Sharp*; it has an overall length of 44.5 m and a draft of 2.9 m. It has 22 berths and carries a crew of eight; the vessel's endurance is about 14 days and it has a range of 3500 nautical miles (University of Delaware 2015). In 2013, the day rate was \$11,725 (National Research Council 2015).

One significant advantage of these larger vessels is the capability to host multiple AUVs, both underwater and surface. AUVs are a "force multiplier" that can greatly increase the survey coverage for a given amount of time; for example, by deploying AUVs at one location and then moving to a separate location to conduct operations using hull-mounted, pole-mounted or towed systems. A pipeline and platform survey described in (Keller, Hamilton and Hird 2015) used a pair of Gavia AUVs in operation 24 hours a day from a 35-m ship. Each AUV could travel for 5 to 6 hours at speeds of 3.5 to 4 knots. A survey crew of nine people was needed, including data processors, as data quality and coverage could not be determined until after each AUV deployment. Over a 26-day deployment, they averaged 45 km of AUV track line per day, but that number includes lost time to transiting to/between survey areas, poor weather and equipment problems that altogether took 41% of their time. On the best day, more than 80 km of track was surveyed.

Expanding the number of AUVs to three or four would require more technicians to process data and maintain the vehicles, but the increase in coverage rate would be greater than the increase in cost. Improvements in autonomy software, such as Seebyte Ltd's Neptune software system,

promise to allow larger numbers of vehicles to operate without a proportional increase in the number of operators (Marine Technology Reporter 2015).

Table 6-7: Summary of Platforms

| Platform | General Use | Description | Effectiveness | Implementability | Cost |
|----------|--|--|---|--|---|
| ROVs | ROVs are primarily used as a platform for environmental characterization and MEC detection and characterization. Working-class ROVs equipped with manipulators are able to directly interact with MEC. | ROVs are integrated sensor platforms that can perform many tasks. Multiple form factors allow ROVs to operate for long periods at depth. Mini-ROVs can be fitted with high-definition cameras and imaging sonar. Inspection-class ROVs can be fitted with magnetometers, other sensors, high-definition cameras, various sonars, and sample collection equipment. Work-class ROVs are capable of performing intrusive investigations and handling MEC. | Mini-ROVs and inspection-class ROVs are highly effective technologies for conducting visual surveys. The ease of deployment coupled with limited support needs and increased safety associated with remotely accessing underwater MEC make ROVs an appealing technology. Inspection-class ROVs are useful tools for investigating specific anomalies and collecting samples. Work-class ROVs are capable of excavating and handling MEC, though they require MEC to be fully exposed on the bottom or minimally buried, as well as in favorable sediment conditions, to be effective. | ROVs have been routinely used for a variety of underwater work. | ROV costs range from low to high based on the form factor (mini, inspection or work-class) and sensors payload. Unlimited depth and bottom time allow for greater productivity. The support vessel is an important consideration in evaluating cost. |
| AUVs | AUVs are an effective platform for environmental characterization technologies and represent an emerging platform for MEC detection and characterization. | AUVs can deploy various sonar and EM sensors over wide areas autonomously for extended periods of time. They require little support and can replace manned survey vessels for sonar or other sensors. AUVs represent an emerging technology platform for EM sensors utilized for MEC detection (Strategic Environmental Research and Development Program 2009). Commercial advancements in towing magnetometers behind AUVs for EM mapping are occurring. Hybrid AUV/ROVs are capable of operating autonomously, but can also be attached to a tether and controlled in real time by a surface operator. | AUVs are most effective when operating in a wide area assessment mode for a large MEC survey. Their ability to deploy over large distances and time periods can make them a safe and cost-effective alternative to deploying sensors from survey vessels. Their effectiveness for MEC detection surveys is greatly reduced by their current inability to accurately record a position and their inability to avoid obstructions when navigating in close proximity to the bottom. | AUVs have been effectively used for environmental characterizations of non-MEC sites. AUVs represent an emerging technology platform for EM activities. | AUVs and hybrid AUV/ROVs are relatively expensive compared to other sensor platforms, and require additional sensors to be effective. Potential cost savings over other technologies is derived through extended, unmanned productivity. |

Table 6-7: Summary of Platforms (Continued)

| Platform | General Use | Description | Effectiveness | Implementability | Cost |
|-----------------|--|--|---|---|--|
| Surface Vessels | Vessels of opportunity are commonly used to deploy towed sensors, ROVs and AUVs for MEC surveying. | The size, and configuration of vessels is determined by the platforms and technologies deployed during a project. A small tethered system (e.g., ROV, towfish) operating in shallow water may require nothing more than a small rigid-hulled inflatable boat, while the deployment of a large tethered system (e.g., work-class ROV) may require a larger vessel with a davit crane capable of deploying and retrieving the over-the-side equipment. | The wide range of available vessels makes them effective platforms for MEC surveying. | Surface vessels are routinely used during investigations. | Costs can range significantly based on the size of the vessel, the crew required to operate the vessel, and related costs such as fuel consumption costs or dock fees. |

Based on U.S. Air Force (2014).

Table 6-8: Effectiveness of Platforms and Technologies When Associated with Various Site Characteristics

| | Site Characteristics | | | | | | | | | | | | | | | | | | | | | | |
|---|----------------------|--------------------|-------------------------------|---|-----------------------------------|------------|-----------------|------------|-------------------------------|---------------------------------------|----------------------------------|----------------------------|---------------------------|-----------------------|---------------------------------|----------------------------|-------------------------|---|--|--------------------------|--|--|--|
| | Low Density Sites | High Density Sites | Small sites (less than 50 ha) | Medium sites (between 50 ha and 500 ha) | Large sites (greater than 500 ha) | Shorelines | Nearshore Zones | Open water | Shallow depth (less than 5 m) | Medium depth (between 5 m and 36.5 m) | Deep depth (greater than 36.5 m) | High visibility conditions | Low visibility conditions | MEC proud of seafloor | MEC buried 0 to 2 m in seafloor | MEC buried deeper than 2 m | Highly variable terrain | Significant areas of clutter and debris on the bottom | Large objects extending vertically from the bottom | Near metallic structures | Areas of increased non-project related vessel activity | Non-project related construction and diving activity | |
| Sensors | | | | | | | | | | | | | | | | | | | | | | | |
| Sub-bottom Profiler | E | E | E | E | E | P | E | E | E | E | E | E | E | E | E | E | E | P | E | E | P | P | |
| Side-scan Sonar | E | E | E | E | E | P | E | E | P | E | E | E | E | E | I | I | E | P | E | E | P | P | |
| Multibeam Echo-sounder | E | E | E | E | E | P | E | E | P | E | E | E | E | E | I | I | E | E | E | E | P | P | |
| Side-scan/Phase Bathymetry Sonar | E | E | E | E | E | P | E | E | P | E | E | E | E | E | I | I | E | P | E | E | P | P | |
| Synthetic Aperture Sonar | E | E | E | E | E | P | E | E | P | E | E | E | E | E | I | I | E | P | E | E | P | P | |
| Magnetometers/Gradiometers | E | P | E | E | E | P | E | E | E | E | E | E | E | E | E | E | P | P | P | P | P | P | |
| Electromagnetic Induction Sensors | E | P | E | E | E | P | E | E | E | E | E | E | E | E | E | P | P | P | P | P | P | P | |
| Optical and Imaging Technology | E | E | E | P | P | P | E | P | E | E | E | E | P | E | I | I | E | E | P | E | P | P | |
| Platforms | | | | | | | | | | | | | | | | | | | | | | | |
| Autonomous Underwater Vehicles | E | E | E | E | P | P | E | E | E | E | E | E | E | E | E | E | P | P | P | E | P | P | |
| Remotely Operated Vehicles | E | E | E | P | P | P | E | E | E | E | E | E | P | E | E | E | E | P | P | E | P | P | |
| Remotely Operated Towed Vehicles | E | E | E | E | E | P | E | E | E | E | E | E | E | E | E | E | P | P | P | E | P | P | |
| Autonomous Surface Vehicles | E | E | E | P | P | P | E | P | E | P | E | E | E | E | E | E | E | E | E | E | P | P | |
| Small Boats | E | E | E | P | I | P | P | P | P | P | P | E | E | E | E | E | E | E | E | E | P | P | |
| Survey Launches | E | E | E | E | P | P | E | P | E | E | E | E | E | E | E | E | E | E | P | E | P | P | |
| Coastal/Regional Research or Commercial Vessels | E | E | E | E | E | I | P | E | I | E | E | E | E | E | E | E | E | E | P | E | P | P | |

Legend: E - Generally Effective, I - Generally Ineffective, P - Potentially Effective

Based on U.S. Air Force (2014)

This Page Intentionally Left Blank.

6.4 Considerations for Survey Design and Implementation

6.4.1 Sensor Configuration and Deployment

The U.S. Army Corps of Engineers Engineering Manual 1110-2-1003, *Hydrographic Surveying* (U.S. Army Corps of Engineers 2013b) is a “best practices” guide for performing hydrographic surveys. Although the U.S. Army Corps of Engineers manual provides an overview on proper setup, configuration, calibration and operation of surface vessel-mounted acoustic sensors, the general concepts are useful for other types of sensors, platforms and applications. Acquiring high-quality acoustic data depends on several factors including:

- ▶ Physical and environmental characteristics of the survey area: water depth, temperature and salinity are necessary for proper equipment calibration.
- ▶ Project data quality objectives: survey purpose and resolution requirements need to be clearly defined. The balance between resolution and range must be considered.
- ▶ Survey speed: sonar data quality can be affected by the speed the sensor travels. Increasing sensor speed reduces the number of times a sound wave can travel to the target and return to the sensor, which reduces resolution.

Configuration of acoustic equipment and the survey design must work in concert to meet project data quality objectives. For example, the size of objects to be detected determines the necessary data resolution, which informs what frequency acoustic sensors to use as well as the altitude of the sensor above the bottom, the survey speed and the swath width for survey lines. Once these variables are defined, a survey plan can be created to achieve comprehensive coverage or space transects appropriately. Similarly, to detect MEC at a WEA, the goals of the survey need to be clearly established. Data resolution requirements as well as equipment and platform availability and cost need to be investigated to aid in selecting an appropriate sensor suite and platform capable of successfully conducting the survey.

Successful surveying relies heavily on understanding oceanographic conditions. Historic weather and climate data for the survey site will indicate the best weather windows for operating in smaller sea states. Salinity levels and temperature changes in water affect the quality of sonar data collected, so these data should be collected to better estimate sound speed through the water column in the survey area. EM 1110-2-1003, *Hydrographic Surveying* (U.S. Army Corps of Engineers 2013b), describes typical hydrographic survey quality control measures, such as tie-lines and bar checks, for undertaking these efforts. Wave, surf, surge and current action in shallow areas are a significant hindrance to towed platforms and should be researched prior to field program deployments. Very shallow water (<10 m) may require use of airborne or modified platforms, such as those that employ sensors floating on the surface rather than sensors that are fully submerged. Man-made activities in the ocean, such as vessel through-traffic, can negatively affect shipboard operations when using over-the-side-gear, especially when towed instruments are involved.

Large variations in topographic relief can slow survey productivity, especially for near-bottom towed systems. For example, mapping of magnetic anomalies is conducted by towing the sensors behind a surface vessel, or by attaching geophysical sensors to ROVs and AUVs. Maintaining a constant offset of the metal detecting platform from the bottom is important when MEC surveys are conducted in areas with topographic relief. While underwater surveys executed with sensors at a constant water depth may be appropriate when the bathymetric

variations are small, bathymetry-following systems ensure uniform target detection. Some platforms are deployed with optical systems, allowing visual and magnetic information to be collected concurrently, but sometimes a combination of geophysical and optical sensors reduces effectiveness. When a towed sensor platform cannot hold position over an item or sufficiently alter its position to achieve a superior viewing angle, the quality of the video or photographic record may be poor due to lighting issues or suspended sediments.

6.4.2 Quality Control

A critical aspect of any technical activity is to ensure that the data quality objectives for the work are met. This includes verifying that the systems in use are performing within acceptable limits and that the targets of interest can be detected reliably and with repeatability in typical conditions for the site. Quality control consists of sensor function tests and verification of positional accuracy. Both are assessed through reacquisition of known control points at an established Instrument Verification Strip (IVS). Verification of positional accuracy is typically achieved through consistent reacquisition of control points at the beginning and end of each survey day. Each positioning system possesses a normal level of accuracy. By repeatedly reacquiring a single object and recording a position, verification of positioning system operability can be assured by comparing the positioning data against expected offsets and all prior verification surveys.

A recommended approach for quality control of mapping and geophysical surveys is to establish this effort at the outset in project-specific work plans. For example, arrange to place ISOs, sized to serve as surrogates for the MEC of interest, in an IVS in areas free of debris to represent MEC items likely to be found at the site (Orca Maritime Inc. 2015, Environmental Security Technology Certification Program 2009). The ISOs can be selected to provide an expected response at various altitudes, which will allow daily performance verification of the sensors compared against models and previous surveys. Multiple surveys of the IVS can be run for each of the various technologies deployed during an investigation. The recorded position of the ISOs in the IVS should be derived from the technology with the positioning system with the lowest overall offset and best accuracy. By surveying the IVS at the start and end of each day, the geophysical sensors can be verified to be delivering the expected detection performance and the “drift” in sensor performance can be documented over time.

Ongoing monitoring of the production survey through implementation of a blind seeding program allows a project team to verify that the production survey is likely to meet data quality objectives or to recognize that problems exist and provide a means to identify root causes and undertake corrective action while still in the field. The objective of a blind seeding program is to provide ongoing monitoring of the quality of the geophysical data collection and target or anomaly selection process as it is performed in the production survey throughout the project. Ideally, the blind seeds should be numerous enough to be encountered on a daily basis. If possible, blind seeding of the project site should occur in accordance with U.S. DoD Environmental Security Technology Certification Program (ESTCP) *Geophysical System Verification (GSV): A Physics-Based Alternative to Geophysical Prove-Outs for Munitions Response* (Environmental Security Technology Certification Program 2009); however, the ability to emplace seeds may be limited due to the need for a diver or working-class ROV to install the seeds. A blind seeding program requires firewalls between the personnel planting the seeds and those evaluating performance, and the personnel performing the data collection and analysis (Environmental Security Technology Certification Program 2009).

6.4.3 Considerations for Use of ROVs

There are several factors to account for when considering ROVs for deployment. Effectiveness of any visual survey can be hampered by low visibility, though the ability to switch between high-definition color and black-and-white video and alter lighting intensity and direction allows ROVs to record better quality video than divers equipped with underwater cameras. ROVs generally need a minimum of 2 feet of visibility to operate around known anomalies, with efficiency increasing with expanding visibility. Areas of fine sediment can hamper working-class ROVs as large thrusters have a tendency to stir up sediments and reduce visibility. Areas of significant bottom debris can also negatively affect ROV actions. Tethers can become snagged in debris, and decreased maneuverability compared to divers can make it difficult to perform visual surveys around, beneath, and between areas cluttered with significant debris. Working-class ROVs are better suited than divers to performing activities in deep water and open areas where safety and productivity concerns create a comparative advantage for ROVs (Carton, King and Bowers 2012).

Wave, surf, surge, depth and current action in the shoreline area have the potential to substantially reduce the stability of an ROV and can damage equipment if water conditions cause the vehicle to impact the bottom. Controlling vessel traffic in the survey area during ROV operations is important to minimize the potential for interference with survey operations. Tethered ROVs are able to survey hundreds of meters from the initial deployment location, which creates a situation where vessels transiting through the survey area may unintentionally sever or become entangled in the tether.

6.5 Recommended Approaches in WEAs

Magnetometers appear to provide the best detection of buried ferrous objects, including possible MEC anomalies, at Atlantic OSC WEA sites due to their ability to detect small buried ferrous objects with the same efficiency as objects exposed on the seabed. The WEAs under consideration have bottoms that consist almost entirely of iron-poor sediment, in which heavy objects like MECs are likely to become buried. Although SAS provides superior areal coverage at high spatial resolution, they do not detect buried objects well. Additionally, commercial development of these WEAs will likely involve excavation, trenching or disturbing seabed materials 2 m below the seabed along the cable route. The smallest MEC considered a concern for the areas investigated is the 155 mm artillery round, which has a magnetic detection range of about 6 m; larger MEC would be detectable from even greater range.

Although magnetometers only detect ferrous metal and do not generally possess the discrimination capabilities of TDEMI, these passive sensors generally have higher production rates in terms of survey speed and are able to collect useable data at higher altitudes than TDEMI sensors. This advantage allows magnetometers to be deployed effectively at underwater sites with high bottom debris density that could potentially obstruct or entangle a platform following close to the bottom.

To maintain a constant offset of the metal detecting platform from the bottom, an AUV may be preferred as the user can program the AUV to maintain a set distance from the seabed. Towed systems rely upon manual letting out or reeling in of cable to adjust the distance off the seabed as required by towed systems and sudden changes in bathymetry may not allow time to adjust the height of the sensor in time resulting in either damage to the equipment or too great a distance

off the seabed for detection. AUVs can also extend a survey into shallower depths than what is typically accessible with towed systems due to vessel draft.

Most AUVs include side-scan sonar; the addition of a magnetometer makes for a comprehensive tool. A survey with track spacing of 4 to 8 m provides substantial overlap for magnetics and highly oversampled backscatter imagery, which would have comparable resolution to the SAS system.

One factor to consider is the position drift that is associated with AUV surveys. Given that AUV's cannot utilize GPS positioning underwater, INS/DVL navigation is required; as outlined in Section 6.1.2.3, INS/DVL navigation is susceptible to positional drift. To minimize drift, the AUV surveys should be broken into areas with survey lines less than a few km. Backscatter imagery from adjacent lines can also be used to help correct for navigational drift of an AUV.

The distance from shore of the WEAs and the size and depth of the area to be surveyed shift the optimal survey platform between a survey launch and a larger vessel, equipped with a surface sonar (such as a PMBS), and also capable of launching one or more survey platforms (e.g., AUVs) to conduct magnetometer and high resolution side scan sonar surveys. For survey areas not far from shore, the higher transit speed of a survey launch relative to a coastal R/V means a smaller fraction of time is spent traveling to and from the survey site. Once survey areas become larger and farther from port, a coastal vessel becomes more cost-effective, since it can carry enough personnel to operate around the clock, support multiple over-the-side systems (e.g., AUVs, tethered systems, hull-mounted sensors) remain in the survey area for days to weeks at a time and process data as the survey progresses. Prior to beginning surveys with platforms that will be near the seafloor, a bathymetric and backscatter survey of the entire area is recommended to aid in mission planning.

7.0 Description of In-field Verification Study Area

7.1 Study Area Description

An in-field verification was performed to develop and optimize methods aiding in the evaluation and management of MEC risks during offshore renewable energy development. The study area selected for the in-field verification is within the Delaware WEA. In-field testing was performed with using the University of Delaware ship (*R/V Daiber*) within a 4.5 km² area of the field blocks of the Delaware WEA (Figure 1-2).

7.2 Physical Characteristics of Delaware WEA

7.2.1 Air Temperature

Temperatures at the sea surface of the study area fluctuate significantly during the year with a mean annual temperature of 10.2 degrees Celsius (°C) (50.4 degrees Fahrenheit [°F]); mean temperature extremes range from 6.8 to 12.9°C (44.2 to 55.2°F) (Table 7-1). The average monthly air temperature range when field work is planned to occur (i.e., during the summer) is 12°C (54°F) (Table 2-6).

Table 7-1: Delaware WEA Seasonal Description

| | Winter | Spring | Summer | Fall |
|--|--------|--------|--------|-------|
| Avg. Sea Surface Temperature (°C) | 6.84 | 9.26 | 11.95 | 12.86 |
| Stratification (kg m ⁻³) (Density difference from depth to surface) | -0.37 | -1.45 | -2.26 | -0.20 |

Source: The Nature Conservancy (2016).

Note: kg m⁻³ - kilogram per cubic meter

7.2.2 Bathymetry and Seafloor Geology

The topography of the continental shelf was shaped largely by sea-level fluctuations caused by past ice ages. The shelf's basic morphology and sediments were derived from the retreat of the most recent ice sheet and the subsequent rise in sea-level.

The study area is within the Delaware WEA (Figure 1-1), characterized by ridge and swale topography in the western blocks, with gentle slopes in the eastern blocks. The study area is on the central Middle Atlantic Bight (MAB), which includes the shelf and slope water from Georges Bank south to Cape Hatteras. The MAB is characterized by a gently sloping bathymetry to the east until about 100 - 200 km offshore. The Delaware WEA has a ridge and swale bathymetric relief with a gentle slope to the east. Ridges are generally about 10 m in height with lengths of 10-50 km. Sediments on the ridge crests tend to contain less fine sand, silt and clay than the swales. The sediment type at the study area is predominantly coarse sand with gravel (65 %), with significant fractions of coarse sand (13%), medium sand (16%), and fine sand (5%) (Table 7-2). Depths in the study area range from 9 – 34 m with approximately 85% of the study area between 15 – 30 m in depth (Table 7-3).

Table 7-2: Sediment Description

| Wentworth Scale (1922) | Silts | Sandy Silt | Fine Sand | Med Sand | Coarse Sand | Coarse Sand w/ Gravel |
|--------------------------------|-------|------------|-----------|----------|-------------|-----------------------|
| Sediment Distribution (% area) | 0.00 | 0.00 | 5.15 | 15.96 | 13.03 | 65.03 |

Sources: The Nature Conservancy (2016); U.S. Geological Survey and University of Colorado (2005)

Table 7-3: Bathymetric Description

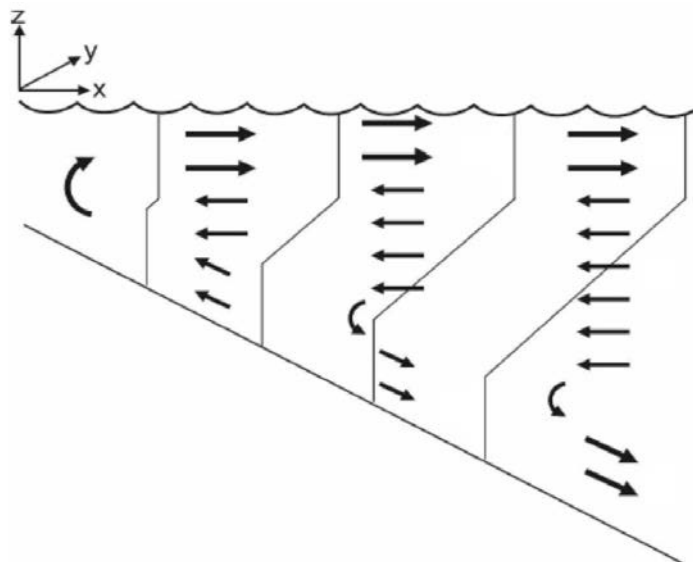
| Bathymetric Relief | W Ridge and Swale, E Gentle Slope | | | | | | | |
|------------------------|-----------------------------------|----------|-----------|-----------|-----------|-----------|-----------|--------|
| Depth Range | 9 - 34 m | | | | | | | |
| Depth Distribution (%) | 0 - 5 m | 5 - 10 m | 10 - 15 m | 15 - 20 m | 20 - 25 m | 25 - 30 m | 30 - 35 m | > 35 m |
| | 0.0000 | 0.0034 | 5.5831 | 26.0844 | 28.5496 | 30.1335 | 9.6442 | 0.0000 |

Source: National Oceanic and Atmospheric Administration (2016f)

Note: m – meter(s)

7.2.3 Currents and Tides

According to Lentz (2008), analysis of current measurements from 33 sites over the MAB continental shelf reveal a consistent mean circulation pattern. Along shelf flow is equatorward and increases with increasing depth from 3 cm per second (cm s^{-1}) at the 15-m isobaths to 10 cm s^{-1} at the 100-m isobath. In the cross-shelf direction (i.e., in the x and z axis of Figure 7-1), the near-surface flow is typically offshore and ranging between 3 to 6 cm s^{-1} . Cross-level estimates show the interior flow is onshore between 0.2 to 1.4 cm s^{-1} , and the near-bottom flow increases linearly with increasing water depth from 1 cm s^{-1} (onshore) in shallow water to 4 cm s^{-1} (offshore) at the 250-m isobath with the direction reversal near the 50-m isobaths (Figure 7-1) (Lentz 2008). Direct observations taken within the Delaware WEA found tidally-driven current amplitudes averaging 7 cm s^{-1} at depths of 30 m (DuVal, Trembanis and Skarke, Characterizing and Hindcasting Ripple Bedform Dynamics: Field Test Of Non-Equilibrium Models Utilizing A Fingerprint Algorithm 2016). However, these observations are not tidally averaged, and are thus not directly comparable to the MAB estimates of Lentz (2008). Due to the dearth of direct bottom current observations across the MAB continental shelf, MAB shelf-wide bottom current estimates remain the best regional estimates available.

Figure 7-1: MAB Cross-Shelf Currents

Note: Schematic of the cross-shelf currents over the MAB adapted from Lentz (2008).

7.2.4 Water Column Profile

Wave climate shows strong seasonal patterns, with wave averages increasing from October through April. Average wave height in the study area during June and July generally range between 0.92 and 0.87, respectively and originate from a southeasterly direction (NOAA NDBC 44009). Sea surface temperature average 11.95°C during the summer months, and temperatures at depths of the study area (i.e., 9 – 34 m) range from approximately 7 to 15°C during June and July (Castelao, Glenn and Schofield 2010). Waters are strongly stratified during summer, with a distinct thermocline at about 20 m depth and a -2.26 kg m^{-3} density difference between water at depth to the surface (Castelao, Glenn and Schofield 2010); (The Nature Conservancy 2016). This stratification may cause issues with surface-based acoustic surveys.

7.2.5 Storms

The study area is located in a region often buffeted by nor'easters, with occasional hurricane activity. Data collected from National Data Buoy Center buoy located offshore of Delaware Bay (Buoys 44009 and 44012) show wind speeds are typically lowest in June and July at 10 knots (12 miles per hour [mph]) to 12 knots (14 mph), and highest in January reaching up to 15 knots (17 mph) in the Delaware Bay area (Bureau of Ocean Energy Management 2012).

Severe weather events during the field effort have the potential to cause structural damage and injury to personnel. Most often, high wind events are associated with extra-tropical cyclones in the winter season but can also be due to tropical cyclones. Hurricane season for the Atlantic Ocean is June 1 through November 30 with a peak in September. On average, about ten storms of tropical storm strength or greater are recorded in the Atlantic basin each year, about half of which reach hurricane level (Bureau of Ocean Energy Management 2012).

7.3 Area Use

Delaware is home to two of the 35 largest U.S. ports: New Castle and Wilmington. The study area is contiguous to active shipping lanes although transportation through the study area is minimal (Bureau of Ocean Energy Management 2012).

The study area is used for recreational and commercial fishing. Recreational fishing was studied for two types of recreational fishers; recreational charter boats and recreational party boats. National Marine Fisheries Service vessel trip report data for chartered fishing vessels and recreational fishing party vessels provides a sum of the total days fished for the calendar year period 2004 – 2008. Between 2004 and 2008, recreational charter fishing boats were present in the study area between 121 and 270 boat days annually. Recreational party fishing boats were present in the study area between 101 and 240 boat days annually. Commercial fishing boat trips between 2004 and 2008, were rare (0 to 265 boat days annually) in the study area compared to the other parts of the surrounding waters (1,399 to 6,355 boat days annually) (Bureau of Ocean Energy Management 2012).

The study area is within the Virginia Capes naval operating area and roughly half of the study area is located in Warning Area 386. The Warning Area 386 air, surface, and subsurface areas are utilized to conduct missile exercises, gunnery exercises, and rocket exercises using conventional munitions, supersonic flight operations, mine warfare training, and laser operations (Bureau of Ocean Energy Management 2012, U.S. Navy 2008).

7.4 Biological Resources

7.4.1 Coastal Habitats

The MAB hosts a range of coastal habitats including barrier islands, sand spits, beaches, dunes, tidal and non-tidal wetlands, mudflats and estuaries; much of which has been impacted to some degree by historical or present human activities (Bureau of Ocean Energy Management 2012). Delaware has approximately 24 miles of oceanfront coastline and coastal resources include extensive tidal wetlands, mudflats, and sandy beaches (Cole, Carter and Arndt 2005).

7.4.2 Critical Marine Habitats and Resources

Mammals classified as endangered under the Endangered Species Act or Depleted under the Marine Mammal Protection Act in the Mid and North Atlantic OCS include the North Atlantic right whale (*Eubalaena glacialis*), the blue whale (*Balaenoptera musculus*), the fin whale (*Balaenoptera physalus*), the humpback whale (*Megaptera novaeangliae*), the sei whale (*Balaenoptera borealis*), the sperm whale (*Physeter macrocephalus*), the bottlenose dolphin (*Tursiops truncatus*), and the west Indian manatee (*Trichechus manatus*) (Bureau of Ocean Energy Management 2012). Of these species, only the North Atlantic right whale, the bottlenose dolphin, and the west Indian manatee were listed as occasional or common in the Mid-Atlantic coastal or shelf habitat. At the study area, there is no critical habitats formally identified for marine mammals (Bureau of Ocean Energy Management 2012). Threatened or endangered sea turtles listed as common in the MAB include the loggerhead sea turtle (*Caretta caretta*) and the leatherback sea turtle (*Dermochelys coriacea*).

There is a potential that water birds and multiple pelagic species may be present from the coastline out to the seaward extent of the study area. A full listing of all endangered birds that can be found in Delaware is available on the Delaware Division of Fish and Wildlife's [website](#).

In the coastal and marine waters of Delaware, the common tern (*Sterna hirundo*), Forster's tern (*Sterna forsteri*), least tern (*Sterna antillarum*), black-crowned night-heron (*Nycticorax nycticorax*), yellow-crowned night-heron (*Nyctanassa violacea*) red knot (*Calidris canutus*), piping plover (*Charadrius melodus*), and black skimmer (*Rynchops niger*) are listed as endangered and may be present during at least part of the year. These species use coastal habitats including beaches, marshes, and intertidal wetlands but may pass through the study area during migration.

Species of bats that currently or historically occur in Delaware are the big brown bat (*Eptesicus fuscus*), the little brown bat (*Myotis lucifugus*), the northern long-eared bat (*Myotis septentrionalis*), the tri-colored bat (*Perimyotis subflavus*), the eastern red bat (*Lasiurus borealis*), the evening bat (*Nycticeius humeralis*), the hoary bat (*Lasiurus cinereus*), and the silver haired bat (*Lasionycteris noctivagans*). However, only the silver haired bat, eastern red bat, and hoary bat would possibly migrate through the study area.

Demersal fish distributions are influenced by latitude and depth, and fish assemblages generally follow isotherms and isobaths (Stevenson 2004). Threatened or endangered marine fish species found off the Mid-Atlantic Coast include the shortnose sturgeon and the Atlantic salmon, which are federally-listed as endangered (Bureau of Ocean Energy Management 2012).

Due to the limited spatial and temporal extent of the in-field verification work, no significant or population-level effects to marine mammals, fish, sea turtles, birds or bats were experienced. No threatened or endangered species were encountered, during the field effort.

7.5 Archaeological Resources

Archaeological resources on the seafloor at the study area include potential historic and pre-contact shipwrecks, which may date from as early at the 16th century to the present. Offshore Delaware and New Jersey have a very high ratio of known or reported shipwrecks per linear mile of coastline (Bureau of Ocean Energy Management 2012). Also, sea-level rise approximately 11,600-11,100 years before present day may have drowned pre-contact sites of human occupation at the study area (Bureau of Ocean Energy Management 2012, Nordfjord 2006).

No potential archaeological resources were encountered during field activities.

7.6 MEC Potentially Present in the Delaware WEA

Munitions are present in the Atlantic OCS as a result of live-fire testing and training, combat operations, sea disposal, accidents, and disposal during emergencies. MEC identification methodologies depend greatly on the size and signature of the expected objects. The CALIBRE Team researched historical and current activities that may have resulted in MEC deposition near WEAs on the Atlantic OCS and identified potential MEC in the study area (Table 7-4).

Table 7-4: Potential MEC in or Near the Delaware WEA

| MEC Item | Projectile/Mine Weight | Fill/Fill Weight | Net Explosive Weight |
|---|---------------------------------------|--|------------------------------------|
| 37 mm, HE, MK II | 1.3 lbs or 1.6 lbs | TNT or tetryl/ approximately 0.1 lb | 0.1 lb |
| 40 mm, HE, HE-T, HE-I, MK II | HE – 2 lbs HE-T – 2 lbs | HE – TNT/ 0.187 lb HE-T – TNT/ 0.17 lb | HE – 0.15 lb HE-T – 0.17 lb |
| 40 mm, AP-T, M81 | 2 lbs | None | 0.0 lb |
| 3-inch HE and practice, M42 | HE – 12.81 lbs Practice – 12.9 lbs | HE – TNT/0.86 lb Practice – Black powder/0.25 lb | HE – 0.86 lb Practice – 0.14 lb |
| 90 mm, HE, M71; HE-T, M71A1 | M71 – 23.3 lbs M7A1 – 39 lbs | HE - TNT/2.04 lbs | HE – 2.04 lbs |
| 120 mm, HE, M73, shell | 50 lbs | TNT/5.24 lbs | 5.24 lbs |
| 6-inch, HE shell, AP projectile | HE- 90.5 lbs AP – 108 lbs | HE – TNT/14 lbs AP – Explosive D/4.5 lbs | HE – 14 lbs AP – 5.4 lbs |
| 155 mm | HE- 95 lbs AP – 100 lbs | HE – TNT/15.17 lbs AP – Explosive D/1.4 lbs | HE – 15.17 lbs AP – 1.68 lbs |
| 8-inch, AP, MK 19, | 261.8 lbs | Explosive D | 3.64 lbs |
| 12-inch, AP projectile, MK15 | 975 lbs | Explosive D/22.2 lbs | 26.6 lbs |
| 16-inch, AP projectile, MK5 | 2,340 lbs | Explosive D | 34 lbs |
| M4 submarine mine, controlled | Over 6,000 lbs | TNT/3,000 lbs | 3,000 lbs |
| German Submarine Mine, TMB (cast aluminum) | 1,475 to 1,625 lbs | 925 to 1,230 lbs | |

Notes:

AP – armor piercing
HE – high explosive
lb(s) – pound(s)

MK - mark
mm – millimeter
TNT - trinitrotoluene

8.0 Application of MEC Risk Assessment to Delaware WEA

8.1 Identification of MEC Potentially Present

The identification of MEC potentially present is based on a review of a variety of records. CALIBRE reviewed documents available from the National Archives and Records Administration, DoD, and various other Government sources relating to ranges, coastal defense, sea disposals and known MEC discoveries on or close to the Atlantic OCS WEAs to identify other areas of potential concern. Additional resources utilized include the U.S. Army Corps of Engineers FUDS [website](#) (U.S. Army Corps of Engineers 2013a), NOAA Historical Map and Chart Collection [website](#) (National Oceanic and Atmospheric Administration 2016a), and the FortWiki Harbor Defense [Portal](#) (Harbor Defense Portal 2015). A significant amount of the documentation reviewed concerning MEC related activities does not include coordinates and reports such information without an exact location. Due to the uncertainties in the location of munitions in the available documentation, MEC locations within a 10-mile radius of the Delaware WEA and between the Atlantic OCS WEA and shore were included as potentially being present in the WEA.

8.1.1 Naval Warfare

During World War I, there was limited German U-boat activity off the U.S. Atlantic Coast with a small number of vessels sunk. However, there was a significant amount of activity off the Atlantic Coast in World War II. The entrance to Delaware Bay was one of the prime hunting areas U-boats as Philadelphia built about one-third of all ships constructed in World War II. However, U-boat attacks occurred during World War I as well. In May 1918, U-151 laid a cluster of mines off Cape Henlopen and later U-117 laid mines near Fenwick Light. The mines from U-117 and U-151 were recovered through 1919. For part of 1942, the Chesapeake and Delaware canal was closed due to the collision of a ship which brought down a bridge across the canal. Ships were forced into the Atlantic when transiting from Norfolk or Baltimore to Philadelphia. U-boats observed the entrance to Delaware and Chesapeake Bays as they constricted the ship traffic. Mine laying and torpedo attacks on shipping were done by U-boats in this area. Between January and June 1942, U-boats sank 17 ships in the vicinity of Cape Henlopen. On 11 June 1942, U-373 laid 15 2,000 TMB mines in the vicinity of the entrance the Delaware Bay. Mine sweepers recovered and destroyed four mines and a fifth detonated sinking the Tug *John R. Williams* which was returning to Cape May. The locations of each of the mines were identified. In 1945, U-858 surrendered at Fort Miles (U.S. Navy at Cape Henlopen 2016).

Anti-submarine activities involved ships and aircraft. Depth charges and depth bombs were used in the anti-submarine activities on the eastern seaboard including in the vicinity of the Delaware WEA. The Hedgehog anti-submarine weapon fired a salvo of 24 mortars in an arc. Each Hedgehog mortar carried a charge of 35 pounds of explosive. Mines were also deployed by U.S. vessels and German U-boats. Minefields such as the one at Fort Miles were removed at the end of hostilities. However, several U-boats operating in U.S. waters were fitted as mine layers but their capacity was only about 65 mines (U-Boat Net 2016). Therefore, the number of mines deployed was probably not particularly large and thus they are unlikely to be present in the study area.

8.1.2 Coastal Defense

Historically, coastal artillery batteries protected major ports and installations. The coastal artillery operated anti-ship artillery or fixed gun batteries in coastal fortifications. The coastal artillery was established in 1794 as a branch of the Army and construction of coastal defenses began. Following the Spanish–American War, U.S. harbor defenses were greatly strengthened and provided with rifled artillery and minefield defenses. Anti-aircraft guns were installed at coastal defense sites starting in World War I. In World War II, 90 mm guns were added to the program as anti-motor torpedo boat (AMTB) batteries.

The World War II minefield at Fort Miles was controlled from on shore with the mines cabled to a command structure. The mine field was composed of 35 mine groups. The mines all are believed to have been removed at the end of the war.

8.1.3 Training Ranges

The Delaware Target Area 1 and 2 (FUDS# C03DE0064) used both practice and high explosive munitions. The rocket training area used practice items with no explosive filler. However, high explosive items from 40 mm to 16-inch could have been used during training. It is likely that the anti-aircraft batteries in the area were used in training. A 37 mm high explosive projectile was recovered from dredge materials in the area.

8.1.4 Sea Disposal of Munitions

Only one known sea disposal appears to lie within 10 nmi of the Delaware WEA. No sea disposal sites were identified between the WEA and shore. Although other disposals may have occurred, no documentation was found during the historical research.

DoD Sea Disposal Site DE-X01 is described in War Department Transportation Service communications from May 1920. The Delaware General Ordnance Depot, Pedricktown, NJ used Transportation Service vessels to dispose of 25 tons of 155 mm projectiles (500 each) “were dumped outside the three-mile limit.” Given the poor description of the disposal site, only a rough estimate can be made of the location.

The Delaware Ordnance Depot history indicates that a “considerable amount of unserviceable ammunition and components containing explosives were taken to sea and dumped” in November 1930 and again in September 1934. The disposal locations are not specified and it is unknown if these items are in the vicinity of the Delaware WEA.

8.1.5 Summary of MEC Related Activities in Delaware WEA

Table 3-6 summarizes the results of the historical research conducted in support of BOEM’s UXO Survey Methodology Investigation findings related to the Delaware WEA.

8.1.6 Summary of MEC Potentially Present from Known Activities in the Delaware WEA

Based on a review of available historical documentation the following MEC were identified as having been used or disposed in the vicinity of the Delaware WEA area. The MEC and their characteristics are summarized in Table 8-1.

Table 8-1: Description of MEC near Delaware WEA

| Item | Projectile/Mine Weight | Fill/Fill Weight | Net Explosive Weight | Hazardous Fragment Distance* |
|--|---------------------------------------|---|--------------------------------------|------------------------------|
| 37 mm, HE, MKII | 1 lbs | TNT or Tetryl/0.05 lb | 0.05 lb | 90 ft |
| 40 mm, HE, HE-T & HEI, MKII | HE – 2 lbs HE-T – 2 lbs | HE – TNT/0.187 lb HE-T – TNT 0.17 lb | HE – 0.187 lb HE-T – 0.17 lb | 132 ft |
| 40 mm, AP-T, M81 | 2 lbs | None | 0.0 lbs | 0 ft |
| 3-inch HE and Practice, M42 | HE – 12.81 lbs Practice – 12.9 lbs | HE – TNT/0.86 lb Practice - Black powder/0.25 lb | HE – 0.86 lbs Practice – 0.14 lbs | 180 ft (Mk27) |
| 90 mm, HE, M71 and HE-T, M71A1 | M71– 23.3 lbs | HE – TNT/2.04 lbs | HE – 2.04 lbs | 288 ft (Comp B) |
| 120 mm, HE, M73 | 50 lbs | TNT/5.24 lbs | 5.24 lbs | |
| 6-inch complete round | HE – 90.5 lbs AP – 108 lbs | HE – TNT/14 lbs AP – Explosive D/4.5 lbs | HE - 14 lbs AP – 5.4 lbs | 394 ft (Mk34) |
| 155 mm Mk [Mark number illegible in documentation] | MkI – 95 lbs | TNT/15.17 lbs 50-50 Amatol/14.38 lbs 80-20 Amatol/13.63 lbs | 15.17 lbs | 395 ft |
| 155 mm complete round | HE (unfuzed) – 95 lbs AP – 100 lbs | HE – TNT/15 lbs AP – Explosive D/1.4 lbs | HE – 15 lbs AP – 1.68 lbs | |
| 8-inch, AP, MK19 | 261.8 lbs | Explosive D | 3.64 lbs | 179 ft |
| 12-inch AP, MK15 | 975 lbs | Explosive D/22.2 lbs | 26.6 lbs | |
| 16-inch AP, MK5 | 2,340 lbs | Explosive D | 34 lbs | 295 ft |
| Hedgehog | 65 lbs | TNT/30 lbs Torpex/35 lbs | 30 lbs 42 lbs | |
| German Naval Torpedo | 2,937 to 3,369 lbs | Hexanite/617 lbs | 740 lbs | |
| M4 submarine mine, controlled | Over 6,000 lbs | TNT/3,000 lbs | 3,000 lbs | |
| German Submarine Mine, TMB (cast aluminum) | 1,475 to 1,625 lbs | 925 to 1,230 lbs | | |

* The distance from a detonation at which there is a 1% probability of being stuck by a fragment that is likely to be fatal (1% Lethality Distance). Distances are in air with no mitigation.

AP – armor piercing
HE – high explosive
lb(s) – pound(s)

MK - mark
mm – millimeter
TNT - trinitrotoluene

These munitions can be generally grouped as follows:

- ▶ Artillery projectiles, and
- ▶ Sea mines.

Other munitions that may be in the area from combat operations include:

- ▶ Anti-submarine warfare munitions, and
- ▶ Torpedoes.

8.2 MEC Hazard Assessment Findings

The MEC hazard assessment consists of determining the likelihood that MEC is present within the renewable energy development area. The MEC hazard assessment included an evaluation of available records from a variety of sources. The findings relating to munitions potentially present in the Delaware WEA are summarized in Table 8-2 with the probability of munitions presence in the area assigned. The UXO-consultant would apply their professional judgment to information in Table 8-2 in conjunction with knowledge of the area potentially disturbed by a given development activity to assign a probability of encounter per Table 5-1 for use in the MEC risk assessment.

8.3 MEC Risk Assessment Results for Delaware WEA

The probability of a MEC incident occurring is dependent upon the product of two factors:

1. Probability of encountering MEC - Factors affecting the probability of encountering MEC related to site history and physical environment.
2. Probability of detonating MEC – Factors affecting the probability of detonating MEC are related to the type of project activity and the sensitivity of the MEC. Since the sensitivity of MEC is dependent on a variety of factors such as whether the item has been through the arming sequence, condition of the munitions components, and the type and condition of the explosives, sensitivity for a given item is very difficult to predict. Thus, the probability of detonating the MEC is determined solely based on the project activity.

The severity of an MEC incident is primarily dependent upon the quantity of high explosives (i.e., net explosive weight) and the location and robustness of receptor.

8.3.1 Semi-quantitative Risk Assessment

The semi-quantitative risk assessment examined the risks to vessels and equipment associated with the Delaware WEA for specific renewable energy area development activities. Table 8-3 through Table 8-5 show the numeric values for each of the factors used in the scoring and the relative risk determination based on the analysis.

8.3.2 MEC Risk Management and Mitigation

A general discussion of MEC risk management and mitigation were provided previously. MEC risk management and the design of the MEC risk mitigation is beyond the scope of the current study.

Table 8-2: Probability of MEC near Delaware WEA

| Potential Source of Munitions | Munitions | Probability of Munitions Between WEA and Shore | Probability of Munitions Within WEA |
|-------------------------------|---|---|---|
| Naval Warfare (WWI and WWII) | Anti-submarine munitions, torpedoes, artillery projectiles | Likely – German U-boats were active off the Atlantic seaboard during WWII. Warships and merchant escorts likely deployed anti-submarine munitions as they transited the area, depth charges may be present. Ship and shore-based guns may have fired on suspected submarines in the area. | Likely – German U-boats were active off the Atlantic seaboard during WWII. Warships and merchant escorts likely deployed anti-submarine munitions as they transited the area, depth charges may be present. Ship based naval guns may have fired on suspected submarines in the area. |
| Coastal Defense Batteries | Artillery projectiles (fixed, semi-fixed) Artillery projectiles (separate loading) | Almost certain - Anti-aircraft batteries were present on the coast and anti-aircraft projectiles have been recovered during beach replenishment. Fixed and semi-fixed projectiles are those expected in this area. | Likely – Although the large caliber guns (separate loading) could reach the nearest portions of the WEA, the number of projectiles likely to be present is small. |
| Training Areas | Artillery projectiles, rockets | Almost certain –Rocket ranges were also present near shore. Only practice rocket use is known. | Unlikely – Weapons used are unlikely to impact the WEA. Some open water training may have occurred but the density of munitions would be low. |
| Sea Disposal of Munitions | Artillery projectiles (fixed, semi-fixed, separate loading) | Unlikely - Although no near shore disposals are documented in this area, disposals prior to WWII were poorly documented and could have occurred near shore. Disposed munitions often do not have all components present and have not gone through the arming sequence. | Moderate – One DoD sea disposal site (DE-X01) is in the area. Sea disposal is poorly documented and other munitions disposal operations may have occurred. Disposed munitions often do not have all components present and have not gone through the arming sequence. |

Page Intentionally Left Blank.

Table 8-3: Probability of Detonation Grades for Site Characterization Activities near Delaware WEA

| Activity | MEC | Probability of Encounter | Sensitivity Factor | Activity Energy Factor | Probability of Detonation (P _c *S*A) | Net Explosive Weight (lbs) | Severity Grade | Risk |
|---------------------|----------------------------------|--------------------------|--------------------|------------------------|---|----------------------------|----------------|-----------|
| | | Table 5-1 | Table 5-2 | Table 5-3 | Table 5-4 | Table 8-1 | Table 5-5 | Table 5-7 |
| Geophysical Survey | Artillery projectiles | 4 | 3 | 1 | 12 | (≤120 mm) <11 | 1 | Low |
| | | | | | | (6-in to 12-in) >11 to 33 | 2 | Low |
| | | | | | | (16-in) >33 to 110 | 3 | Medium |
| | Sea mines | 1 | 4 | 1 | 4 | >550 | 5 | High |
| | Anti-submarine warfare munitions | 2 | 3 | 1 | 6 | >11 to 33 | 2 | Low |
| >33 to 110 | | | | | | 3 | Medium | |
| Torpedoes | 1 | 3 | 1 | 3 | >550 | 5 | High | |
| Geotechnical Survey | Artillery projectiles | 1 | 3 | 2 | 6 | (≤120 mm) <11 | 1 | Low |
| | | | | | | (6-in to 12-in) >11 to 33 | 2 | Low |
| | | | | | | (16-in) >33 to 110 | 3 | Medium |
| | Sea mines | 1 | 4 | 2 | 8 | >550 | 5 | High |
| | Anti-submarine warfare munitions | 1 | 3 | 2 | 6 | >11 to 33 | 2 | Low |
| >33 to 110 | | | | | | 3 | Medium | |
| Torpedoes | 1 | 3 | 2 | 6 | >550 | 5 | High | |

Note: Characterization of meteorological resources typically involves installation of a meteorological mast is installed in a manner similar to a monopile foundation or jacket structure. This is addressed in Table 8-5.

Table 8-4: Risk Scores for Substructure and Foundation Activities near Delaware WEA

| Activity | MEC | Probability of Encounter | Sensitivity Factor | Activity Energy Factor | Probability of Detonation (P _c *S*A) | Net Explosive Weight (lbs) | Severity Grade | Risk |
|--|----------------------------------|--------------------------|--------------------|------------------------|---|----------------------------|----------------|-----------|
| | | Table 5-1 | Table 5-2 | Table 5-3 | Table 5-4 | Table 8-1 | Table 5-5 | Table 5-7 |
| Installation of Monopiles or Foundations | Artillery projectiles | 4 | 3 | 5 | 60 | (≤120 mm) <11 | 1 | Low |
| | | | | | | (6-in to 12-in) >11 to 33 | 2 | Medium |
| | | | | | | (16-in) >33 to 110 | 3 | Medium |
| | Sea mines | 1 | 4 | 5 | 20 | >550 | 5 | High |
| | Anti-submarine warfare munitions | 2 | 3 | 5 | 30 | >11 to 33 | 2 | Low |
| | | | | | | >33 to 110 | 3 | Medium |
| Torpedoes | 1 | 3 | 5 | 15 | >550 | 5 | High | |
| Installation of Scour Protection Systems | Artillery projectiles | 4 | 3 | 5 | 60 | (≤120 mm) <11 | 1 | Low |
| | | | | | | (6-in to 12-in) >11 to 33 | 2 | Medium |
| | | | | | | (16-in) >33 to 110 | 3 | Medium |
| | Sea mines | 1 | 4 | 5 | 20 | >550 | 5 | High |
| | Anti-submarine warfare munitions | 2 | 3 | 5 | 30 | >11 to 33 | 2 | Low |
| | | | | | | >33 to 110 | 3 | Medium |
| Torpedoes | 1 | 3 | 5 | 15 | >550 | 5 | High | |

Table 8-5: Risk Scores for Cable Installation Activities near Delaware WEA

| Activity | MEC | Probability of Encounter | Sensitivity Factor | Activity Energy Factor | Probability of Detonation (P _e *S*A) | Net Explosive Weight (lbs) | Severity Grade | Risk |
|---|----------------------------------|--------------------------|--------------------|------------------------|---|----------------------------|----------------|-----------|
| | | Table 5-1 | Table 5-2 | Table 5-3 | Table 5-4 | Table 8-1 | Table 5-5 | Table 5-7 |
| PLGR Operations | Artillery projectiles | 4 | 3 | 3 | 36 | (≤120 mm) <11 | 1 | Low |
| | | | | | | (6-in to 12-in) >11 to 33 | 2 | Low |
| | | | | | | (16-in) >33 to 110 | 3 | Medium |
| | Sea mines | 1 | 4 | 3 | 12 | >550 | 5 | High |
| | Anti-submarine warfare munitions | 2 | 3 | 3 | 18 | >11 to 33 | 2 | Low |
| | | | | | | >33 to 110 | 3 | Medium |
| Torpedoes | 1 | 3 | 3 | 9 | >550 | 5 | High | |
| Cable Installation (Jetting or Ploughing) | Artillery projectiles | 4 | 3 | 4 | 48 | (≤120 mm) <11 | 1 | Low |
| | | | | | | (6-in to 12-in) >11 to 33 | 2 | Medium |
| | | | | | | (16-in) >33 to 110 | 3 | Medium |
| | Sea mines | 1 | 4 | 4 | 16 | >550 | 5 | High |
| | Anti-submarine warfare munitions | 2 | 3 | 4 | 24 | >11 to 33 | 2 | Low |
| | | | | | | >33 to 110 | 3 | Medium |
| Torpedoes | 1 | 3 | 4 | 12 | >550 | 5 | High | |
| Cable Installation (Concrete Mattress) | Artillery projectiles | 4 | 3 | 3 | 36 | (≤120 mm) <11 | 1 | Low |
| | | | | | | (6-in to 12-in) >11 to 33 | 2 | Low |
| | | | | | | (16-in) >33 to 110 | 3 | Medium |
| | Sea mines | 1 | 4 | 3 | 12 | >550 | 5 | High |
| | Anti-submarine warfare munitions | 2 | 3 | 3 | 12 | >11 to 33 | 2 | Low |
| | | | | | | >33 to 110 | 3 | Medium |
| Torpedoes | 1 | 3 | 3 | 9 | >550 | 5 | High | |

| Activity | MEC | Probability of Encounter | Sensitivity Factor | Activity Energy Factor | Probability of Detonation (P _e *S*A) | Net Explosive Weight (lbs) | Severity Grade | Risk |
|---|----------------------------------|--------------------------|--------------------|------------------------|---|----------------------------|----------------|--------|
| Cable Installation (Armoring with Rock) | Artillery projectiles | 4 | 3 | 4 | 48 | (≤120 mm) <11 | 1 | Low |
| | | | | | | (6-in to 12-in) >11 to 33 | 2 | Medium |
| | | | | | | (16-in) >33 to 110 | 3 | Medium |
| | Sea mines | 1 | 4 | 4 | 16 | >550 | 5 | High |
| | Anti-submarine warfare munitions | 2 | 3 | 4 | 24 | >11 to 33 | 2 | Low |
| | | | | | | >33 to 110 | 3 | Medium |
| Torpedoes | 1 | 3 | 4 | 12 | >550 | 5 | High | |

9.0 In-field Verification Methods and Procedures

9.1 Design of the In-field Verification Study

WEA environmental conditions, personnel requirements, safety, positional accuracies, sensor availability, cost, and vessel logistics were all considered in selecting the appropriate technologies for the in-field verification. Those technologies selected for in-field verification include optical sensors, side-scan sonar, and a cesium vapor magnetometer sensor. Sub-bottom profilers, SAS, and multibeam sonar were not considered ideally suited for the project objectives. While each of these have strengths in given environments; magnetometry, optical sensors, and high-resolution side-scan were considered to best meet the requirements determined by the review presented in Section 6.0.

9.1.1 Sensor Selection

For a survey in which the objects of interest are exposed on the seafloor, the SAS provides the greatest areal coverage at high spatial resolution. However, the Delaware WEA (and the others in the Atlantic OCS) is relatively shallow, and thus high-resolution side-scan is deemed sufficient for coverage rates and resolution in wide area assessment. Further, the Atlantic WEAs have bottoms that consist almost entirely of non-cohesive sediment, in which heavy objects like MEC are likely to become buried. Due to the likely excavation depths (i.e., up to 2 m) of future commercial development of these WEAs; the tool of choice then becomes a magnetometer. The minimum MEC for the development activities is the 155 mm artillery round, with an anticipated magnetic detection range of 8 m or less. Most AUVs include a high-resolution side-scan sonar; the addition of a magnetometer makes for an appropriate tool. A survey with track spacing of 8 m provides substantial overlap for magnetics and highly oversampled backscatter imagery, which for close range has resolution comparable to the SAS system. Furthermore, the backscatter imagery from adjacent lines can be used to help correct for navigational drift of the AUV (refer to Section 9.3.3.2).

9.1.2 Selected Platform for In-field Verification

The distance from shore of the WEAs and the size and depth of the area to be surveyed shift the optimal survey platform between a survey launch and a coastal R/V, equipped with one or more AUVs and phase bathymetry side-scan sonar. The wide swaths of side-scan sonars can be used to see upslope during a survey from deeper water to shallow to determine if hazards are present, but swath width is a multiple of sonar altitude, and at some point the deeper draft of a coastal vessel restricts operations. AUVs, deployed from either type of vessel, can extend the survey into very shallow depths. For survey areas not far from shore, the higher transit speed of a survey launch relative to a coastal or oceanic R/V means a smaller fraction of time is spent traveling to and from the survey site. Once survey areas become larger and farther from port, a coastal vessel becomes more cost-effective, because it can carry enough personnel to operate around the clock and support multiple AUVs and can remain in the survey area for many days to launch and recover the AUVs, servicing them and processing data as the survey progresses. To minimize drift, the AUV surveys were broken into areas with survey lines limited to a few km.

Once again, physical characteristics of the WEA, personnel requirements, safety, positional accuracy, cost, and vessel logistics were all considered in selecting the appropriate technologies for the in-field verification. With these requirements, pole-mounted sensors, and an AUV were

deployed from the R/V Daiber, a large survey launch (Table 9-1), during the in-field verification. Towed vehicles were not suitable for the project objectives due to the shallow, variable seafloor bathymetry, which is present in much of the Delaware WEA. Towed vehicles have difficulty maintaining constant altitudes from the seafloor in areas of variable bathymetry. AUV's, however, are capable of bottom-following modes, and can maintain the constant altitudes and transect following required for high-precision surveys. ROV's are an industry standard for visual observations and detailed surveying, and in small form factors, are affordable and easily deployable from any vessel of opportunity.

Table 9-1: Vessel Specifications – R/V Joanne Daiber

| <i>R/V Joanne Daiber</i> | |
|---|---------------------------------|
| Hull | |
| Manufacturer: | Newton Boats, Research 46 |
| Length: | 14 m (46-foot) |
| Beam: | 4.9 m (16-foot) |
| Draft: | 1.2 m (4-foot) |
| Propulsion: | Twin Cummins Diesel QSB 355 HP |
| Fuel Capacity: | 400 gallons |
| Cruising speed: | 18 knots |
| Cruising Range: | 648 km (350 miles) with reserve |
| Maximum Load Capacity: | 2 crew plus 18 researchers |
| Electronics | |
| Garmin electronics package | |
| Multifunction Displays (2 on fly bridge and one in main cabin) | |
| Depth Sounder | |
| Radar | |
| VHF radios, AIS, EPIRB | |
| Mechanical | |
| 2,000 pound A-frame with winch | |
| 800 pound side davit with winch | |
| 15 KW Kohler generator | |
| scientific counter space including flow through salt water sink | |

9.1.3 Selected Positioning Techniques for In-field Verification

Of the positioning technologies evaluated, USBL underwater positioning system was deemed most suitable for the in-field verification. LBL positioning requires dedicated time for the placement of transponders and accurate surveying of the transponder positions. Further, work areas are then limited to within the LBL grid network, which must be repositioned and resurveyed for work in new areas. For the in-field verification, the plan was to use USBL to obtain accurate positions for the ISOs in the IVS and the blind seeds in the survey areas.

9.2 Mobilization

Mobilization included preparing for each of the field activities, gathering and checking necessary equipment, and organizing and assembling trained field personnel. Equipment and materials were assembled and checked (i.e., calibration and battery checks) prior to transport to the site.

All field personnel received site-specific health and safety training and familiarization with the planned tasks prior to commencing work. The required health and safety equipment was reviewed with the Boat Captain and on site education and briefings were given by the University of Delaware Principal Investigator at the site.

The University of Delaware Principal Investigator prepared a schedule in coordination with on site personnel to minimize the potential for delays and schedule conflicts. The University of Delaware Principal Investigator was responsible for acquiring equipment, checking to see that the necessary equipment was on site, and maintaining the schedule. Early and continuous coordination with the vessel and crew was conducted to obtain approval for the equipment and methods used.

Field work occurred over July 12 and from July 18 to 28 2016 in the Delaware WEA. Initial site selection and mapping took place on July 12, 2016. Site seeding with munitions surrogates and establishment of the IVS and preparation took place July 18-19, 2016. Detection team operations were conducted from July 20-28, 2016. Daily operations are summarized in the In-Field Testing and Methodology Verification Trip Report (Appendix A).

9.2.1 Equipment

On arrival at the port, the equipment was inspected for damage and operability checks were performed. The batteries were charged and operational checks were performed on all equipment per manufacturer's instructions. Most sensors are factory calibrated and do not require field calibration. To ensure that the sensors were performing properly, they were checked in both a dry and wet environment prior to start and at the end of the fieldwork.

9.2.2 Personnel

University of Delaware provided personnel with expertise and functional capability to include dive support and operation of the AUV and R/V *Daiber*. The seed deployment team placed the IVS and blind seeds and consisted of personnel separate from those composing the detection survey team. The detection survey team tested survey methods for detecting MEC and were tasked with determining the optimal methods for locating the munitions surrogates (ISOs). The detection survey team independently analyzed the data and identified magnetic anomalies and selected targets of interest.

9.3 Prepare Study Area

The technology review established that no one sensor is capable of effectively conducting both wide area assessment for large-region coverage, and target interrogation for MEC identification. Therefore, this in-field verification effort employed a multi-scale approach MEC detection and identification. This approach combines:

- 1) Hull-mounted, high-resolution sonar for wide area assessment,
- 2) Near-bed, tight coverage surveying using magnetometry and high-resolution side-scan surveying by AUV for target verification, and
- 3) Target identification using AUV or ROV optical surveying.

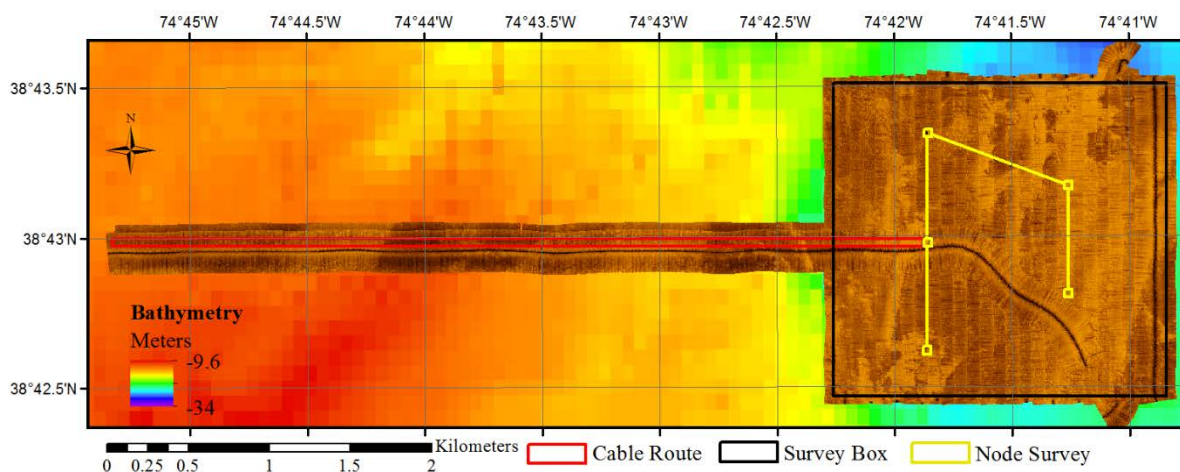
This combination of multi-phased surveying and target identification through the synthesis of multiple remote sensing technologies should maximize the potential for MEC detection.

The in-field verification effort consisted of four parts:

- 1) Surface vessel wide area assessment,
- 2) Simulated monopile network survey,
- 3) Cable route survey, and
- 4) Optical verification.

The study area consisted of a 2 x 2 km box and 5 km cable route (Figure 9-1). To prepare these study areas, the IVS and blind seeds were emplaced at the start of the in-field verification. The test strip conformed to the ESCTP IVS as outlined by the Geophysical System Verification Report (Environmental Security Technology Certification Program 2015b) and modified for the marine environment (Section 9.3.1). Within the 2 x 2 km study area, three seeded test fields were established. The test fields were within or near the pre-established monopile network survey (Figure 9-1). Additional seeds were placed along a 5 km “cable route” to demonstrate the selected technologies for a cable route survey.

Figure 9-1: Side-scan Sonar Coverage of Cable Route and 2 x 2 km Survey Box Collected 20 July 2016



On 12 July 2016, the preselected survey areas were mapped by surface vessel phase-measuring bathymetric sonars (PMBS) sonar by the seed deployment team to determine whether targets or obstructions were already present within the study area. No targets or obstructions were observed by the team. Seeding operations commenced on 18 July 2016 with the placement of the IVS.

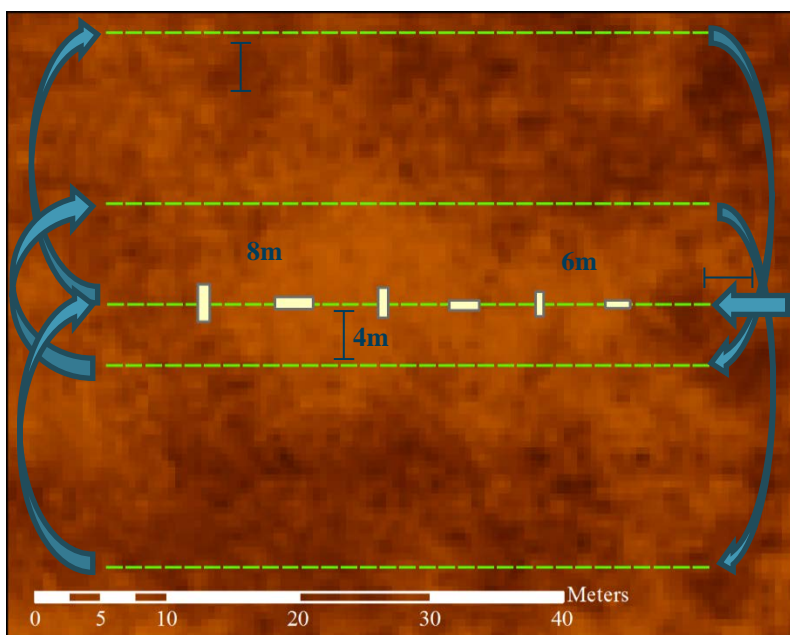
Team members not privy to the seeded test field operations conducted the blind detections surveys. The detection survey team was tasked with conducting a wide area assessment survey of the 2 x 2 km box, followed by the monopile network survey. After completion of these surveys, the 5 km cable route survey was conducted. A sample of targets identified in both the area and route surveys was visually verified.

9.3.1 Instrument Verification Strip Survey

The IVS was to be placed near the test site, but away from the seeded surrogates or other metallic debris and at a depth as close to the survey depth as possible. The IVS consisted of

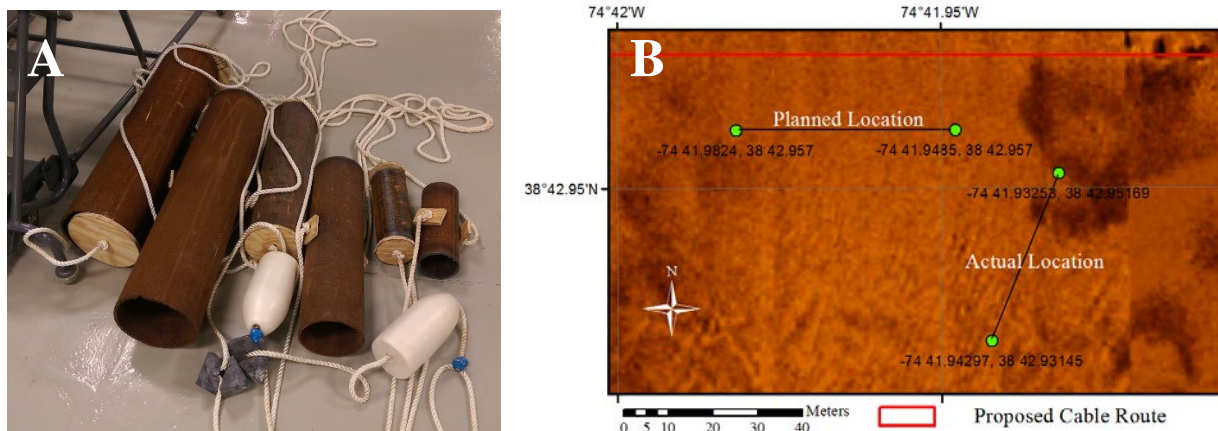
Naval Research Laboratory's NRL/MR/6110-09-9183, "Industry Standard Objects" Guidance (Naval Research Laboratory 2009) for the purpose of calibrating the sensors prior to embarkation. Adapted for application to the marine environment, the IVS consisted of six surrogates (two 8-inch, two 6-inch, and two 4-inch ISO) oriented parallel or orthogonal to the survey transect (Figure 9-2). Each surrogate was spaced out 6 m along a ½-inch nylon line, weighted at each end and attached to subsurface floats (Figure 9-3A). To monitor sensor performance and navigation drift, a specific IVS mission was designed for the University of Delaware's Gavia AUV. The mission, represented in Table 9-2, consisted of two lines along the strip in opposite directions (to monitor latency), a parallel transect offset 4 m (half the standard mission line space), a parallel transect offset by 8 m (standard mission line spacing), and two lines offset 20 m (to monitor system noise). The sensors surveyed the IVS to establish a baseline response and validate instrument performance prior to, and at the end of each day.

Figure 9-2: IVS Configuration and AUV Mission Route



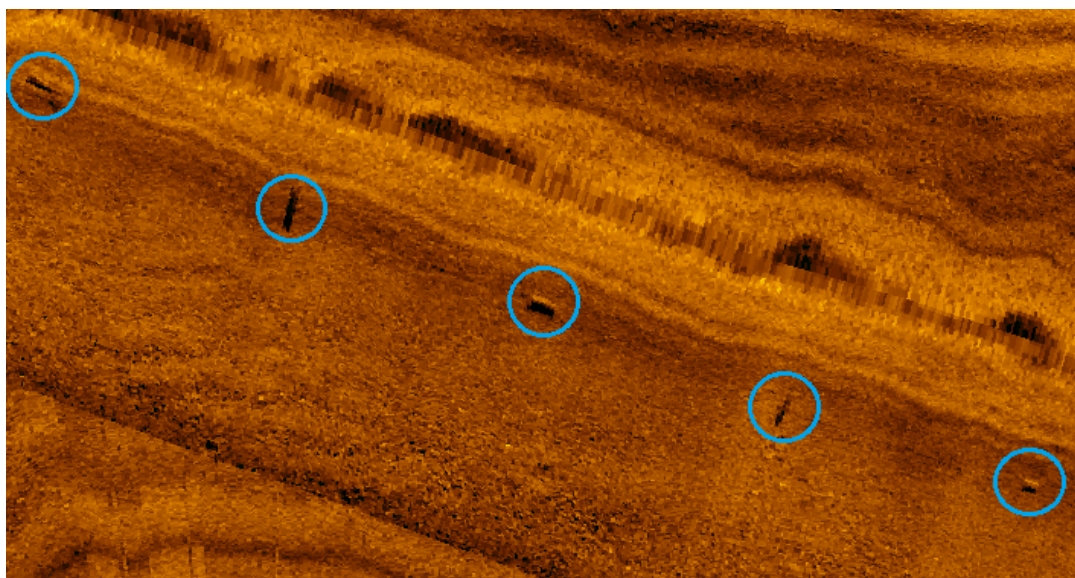
While the intended orientation was East-West, difficulties with IVS placement resulted in Southwest-Northeast orientation (Figure 9-3B). Due to conditions at the site at deployment, precise positioning of the IVS was not verified by USBL tracked divers as initially planned. Subsequent mapping efforts reacquired the IVS and determined that the IVS was otherwise ideally laid out, with surrogates appropriately spaced and oriented (Figure 9-4).

Figure 9-3: IVS Items and Location



The IVS (A) was deployed in the vicinity of the planned location, but laid out (B) in a NE-SW orientation instead of the planned E-W orientation.

Figure 9-4: IVS Items and Location



Side-scan Sonar Imagery of a Portion of the IVS. The munitions surrogates are highlighted. Note the alternating orientation evident in the imagery.

9.3.2 Blind Seeding

Surrogate seeding commenced 19 July 2016. Seeds were placed in five locations along the cable route, and within three sites along the monopile note network. In all, 62 seeds were placed at the site.

Surrogates consisted of 8-inch, 6-inch, 4-inch and 2-inch diameter (inner diameter) schedule 40 steel pipes. The 4-inch and 2-inch surrogates were cut to length per Naval Research Laboratory's NRL/MR/6110-09-9183, "Industry Standard Objects" Guidance (Naval Research Laboratory 2009), while larger seed sizing was informed by historical documentation for 8-inch

artillery shells (36 inches long), and 155 mm artillery shells (24 inches long). Each seed was measured for length, inner diameter, wall thickness, and weight prior to deployment, and labeled with an identification number (Figure 9-5A; Appendix B).

Figure 9-5: Munitions Surrogates and USBL Puck



Munitions Surrogates and USBL Puck. Munitions surrogates (A – left side) were initially lowered on a slack-line with USBL puck (B – right side) attached. The USBL was abandoned for the later deployments due to complications from a strong thermocline. Vessel GPS was used to mark the remainder of the surrogate positions.

Seeds were deployed from the surface vessel via slack-line. Attached to the slack-line was a remote USBL tracking (Figure 9-5B). Both the ship and USBL positions were recorded for each surrogate. While initial cable route deployments suggested the USBL was performing correctly, issues arose with sites deeper than 15 m, where a strong thermocline affected system performance. Where unreliable USBL positions were present, seed positions were recorded using the surface vessel’s position. Seeding was completed within a day. The size breakdown and area placement are described in Table 9-2.

Table 9-2: Number and Size of Surrogates Placed at Each Seeding Site

| Site | 8-inch | 6-inch | 4-inch | 2-inch | Subtotal |
|-----------------|----------|-----------|-----------|-----------|-----------|
| Cable Route 1 | 0 | 2 | 2 | 1 | 5 |
| Cable Route 2 | 1 | 2 | 1 | 1 | 5 |
| Cable Route 3 | 0 | 3 | 3 | 0 | 6 |
| Cable Route 4 | 1 | 1 | 2 | 1 | 5 |
| Cable Route 5 | 0 | 3 | 2 | 1 | 6 |
| <i>Subtotal</i> | 2 | 11 | 10 | 4 | 27 |
| Node 1 Route | 1 | 4 | 3 | 3 | 11 |
| Node 3 | 1 | 5 | 4 | 2 | 12 |
| Node 4 | 1 | 6 | 3 | 2 | 12 |
| <i>Subtotal</i> | 3 | 15 | 10 | 7 | 35 |
| Total | 5 | 26 | 20 | 11 | 62 |

9.3.3 Seeded Area Blind Survey

9.3.3.1 Surface Vessel Wide Area Assessment

A high-resolution hull-mounted sonar survey was completed across the 2 by 2 km study area to simulate a wide area assessment. The survey used an [EdgeTech 6205](#) PMBS. This sonar system

is a portable, pole-mounted unit and can be fitted to a vessel of opportunity. The sonar is equipped with a dual-frequency 230/550 kHz side-scan sonar capable of up to approximately 400 m swath width and decimeter resolution, in addition to a 550 kHz bathymetric sonar with up to 200 m swath and similar resolution. It is combined with a Coda Octopus F190R+ inertial motion unit, which, coupled with RTK/PPK GPS, is capable of positional accuracy down to 1 cm (expected offshore down to 10 cm or less). Surveying can be conducted at speeds of up to 8 knots, depending on ideal sonar resolution. Both low and high frequency side-scan and high frequency bathymetry and backscatter are collected simultaneously; this yields four separate data products at once, including real time textural and 3-dimensional maps of the seafloor. The system is capable of a wide across track footprint of 8-times water depth, while still meeting the [International Hydrographic Organization](#) special order.

Using the University of Delaware's R/V *Joanne Daiber*, the survey mapped the study area using an initial track spacing of three times the local water depth, which resulted in greater than 100 % overlap in bathymetry and 200 % overlap in side-scan sonar data. Navigational and vessel motion data was collected real time and was post processed for improved data quality. Sound velocity profiles were taken every hour to account for local spatial and temporal effects of acoustic refraction on sonar data. Bathymetric and side-scan sonar data were collected redundantly, with raw data storage and real time sonar processing for immediate data products.

9.3.3.2 Monopile Network Survey

AUV magnetometer surveys were conducted over a simulated monopile wind generator network consisting of six monopile nodes with connecting cable network. This survey tested the effects of survey altitude, transect spacing, and transect orientation to establish the most efficient survey parameters to identify the presence of surrogate MEC items. These surveys were conducted using a Gavia AUV. The Gavia AUV is a modular designed vehicle customizable to individual projects. Available sensor modules include a Marine Sonics high-resolution side-scan sonar, dual-frequency 900/1800 kHz, a GeoAcoustics GeoSwath 500 kHz PMBS, 2 megapixel Point Grey Color Grasshopper Camera, and environmental sensors (e.g., salinity, temperature, dissolved oxygen, and turbidity). The Gavia AUV used is navigated by a Kearfott T-24 "SEANAV" INS coupled with an RD Instruments 1200 kHz Workhorse DVL. The DVL measures velocity of the vehicle over the seafloor and provides these measurements to the INS to constrain navigational drift error. While on the surface, a WAAS-capable L1/L2 receiver GPS in the AUV's sail provided position fixes to the INS before missions. When submerged, the published drift rate for the INS with an integrated DVL during submerged operation is 0.1% of distance traveled. Additional methods in survey design can further constrain AUV positional error. The Gavia has a depth rating of up to 500 m, and can run for over 3.5 hours and cover up to 20 linear km per mission. For this study, a marine magnetometer developed for the University of Delaware AUV in an ESTCP funded program (MR-201002) was used for the targeted magnetometer surveys. The AUV magnetometer module houses a Geometrics G-880AUV self-oscillating split-beam cesium vapor (non-radioactive ^{133}Cs) total field magnetometer with automatic hemisphere switching coupled with an Applied Physics 539 fluxgate compass (Environmental Security Technology Certification Program 2015a).

Surveying consisted of AUV magnetometer and high-resolution side-scan sonar over 40 x 20 m boxes around pre-established monopile locations (Figure 9-1). The AUV also surveyed inter-array cable routes between these monopile node surveys. Node surveys were conducted with an initial track spacing of 8 m or less to provide substantial overlap for magnetics and highly

oversampled backscatter imagery. The backscatter imagery from adjacent lines was used to help correct for navigational drift of the AUV.

To address buried MEC, repetitive surveys were conducted over areas determined by the detection study team to have surrogate targets. These surveys were adjusted 2 m vertically to simulate materials buried up to 2 m deep, and test the effective range of the system to detect buried MEC. For instance, an AUV magnetometer survey typically planned for 2 m altitudes were adjusted to 4 m altitudes. Since buried MEC detection by magnetometry is a function of distance between sensor and object and not sediment overburden, this adequately simulates buried MEC. Transect spacing and orientation were varied to determine the optimal survey methods for MEC detection.

The AUV was deployed from the R/V *Joanne Daiber*. Data was stored onboard the AUV during missions and was downloaded each time the AUV was recovered. After each mission, the AUV was recovered by the surface team for data processing, vehicle servicing, and battery replacement. The survey team had three separate batteries modules, allowing for AUV mission turnaround times of less than one hour. Up to three missions were conducted each day.

9.3.3.3 Cable and Pipeline Route Test Surveys

Cable route test surveys were completed to account for the conditions present in cable laying areas for renewable energy power cables. Long linear transects, typical in these surveys, may impact sensor platform navigational accuracy and therefore the platform's effective coverage of planned cable routes.

To test whether the chosen platforms can adequately navigate along a predetermined cable route and detect MEC, surrogates (ISOs) were deployed in series along a 5 km transect. Munitions surrogates were placed by the seeding team at 1 km intervals along the transect. The detection survey team was not privy to the locations of the surrogates, but was given the bounding coordinates of the cable route.

These surveys were conducted using the setup and methodology described in Sections 9.3.3.1 and 9.3.3.2. Transect spacing, sensor height, survey speed and other parameters were set to determine optimal combinations. To minimize drift, the AUV surveys were broken into areas with survey lines less than a few km.

9.3.3.4 Targeted Optical Survey

A subset of the magnetometer survey targets identified by the detection survey team were reacquired and verified using visual means. This was performed using the AUV's onboard camera in visual surveys. Reacquisition of targets via the AUV camera surveys could also be used to establish navigational performance.

The AUV used is equipped with a 2 megapixel Point Grey Grasshopper color camera capable of multiple photos per second. In standard camera surveys, photos capture $>2.7 \text{ m}^2$ of seafloor and can clearly image objects smaller than 10 cm. Each image is geo-referenced and tagged with pertinent metadata. The navigation accuracy of the AUV, which is described in Section 6.2.1, proved sufficient for re-locating objects previously identified by magnetometer or sonar. The mission endurance of the vehicle allowed for the imaging of multiple targets over a larger spatial domain.

After reaching the target, the AUV camera systems recorded images of the object from a variety of distances and angles to allow for its definitive identification. AUV images are geo-referenced with the AUV's position and stored onboard the vehicle. These were recovered after each mission to verify detection and navigational accuracy. AUV navigation, video and sonar imagery is recorded on the surface vessel in real time. Imagery was reviewed by team personnel and each object was classified as either a MEC surrogate (positive identification) or other (negative identification). Results of the targeted optical survey were used to answer the study question of whether sensors tested during this investigation can distinguish between the munitions surrogates and other features on the seafloor surface.

9.4 Navigation and Mapping System

Data was collected using a RTK-GPS (e.g., Trimble, Leica, Topcon, or other system) that met the project data quality objectives. Times from the survey equipment internal clock and survey support vessel GPS satellite clock were used to time-stamp both position and sensor data information for later correlation. Position dilution of precision or horizontal variance calculations were provided as part of the data stream. The GPS simultaneously recorded position along with geophysical response data. The Universal Transverse Mercator, Zone 18 N coordinate system was used and referenced to the National Geodetic Survey NAD83. The investigation reviewed the survey tracks and monitored the position of the surveying equipment with respect to the intended track during the data collection phase to ensure coverage of the areas of interest. Location tracking and transect identification was accomplished using the onboard navigation equipment.

9.5 Combined Surface Vessel Wide Area Assessment and Target Interrogation Method Assessment

The sensor platform's performance was evaluated by its ability to correctly detect, navigate to, and identify the surrogate MEC. Various mission methodologies were used to test and maximize the platform's effectiveness. The field effort tested the proposed technology and methodological framework in four separate ways:

- ▶ First, this test determined whether a high-resolution, hull-mounted system can be used to effectively identify areas of interest for target interrogation.
- ▶ Second, this field effort tested the ability and effectiveness of the selected platform and sensor suite (e.g., magnetometry, side-scan sonar, optical survey) to properly identify and accurately survey surficial and buried MEC.
- ▶ Third, this field test determined whether the selected platform can effectively detect MEC in both focused-area and cable route surveys.
- ▶ Lastly, this approach determined whether the combined surface vessel wide area assessment and target interrogation method is a cost-effective and efficient manner in which to search for and identify MEC within the WEAs.

9.6 Demobilization

Upon completion of the technology demonstration and the vessel returning to port, all equipment was offloaded and inspected for damage. The raw and processed data files were archived at University of Delaware and were transferred to BOEM for retention. Equipment was cleaned, crated, and shipped to the technology providers' warehouse.

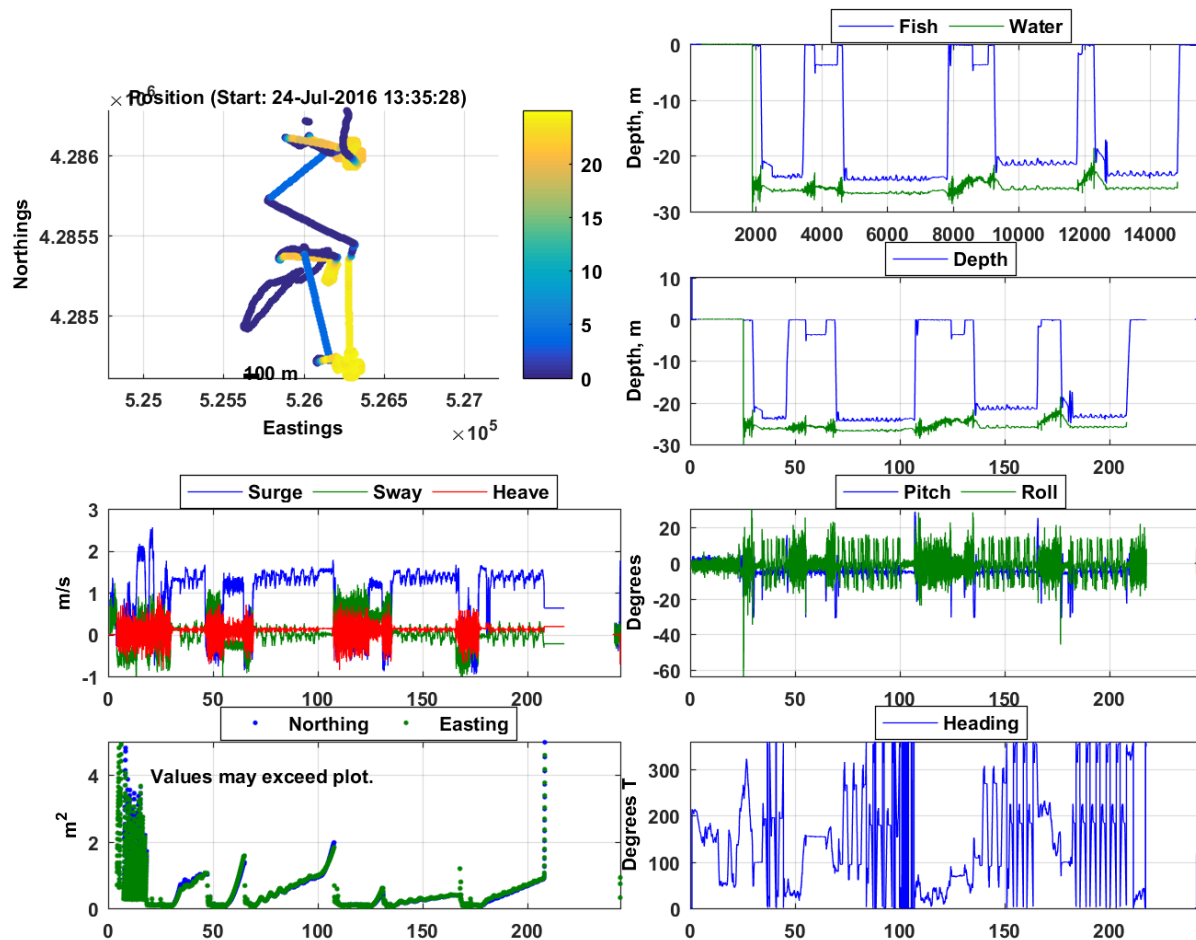
10.0 In-field Verification Results

10.1 Data Processing

10.1.1 Initial Processing

All data was processed daily by the team and used to monitor system performance and inform subsequent mission efforts. This included processing of magnetometer, side-scan sonar, and AUV mission logs (e.g., navigation, altimetry, attitude). A sample of the AUV mission data is presented in Figure 10-1.

Figure 10-1: Gavia AUV Mission Log Example Navigation Plot



10.1.1.1 Magnetometry

Magnetometer data was processed using Geometrics MagPick and MagComp software. Raw magnetometer data was parsed from Gavia XML files and separated into individual missions. Basestation magnetic data was collected daily from the Fredricksburg, VA station via Intermagnet.org to correct for diurnal variations to the local magnetic field. Data was then run through MagComp to remove vehicle noise, using calibration coefficients determined via calibration runs prior to the field effort. A set of coefficients were calculated for each battery

used on the AUV to account for variations in discharge behavior between batteries. Final data was exported in *.csv format and uploaded into the Chesapeake Technologies, Inc. SonarWiz sonar processing suite for mag picking and comparison to side-scan sonar data by the detection team.

10.1.1.2 Side-scan Sonar

Surface vessel PMBS sonar was collected and processed using the Chesapeake Technologies, Inc. SonarWiz sonar processing suite. AUV side-scan sonar data was also processed using SonarWiz. Sonar data processing followed industry standard procedures for side-scan data, focusing on gain corrections to remove the variation in across-track brightness inherent in side-scan sonar performance in order to achieve the most representative mosaic of the seafloor. Standardized gain settings were chosen to make the sonar data as internally consistent as possible between different daily mission datasets. Raw EdgeTech (*.jsf) and Marine Sonics (*.mst) sonar files were imported using a time-varying gain, to compensate for signal loss on the outer swath of the sonar files. Once the files were imported, bottom tracking corrections were applied if automatic bottom tracking had failed. Once verified or corrected, an empirical gain normalization correction was applied. This gain correction makes the data set consistent from a file-to-file basis, removing gain biases caused by variations in backscatter intensity from differing sediments between each file. This produces an internally consistent mosaic. Processed sonar mosaics were gridded and exported as Google Earth (*.kmz) and standard image (*.geotiff) formats.

10.1.1.3 Imagery

AUV camera imagery is geotagged and referenced with vehicle position and attitude data at the time of collection. Images were processed and compiled into “film strips” and Google Earth (*.kmz) by AUV transect for geo-referencing to sonar data targets.

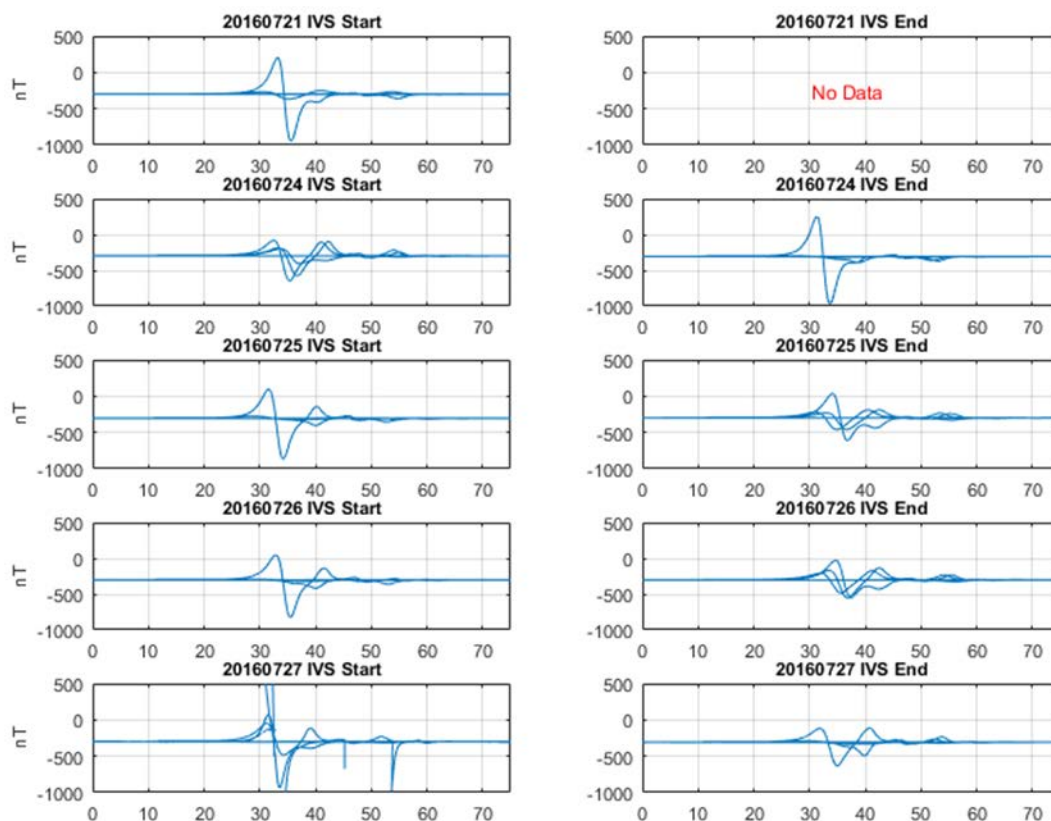
10.1.2 Detection Team Target Identification

The detection team utilized a sequential approach to the analysis and interpretation of both magnetometer and side-scan sonar data described in detail below.

First, the repeated IVS surveys conducted at 2 m altitude over known targets (8-inch, 6-inch, and 4-inch munitions surrogates) were used as a reference for target strength and magnetometer anomaly size determination. Signatures of the targets in the IVS survey data are readily apparent (Figure 10-2). Note that no 2-inch surrogates were included in the IVS.

The magnetometer anomalies for each of the target types (8-inch, 6-inch, and 4-inch) from the IVS were used as a reference table (Table 10-1). These IVS reference values are directly applicable to most of the production surveys that were run at an identical altitude of 2 m. However, for the higher elevation missions designed to test the effects of burial we extrapolated the magnetic response from the IVS at 2 m upwards to altitudes of 4 and 8 m in order to establish a likely response for each size surrogate using a reduction in magnetic anomaly strength proportional to the change in altitude cubed.

Figure 10-2: Magnetometer Signal from IVS missions Over Duration of Field Effort



Note: Daily variation in signal was determined to be a product of navigational drift between missions (Section 10.3).

Table 10-1: Typical Magnetometer Response for Surrogates by Size at 2 m Altitude

| IVS Surrogate Size | Magnetic Anomaly |
|--------------------|------------------|
| 2-inch | N/A |
| 4-inch | <30 nT |
| 6-inch | ~50-150 nT |
| 8-inch | >200 nT |

Once informed by the IVS surrogate responses the detection team proceeded to sequentially evaluate the magnetometer and the side-scan sonar data with the following progression:

- 1) First, the detection team performed pick of anomalies based only on magnetometer data and using a combination of SonarWiz threshold auto-detection together with manual review and adjustment to account for any targets not picked up by the threshold filter (described in Section 10.1.2.1).
 - a. To assess the effect of burial on magnetometer based detection, the picks were performed first on the 6 m altitude mission performed on Node 3.

- b. Next, the same approach was used to pick targets again using mag only data for the 4 m altitude mission of Node 3.
 - c. Finally, the same approach was used to pick targets using mag only data for 2 m altitude mission of Node 3. Target location and anomaly strength for each of these three passes were recorded separately to a datasheet for the final analysis.
- 2) Separately from the magnetometer data analysis, sonar targets were selected from the side-scan sonar data only. This consisted of reviewing the sonar waterfall for each survey line and manually picking out sonar targets. Each target was marked for position (latitude and longitude). This is described in more detail in Section 10.1.2.2.
 - 3) After all magnetometer only picks had been made for targets in each node and cable route, then and only then were the mag picks overlaid onto the side-scan sonar mosaic. At this stage, the detection team also included the sonar target overlays together with the magnetometer targets.
 - 4) Step 3 was used to further discriminate any magnetic anomalies that may have come from multiple close targets by visually comparing the magnetometer anomalies to the side-scan sonar mosaic.
 - 5) Utilizing the magnetic responses to determine ferrous objects and the side-scan mosaic, the detection team then estimated the size of each magnetic positive sonar target.

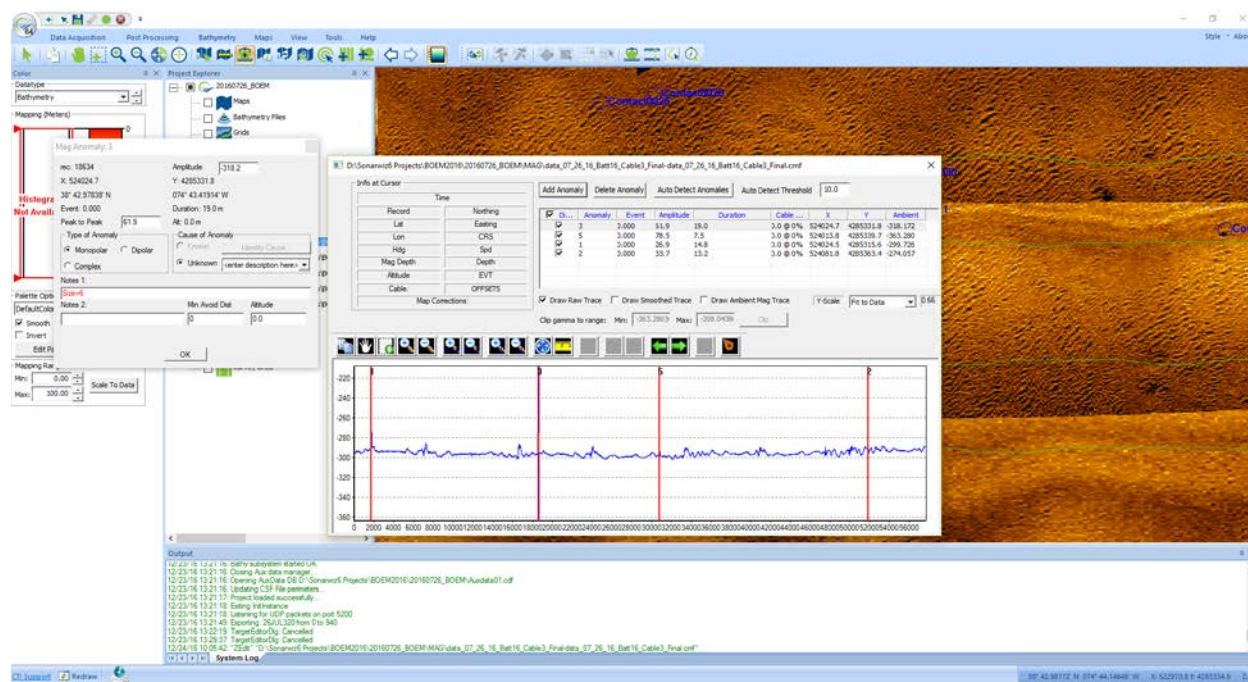
Two sets of summary tables were produced from 1) magnetometer only targets with position and size estimate and 2) magnetometer informed side-scan sonar targets. These tables were used to evaluate system performance.

10.1.2.1 Magnetometry Anomaly Picking

The processed and corrected magnetometer data was imported into Chesapeake Technology, Inc.'s SonarWiz software so that magnetic anomalies could be identified. Each time series file was selected and "Auto Detect Anomalies" was used with a threshold of 10.0 nT, which was determined to be the most effective threshold for detecting anomalies compared to manual interpretation. Detected anomalies were manually verified, and any apparent anomalies undetected by the previous process were manually selected (Figure 10-3). The manual inspection consisted of searching for dipole signatures having a distinct enough signal to allow it to be discernable from the background noise.

Size estimation for anomalies begin after a list of anomalies was produced and manually inspected for each magnetometer time series. This process involved comparing the IVS peak to peak amplitudes to a known list of sizes of munitions in that strip. This comparison established a range of peak to peak amplitude values for each size surrogate: 4-inch, 6-inch, and 8-inch. Then, those established ranges for each size class were used to categorize the sizes of the anomalies in each magnetometer data set from the survey sites. The size class estimate was then inputted into the "Notes 1:" section under the editor in the magnetometer anomaly list. It is important to note that the range of values of the size classes for the peak to peak amplitude of the magnetometer signal was a function of the height the vehicle was traveling over the seabed.

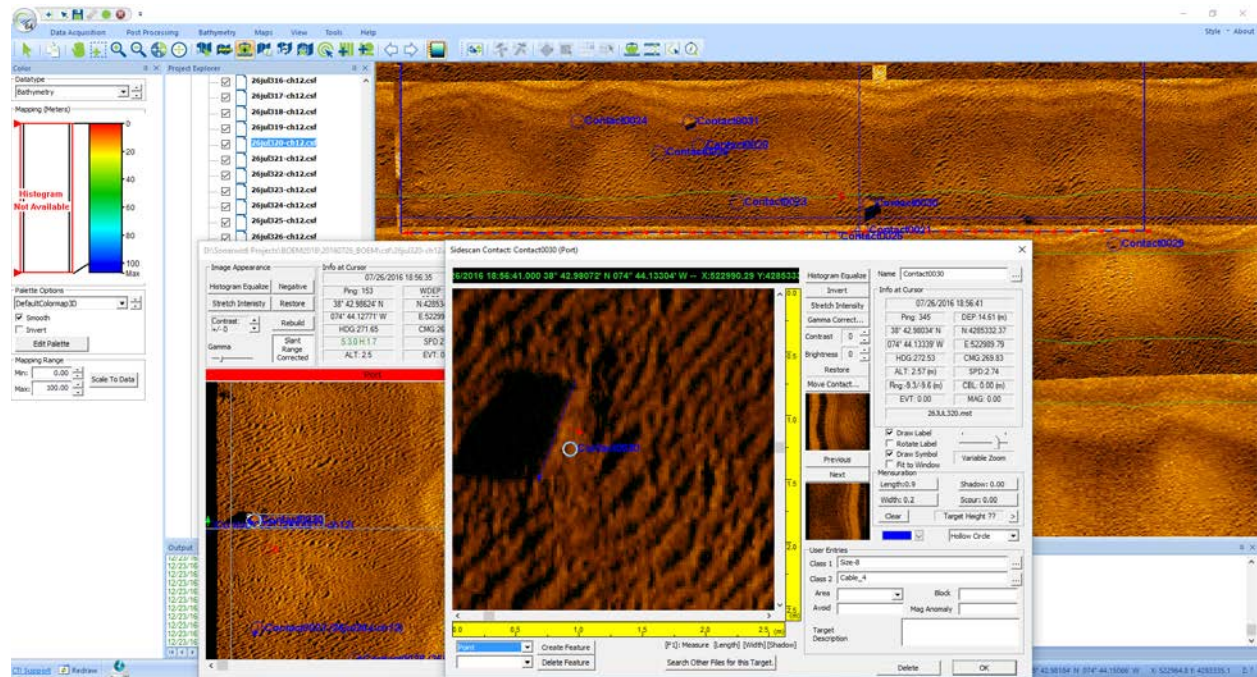
Figure 10-3: Magnetometer Anomalies Signal with Four Auto-detected Anomalies and Size Class



10.1.2.2 Side-scan Sonar Target Selection

Once the side-scan sonar data was processed, targets were then selected in SonarWiz sonar processing software, as well. Each sonar file was opened in “digitizing view” and scrolled through the waterfall view to search for linear features in terms of a feature sitting proud of the seabed or the shadow that feature created via the low grazing angle. When a target was located, a contact was created that cataloged the latitude and longitude (Figure 10-4). The location where the contact was found was cataloged in the “Class 1” section in user entry. Length and width were measured for each contact and that information was used to inform the diameter of the identified target. Each width was rounded to the closest size class: 2-inch, 4-inch, 6-inch, 8-inch, and was cataloged in the “Class 2” section in user entry, which was used as the size estimation of the target. If the linear feature on the seabed was not easily defined but there was a distinct linear shadow, the width of the shadow was measured, which gave the target height that was then rounded to the closest class available and inputted into the “Class 2” section in user entry. This method ensured that every target was given a site location and a size estimate.

Figure 10-4: Contact with Length and Width Measured and Position, Site, and Size Estimate Cataloged



There were numerous files that had multiple targets. Each target within the file would be selected and saved as a unique contact. However, the same target that showed up in consecutive files would not be saved as a unique contact in each file; the file names of the contacts that had previously been selected appear on all new files. Conversely, targets that appeared on parallel lines (i.e., the next transect over) would be saved as a unique contact, allowing for the evaluation of navigation drift. The position of the selected targets in a sonar file is not an absolute position therefore, selecting the same target on adjacent lines ensures multiple positions are considered to increase the precision relative to the actual contact itself.

10.2 Performance Analysis

Performance analysis was conducted by the seed deployment team. Analysis focused on navigational performance, total number of surrogates located, target selection by sensor type, and surrogate size estimation. Navigational performance was observed via drift in target position within the IVS missions over the course of the field effort. Target identification, surrogate sizing and surrogate identification was evaluated by comparing detection team magnetometer and side-scan sonar targets to seed positions verified by the seed deployment team. Due to difficulties with the initial USBL measurements, this required the separate processing and identification of targets from the AUV side-scan sonar data by the detection team. Identified targets from each mission day were then compared to positions estimates from both the vessel and USBL data (for data in which the USBL was operating correctly). Final reference target positions were then selected by those that most closely conformed to the positions recorded by the detection team. Of the 62 surrogates deployed, 54 were reacquired by the seed deployment team; 8 targets were not relocated after deployment (Table 10-2 and Table 10-3). These missing surrogates consisted only of 4-inch and 2-inch surrogates, while all 8-inch and 6-inch targets were reacquired (Table 10-3). At least two 4-inch surrogates and two 2-inch surrogates were placed outside of AUV

sonar coverage, based on the locations recorded by the deployment team. The remaining surrogates were either not detectable due to: sensor resolution / capabilities, inability of the deployment and search teams to recognize surrogate in the data, surrogate not placed in topside recorded position, or subsequently buried or moved by outside forces. All subsequent analysis is based off of the 54 surrogates relocated by the seeding team (Table 10-2) for consistency between detected targets, target location, and target size/type identification performance by the search team. Proper performance analysis of target location and identification require that target locations are known to the deployment team.

Table 10-2: Number and Size of Surrogates Relocated at Each Site by Seeding Team

| Site | 8-inch | 6-inch | 4-inch | 2-inch | Subtotal |
|-----------------|----------|-----------|-----------|----------|-----------|
| Cable Route 1 | 0 | 3 | 2 | 1 | 6 |
| Cable Route 2 | 1 | 2 | 1 | 1 | 5 |
| Cable Route 3 | 0 | 3 | 3 | 0 | 6 |
| Cable Route 4 | 1 | 1 | 2 | 0 | 4 |
| Cable Route 5 | 0 | 2 | 2 | 0 | 4 |
| <i>Subtotal</i> | 2 | 11 | 10 | 2 | 25 |
| Node 1 Route | 1 | 4 | 1 | 0 | 6 |
| Node 3 | 1 | 5 | 4 | 2 | 12 |
| Node 4 | 1 | 6 | 2 | 2 | 11 |
| <i>Subtotal</i> | 3 | 15 | 7 | 4 | 29 |
| Total | 5 | 26 | 17 | 6 | 54 |

Table 10-3: Number and Size of Surrogates Not Relocated by Seeding Team

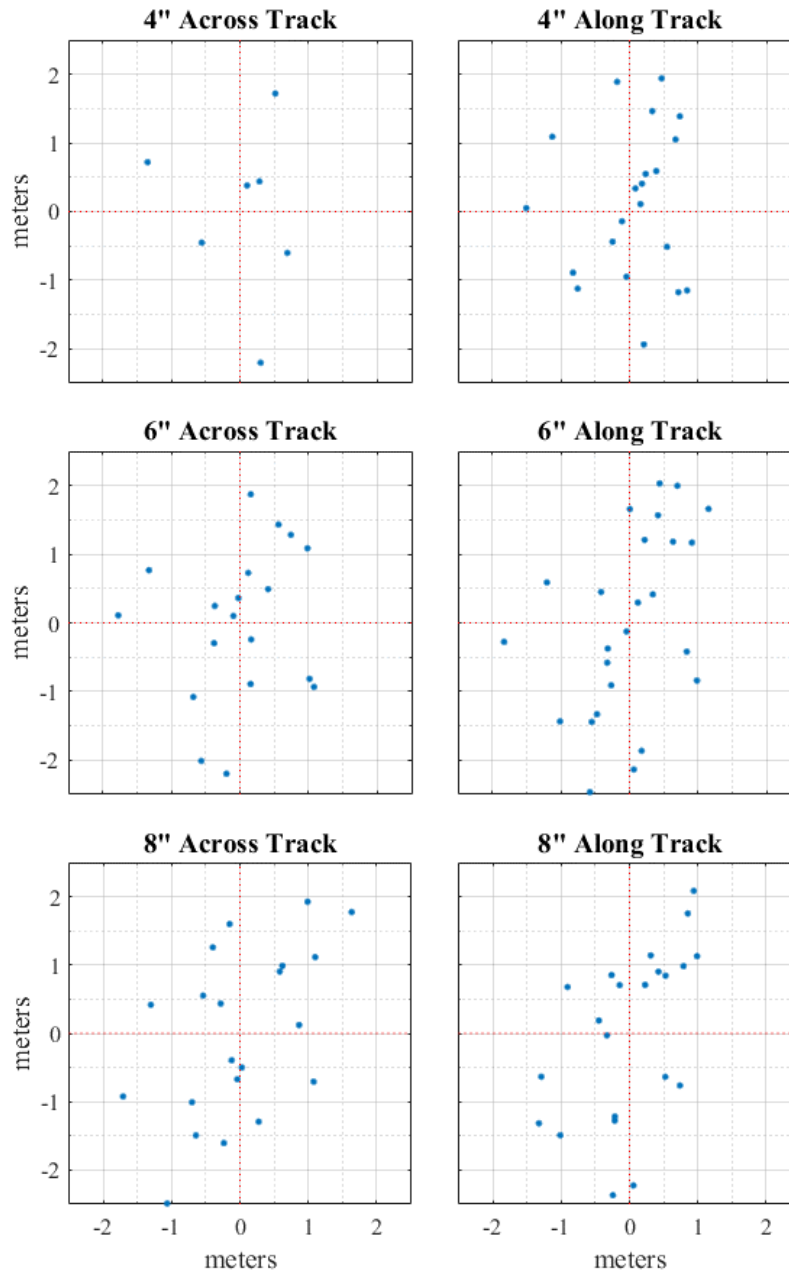
| Site | 4-inch | Comments | 2-inch | Comments |
|-----------------|----------|--|----------|--|
| Cable Route 1 | 0 | None | 0 | None |
| Cable Route 2 | 0 | None | 0 | None |
| Cable Route 3 | 0 | None | 0 | None |
| Cable Route 4 | 0 | None | 1 | Not detected |
| Cable Route 5 | 0 | None | 1 | Not detected |
| <i>Subtotal</i> | 0 | None | 2 | None |
| Node 1 Route | 2 | Located outside of AUV survey coverage | 3 | Located outside of AUV survey coverage or otherwise not detected |
| Node 3 | 0 | None | 0 | None |
| Node 4 | 1 | Not detected | 0 | None |
| <i>Subtotal</i> | 3 | None | 3 | None |
| Total | 3 | None | 5 | None |

10.2.1 Navigation

Positional uncertainties in the actual IVS position were on the order of about 1 m, thus not allowing for determination of navigational accuracy of the AUV by comparing the IVS position to AUV reported positions without incorporating those uncertainties. Instead, AUV navigational

drift was determined by examining the individual target locations for each IVS mission, and determining the positional “scatter” over the course of the field effort. A local mean was determined for each IVS surrogate, to which each reported position was compared. Figure 10-5 illustrates the scatter for each IVS surrogate. Surrogate positional scatter never exceeded 2.5 m relative to the local mean throughout the field effort.

Figure 10-5: IVS Surrogate Positional Scatter Over Field Effort



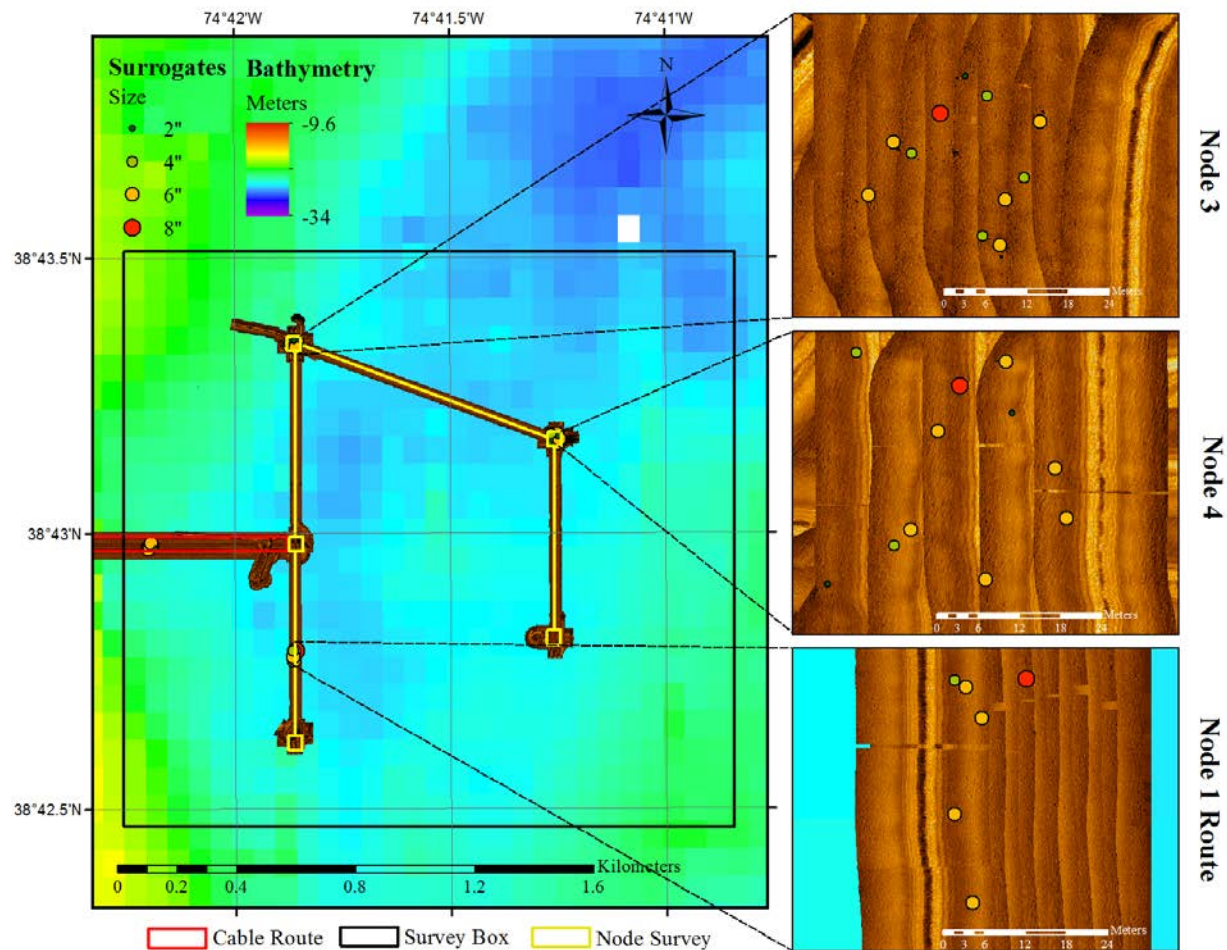
10.2.2 Node Mission Performance

Node missions were conducted at a standard altitude of 2 m and transect spacing of 8 m. Transects were laid out both in a North-South and East-West direction, with anticipation of

better coverage and increased overlap necessary to detect smaller surrogates. Missions were conducted at a speed of 3 knots, with magnetometry collected at 10 hertz; theoretically, this sampling rate and speed should resolve objects as small as 15 cm should the signal be greater than the system noise (<10nT) at 2 m altitude. High-resolution side-scan (1800 kHz) was collected at a range setting of 20 m, resulting in resolutions of <10 cm. Each node mission covered a 40 by 40 m area around a simulated monopile node and 0.6 km cable route linking the nodes for the in-field verification (Figure 9-1).

Surrogates were placed on the route between Nodes 1 and 2, in Node 3 and in Node 4 (see Figure 10-6). No targets were selected by the detection team outside of these areas, although both false positives and false negatives occurred within these missions. The results are presented in terms of the total number of surrogates detected per mission (Section 10.2.2.1) and target identification per mission (Section 10.2.2.2) for both magnetometer and side-scan sonar. Magnetometry, due to its ability to potentially detect both surficial and buried targets, is treated as the primary sensor for detection. The detection team used magnetometry to aid in selection of side-scan sonar targets, confirming whether magnetics were present in questionable surface targets.

Figure 10-6: Node Mission Overview



10.2.2.1 Target Detection

The target detection threshold for the in-field verification was the detection of all 155 mm (6-inch) surrogates or larger. Magnetometer detection results are shown in Table 10-4. With magnetometry alone in standard mission parameters, the detection of all 6-inch or larger surrogates was not achieved. Only in Node 4 were all 6-inch surrogates located, and only in Node 3 was an 8-inch surrogate located. With smaller surrogates, half of the 4-inch surrogates were located in Node-3 and Node-4. No 2-inch surrogates were located by magnetometer. False positives were low, with only two 6-inch and one 4-inch targets claimed in total.

Table 10-4: Target Detection by Surrogate Size for Node Missions using Magnetometry

| Region | Altitude (m) | Line Spacing (m) | # Surrogates | # Detected | % Detected | # False Positives |
|-------------------------|--------------|------------------|--------------|------------|------------|-------------------|
| 8-inch Surrogate | | | | | | |
| Node 1 Route | 2 | 8 | 1 | 0 | 0 | 0 |
| Node 3 | 2 | 8 | 1 | 1 | 100 | 0 |
| Node 4 | 2 | 8 | 1 | 0 | 0 | 0 |
| 6-inch Surrogate | | | | | | |
| Node 1 Route | 2 | 8 | 4 | 1 | 25 | 0 |
| Node 3 | 2 | 8 | 5 | 1 | 20 | 1 |
| Node 4 | 2 | 8 | 6 | 6 | 100 | 1 |
| 4-inch Surrogate | | | | | | |
| Node 1 Route | 2 | 8 | 1 | 0 | 0 | 0 |
| Node 3 | 2 | 8 | 4 | 2 | 50 | 1 |
| Node 4 | 2 | 8 | 2 | 1 | 50 | 0 |
| 2-inch Surrogate | | | | | | |
| Node 1 Route | 2 | 8 | 0 | 0 | NA | 0 |
| Node 3 | 2 | 8 | 2 | 0 | 0 | 0 |
| Node 4 | 2 | 8 | 2 | 0 | 0 | 0 |

Side-scan sonar target detection, aided by magnetometry, shows significantly better results (Table 10-5). However, considering that the majority of MEC are likely buried or partially buried (70 % according to Environmental Security Technology Certification Program (2010)), these results are only representative the portion of MEC on the sediment surface. Regardless, all 6-inch or larger surrogates were located in all node missions using side-scan aided by magnetometry. In both Node 1 Route and Node 4 missions, all 4-inch surrogates were also located. Only in Node 3 were the 2-inch surrogates located. False targets were again low, with only four false targets combined.

Table 10-5: Target Detection by Surrogate Size for Node Missions using Side-scan Sonar Aided by Magnetometry

| Region | Altitude (m) | Line Spacing (m) | # Surrogates | # Detected | % Detected | # False Positives |
|-------------------------|--------------|------------------|--------------|------------|------------|-------------------|
| 8-inch Surrogate | | | | | | |
| Node 1 Route | 2 | 8 | 1 | 1 | 100 | 1 |
| Node 3 | 2 | 8 | 1 | 1 | 100 | 0 |
| Node 4 | 2 | 8 | 1 | 1 | 100 | 0 |
| 6-inch Surrogate | | | | | | |
| Node 1 Route | 2 | 8 | 4 | 4 | 100 | 0 |
| Node 3 | 2 | 8 | 5 | 5 | 100 | 0 |
| Node 4 | 2 | 8 | 6 | 6 | 100 | 1 |
| 4-inch Surrogate | | | | | | |
| Node 1 Route | 2 | 8 | 1 | 1 | 100 | 2 |
| Node 3 | 2 | 8 | 4 | 2 | 50 | 0 |
| Node 4 | 2 | 8 | 2 | 2 | 100 | 0 |
| 2-inch Surrogate | | | | | | |
| Node 1 Route | 2 | 8 | 0 | 0 | NA | 0 |
| Node 3 | 2 | 8 | 2 | 2 | 100 | 0 |
| Node 4 | 2 | 8 | 2 | 0 | 0 | 0 |

10.2.2.2 Target Identification

The detection team estimated sizes for each target located. In both magnetometry and side-scan sonar, multiple targets picked by the detection team were often associated with each surrogate. If the target estimation varied among a set of targets associated with one surrogate, the largest size estimated was selected for the final size estimate, since the largest target would effectively have the most potential to cause harm to offshore energy development.

For magnetometry, size was determined by the amplitude of the magnetic signal (Table 10-6). The sole 8-inch target, located in Node 3, was correctly sized, as were the sole 6-inch surrogates located in Node 3 and Node 1 Route. Of the six 6-inch surrogates in Node 4, half were correctly sized. With 4-inch surrogates, 2 of 3 were correctly sized in Nodes 3 and 4.

For side-scan sonar, targets confirmed by both side-scan and magnetometry were measured within the side-scan imagery for diameter and length. These measurements were used estimate size. The results are shown in Table 10-7. Two of three 8-inch surrogates were properly identified. With 6-inch surrogates, half were correctly identified in Node 1 Route, but only a third of those located in Node 4 and none of the 6-inch surrogates in Node 3. Performance improved with 4-inch surrogates, where all 4-inch surrogates within Node 1 Route and Node 4 were correctly identified, and half in Node 3. The detected 2-inch targets in Node 3 were not correctly identified.

Table 10-6: Target Identification by Surrogate Size for Node Missions using Magnetometry

| Region | Altitude (m) | Line Spacing (m) | # Detected | # Correctly Sized | % Correctly Sized |
|-------------------------|--------------|------------------|------------|-------------------|-------------------|
| 8-inch Surrogate | | | | | |
| Node 1 Route | 2 | 8 | 0 | 0 | NA |
| Node 3 | 2 | 8 | 1 | 1 | 100 |
| Node 4 | 2 | 8 | 0 | 0 | NA |
| 6-inch Surrogate | | | | | |
| Node 1 Route | 2 | 8 | 1 | 1 | 100 |
| Node 3 | 2 | 8 | 1 | 1 | 100 |
| Node 4 | 2 | 8 | 6 | 3 | 50 |
| 4-inch Surrogate | | | | | |
| Node 1 Route | 2 | 8 | 0 | 0 | NA |
| Node 3 | 2 | 8 | 2 | 1 | 50 |
| Node 4 | 2 | 8 | 1 | 1 | 100 |
| 2-inch Surrogate | | | | | |
| Node 1 Route | 2 | 8 | 0 | 0 | NA |
| Node 3 | 2 | 8 | 0 | 0 | NA |
| Node 4 | 2 | 8 | 0 | 0 | NA |

Table 10-7: Target Identification by Surrogate Size for Node Missions using Side-scan Sonar Aided by Magnetometry

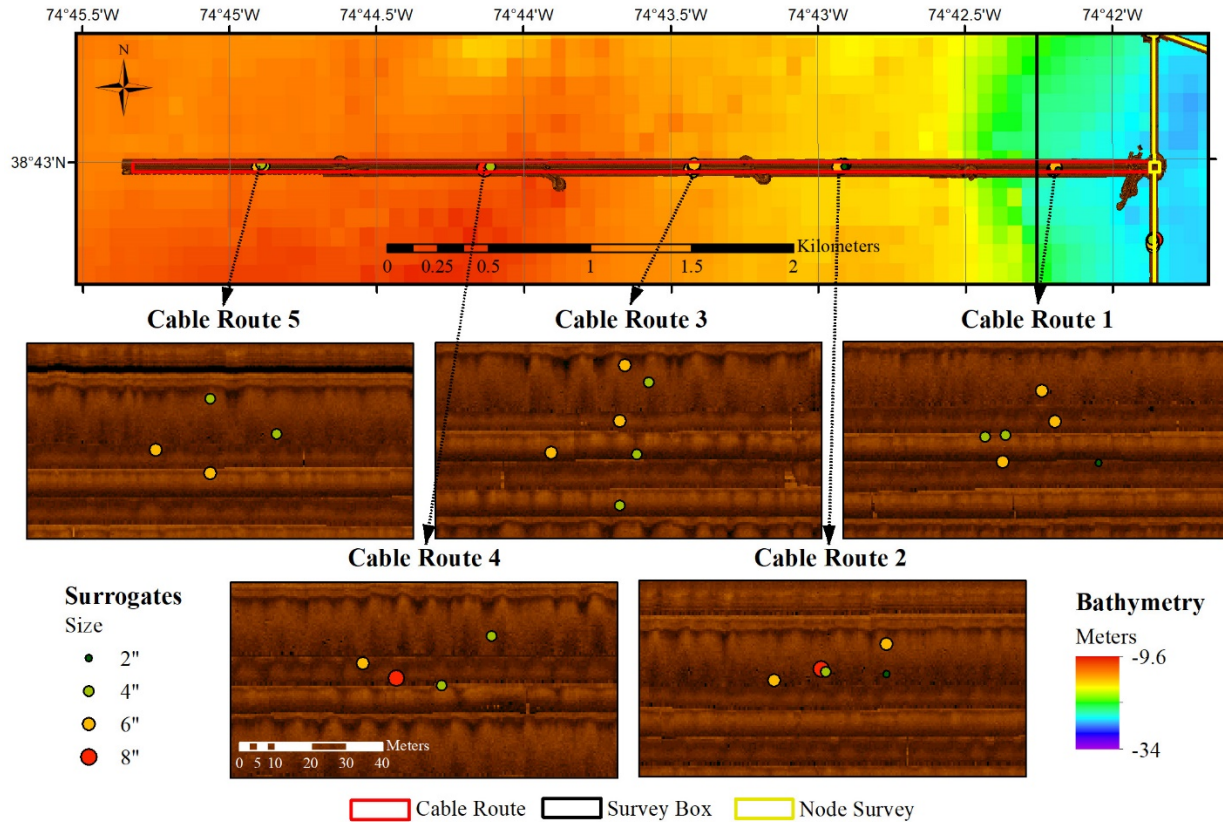
| Region | Altitude (m) | Line Spacing (m) | # Detected | # Correctly Sized | % Correctly Sized |
|-------------------------|--------------|------------------|------------|-------------------|-------------------|
| 8-inch Surrogate | | | | | |
| Node 1 Route | 2 | 8 | 1 | 1 | 100 |
| Node 3 | 2 | 8 | 1 | 0 | 0 |
| Node 4 | 2 | 8 | 1 | 1 | 100 |
| 6-inch Surrogate | | | | | |
| Node 1 Route | 2 | 8 | 4 | 2 | 50 |
| Node 3 | 2 | 8 | 5 | 0 | 0 |
| Node 4 | 2 | 8 | 6 | 2 | 33.33 |
| 4-inch Surrogate | | | | | |
| Node 1 Route | 2 | 8 | 1 | 1 | 100 |
| Node 3 | 2 | 8 | 2 | 1 | 50 |
| Node 4 | 2 | 8 | 2 | 2 | 100 |
| 2-inch Surrogate | | | | | |
| Node 1 Route | 2 | 8 | 0 | 0 | NA |
| Node 3 | 2 | 8 | 2 | 0 | 0 |
| Node 4 | 2 | 8 | 0 | 0 | NA |

10.2.3 Cable Route Mission Performance

Cable route missions used the same mission parameters as node missions, with 2 m altitude and 8 m spacing as the standard settings. Missions were only composed of East-West transects, all 1 km in length to reduce navigational drift. Cable route missions were also conducted at 3 knots,

with the same sampling settings used in the node missions for magnetometry and side-scan sonar. Each cable route mission covered a 1000 by 50 m area, totaling the 5 km length of the simulated cable route in the in-field verification (Figure 10-7).

Figure 10-7: Cable Route Mission Overview



10.2.3.1 Target Detection

Magnetometer detection results are shown in Table 10-8. Unlike the node missions, all 8-inch surrogates were identified by magnetometer. However, only one of three 6-inch surrogates were located in both Cable 1 and Cable 3 missions, and only half in Cable 2. None of the 6-inch surrogates were located in Cable Routes 4 or 5. Results are similar with smaller surrogates, although two of three 4-inch surrogates were located in Cable 3. Once again, no 2-inch surrogates were located. False positives were slightly higher than in node missions, but no more than four false targets occurred in any one mission (Cable Route 5).

Table 10-8: Target Detection by Surrogate Size for Cable Route Missions using Magnetometry

| Region | Altitude (m) | Line Spacing (m) | # Surrogates | # Detected | % Detected | # False Positives |
|-------------------------|--------------|------------------|--------------|------------|------------|-------------------|
| 8-inch Surrogate | | | | | | |
| Cable Route 1 | 2 | 8 | 0 | 0 | NA | 0 |
| Cable Route 2 | 2 | 8 | 1 | 1 | 100 | 0 |
| Cable Route 3 | 2 | 8 | 0 | 0 | NA | 0 |
| Cable Route 4 | 2 | 8 | 1 | 1 | 100 | 0 |
| Cable Route 5 | 2 | 8 | 0 | 0 | NA | 1 |
| 6-inch Surrogate | | | | | | |
| Cable Route 1 | 2 | 8 | 3 | 1 | 33.33 | 1 |
| Cable Route 2 | 2 | 8 | 2 | 1 | 50 | 0 |
| Cable Route 3 | 2 | 8 | 3 | 1 | 33.33 | 0 |
| Cable Route 4 | 2 | 8 | 1 | 0 | 0 | 0 |
| Cable Route 5 | 2 | 8 | 2 | 0 | 0 | 3 |
| 4-inch Surrogate | | | | | | |
| Cable Route 1 | 2 | 8 | 2 | 0 | 0 | 0 |
| Cable Route 2 | 2 | 8 | 1 | 0 | 0 | 1 |
| Cable Route 3 | 2 | 8 | 3 | 2 | 66.67 | 1 |
| Cable Route 4 | 2 | 8 | 2 | 1 | 50 | 1 |
| Cable Route 5 | 2 | 8 | 2 | 0 | 0 | 0 |
| 2-inch Surrogate | | | | | | |
| Cable Route 1 | 2 | 8 | 1 | 0 | 0 | 0 |
| Cable Route 2 | 2 | 8 | 1 | 0 | 0 | 0 |
| Cable Route 3 | 2 | 8 | 0 | 0 | NA | 0 |
| Cable Route 4 | 2 | 8 | 0 | 0 | NA | 0 |
| Cable Route 5 | 2 | 8 | 0 | 0 | NA | 0 |

As with Node mission results, all 8-inch and 6-inch surrogates were located using side-scan sonar aided by magnetometry. In Cable Routes 2 and 4, all 4-inch targets were also located, although only two of three were located in Cable 3 and none in Cable Routes 1 and 5. As with magnetometry alone, no 2-inch surrogates were located. False positives were significantly higher in side-scan targets, with all missions containing at least two false positives, and one (Cable Route 5) containing seven false positives. Refer to Table 10-9.

Table 10-9: Target Detection by Surrogate Size for Cable Route Missions using Side-scan Sonar Aided by Magnetometry

| Region | Altitude (m) | Line Spacing (m) | # Surrogates | # Detected | % Detected | # False Positives |
|-------------------------|--------------|------------------|--------------|------------|------------|-------------------|
| 8-inch Surrogate | | | | | | |
| Cable Route 1 | 2 | 8 | 0 | 0 | NA | 0 |
| Cable Route 2 | 2 | 8 | 1 | 1 | 100 | 0 |
| Cable Route 3 | 2 | 8 | 0 | 0 | NA | 0 |
| Cable Route 4 | 2 | 8 | 1 | 1 | 100 | 1 |
| Cable Route 5 | 2 | 8 | 0 | 0 | NA | 0 |
| 6-inch Surrogate | | | | | | |
| Cable Route 1 | 2 | 8 | 3 | 3 | 100 | 1 |
| Cable Route 2 | 2 | 8 | 2 | 2 | 100 | 0 |
| Cable Route 3 | 2 | 8 | 3 | 3 | 100 | 1 |
| Cable Route 4 | 2 | 8 | 1 | 1 | 100 | 1 |
| Cable Route 5 | 2 | 8 | 2 | 2 | 100 | 1 |
| 4-inch Surrogate | | | | | | |
| Cable Route 1 | 2 | 8 | 2 | 0 | 0 | 2 |
| Cable Route 2 | 2 | 8 | 1 | 1 | 100 | 2 |
| Cable Route 3 | 2 | 8 | 3 | 2 | 66.67 | 1 |
| Cable Route 4 | 2 | 8 | 2 | 2 | 100 | 3 |
| Cable Route 5 | 2 | 8 | 2 | 0 | 0 | 6 |
| 2-inch Surrogate | | | | | | |
| Cable Route 1 | 2 | 8 | 1 | 0 | 0 | 0 |
| Cable Route 2 | 2 | 8 | 1 | 0 | 0 | 0 |
| Cable Route 3 | 2 | 8 | 0 | 0 | NA | 0 |
| Cable Route 4 | 2 | 8 | 0 | 0 | NA | 0 |
| Cable Route 5 | 2 | 8 | 0 | 0 | NA | 0 |

10.2.3.2 Target Identification

Target identification by magnetometer are shown in Table 10-10. One of two 8-inch surrogates, located in Cable 2, was correctly sized. Of the detected 6-inch surrogates, those located in Cable Routes 2 and 3 were correctly identified (two of three total). With 4-inch surrogates, two of three surrogates identified in Cable Routes 3 and 4 were correctly sized. No 2-inch surrogates were located to provide size estimation results.

The results for side-scan sonar are shown in Table 10-11. All 8-inch surrogates were properly identified. With 6-inch surrogates, only one surrogate in five missions was correctly identified. Performance improved with 4-inch surrogates, as with node missions, where all 4-inch surrogates within Cable Routes 2 and 4 were correctly identified, and half in Cable Route 3. No 2-inch surrogates had been identified to be sized.

Table 10-10: Target Identification by Surrogate Size for Cable Route Missions using Magnetometry

| Region | Altitude (m) | Line Spacing (m) | # Surrogates | # Detected | # Detected Correctly Sized | % Detected Correctly Sized |
|-------------------------|--------------|------------------|--------------|------------|----------------------------|----------------------------|
| 8-inch Surrogate | | | | | | |
| Cable Route 1 | 2 | 8 | 0 | 0 | NA | NA |
| Cable Route 2 | 2 | 8 | 1 | 1 | 1 | 100 |
| Cable Route 3 | 2 | 8 | 0 | 0 | NA | NA |
| Cable Route 4 | 2 | 8 | 1 | 1 | 0 | 0 |
| Cable Route 5 | 2 | 8 | 0 | 0 | NA | NA |
| 6-inch Surrogate | | | | | | |
| Cable Route 1 | 2 | 8 | 3 | 1 | 0 | 0 |
| Cable Route 2 | 2 | 8 | 2 | 1 | 1 | 100 |
| Cable Route 3 | 2 | 8 | 3 | 1 | 1 | 100 |
| Cable Route 4 | 2 | 8 | 1 | 0 | NA | NA |
| Cable Route 5 | 2 | 8 | 2 | 0 | NA | NA |
| 4-inch Surrogate | | | | | | |
| Cable Route 1 | 2 | 8 | 2 | 0 | NA | NA |
| Cable Route 2 | 2 | 8 | 1 | 0 | NA | NA |
| Cable Route 3 | 2 | 8 | 3 | 2 | 1 | 50 |
| Cable Route 4 | 2 | 8 | 2 | 1 | 1 | 100 |
| Cable Route 5 | 2 | 8 | 2 | 0 | NA | NA |
| 2-inch Surrogate | | | | | | |
| Cable Route 1 | 2 | 8 | 1 | 0 | NA | NA |
| Cable Route 2 | 2 | 8 | 1 | 0 | NA | NA |
| Cable Route 3 | 2 | 8 | 0 | 0 | NA | NA |
| Cable Route 4 | 2 | 8 | 0 | 0 | NA | NA |
| Cable Route 5 | 2 | 8 | 0 | 0 | NA | NA |

Table 10-11: Target Identification by Surrogate Size for Cable Route Missions using Side-scan Sonar Aided by Magnetometry

| Region | Altitude (m) | Line Spacing (m) | # Surrogates | # Detected | # Detected Correctly Sized | % Detected Correctly Sized |
|-------------------------|--------------|------------------|--------------|------------|----------------------------|----------------------------|
| 8-inch Surrogate | | | | | | |
| Cable Route 1 | 2 | 8 | 0 | 0 | NA | NA |
| Cable Route 2 | 2 | 8 | 1 | 1 | 1 | 100 |
| Cable Route 3 | 2 | 8 | 0 | 0 | NA | NA |
| Cable Route 4 | 2 | 8 | 1 | 1 | 1 | 100 |
| Cable Route 5 | 2 | 8 | 0 | 0 | NA | NA |
| 6-inch Surrogate | | | | | | |
| Cable Route 1 | 2 | 8 | 3 | 3 | 0 | 0 |
| Cable Route 2 | 2 | 8 | 2 | 2 | 0 | 0 |
| Cable Route 3 | 2 | 8 | 3 | 3 | 0 | 0 |
| Cable Route 4 | 2 | 8 | 1 | 1 | 0 | 0 |
| Cable Route 5 | 2 | 8 | 2 | 2 | 1 | 50 |
| 4-inch Surrogate | | | | | | |
| Cable Route 1 | 2 | 8 | 2 | 0 | NA | NA |
| Cable Route 2 | 2 | 8 | 1 | 1 | 1 | 100 |
| Cable Route 3 | 2 | 8 | 3 | 2 | 1 | 50 |
| Cable Route 4 | 2 | 8 | 2 | 2 | 2 | 100 |
| Cable Route 5 | 2 | 8 | 2 | 0 | NA | NA |
| 2-inch Surrogate | | | | | | |
| Cable Route 1 | 2 | 8 | 1 | 0 | NA | NA |
| Cable Route 2 | 2 | 8 | 1 | 0 | NA | NA |
| Cable Route 3 | 2 | 8 | 0 | 0 | NA | NA |
| Cable Route 4 | 2 | 8 | 0 | 0 | NA | NA |
| Cable Route 5 | 2 | 8 | 0 | 0 | NA | NA |

10.2.4 Mission Variations

All node and cable route surveys were conducted using 2 m altitude and 8 m transect spacing based off initial recommendations from the technology review. To examine the effect of altitude and transect spacing on performance, a select number of missions were conducted with variations in altitude and transect spacing. Additionally, increasing the AUV altitude above the seabed was used to simulate surrogate burial: distance between the target and the magnetometer determines signal strength, not the medium in between, unless it contains ferrous materials. Thus, with seawater and non-ferrous sands present at the field site, increasing the altitude from 2 to 4 m would simulate 2 m surrogate burial. Variations in line spacing were examined to determine whether performance improved with enough significance to justify narrower transect spacing, which in turn would increase the total survey time required. Based off initial performance with 8 m spaced transects, wider transect spacing was tested as it would not have improved detection results. All simulated burial and variable spacing missions were conducted over Node 3, where the detection team was most confident in the presence of surrogates.

10.2.4.1 Simulated Burial

Simulated burial missions were flown at two separate altitudes: 4 and 6 m. This simulated 2 and 4 m burial respectively. The results are presented in Table 10-12. Most notable is the improvement over the standard Node 3 mission: an additional 6-inch and 4-inch surrogate are located, as well as both 2-inch surrogates. Further, all 8-inch and 6-inch surrogates are correctly identified. However, target identification was not successful at 4 m altitude for targets less than the 6-inch surrogates. At 6 m altitude, an additional 6-inch surrogate is located, although only one 4-inch and neither 2-inch surrogates were found. This suggests that buried even up to depths of 4 m, a 155 mm MEC can possibly be detected, although target identification was less successful for 6-inch surrogates at this altitude.

10.2.4.2 Variations in Transect Spacing and Altitude

Transect spacing was decreased to 4 m to test whether detection and identification rates would increase. Two missions were conducted: one at the standard 2 m altitude, and a second at 4 m altitude. The latter would then additionally test the effect of 4 m spacing on simulated buried targets. To maintain mission duration, 4 m spaced transects required that only North-South transects were run, instead of the standard North-South and East-West transects of the 8 m spaced missions.

The results from magnetometer picking are included in Table 10-13. With the 2 m altitude, 4 m spaced mission, detection rates improved over the standard 8 m spaced mission, with two additional 6-inch surrogates located, and one additional 4-inch surrogate detected. However, the 2-inch surrogates were not located. Target identification was also improved over standard missions, with two of three 6-inch surrogates correctly identified, and all located 8-inch and 4-inch targets correctly identified. Target detection was identical when altitude was increased to 4 m and 4 m spacing maintained, but the increase in altitude did impact target identification: only one 6-inch surrogate and neither of the detected 4-inch surrogates were correctly identified.

Although the primary motive for the simulated burial missions was to test the performance of the magnetometer, increased altitude has consequences for the performance of side-scan sonar. With increased altitude, resolution may decrease, but swath width may increase. This creates the potential to cover, or in the case of “lawnmower” surveying, more sonar overlap, but potentially at the expense of resolution and target detection and identification. In this experiment, the influence of increasing the altitude (Table 10-14) to 4 m altitude had negligible effect on target detection based on the side-scan data. In fact, an additional 4-inch surrogate was located versus the standard 2 m altitude mission. Similarly, target identification does not appear to have been negatively affected: target identification improved across 8-inch, 6-inch, and 4-inch surrogates. The increase to 6 m altitude, however, does appear to have a negatively impacted detection. One 6-inch surrogate was missed, while only one 4-inch surrogate and neither of the 2-inch surrogates was located. Further, successful surrogate identification rates decreased.

With variations in transect spacing, (Table 10-15), the 4 m spaced mission did not result in an improvement in detection: one less 4-inch surrogate was located, and overall target identification did not improve. At 4 m altitude and 4 m spacing, performance further decreased: only four of the five 6-inch surrogates present were found and none of the 2-inch surrogates were located. Target identification performance further decreased, with only one 6-inch and one 4-inch surrogate correctly identified.

Table 10-12: Target Detection and Identification by Surrogate Size for Simulated Burial Missions using Magnetometry

| Region | Altitude (m) | Line Spacing (m) | # Surrogates | # Detected | % Detected | # False Positives | # Detected Correctly Sized | % Detected Correctly Sized |
|-------------------------|--------------|------------------|--------------|------------|------------|-------------------|----------------------------|----------------------------|
| 8-inch Surrogate | | | | | | | | |
| Node 3 | 4 | 8 | 1 | 1 | 100 | 0 | 1 | 100 |
| Node 3 | 6 | 8 | 1 | 1 | 100 | 0 | 1 | 100 |
| 6-inch Surrogate | | | | | | | | |
| Node 3 | 4 | 8 | 5 | 2 | 40 | 0 | 2 | 100 |
| Node 3 | 6 | 8 | 5 | 3 | 60 | 1 | 2 | 66.67 |
| 4-inch Surrogate | | | | | | | | |
| Node 3 | 4 | 8 | 4 | 3 | 75 | 0 | 0 | 0 |
| Node 3 | 6 | 8 | 4 | 1 | 25 | 0 | 0 | 0 |
| 2-inch Surrogate | | | | | | | | |
| Node 3 | 4 | 8 | 2 | 2 | 100 | 0 | 0 | 0 |
| Node 3 | 6 | 8 | 2 | 0 | 0 | 0 | 0 | NA |

Table 10-13: Target Detection and Identification by Surrogate Size for Variable Transect Spacing and Altitude Missions using Magnetometry

| Region | Altitude (m) | Line Spacing (m) | # Surrogates | # Detected | % Detected | # False Positives | # Detected Correctly Sized | % Detected Correctly Sized |
|-------------------------|--------------|------------------|--------------|------------|------------|-------------------|----------------------------|----------------------------|
| 8-inch Surrogate | | | | | | | | |
| Node 3 | 2 | 4 | 1 | 1 | 100 | 0 | 1 | 100 |
| Node 3 | 4 | 4 | 1 | 1 | 100 | 0 | 1 | 100 |
| 6-inch Surrogate | | | | | | | | |
| Node 3 | 2 | 4 | 5 | 3 | 60 | 0 | 2 | 66.67 |
| Node 3 | 4 | 4 | 5 | 3 | 60 | 0 | 1 | 33.33 |
| 4-inch Surrogate | | | | | | | | |
| Node 3 | 2 | 4 | 4 | 2 | 50 | 0 | 2 | 100 |
| Node 3 | 4 | 4 | 4 | 2 | 50 | 0 | 0 | 0 |
| 2-inch Surrogate | | | | | | | | |
| Node 3 | 2 | 4 | 2 | 0 | 0 | 0 | 0 | NA |
| Node 3 | 4 | 4 | 2 | 0 | 0 | 0 | 0 | NA |

Table 10-14: Target Detection and Identification by Surrogate Size for Variable Altitude Missions using Side-scan Sonar Aided Magnetometry

| Region | Altitude (m) | Line Spacing (m) | # Surrogates | # Detected | % Detected | # False Positives | # Detected Correctly Sized | % Detected Correctly Sized |
|-------------------------|--------------|------------------|--------------|------------|------------|-------------------|----------------------------|----------------------------|
| 8-inch Surrogate | | | | | | | | |
| Node 3 | 4 | 8 | 1 | 1 | 100 | 0 | 1 | 100 |
| Node 3 | 6 | 8 | 1 | 1 | 100 | 0 | 1 | 100 |
| 6-inch Surrogate | | | | | | | | |
| Node 3 | 4 | 8 | 5 | 5 | 100 | 3 | 3 | 60 |
| Node 3 | 6 | 8 | 5 | 4 | 80 | 2 | 2 | 50 |
| 4-inch Surrogate | | | | | | | | |
| Node 3 | 4 | 8 | 4 | 3 | 75 | 0 | 2 | 66.67 |
| Node 3 | 6 | 8 | 4 | 1 | 25 | 0 | 0 | 0 |
| 2-inch Surrogate | | | | | | | | |
| Node 3 | 4 | 8 | 2 | 2 | 100 | 0 | 0 | 0 |
| Node 3 | 6 | 8 | 2 | 0 | 0 | 0 | 0 | NA |

Table 10-15: Target Detection and Identification by Surrogate Size for Variable Transect Spacing using Side-scan Sonar Aided Magnetometry

| Region | Altitude (m) | Line Spacing (m) | # Surrogates | # Detected | % Detected | # False Positives | # Detected Correctly Sized | % Detected Correctly Sized |
|-------------------------|--------------|------------------|--------------|------------|------------|-------------------|----------------------------|----------------------------|
| 8-inch Surrogate | | | | | | | | |
| Node 3 | 2 | 4 | 1 | 1 | 100 | 0 | 1 | 100 |
| Node 3 | 4 | 4 | 1 | 1 | 100 | 0 | 0 | 0 |
| 6-inch Surrogate | | | | | | | | |
| Node 3 | 2 | 4 | 5 | 5 | 100 | 4 | 0 | 0 |
| Node 3 | 4 | 4 | 5 | 4 | 80 | 3 | 1 | 25 |
| 4-inch Surrogate | | | | | | | | |
| Node 3 | 2 | 4 | 4 | 1 | 25 | 1 | 1 | 100 |
| Node 3 | 4 | 4 | 4 | 1 | 25 | 0 | 1 | 100 |
| 2-inch Surrogate | | | | | | | | |
| Node 3 | 2 | 4 | 2 | 2 | 100 | 0 | 0 | 0 |
| Node 3 | 4 | 4 | 2 | 0 | 0 | 0 | 0 | NA |

Page Intentionally Left Blank.

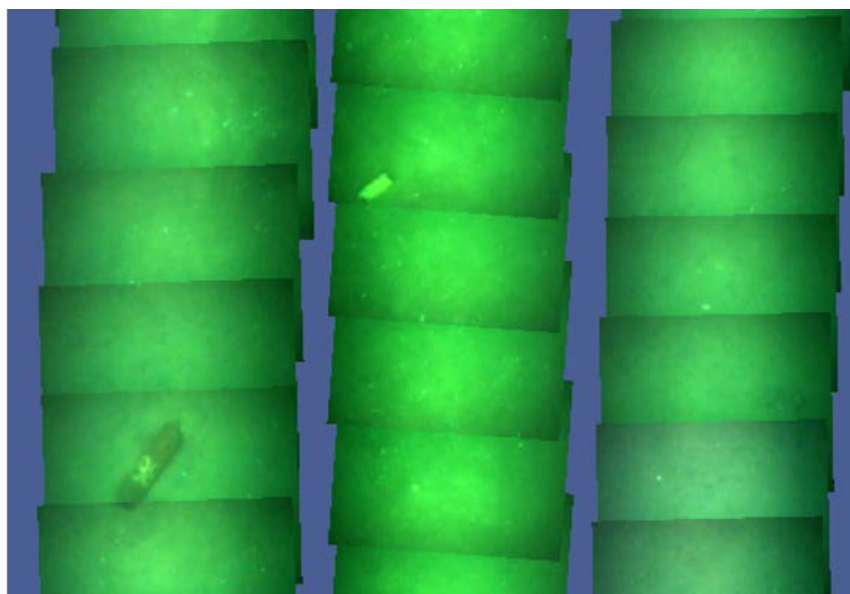
10.2.5 Optical Survey

Optical survey missions were conducted with the AUV to reacquire and confirm the presence and type of surrogates initially identified by the detection team. This tested the ability of the detection team to properly report the location of surrogates with such accuracy as to allow for reacquisition by the same or other means.

To achieve the best possible coverage and resolution, a photo test mission was conducted over the IVS. Three different vehicle altitudes were tested: 3, 2.5 and 2 m. Preliminary analysis determined the 2 m altitude rendered the best conditions for target identification. All photo missions were conducted at 2 m altitude.

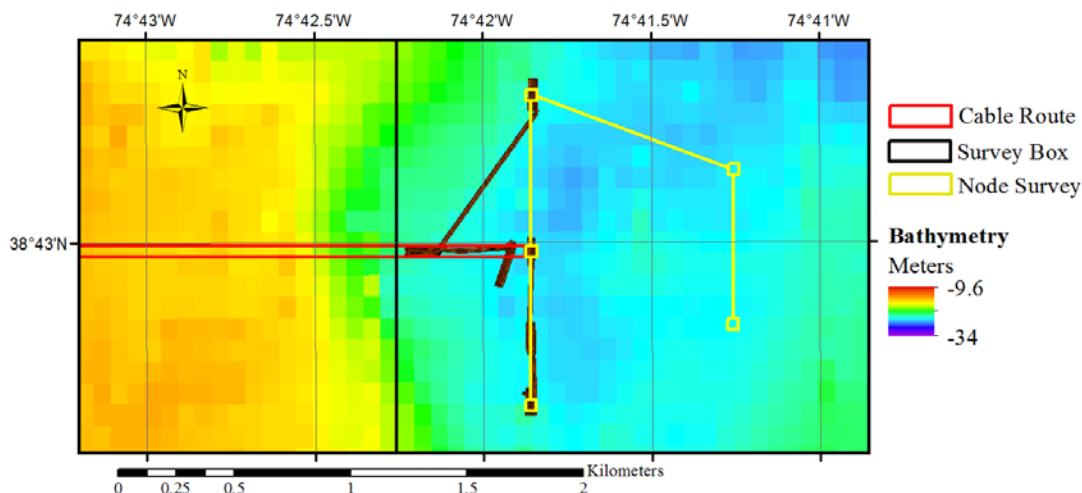
Missions were constructed in “lawnmower” patterns over groupings of targets identified by the detection team. This would also allow for the mosaicking of a group targets (Figure 10-8). Three photo missions were conducted, focusing on Node 1, Node 1 Route, Node 3, and Cable Route 1.

Figure 10-8: Section of Photomosaic from Node 3 Optical Survey



Note the 6- and 4-inch surrogates in the image.

Within Node 1, targets picked by the detection team appeared only in side-scan, but not in magnetometer. The photo mission revealed that the targets were not surrogates, but rather geological features (e.g. boulders). On the route between Nodes 1 and 2 (referred to as Node 1 Route), both magnetometer and side-scan targets were present, and were verified by photograph. Both Node 3 and Cable Route 1 missions reacquired targets and confirmed the presence of surrogates as well (Figure 10-9).

Figure 10-9: Overview of AUV Camera Missions Collected 28 July 2016

Side-scan sonar is presented to better illustrate the areas covered.

10.3 Discussion

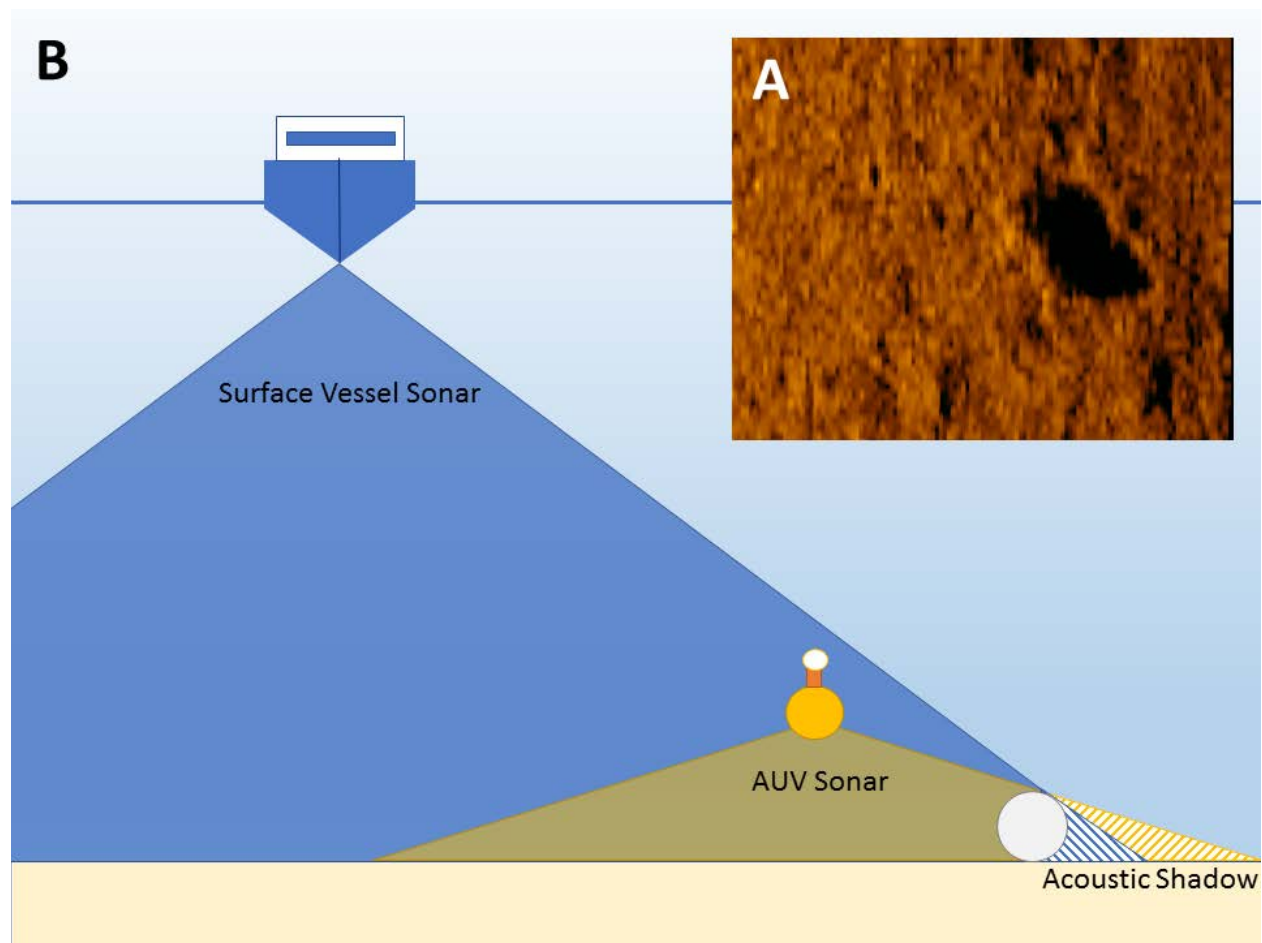
10.3.1 Wide Area Assessment

The wide area assessment tested the ability of the selected high-resolution, hull-mounted PMBS to effectively identify areas of interest for target interrogation, as well as provide useful geophysical data for seabed sediment classification, bathymetry and locating potential hazards to AUV operations. During the in-field verification, the entire study area was mapped with over 200% side-scan coverage and 100% bathymetric coverage. Important geophysical data was collected for site characterization and no obstructions to AUV missions were determined to be present.

Despite the significant coverage, no targets could be clearly identified from the PMBS data. The resolution of the system was deemed sufficient to detect the larger objects; as noted before, similar systems with lower resolution had been used with success (Edwards, et al. 2012). Upon conducting the AUV surveys, it was determined that the acoustic signature of the surrogates was too similar to the acoustic reflectivity of the surrounding seabed (Figure 10-10A). In comparison, the sediments in the study area mapped by Edwards et al., (2012) were much less acoustically reflective, and the acoustic signature of the MEC more apparent. Alternatively, while the system used for the in-field verification had the theoretical resolution to resolve the surrogates, the surrogate signatures was at times masked by the surrounding sediments.

The most apparent signature of the surrogates, as identified from the AUV side-scan sonar, was the acoustic shadow created by the targets. The length of the acoustic shadow is determined not only by the height of the object above the seabed, but also the grazing angle of the sonar. A steeper grazing angle, as presented by the ship-borne PMBS, results in a much shorter acoustic shadow than a shallower grazing angle, which occurred in the AUV surveys (Figure 10-10B). Thus, the AUV, with both magnetometer and side-scan, became the primary means by which to locate the surrogates.

Figure 10-10: Illustration of Effects of Grazing Angles



An example sonar image (A) of a 6-inch surrogate illustrates the similar acoustic backscatter intensity between the surrogates and the sediment. The acoustic shadow becomes the important identifier. (B) Diagram illustrating the effects of the grazing angles from the surface vessel sonar (steeper angle) versus the AUV sonar (shallower angle) on acoustic shadow length.

10.3.2 AUV Platform and Sensor Suite Performance

The primary tool for target location and identification in the in-field verification was the AUV platform, focusing on magnetometry and side-scan sonar. Both were tested and analyzed separately for the ability to accurately locate surrogates and provide information to estimate surrogate size. The selected magnetometer served as the primary instrument, as it is capable of detecting both surficial and buried targets. The study tested the ability of the magnetometer to detect buried surrogates, of depths up to 4 m through “simulated burial” missions. The sensor performance as analyzed by detection on an individual transect basis (i.e., the selection of individual targets per file versus averaging over the whole mission; see Appendix C, C.1) and target geolocation and size estimation (Appendix C, C.2) will be discussed in this section. Performance of the overall system and methodological approach are discussed in the following sections.

10.3.2.1 IVS Metrics

Navigational variation as calculated from the IVS never exceeded 2.5 m in radius, or well within the 5 m positional radius for targets stipulated by the study. There was no significant difference

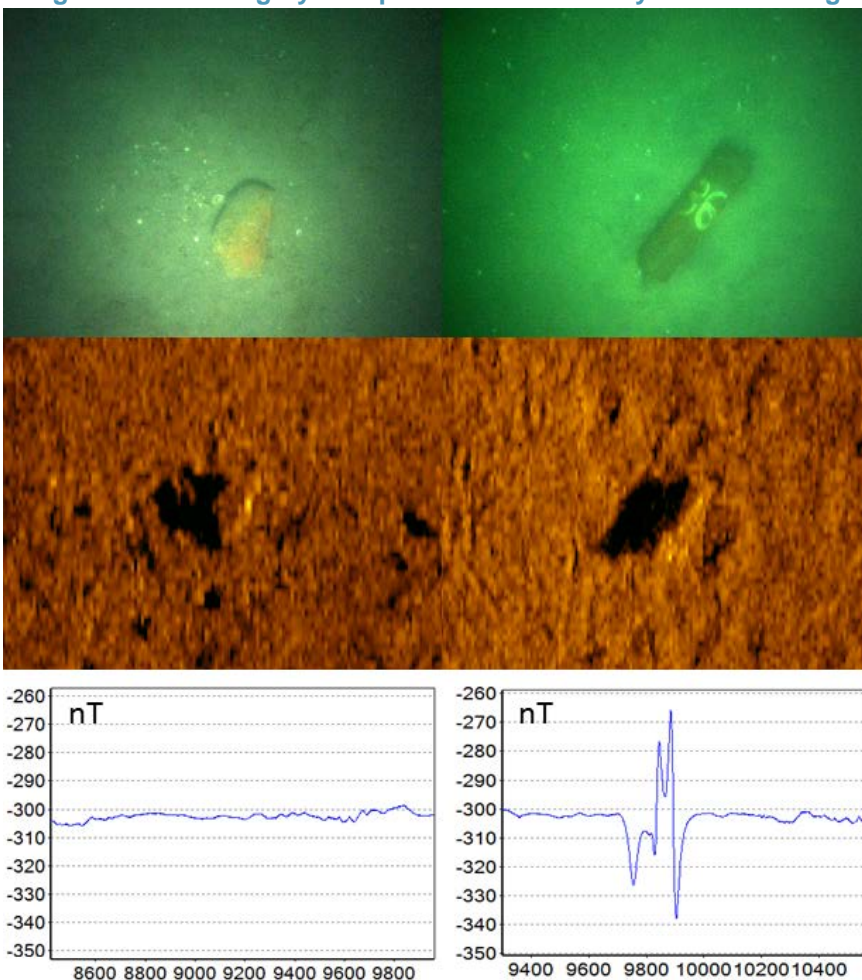
between positions recorded for surrogates oriented along-track or across-track, suggesting that scatter was attributable to vehicle navigational drift or positional uncertainties rather than uncertainties in determining absolute surrogate positions (i.e., reported target point by the detection team) within the side-scan data. Variation in magnetic signal across IVS missions is likely related to this same navigational drift: if the vehicle is running up to 2.5 m off the intended mission plan, then the magnetic signal would be expected to decrease as the cube of the distance, or on the order of 15x signal loss (for a 6-inch surrogate at 2 m altitude this is approximately a 100 nT signal drop). This variation in signal would be far greater than the noise inherent to the cesium magnetometer (<10 nT).

10.3.2.2 Magnetometer

The inclusion of the magnetometer in the sensor suite was to provide the ability to differentiate surficial targets, identified by the side-scan sonar, with ferrous signatures (i.e. surrogates) from those without (e.g., boulders, fish pots). Also, the system provides the ability to detect surrogates that were buried or obscured from detection by side-scan sonar. With regards to surficial targets, the magnetometer proved useful in conjunction with side-scan; several false-positive targets were identified in Node 1 by the detection team upon initial review of the side-scan sonar. However, when combining magnetics, the detection team determined that the Node 1 targets were not surrogates, and would be false positives if only relying on the sonar data. These targets were later identified as boulders in the AUV camera missions (Figure 10-11).

As a standalone detection sensor, the magnetometer did not prove effective. This is best illustrated by looking at target identification rate (see Appendix C), which analyzes how effective the detection team was at identifying targets from the data per transect. It must be noted that these rates consider that multiple targets may be identified for only one

Figure 10-11: Imagery Comparison of Previously Identified Targets

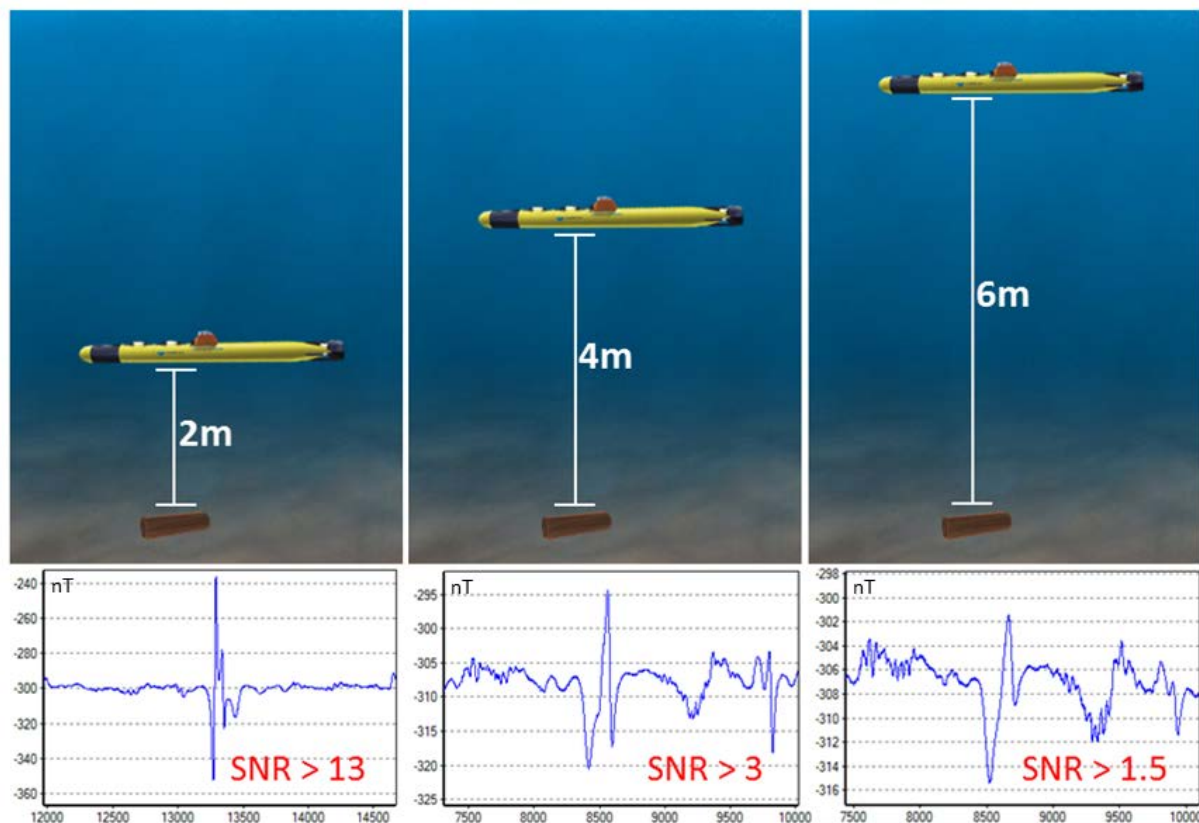


The geologic target (left) had only a side-scan signature associated with it, while the surrogate (right), had both a side-scan sonar and magnetic signature.

individual object on the seafloor should there be multiple instances of the object in the data (e.g. the same object seen in two separate transects). When looking at all node missions combined, the target identification rate was only 53.66% (Table C-1). In combined cable route missions, this number decreased to 26.47%. The range-limited nature of the magnetometer is likely the main contributor to this performance; the default line spacing (8 m) was likely too wide to effectively detect the smaller surrogates. The difference in the performance between node surveys and cable surveys reflects that node surveys were run in both North-South and East-West, while cable routes only East-West. This effectively doubled the coverage by the magnetometer in the node surveys, and thus doubled the detection rate versus cable route surveys.

Simulated burial missions were run at 4 and 6 m altitudes in Node 3 to simulate 2 and 4 m surrogate burial respectively. The detection performance for a standard 155 mm surrogate is shown in Figure 10-12. In standard 2 m altitude missions, the surrogate signal to noise ratio (SNR) was in excess of 13, thus serving as the baseline response. This response dropped appreciably in the 4 m altitude mission to a SNR above 3, but this is expected; the signal should drop as a cube of the distance. Despite this drop, the 155 mm surrogate was still clearly discernable in the data. At 6 m altitude, the signal was less detectable by amplitude, with signal amplitude only half again greater than the noise. However, the dipole signal characteristic of the surrogates was still clearly visible, and the target therefore detectable. This is reflected in the target identification rate by the detection team; there was no appreciable drop in overall target detection rate for the 4 and 6 m altitude missions (63.63% and 46.67%) versus the standard 2 m altitude missions (53.66%).

Figure 10-12: Magnetometry SNR Ratio for 6-inch Surrogate at Various Altitudes



The threshold for correctly positioned targets was selected by the study to be all targets within a 5 m radius of the known seed positions. Anything beyond that threshold would be counted as improperly positioned or a “bad target”, since such a reported position would make it difficult to relocate the actual surrogate. More targets picked by magnetometer in the node missions were on the whole more accurately positioned than the cable route (70.38% vs 37.5% within 5 m radius of known target) (see Appendix C C.2.1). Similar to the issue with target identification, error in target locations were more likely a factor of coverage than navigational error although navigational drift did contribute to the positional error (as discussed in Section 10.3.2.3). For the magnetometer, the data is reported as one data point in time and space, or more simply recorded as a signal at the position of the vehicle. Thus, a target picked would be placed at the point of the magnetometry detection, not the actual target location. This may be improved by interpolating the magnetometer to create a 3D grid, although interpolating coarsely spaced data may introduce additional errors.

The main contributing factor to variation in size estimation for the magnetometer is distance between the object and the sensor. If the surrogate was directly under the magnetometer (as with the IVS), the correct size estimation was more likely. If the surrogate was a few meters off the AUV transect, the size estimate would more likely be smaller than the actual target (due to the signal loss described above). This is supported in the data. Of the incorrectly categorized surrogates, 85.71% were categorized as smaller than the actual target in the node surveys, and 75% were categorized as smaller in the cable route surveys (Table C-3).

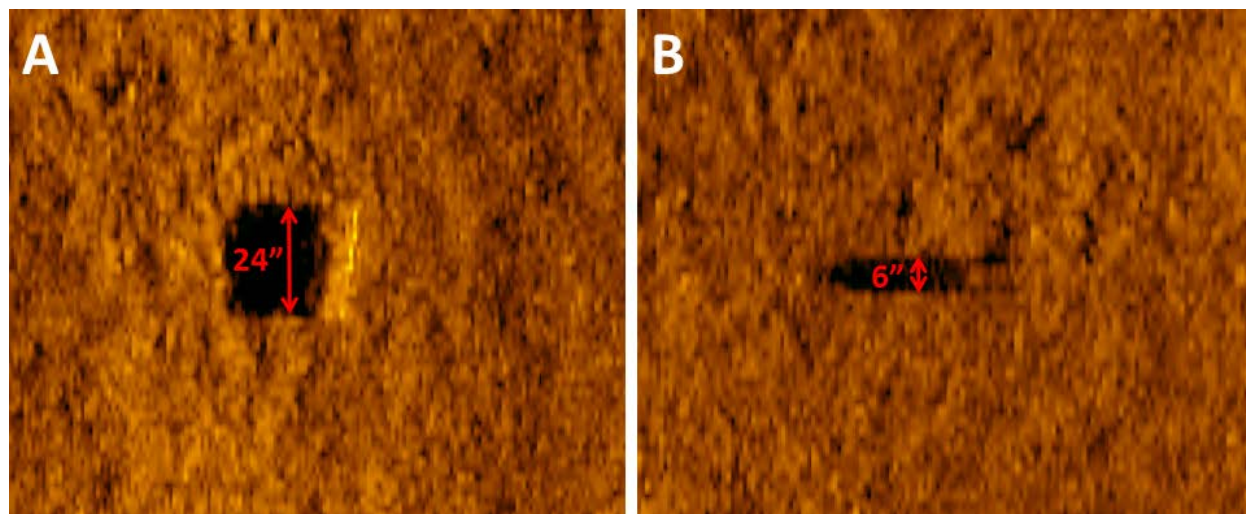
10.3.2.3 Side-scan Sonar

Side-scan sonar was more effective for target identification and size estimation. Node and cable route missions utilized the 1800 kHz side-scan sonar on the AUV, which could be gridded at resolutions of 10 cm or less. In theory, this would allow for the detection of objects smaller than the 2-inch surrogates used as the minimum ISO size in the in-field verification. However, as noted above, the acoustic signature of the surrogates was masked by the reflectivity of the seabed sediments. Thus, the main identifying characteristic became the acoustic shadow.

The acoustic shadows provided clear evidence for the presence of 6-inch or larger surrogates, as evidenced by the location of all 6-inch or larger surrogates in the study. However, smaller targets were less clearly identified, or went otherwise undetected. While the shallow grazing angle from the AUV side-scan improved detection by lengthening the acoustic shadow, the 4-inch and 2-inch surrogates were only slightly proud of the seabed, and therefore less distinctive from surrounding seabed clutter (e.g., boulders, cobbles, bedforms). Thus, detection of 4-inch or smaller targets was more variable.

Overall, side-scan sonar was more effective for target identification than magnetometry. In node missions, detection rate was 85.51% (Table C-2). As with magnetometry, detection dipped in cable routes to 56.34%, which is still better than overall magnetometer performance. Similar to the issue with magnetometry, the improved object detection in node missions versus cable route missions is due to the mission design; the cross-directional mission plans for the node surveys would negate issues with surrogate orientation. For instance, a surrogate located across-track (Figure 10-13A) may not have as distinctive acoustic shadow (being only as wide as the diameter of the object), as would a surrogate located along-track (full-length acoustic shadow; Figure 10-13B). Should a surrogate oriented across-track be encountered on a node mission and go undetected in one transect direction (e.g., East-West), it would appear along-track in the other transect direction (e.g., North-South) and thus be more detectable. Cable missions, composed only of East-West transects, would not have this advantage.

Figure 10-13: Effect of Orientation on Acoustic Shadow of 6-inch Surrogate



Comparison of acoustic shadows of a 6-inch Surrogate in Node 4 oriented across-track (A) and along-track (B).

Target location by side-scan was significantly better than in side-scan than the magnetometer due to the increased data coverage. In the node survey, 92.5% of the targets were within the 5 m

buffer, while in the cable route, 58.62% fell within the buffer (Table C-4). While this is a similar drop in performance as the target detection rates between node and cable routes, the decrease in positional accuracy in cable missions is less a factor of total coverage as it is due to the increase in navigational drift. AUV navigation is typically poorer in long straight transects as found in the cable routes than it is in short, “lawnmower” patterns as used in the node missions. In a straight line, the DVL INS has a nominal drift of 0.1% of the distance travel (on the order of 1 m per km traveled). This can be minimized by designing missions to have shorter transects with opposing directions (i.e. running east, then back west). While the cable route missions were only 1 km transects, this accumulated navigational error was greater than that of the node missions, resulting in the decrease in accuracy for target locations.

Target size estimation using side-scan data did not prove to be more accurate than with the magnetometer. Only 42.34% of surrogates were correctly identified in the node missions, while 47.06% were correctly identified in the cable route missions. The potential cause for this error in cable route missions may be relatable to the orientation of the target relative to the sonar. If aligned normal to or at an angle to the sonar, the object would likely present an acoustic shadow smaller than the actual object, and thus would be categorized incorrectly. This is evidenced by the 83.33% of targets in cable route missions identified as smaller than the actual target by the detection team. This, however, should not have been an issue in the node missions, where transects were run both North-South and East-West. While the rate of under-sized targets in node missions (54.69%) dropped relative to cable route missions, there was a corresponding rise in targets identified as larger than the actual surrogate (from 16.67% of targets in cable route missions to 45.31% of targets in node missions), rather than an increase in properly categorized targets. A potential explanation for the over estimates in size may be user input error; side-scan targets were manually measured in the digital data, which would be dependent upon the proper identification of the edges of the acoustic shadow. This error could also explain some targets that were categorized as smaller than the respective surrogates by the detection team.

10.3.3 Node and Cable Mission Methodology Performance

The in-field verification examined not only the performance of the selected platform, but also methods by which to maximize coverage while maintaining an acceptable threshold for MEC detection. The mission types, both node and cable route, were designed specifically for the University of Delaware’s AUV, although are applicable and adaptable to any platform using a similar sensor suite. The previous section examined the detection rates and size estimation of surrogates as a function of sensor type onboard the AUV, and in part, discussed the results in light of mission type. This section examines the total surrogates located (see Section 10.2.2) as a function of mission type, and the effect of varying mission spacing and altitude on overall performance.

10.3.3.1 Node Performance

Standard node missions were conducted at 2 m altitude with 8 m line spacing to maximize the coverage, but allow for detection of smaller surrogates by the magnetometer. This mission plan, from the standpoint of side-scan alone, succeeded in locating all 6-inch and larger targets. Using only the magnetometer, just 33.33% of 8-inch surrogates were found, and 53.33% of 6-inch surrogates. Variations in spacing and altitude were then tested to see the influence on detection by magnetometer.

Node 3, which was confirmed by the detection team initially to contain surrogates, became the test site. With magnetometer detections in the standard Node 3 mission, the single 8-inch surrogate was located, but only one of five 6-inch surrogates, two of four 4-inch surrogates and neither of the 2-inch surrogates were located. These results serve as the baseline. When decreasing the mission spacing from 8 to 4 m, while maintaining a 2 m altitude, the magnetometer performance improves: an additional 6-inch and 4-inch surrogate are located. Increasing the altitude to 4 m, but maintaining the 8 m line spacing yielded similar results, although both 2-inch surrogates were also located. At 4 m altitude with 4 m spacing, three of five 6-inch surrogates were located, but only two of four 4-inch and no 2-inch surrogates. This pattern is repeated with 6 m altitude mission, where three of five 6-inch surrogates were located, but with no 4-inch surrogates located either.

With side-scan, the all 8-inch and 6-inch surrogates were located by side-scan. Two of four 4-inch surrogates and both 2-inch surrogates were located. Variations in missions spacing and altitude did not improve the base performance in most tests, and in the cases of 4 m altitude/4 m spacing and 6 m altitude, resulted in only four of five 6-inch surrogates located. This likely reflects the change from the standard 8 m spaced mission plans from running both North-South and East-West transects to just North-South transects with the 4-m spaced mission. On the other hand, the 4 m altitude, 8 m spaced mission did result in all but one 4-inch surrogate located.

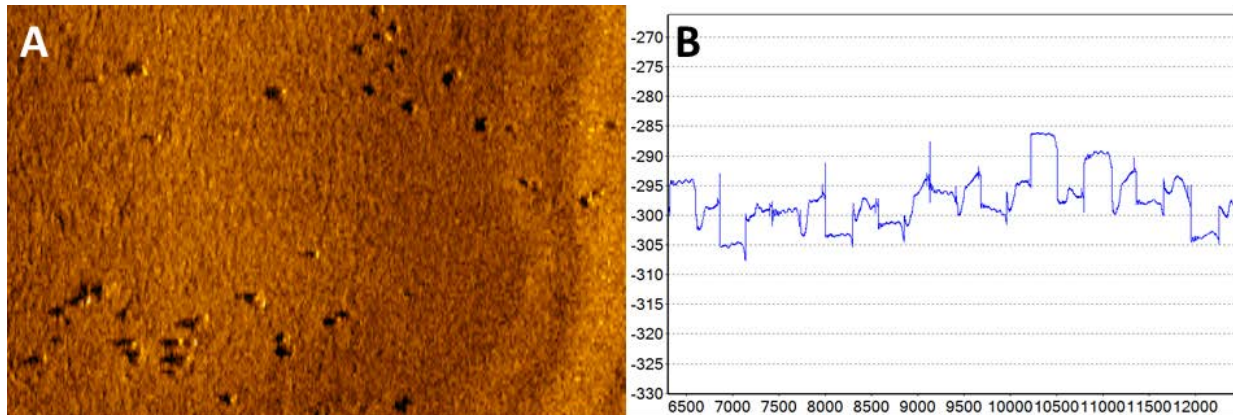
Combined, both magnetometer and side-scan detected the most surrogates in Node 3 with 4 m altitude and 8 m spacing, although the results may not be significantly improved over the standard mission plan; only one more 4-inch surrogate was located in the side-scan, which had already been located with the magnetometer, and the additional 2-inch surrogates located with the magnetometer were already located in the side-scan. Also taking into account buried MEC, increasing the mission altitude to 4 m would make detecting MEC buried 2 m below the surface (and thus 6 m from the sensor) more difficult: no 4-inch or 2-inch surrogates were located in the 6 m altitude mission with magnetometer. If the threshold of detection by size is 155 mm artillery projectile (6-inch surrogate), the 4 m altitude is acceptable, although 2 m altitude may allow for more confidence in the detection of buried 155 mm shells. Accurate sizing and detection rates were highest with 2 m altitude and 4 m spacing; tighter spacing allowed for better characterization by magnetometer although the side-scan sonar run at 4 m spacing did detect one fewer 6-inch surrogate. Further combined metrics are discussed in Appendixes C and D.

10.3.3.2 Cable Route Performance

All cable route missions were conducted with 2 m altitude and 8 m line spacing, with 1 km long transects. With the side-scan sonar, all 6-inch or larger surrogates were located, while five of ten 4-inch surrogates and no 2-inch surrogates were found. With the magnetometer, all 8-inch surrogates were located, but only three of eleven 6-inch surrogates, two 4-inch surrogates and no 2-inch surrogates were located. The relatively poor performance of the magnetometer in cable routes versus node-routes likely reflects the issue of navigation and coverage discussed in Section 10.3.2; missions were only run with East-West transects and long transects increase navigational drift. However, the selection of 1 km long lines versus running the entire length of the 5 km long cable route was intended to minimize navigation drift without sacrificing coverage. Adding crossing transects orthogonal to the primary line direction (e.g. adding North-South transects) may increase detection.

Increased false positives on the cable route, particularly Cable Route 5, can be linked to two causes, one regarding side-scan sonar and one magnetometry. Regarding the first, on the western edge of the cable route, a number of surrogate size features appeared in the sonar. The exact nature of these targets was never discovered, although these may be either biological or geological in nature (Figure 10-14A). Secondly, in the initial transect or two (survey lines) of the Cable Route 5 mission, the AUV had difficulty maintaining altitude. This resulted in the vehicle oscillating in altitude and increased noise in the magnetometer data. A number of false magnetometer targets occurred on these transects (Figure 10-14B), suggesting a probable link.

Figure 10-14: Examples of Data that could Result in False-positive Identifications



(A) Example of geological or biological targets in the Cable 5 mission survey. (B) False targets in magnetometer caused by oscillations in AUV altitude.

10.3.4 Multi-Platform Methodology Assessment

A multi-platform approach was selected to maximize the efficiency and effectiveness of MEC detection and identification. The approach was a combination of a wide area assessment using a hull-mounted, phase-measuring bathymetric and side-scan sonar and autonomous underwater vehicle with high-resolution side-scan sonar, magnetometer, and camera. A wide area assessment should characterize the physical conditions at site and potentially detect some surficial targets for further inspection by AUV. Coverage rate is maximized, and cost potentially minimized, by conducting a wide area assessment, although resolution may be limited and target detection and identification less effective. Conversely, more focused surveys using an AUV should maximize detection and proper MEC identification, although coverage is limited by the range of the vehicle and sensors onboard. Thus, the combination of the two platforms should, ideally, emphasize the strengths of both approaches in a manner that would maximize efficiency and minimize costs, while overcoming limitations that would otherwise be a factor when used separately.

The entire wide area assessment in the in-field verification was conducted within 6 hours, encompassing the 5 km cable route and 2 by 2 km box. Bathymetry and dual-frequency sonar was collected simultaneously. The data provided information for sediment classification, seafloor topography, and potential obstructions to AUV missions. As discussed in Section 10.3.1, no targets were directly located from the wide area assessment, although in other locations with different sediments, positive target detection may be possible. The survey was conducted at 7 knots, with 100% bathymetric coverage and 200% side-scan coverage. The coverage rate was effectively 1.6 km² per hour with 125 m swath width and less than 0.5 m

resolution. This rate does not account for stops conducted to collect the sound velocity profiles necessary to process bathymetric sonar, which could be nullified through the use of a moving velocity profiler. Given an 8-hour survey window, over 14 km² could potentially be surveyed. The coverage rate and area could be doubled if only 100% side-scan coverage was required.

AUV coverage rates were more limited, but the purpose of the AUV was to maximize target detection and identification, not conduct a wide area assessment. This is achievable by much higher resolution data gathered with precision using an autonomous platform. Each AUV deployment during the in-field verification spanned up to 3 hours, covered up to 16.5 linear km, and consisted of one or more discrete missions (with a mission defined as one individual node or cable route section). However, this included the collection of range-limited sensors, including 1800 kHz side-scan sonar (swath width 20 m) and magnetometry (effective range of 10 m or less), with high-resolution or high sampling rates (<10 cm with side-scan sonar and 10 hertz sampling with magnetometer). Given these parameters, coverage rates for the AUV 1800 kHz sonar would be 0.108 km² per hour, while magnetometry coverage rate would be at most 0.05 km² per hour.

In terms of effectiveness, approximately half of the threshold targets (6-inch) were located by magnetometer, and all were located by side-scan sonar.

The estimated time to cover all five 40 by 40 m nodes and all five 1 km by 0.05 km cable route sections was 183 minutes and 525 minutes respectively, excluding preparation and launch time for the AUV (approximately 45 minutes per battery change). Although each node mission was conducted individually, this would require the equivalent of one AUV deployment to survey five 40 by 40 m nodes and three AUV deployments to survey five 1 by 0.05 km sections of cable route.

For better detection by magnetometer, line spacing would need to decrease from 8 to 4 m, effectively halving the coverage rate of the AUV. This in turn would double the time, and thus double the cost, to conduct surveying over the in-field verification site, and effectively it would require two 3-hour AUV deployments to survey five to six 40 m by 40 m nodes and five 3.5 hour AUV deployments to cover a 5 by 0.05 km cable route. Accounting for preparation time with vehicle, effectively all node missions would take one eight-hour day, and all cable route missions three seven-hour days.

10.4 Conclusions and Recommendations

The goal of this research effort is to investigate technologies and methods for MEC detection, through historical research, geophysical site characterization, technological review, and an in-field verification effort. The purpose of the in-field verification was to demonstrate the technologies and methods selected by the review process, and utilize the results to optimize MEC detection. The data quality objectives for this project focus on goals directly related to the in-field verification process. Each data quality objective is addressed in the following section. Conclusions are drawn from the in-field verification, and recommendations offered to assist in developing MEC detection studies.

10.4.1 Environmental Interference and Compensation

Environmental sources of error in magnetics (i.e., diurnal variation) were accounted for in post processing. Due to the location of the site offshore, diurnal variation could not be measured locally, but rather, was compensated for by using a regional U.S. Geological Survey base station.

The location of the base station was over 240 km from the field site, but provided acceptable data for diurnal correction. This process could further be optimized by providing a more local base station, placed at the closest possible terrestrial site and therefore more sensitive to minor local variations that were not captured in the regional data set used this study.

In situ environmental interference for the AUV were accounted for in the wide area assessment. Any impediment to AUV missions could be identified from the surface vessel survey. Smaller, more local sources of noise were noted in the sonar from the AUV during mission data review. These include man-made objects that were not ISOs placed by the study, such as fishing gear, which can influence magnetics.

The use of an IVS was instituted to monitor and potentially compensate sensor drift, particularly in the magnetometer. Differences in magnetic response over the course of the in-field verification are attributable to navigational drift more so than sensor drift, as addressed in Section 10.3.2.1. The IVS was designed with two ISOs for each anticipated MEC at the site, oriented in along and across-track. The bi-directional alignment accounts for the potential influence of MEC orientation relative to the sensor on the signal. This proved useful in characterizing the potential magnetic signature of ISO's in the study.

The spacing of each ISO, at 6 m apart, was not ideal. The signal for the larger ISOs partially masked the signal from the smaller ISOs in the immediate vicinity. The design of the ISO could be updated to account for variation in signal amplitude with various sized objects.

Further, the IVS utilized in this study was an adaptation of IVS design utilized in terrestrial efforts. The complication inherent to marine surveying limit the ability of any platform to precisely survey the IVS with the degree necessary to limit variation in IVS signal to only that caused by sensor drift, and not those caused by navigational drift. Future marine IVS design should account for and incorporate a design to minimize signal variation caused by navigational drift. To optimize the process, experimenting with IVS design on land prior to deployment is recommended.

10.4.2 Distinguishing ISOs

The utilization of multiple platforms with multiple sensors in the in-field verification was to provide as much data as possible to detect and confirm the identity of ISOs and minimize false-positive detections. The wide area assessment missions were designed to ensure at least 100% bathymetric coverage of the survey area. Since the PMBS bathymetric coverage is approximately 50% of the side scan sonar coverage, the side scan sonar coverage while achieving 100% bathymetric coverage was about 200%. The magnetometer coverage at the necessary resolution was less than that of the side scan sonar and the AUV missions designed to ensure adequate coverage with the magnetometer, achieved a greater than 200% coverage with the AUV side-scan sonar. Further, standard node missions were designed to provide two separate orientations (e.g., North-South and East-West) to provide an additional viewing angle to further distinguish between ISO and environmental noise. The inclusion of a high-resolution sonar with the magnetometer provided an important source for not only surficial ISO detection, but also identification of false targets. The use of optical surveying provided further confirmation regarding surficial targets of questionable nature. To distinguish ISOs then, it is optimal to design surveys to maximize overlap and coverage by multiple sensors, particularly the inclusion of sensors that account for the limitations of magnetometry.

10.4.3 Evaluating ISO Identification

The focus of the in-field verification was to detect both surficial objects, and those which may have become buried by physical and geological processes subsequent to their deposition. Further, the study examined the ability to identify the type of target that may not otherwise be visible in optical surveys. The magnetometer was included to satisfy this objective. Magnetic signal is proportional to amount of magnetic material in an object, given a fixed distance between the object and sensor. Thus, both surficial and buried objects should be identifiable by their magnetic signature with careful control of sensor positioning, although surficial targets may also be identifiable through sonar signature.

Surficial ISO target detection was largely more successful in side-scan sonar; all 6-inch or larger surrogates were located by side-scan using the methods employed by this study. These results may be interpreted to emphasize the strength of sonar for target detection, but more so the consequences of mission design on optimizing detection by magnetometry.

The standard transect spacing (8 m) used in this study was not optimal for 6-inch ISO detection by magnetometer. Tighter transect spacing would likely prove more successful, as indicated by the results for the variable line spacing experimentation (Section 10.2.4). However, the optimal line spacing for this study may not be applicable to others. Should larger munitions be selected as the targets of interest, 8 m or wider transect spacing would likely be sufficient to permit their detection. To optimize detection by magnetometry, it is necessary to initially experiment with line spacing prior to conducting production surveys. This may be experimented over a seeded patch or an IVS.

Target size estimation by sonar was not always more successful than magnetometry. Confusion over the identity of a surrogate was attributed to the signature of surrogates at normal or oblique orientations to the sonar. This emphasizes the use of multiple transect directions (e.g. both North-South and East-West) to minimize the potential for improper identification, especially addressing the potential to identify a larger MEC as something smaller. Since magnetics will be less susceptible to the influence of orientation on signal (overall amplitude should not change by orientation, although the dipole signature may be less apparent when the target is aligned normal to the sensor) and can distinguish between ferrous and non-ferrous targets, magnetics should be used to inform and confirm the nature and identity of a target detected by sonar.

ISO burial was simulated by running AUV mission altitudes at 2 and 4 m above standard mission altitudes (i.e., simulated burial missions were run at 4 and 6 m altitude) for the selected AUV. This simulated 2 and 4 m burial. Analysis, based on a small data set, determined that the threshold target size (155 mm) was detected 50% of the time by the selected system at burial depths up to 4 m with 8 m line spacing. Alternatively, 155 mm or larger surrogates could be detectable when buried up to 2 m if missions were conducted at 4 m altitudes with 8 m line spacing. However, the latter is not recommended; the SNR was not ideal to ensure detection unless the target is located directly beneath the sensor. Prior to use of a given sensor, it is recommended to experiment with and characterize the effects of altitude, and thus burial, on the detectability of the minimum size target MEC. These may be conducted over a seeded area or IVS. Further it is recommended to run IVS surveys not only at the standard mission altitude, but to periodically conduct IVS surveys at higher altitudes to simulate burial for the identification of buried MEC in production surveys. Again, survey spacing and multiple transect orientations should be experimented with to optimize the process for buried targets.

10.4.4 ISO Detectable Range

The detectable range for ISOs was experimented with by varying the spacing and altitude of the missions conducted over a seeded area. The results of the production surveys in the in-field verification using preselected mission transect spacing and orientation, and altitude suggest that this process is necessary to optimize detection. The experimental missions were not conducted prior to the start of production missions, nor were subsequent production missions altered based on the preliminary results of the experimental missions. Future studies should perform such experiments prior to conducting MEC detection surveys to optimize detection by the selected sensors and platforms.

The final results of the in-field verification indicate that the selected mission transect spacing (8 m) was not adequate to detect the threshold surrogate size with the magnetometer over horizontal distances. Rather, reducing that spacing to one-half of the selected transect spacing would have improved detection rates. Further, designing missions with only one transect orientation had a negative effect on detection, and that missions conducted with two transect orientations (e.g., North-South and East-West) would improve detection further. On the other hand, the results from the simulated burial missions suggest that the selected mission altitude (2 m) was more than adequate to detect the 6-inch surrogates buried at 2 m or deeper vertically. Again, the vertical detection threshold may be optimized through field experimentation of a seeded area or over an IVS, and will be determined by the minimum size MEC set as the threshold for detection. The minimum size MEC of concern is established through the MEC risk assessment.

10.4.5 Cost and Coverage Rate

The effective coverage rates of the platforms and sensors selected were discussed in detail in Section 10.3.4. The results for the in-field verification indicate that the chosen area could effectively be surveyed within 5 days with the selected technology (assuming 8-hour work days), including the wide area assessment over the 2 by 2 km box, five monopile nodes, and a 5 km cable route, should a reduction in transect spacing be implemented as recommended to improve magnetometer results. Mobilization for the study included 0.5 days to prepare the survey vessel and PMBS sonar, while the AUV preparation took one day of mobilization and testing. This does not account for any maintenance or testing in the preceding months prior to the in-field verification.

Based on the daily rate for the University of Delaware survey vessel *R/V Daiber*, PMBS sonar, AUV, and personnel time, daily rates were estimated at \$10,000. Broken down into cost per unit area, the estimated rate for the wide area assessment is \$336 per square km, assuming up to 14 square km per day. The AUV coverage rate could be estimated in linear km cover, which is estimated at \$279 per linear km, given two missions per day. The development, placement, and preliminary surveying of the IVS took two days (not including sourcing materials), with the IVS costing approximately \$500 for materials and labor. All cost estimates should also be considered in terms of data collected, since multiple sensors were collecting data simultaneously.

11.0 Post-Storm Season Assessment

11.1 Introduction

11.1.1 Background

Interest in the mobility of MEC in the underwater environment led to a follow on task to investigate the position and burial of the surrogates deposited for the BOEM In-Field Testing and Methodology Verification (Section 9.0). Previous mine burial studies (Traykovski, Richardson, et al. 2007, Trembanis, et al. 2007) and ongoing DoD MEC mobility studies (Calantoni 2017, Traykovski, Continuous Monitoring of Mobility, Burial and Re-Exposure of Underwater Munitions in Energetic Near-Shore Environments, MR-2319 2017, Puleo 2017) have and continue to examine MEC mobility under increasing energetic events (i.e., storm generated waves and currents). These studies observed, scour, burial, and in specific instances, mobility (Calantoni 2017), depending on object size and density, local sediment type, and the duration and magnitude of near-bed currents. In the months following the July 2016 in-field verification, during the hurricane and Nor'easter storm season, multiple instances of significant wave events (defined here as the potential to generate mass sediment transport) occurred in the vicinity of the study area (see Section 11.1.2). Given that positions of the surrogates at completion of the July 2016 field effort are known, an additional field effort was undertaken to reacquire the surrogates and determine whether: a) the surrogates became mobile during energetic conditions, b) the surrogates underwent *in situ* scour and burial during energetic conditions, or c) no mobility or burial occurred. Additionally, the follow up study incorporates and evaluates recommendations resulting from the 2016 field effort (Section 10.4).

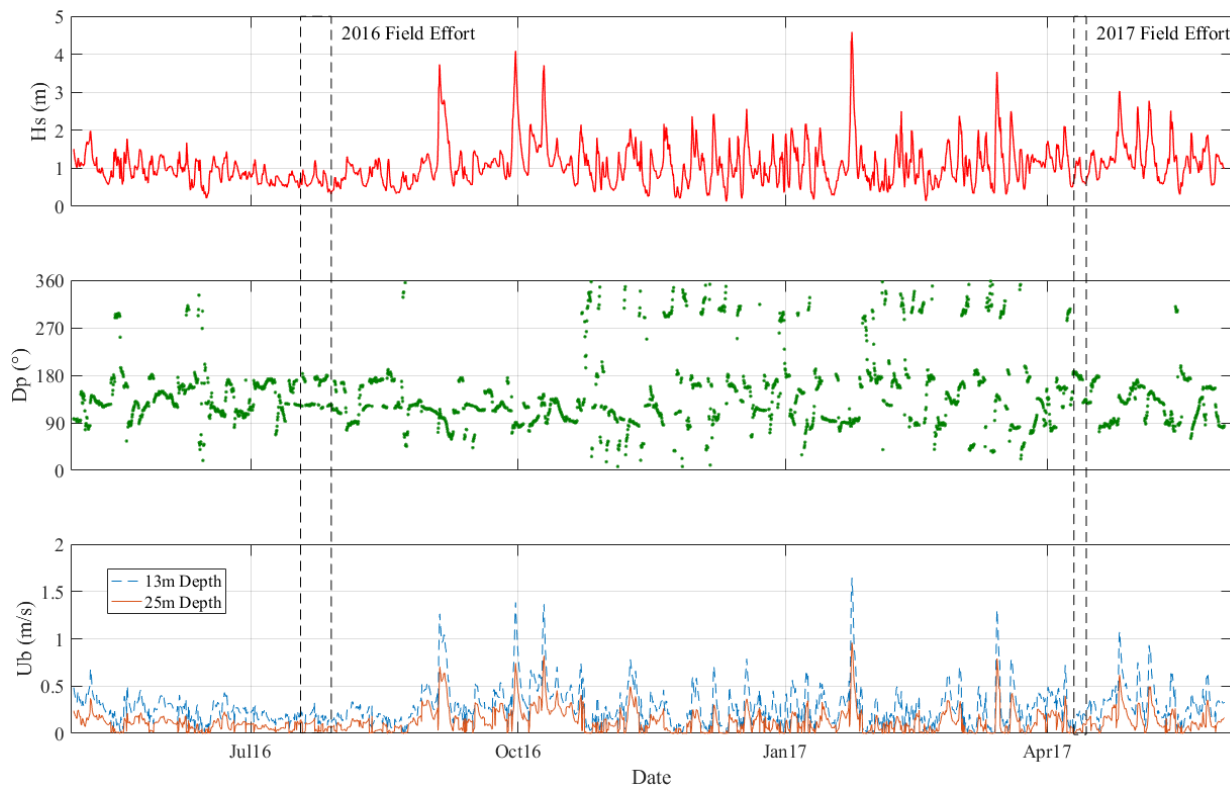
The field effort incorporated another wide area assessment (WAA) of the entire field area, which consisted of a 2 x 2 km box and 5 x 0.05 km cable route, to establish whether large scale alteration to seabed morphology occurred (Section 11.2.1). Surveying utilized the same vessel-mounted dual frequency 230/550 kHz Edgetech 6205 phase measuring bathymetric and side-scan sonar mounted to the same vessel, the *R/V Daiber*, utilized by the 2016 field effort. Subsequently, targeted AUV missions were conducted over selected areas previously containing surrogate munitions. These missions utilized the same AUV and magnetometer deployed in the 2016 missions, incorporating improvements to the mission design based on findings from the 2016 field effort (Section 10.4). The mission sites were prioritized based on conditions representative of the different sediment types, bathymetric slope and depth, and surrogates present throughout the field area. An IVS, modified based on recommendations developed from the 2016 field effort (Section 10.4.1), was placed on site and mapped with the AUV daily.

11.1.2 Hydrodynamic Record

The interim period between the final 2016 field effort and the beginning of the 2017 field effort spanned 255 days. No direct instrumentation was present on the site to record hydrodynamic conditions, but as suggested in Section 2.0, regional wave climate is recorded at NOAA Buoy 44009, which lies approximately 28 km south of the study site and at a similar distance from shore (30.5 kilometers). In DuVal et al. (2016), measurements from Buoy 44009 were found to have a strong correlation to hydrodynamic conditions measured *in situ* at Site 11 (Redbird Artificial Reef), which lies only 3 km SW of the current study area. However, during the duration of the interim period between the 2016 and 2017 field effort, Buoy 44009 was down for maintenance, leaving no equivalent buoy record within 120 km of the study area. A similar

incident occurred during the course of the study conducted by DuVal et al., (2016). To fill in the data gap, DuVal et al., used hindcasting data from the NOAA WaveWatch III. Using the most local data node, the authors found a strong correlation ($r^2 = 0.95$) to *in situ* data when correcting the data with a linear transform. Based on these results, this current study performed the same linear transform to local WaveWatch III hindcast data for the duration of the interim period to fill in the data gap for the local hydrodynamic record. The record is shown in Figure 11-1.

Figure 11-1: Hydrodynamic Record for BOEM Study Area Derived from NOAA WaveWatch III



The estimates show significant wave height (Hs), dominant wave direction (Dp), and near-bed wave orbital velocity (Ub).

The WaveWatch III record indicates five events in which the significant wave height (Hs) topped 3 m (with one topping 4 m), each with wave orbital velocities in excess of 0.5 m/second in the deepest part of the study area. The events were, by comparative standards, not large events, but had enough energy to initiate sediment transport at the site (see Section 11.3.1), indicating the potential for surrogate scour, burial, or mobility to occur. The 2016 and 2017 field efforts are outlined for comparison, where minimal wave energy was observed. Subsequent sediment mobility and bedform predictions used in this section are based on this WaveWatch III record.

11.2 Field Effort

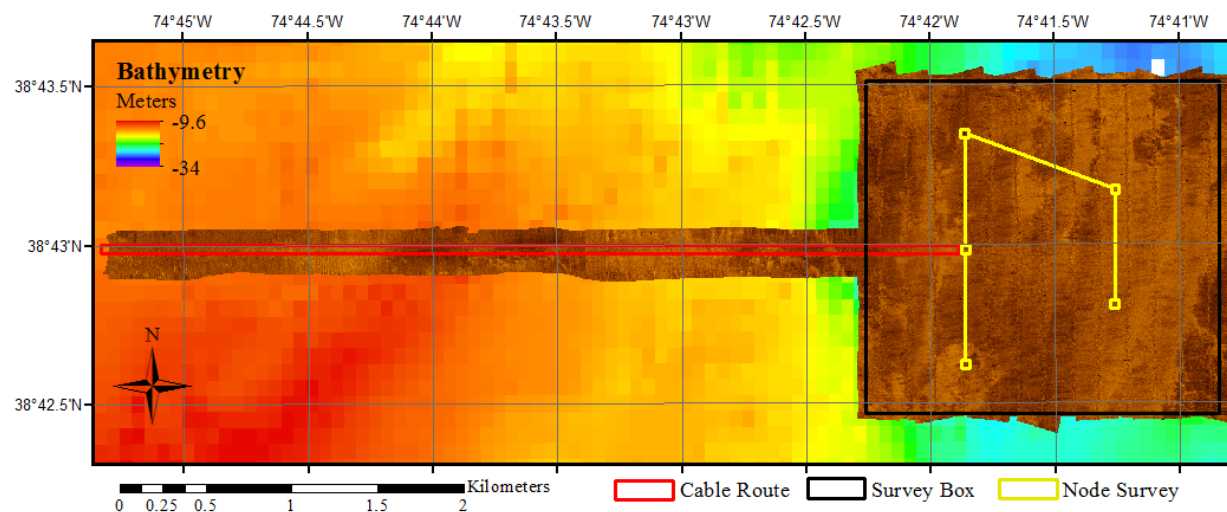
The field effort for the follow on study took place from April 10-14, 2017. The daily operations are outlined in the Post-Trip report (see Appendix E). Many of the daily field efforts were conducted using the same technology and methods described in Section 9.0. Deviations from the methods described in Section 9.0 are discussed in the subsections below. In regards to the technology used, it should be noted that the battery modules used on the AUV during the 2016 operations were being serviced during the period that the 2017 field effort took place, requiring

the use of replacement batteries. This necessitated calibration missions to account for differences in vehicle noise in the magnetometer data. The calibration missions were conducted in the Delaware Bay on April 11, 2017. The missions consisted of a 100 x 100 m box route conducted in the water column and away from potential environmental noise (e.g., ferrous debris on the seabed). Two batteries were calibrated, both with SNR improvement > 5 (a SNR > 4 is recommended by the manufacturer, M. Tchernychev personal communication).

11.2.1 WAA

The WAA was conducted on April 10, 2017 using the Edgetech 6205 PMBS. While the previous WAA was conducted with 100% overlap in bathymetry and 200% overlap in side-scan in the 2016 missions, the 2017 mission lines were spaced wider to allow for, at minimum, 100% bathymetric coverage and 100% overlap in side-scan sonar, or half of the overlap of the 2016 mission. This allowed for less surveying time while still obtaining greater than 100% side-scan sonar coverage, and thus provided more realistic coverage rates expected for commercial WAA. The results from the WAA are shown in Figure 11-2. A comparative analysis to the sediment distribution of the 2016 dataset is discussed in Section 11.3.2. As determined in Section 10.0, the WAA was unable to detect any surrogates, but provided necessary bathymetric and sediment morphological characterization for the site.

Figure 11-2: WAA conducted on April 10, 2017



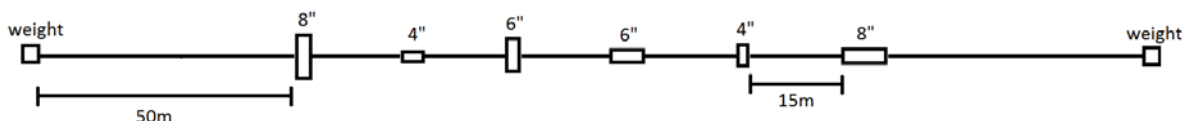
Sonar mosaic is gridded at 0.5 m. Brighter pixels indicate higher acoustic reflectivity.

11.2.2 IVS

The IVS used during the 2016 field effort was the first iteration based on recommendations for establishing an IVS in terrestrial settings (Environmental Security Technology Certification Program 2015b, 2009). As anticipated, the design was experimental for application underwater and the results from the 2016 field effort led to a number of recommendations to improve IVS design and mission plans (Section 10.4). In response to these recommendations, the IVS for the 2017 mission was redesigned (Figure 11-3). First, the spacing between the IVS surrogates was increased from 6 to 15 m, in order to reduce the potential for signal overlap, which masked the signal of individual surrogates in the 2016 IVS missions. Additionally, the order of the surrogate types was modified, placing the largest surrogates on opposite sides of the strip, further decreasing the likelihood of overlap between the largest objects. This also facilitated launch and

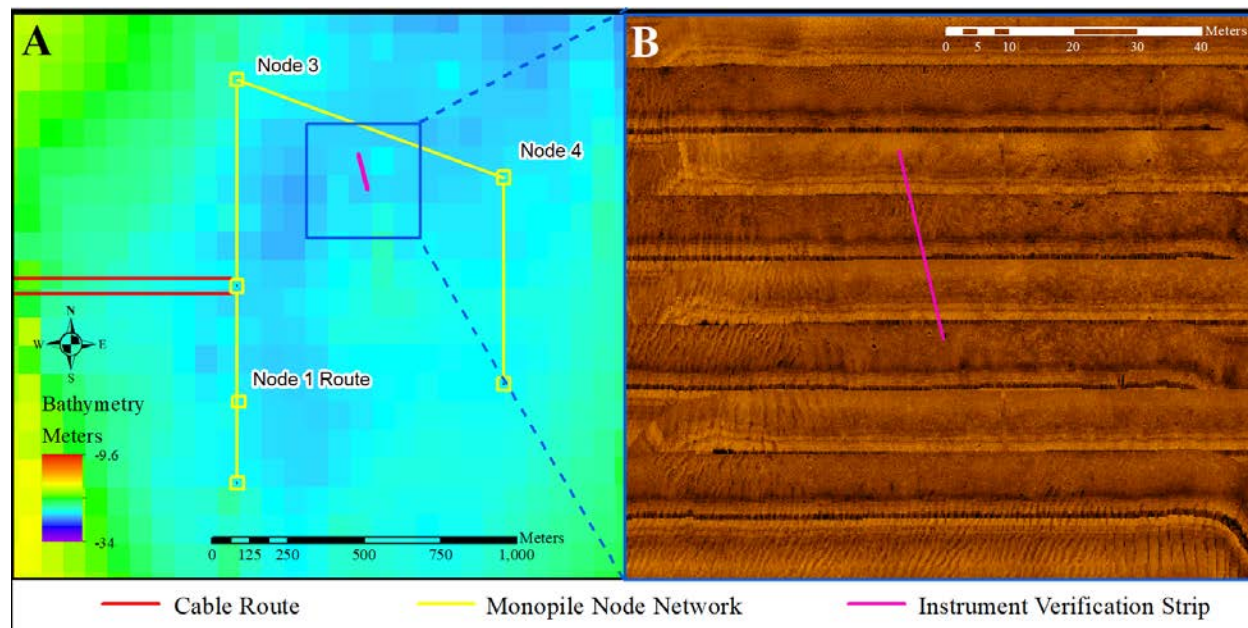
recovery; instead of having the two heaviest objects on one end of the strip, which significantly complicated launch and recovery of the IVS in the 2016 mission, the order of objects from heaviest (8-inch), to lightest (4-inch), to the medium weight (6-inch), and reverse, more evenly distributed the weight, making the IVS deployment more manageable. As well, the spacing of the ground line weights (on either end of the strip) was increased to 50 m, or double the water depth at the site, to ensure that no weight was hanging in the water column when the first surrogates were lowered. Lastly, the surrogates themselves were detachable, unlike the previous design, which allowed for the surrogates to be removed upon retrieval and the ground line fed through block and tackle, much like fishing gear. Surface markers on polypropylene line ran up from the ground weights to facilitate reacquisition and retrieval of the IVS.

Figure 11-3: Redesigned IVS



The IVS deployment occurred on April 10, 2017 after completion of the WAA. The intended placement for the IVS was in the middle of the WAA, to allow for reduced transit time between the IVS and the three node mission sites (Node 1 Route, Node 3, and Node 4). However, after deployment the IVS was closer to Nodes 3 and 4 (Figure 11-4A). Reacquisition by the AUV on April 12, 2017 determined that the IVS lay primarily in a pocket of coarse sediment without bedforms, surrounded by coarse sediment ripple bedforms fields (Figure 11-4B).

Figure 11-4: Location of 2017 IVS and Morphological Setting

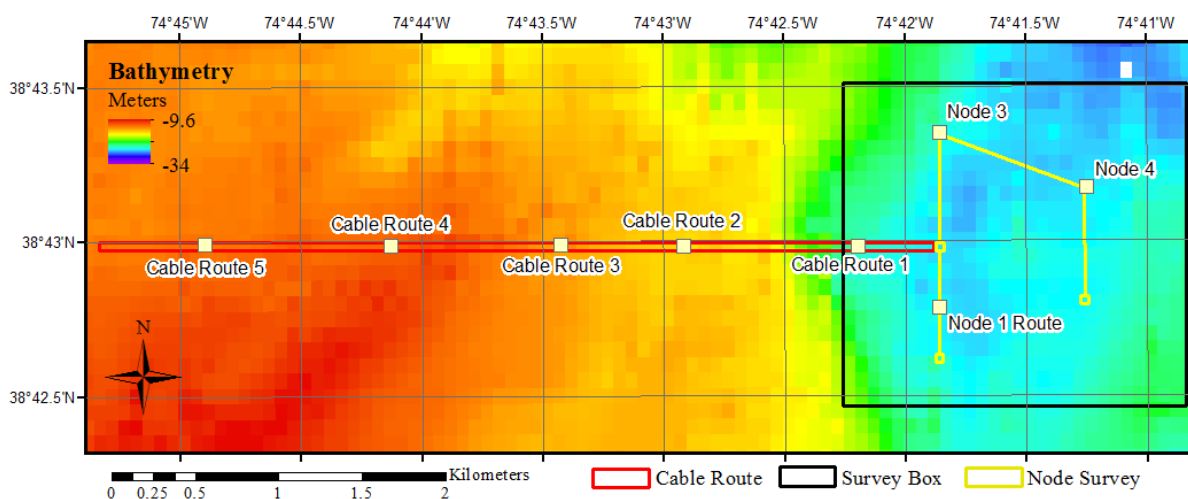


11.2.3 AUV Missions

AUV side-scan sonar and magnetometer missions for the follow up study were conducted over selected areas (Node 1 Route, Node 3, and Node 4, as well as Cable Routes 1, 2 and 5) where surrogate munitions were placed in July 2016. These sites were prioritized to include different sediment types, bathymetric slope and depth, and surrogates present throughout the field area.

Instead of re-conducting the entire cable route missions from the 2016 field effort, the missions were focused only over the areas where surrogates were placed in 2016 (Figure 11-5). All missions were initially designed to conduct the same survey route: the AUV would run a 2 m altitude mission with 4 m spaced transects over the 40 x 40 m area over which the surrogates were initially deployed (see Section 9.0). The transect lines would run both N-S and E-W, as suggested by the recommendation from the 2016 field effort (see Section 10.4). After this, an area 24 m beyond the 40 x 40 m box would be surveyed in case surrogate mobility occurred.

Figure 11-5: Overview of BOEM In-field Verification 2016 Study Site and Surrogate Locations



AUV missions were conducted April 12-14, 2017, starting with Nodes 3 and 4. After preliminary magnetometer analysis, it was determined that no surrogates moved beyond the 40 x 40 m box in which the surrogates were initially placed for either Nodes 3 or 4. While Node 1 Route was conducted as planned, all cable route missions were then altered to conduct only the 40 x 40 m box with N-S and E-W lines in order to reduce overall mission time (mission reduction was an hour for each area) and allow for additional mission testing. After the completion of the target area missions, two additional missions were conducted. The first was a 6 m altitude mission over Node 3, to determine whether 6-inch surrogates could still be detected if buried at the site despite higher altitude (as requested by BOEM). The second mission was a camera mission over Node 3 to ground-truth bedforms and confirm whether scour and burial occurred as it appeared in preliminary data analysis. The camera, however, did not perform properly and no photographs were taken due to a network fault that is now being addressed by the AUV manufacturer. The field effort concluded with the recovery of the IVS following the camera mission on April 14, 2017.

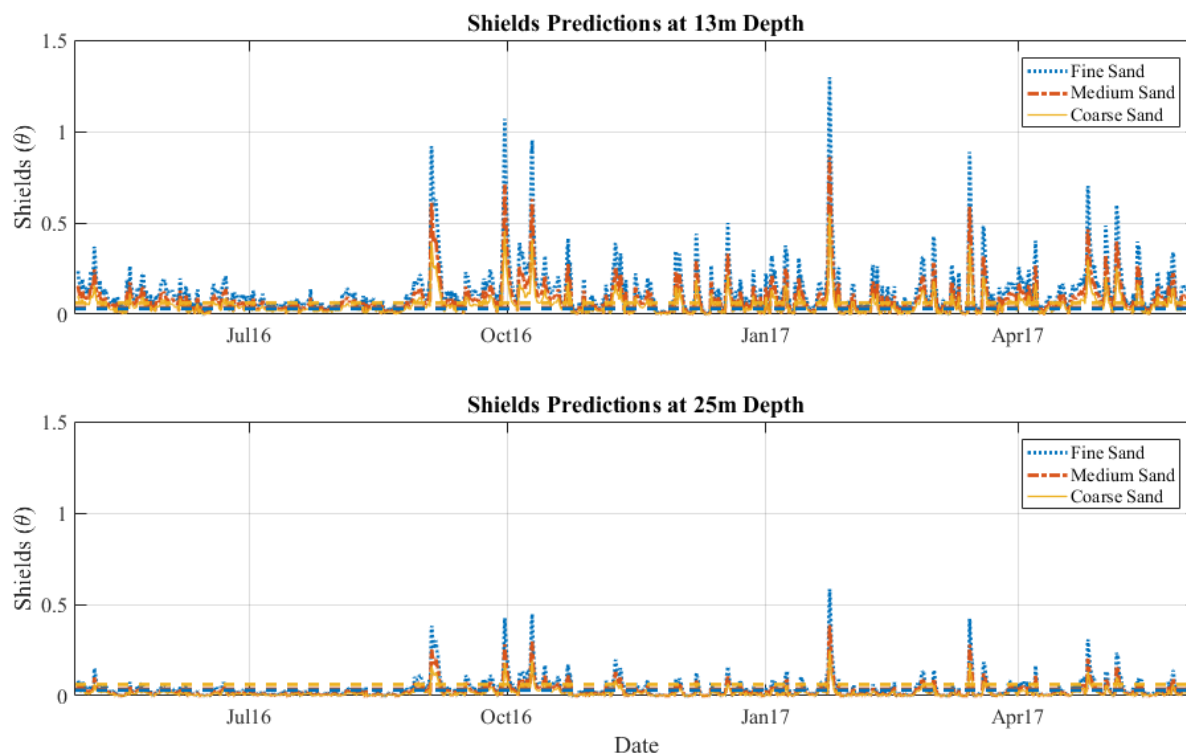
11.3 Results

Raw sonar and magnetometer data were processed using the same methods discussed in Section 10.1. Particular focus was given to comparisons between 2016 and 2017 data sets. This includes comparison of sediment distribution, surface morphology, and target locations. AUV navigational precision was monitored through repetitive IVS missions, to ensure any apparent mobility in surrogates in the 2017 data was not due to navigational error. All hydrodynamic data and derived morphological predictions are based on NOAA WaveWatch III data discussed in Section 11.1.2.

11.3.1 Hydrodynamics and Projected Sediment Transport

While five events with significant energy were identified during the interim period between the 2016 and 2017 field efforts, various additional factors play a role in whether significant sediment transport, and subsequently the potential for scour, burial, or mobility, occurred in the study area. Sediment size and depth are two primary factors. Calculating the threshold of sediment motion for representative sediment types found in the region, and the minimum and maximum depths at the site, provide an overall boundary for expected conditions at the study area. Given that Site 11, which was heavily characterized with over 40 sediment samples taken in the study by DuVal et al., (2016), lies only 3 km SW of the BOEM study area, the threshold of sediment motion was estimated using the Shields parameter and the representative sample sizes from DuVal et al., (2016) in their study: 0.17, 0.4, and 1 mm (e.g., fine sand, medium sand, and coarse sand). The Shields parameter is a non-dimensionalized parameter indicating the potential for sediment motion, calculated by the ratio of the shear stress exerted by near bed currents on the sediment to the physical characteristics of the sediment in water. When the Shields parameter exceeds a threshold value unique to the sediment size and density, the initiation of sediment motion is anticipated. Shields estimates for the representative sediment sizes have been calculated at the shallowest (13 m) and deepest (25 m) areas in the BOEM study area to provide bounding conditions at the site (Figure 11-6). The five events highlighted in Section 11.1.2 again appear most prominently, indicating that at both shallow and deep sites, all expected sediment types would be in motion during these events. Therefore, significant sediment transport would be anticipated at the site, with the potential formation of ripple bedforms in coarse sediments. These bedforms are important for their impact on the optical or sonar detection of objects on the sediment surface, potentially obscuring the surrogates within the ripple field.

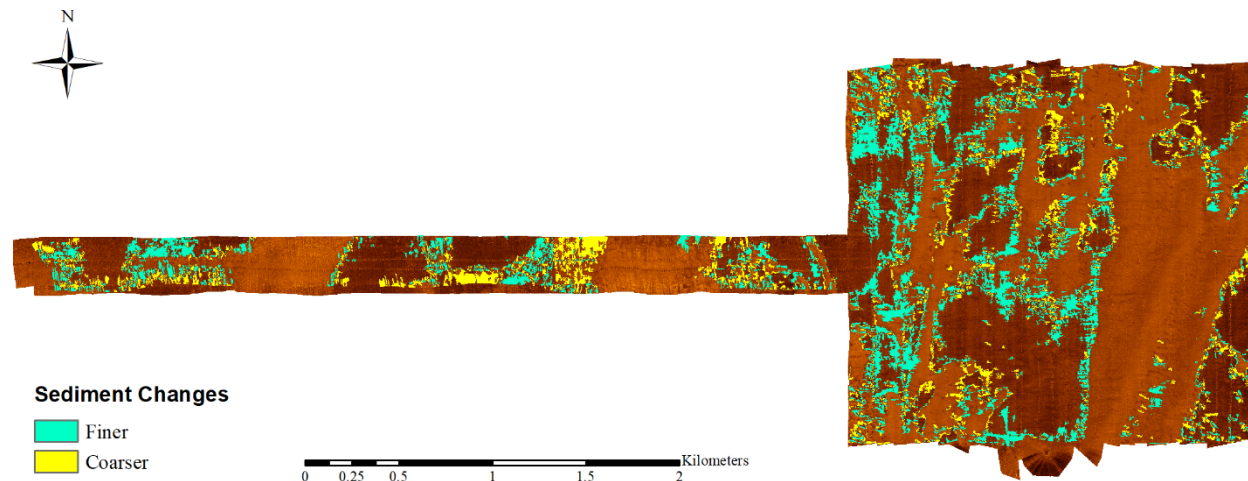
Figure 11-6: Shields Parameter Estimates of Sediment Motion for Representative Sediment Types at the BOEM Study Area



11.3.2 WAA and Observed Morphological Modification

While no direct observations were collected during the interim period between field efforts, a comparison of sediment distribution at the site can be made with the sonar data collected during the WAA. This provides insight to overall sediment transport integrated over the entire interim period, although individual events of sediment transport can only be estimated (see Section 11.3.1). Here, side-scan sonar data collected by the Edgetech 6205 at 230 kHz was brought into ESRI ArcGIS, where imagery classification tools were used to isolate primary sediment types at the study area. While much variability exists in the study area, two primary backscatter groups appear: more absorbent (darker) and more reflective (lighter). Through previous studies Trembanis et al., (2013); Raineault et al., (2013), acoustic reflectivity can be related to sediment size, with coarser material having more reflective properties than fine materials. Thus, the data can be divided into two primary sediment groups: coarser (lighter returns) and finer (darker returns). Using ArcGIS, raster images of the sonar data collected in 2016 and 2017 were classified and filtered to remove noise, using the recommended workflow for supervised classification by ESRI (see <http://desktop.arcgis.com/en/arcmap/latest/extensions/spatial-analyst/image-classification/image-classification-using-spatial-analyst.htm>). Once the noise was removed, the classification raster were verified by manual comparison to the original data sets. Finalized results were then compared, with changes between the 2016 and 2017 datasets represented as areas where sediment became coarser or finer. The results are highlighted in Figure 11-7.

Figure 11-7: Sediment Changes between 2016 and 2017 WAAs



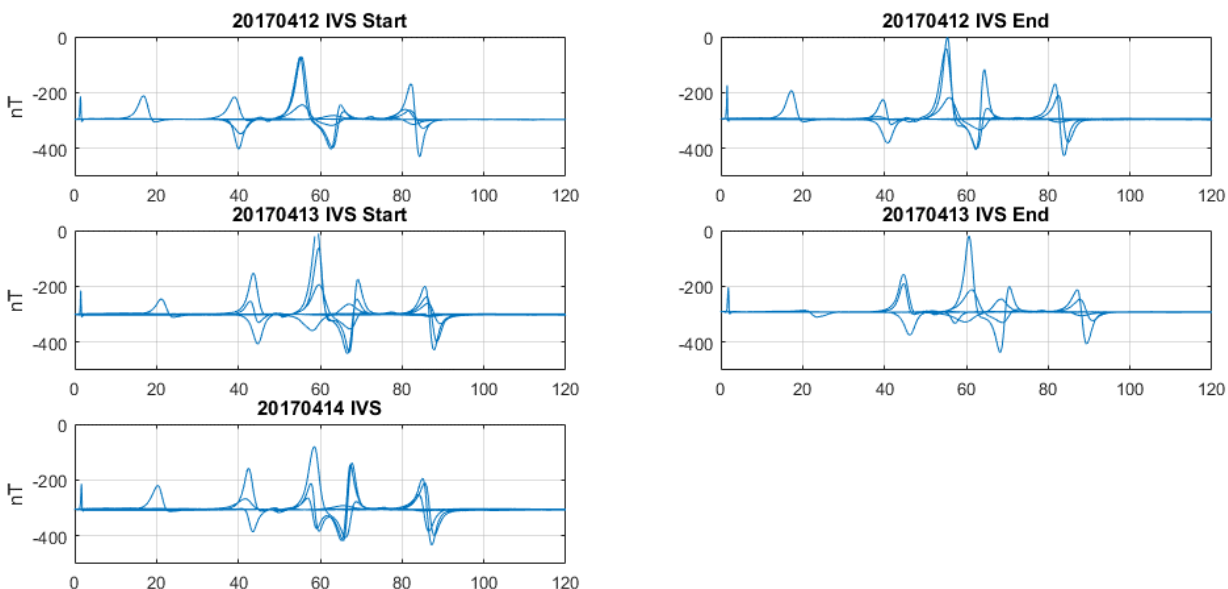
Estimates of the amount of area with an increase in coarse sediment and fine sediment suggest that nearly double the area became finer (about 625,000 m²) than coarser (about 337,500 m²). However, variations in gain between data sets and vessel motion effects in the data can introduce noise, and as such the numbers should not be taken in such strict precision, but rather as the order of magnitude of relative change (i.e., 2:1 increase in area of fine sediment coverage) (DuVal 2014). More qualitatively, the data indicates boundary shifts for sediment, which may indicate anticipated bedform formation for an area, or the potential for scour or burial of an object. Areas with coarser sediment are more likely than areas with fine sediment to form large-wave orbital ripples, in which objects remain proud of the bed, but may be obscured. Areas with finer

sediment may not have bedforms, but objects may scour and bury. Such observations were made in previous mine burial studies (Traykovski, Richardson, et al. 2007). The direction of the shifting of sediment boundaries may also indicate dominant direction of current forcing. Qualitatively, the results of the comparison do not yield any clear indication of a primary directional forcing, although the WaveWatch III data suggest most wave directional forcing came from NE – SE directions, or the typical approach of Nor'easter and extra-tropical storms.

11.3.3 IVS and AUV Navigation

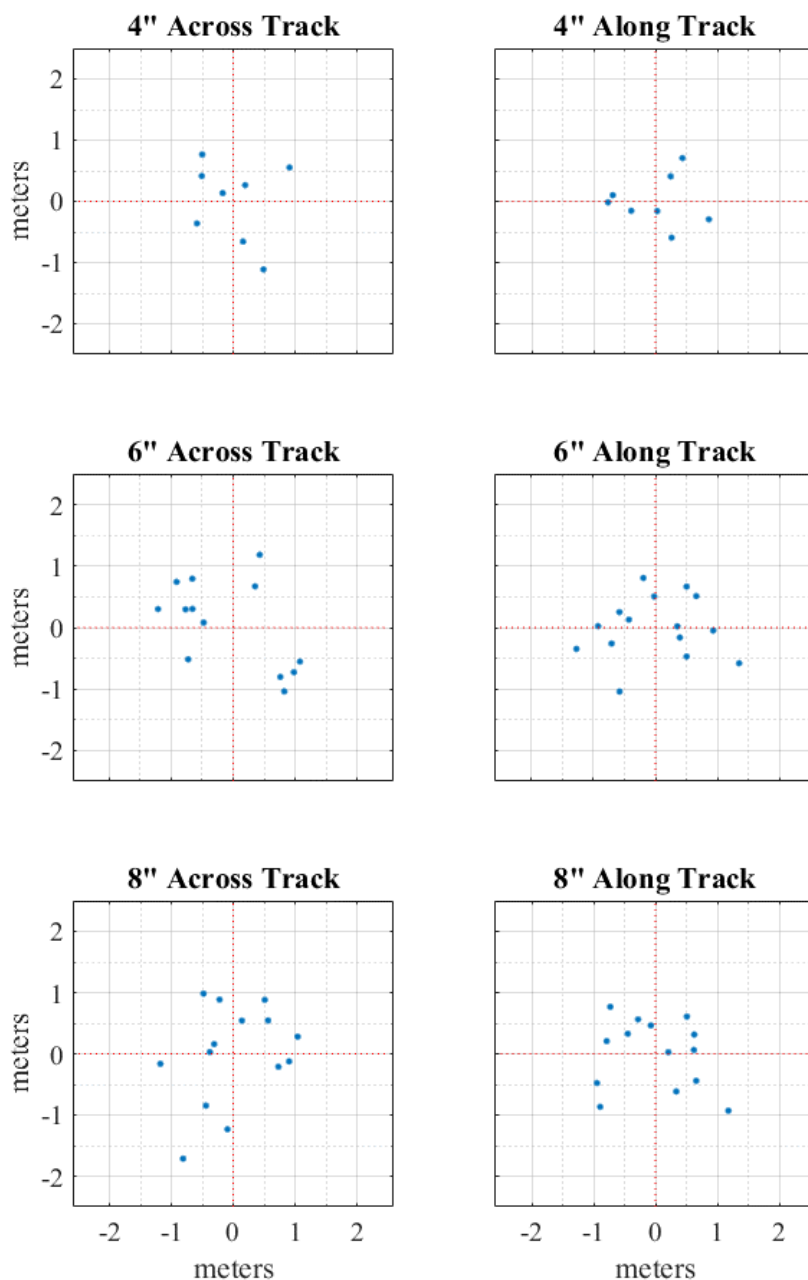
IVS missions were conducted each time the vehicle underwent a battery replacement. For missions conducted on April 12 -13, this occurred twice, while only one IVS mission was conducted on April 14, 2017. The magnetometer data collected on the IVS missions are presented in Figure 11-8. The results illustrate the difference in the new IVS design, as compared to the results of the 2016 IVS (Section 10.1.2). Whereas individual target signals were less discernable in the 2016 IVS data, the 2017 data shows clearly discernable targets; although difficult to discern at this scale, both of the smallest targets, the 4-inch surrogates, were accounted for in all five IVS missions. While four less IVS missions were conducted in 2017, the results appear less variable overall than the 2016 IVS missions.

Figure 11-8: IVS Magnetometer Results for the 2017 Field Effort



In addition to monitoring variation in magnetometer performance, the IVS provides a baseline for navigational performance of the AUV during the field effort, as discussed in Section 10.2.1. Using the targets picked from the side-scan sonar, the scatter of the targets indicates the precision of the AUV's navigation, and the positional accuracy of targets expected during production missions. The IVS target scatter is presented in Figure 11-9. While as much as 2.5 m variation was experienced from a "local mean" in target locations for IVS surrogates in the 2016 data, no more than 1.75 m variation was identified in the 2017 IVS data. Again, four less missions were conducted in 2017, which may account for less overall variation, but the results indicate improvement in AUV navigational performance over the 2016 data.

Figure 11-9: IVS Magnetometer Results for the 2017 Field Effort



11.3.4 Surrogate Target Detection

Side-scan sonar targets and magnetometer picks identified in the 2017 dataset were compared to the last known surrogate positions from 2016. As anticipated from the estimations of sediment threshold of motion calculations, the majority of surrogates were not easily identifiable in side-scan sonar data, either being buried in finer sediments, obscured in ripple bedforms, or confused in heavily cluttered areas (e.g., biology, debris). Thus, magnetometry became the primary means to identify targets. Side-scan sonar targets without associated magnetometer data were filtered out. Additionally, any magnetometer pick that did not have any additional picks in the vicinity were flagged; the modified mission plan for 2017 was designed to ensure enough coverage

overlap in magnetometry that any one surrogate should be seen at multiple instances in the data. While all missions were conducted in similar fashion (aside from the removal of the wider search patterns discussed in Section 11.2.3), the results are broken into node missions and cable route missions to facilitate data presentation and discussion. Each figure shows all of the selected and filtered magnetometer and side-scan picks associated with the surrogates from multiple transects or missions. Thus, multiple targets and picks are shown for each surrogate.

11.3.4.1 Node Missions

All node mission lie in depths greater than 20 m, and were exposed to lesser forcing than the shallower cable route missions (Section 11.3.1). Despite this, the majority of surrogates in Node 1 Route and Node 3 were not identifiable in the side-scan data (Figure 11-10). Here, small ripple bedforms were present, but analysis from the sediment classification indicate that these sites were composed of finer sediments. Although ripple bedforms have the potential to obscure targets, the objects that were identifiable in side-scan sonar data were largely proud of the seabed, and readily identifiable. Despite the lack of side-scan sonar targets, magnetometer picks are present in the vicinity of the last reported surrogate locations. This indicates that the majority of surrogates in Node 1 Route and Node 3 underwent scour and burial, and were largely not mobilized. Although some offset exists between reported positions and targets, the distances (<5 m) are not great enough to rule out navigational offset between mission 2016 and 2017 datasets. Surrogates that were buried or obscured or proud are listed by type in Table 11-1.

Figure 11-10: Node Mission Target Results from the 2017 Field Effort

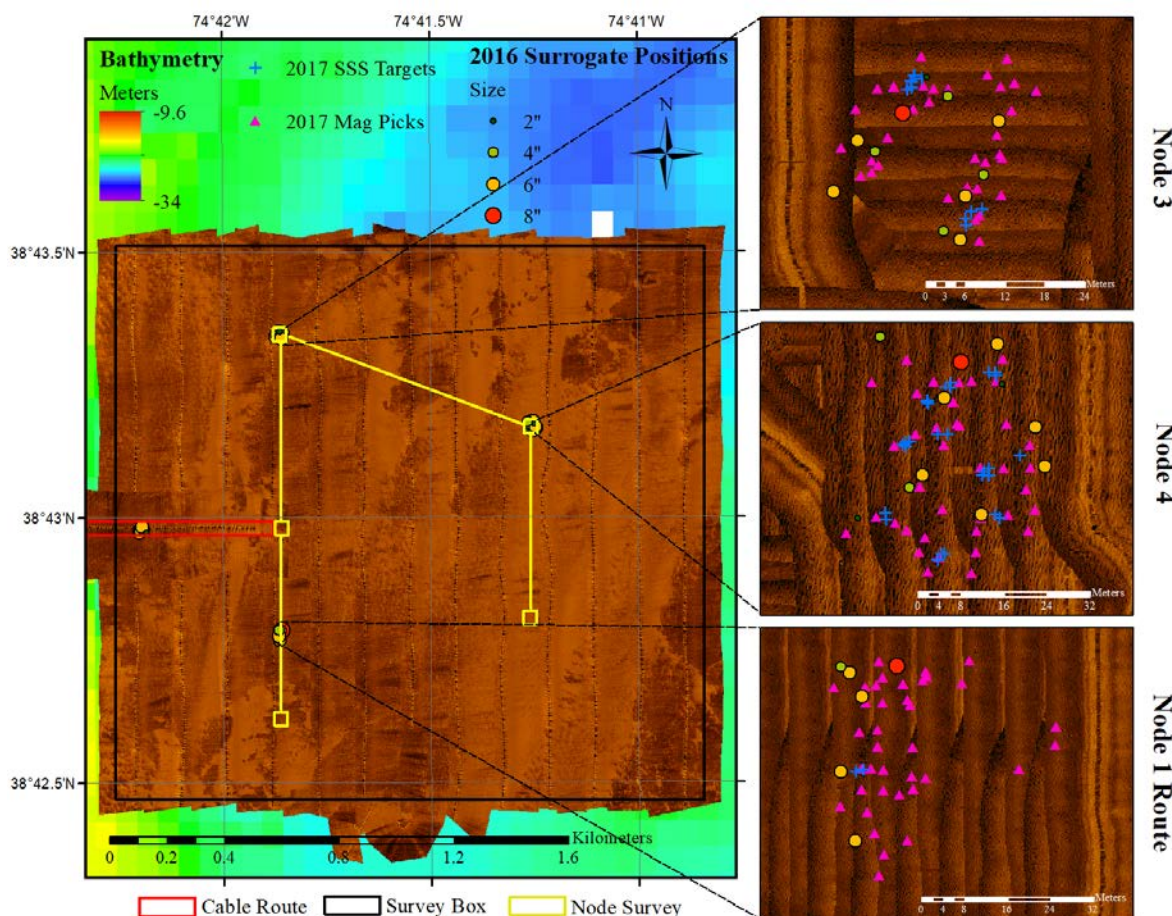
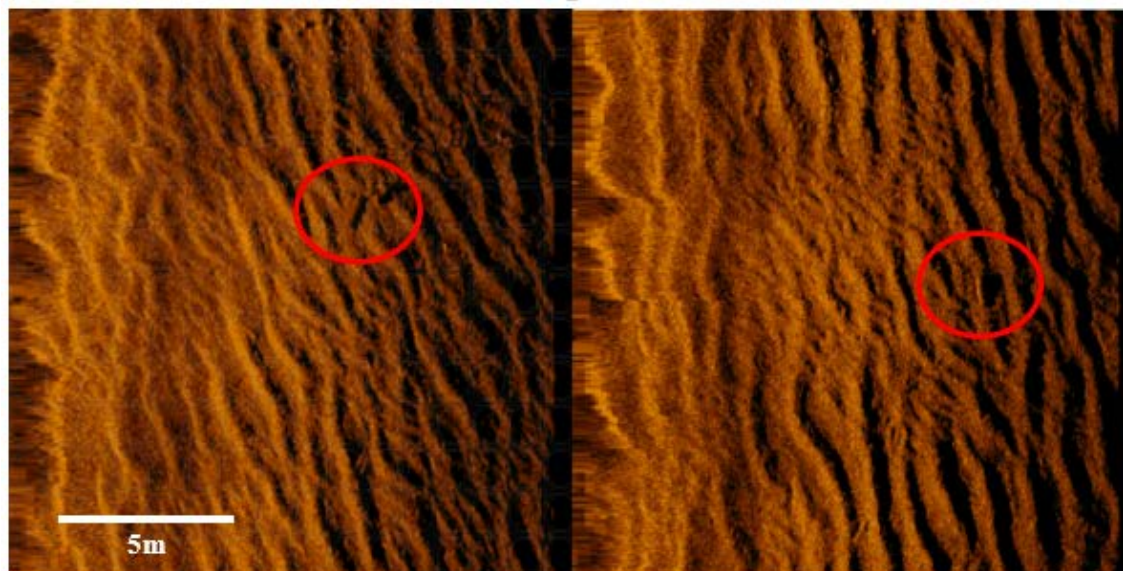


Table 11-1: Node Mission Target Results from the 2017 Field Effort

| Site | Depth (m) | Sediment Texture | 8-inch Proud | 8-inch Buried/ Obscured | 6-inch Proud | 6-inch Buried/ Obscured | 4-inch Proud | 4-inch Buried/ Obscured | 2-inch Proud | 2-inch Buried/ Obscured |
|--------------|-----------|------------------|--------------|----------------------------|--------------|----------------------------|--------------|----------------------------|--------------|----------------------------|
| Node 1 Route | 24 | Fine | 0 | 1 | 1 | 3 | 0 | 1 | 0 | 0 |
| Node 3 | 25 | Fine | 1 | 0 | 1 | 4 | 0 | 4 | 0 | 2 |
| Node 4 | 25 | Coarse | 1 | 0 | 6 | 0 | 0 | 2 | 0 | 2 |

While most surrogates were buried in Node 1 Route and Node 3, the majority were exposed in Node 4. Compared to Node 1 Route and Node 3, the sediment type in Node 4 was coarser, and the entire mission area was characterized by large-wave orbital ripple bedforms. Within the ripple bedforms, surrogates were found to both align with the dominant ripple crest direction, and lie at orthogonal angles to the crests, as illustrated by Figure 11-11. Although no definitive mobility could be confirmed in Node 1 Route and Node 3, all side-scan sonar targets and magnetometer picks for Node 4 do not correspond to the 2016 data set, which suggests mobility occurred. However, the targets and picks in the Node 4 mission are all 9 – 12 m to the SW of the 2016 locations, and the position of the objects relative to each other remains mostly consistent with the 2016 locations. This suggests that a large navigation offset, either in one or both of the 2016 and 2017 Node 4 missions. Since there are no additional missions by which to compare surrogate positions, it cannot be easily determined if navigational offset is purely the cause. Regardless, the apparent translation of the surrogates to the SW, without distortion to the orientation of the objects relative to each other, is enough to raise skepticism for the case of mobility.

Figure 11-11: Side-scan Sonar Data showing 6-inch Surrogates Orthogonal to and In-line with Dominant Ripple Crest Direction



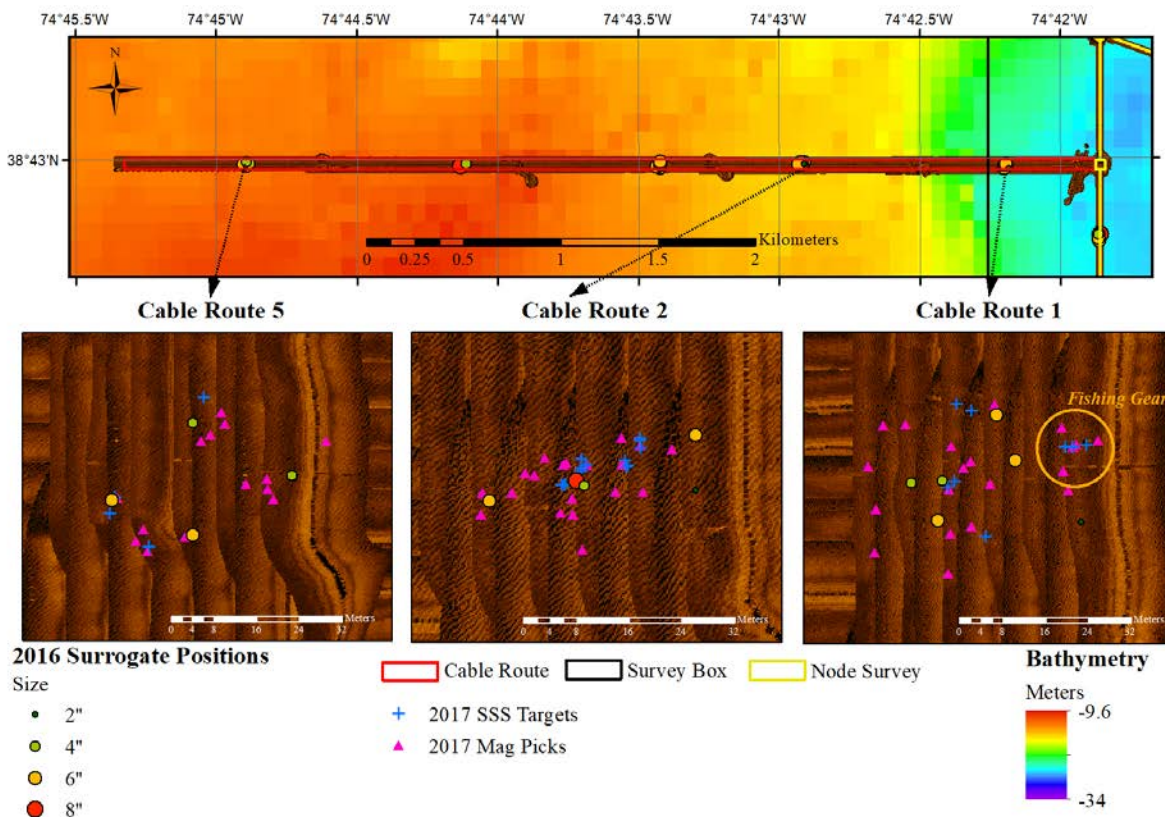
11.3.4.2 Cable Route Missions

During all three cable route missions, at least two surrogates were identified in side-scan sonar data (Table 11-2). Smaller ripple bedforms were present on Cable Route 1, while ripple bedforms characterized Cable Route 2 (Figure 11-12). On Cable Route 5, large orbital ripples had undergone considerable erosion, with rounded, flattened ripple crests that had fresh, smaller ripples formed over the top. On Cable Route 1, the magnetometer picks and side-scan sonar targets were considerably more scattered, although no consistent cluster of targets are present to indicate that any object was actually mobilized; the cause may be linked to AUV navigational offsets causing target scattering or unexpected magnetometer noise. The large cluster of targets to the east of the reported surrogate positions were associated with a benthic fish or whelk trap in the side-scan sonar data, not a mobile surrogate. There were, however, no targets in the immediate vicinity of a 6-inch surrogate previously located near the current location of fish trap. It is difficult to determine whether the signal was masked by the magnetic signal of the fish trap, or if the surrogate had become mobile and moved to the SW, where a cluster of magnetic picks were made. These picks have lower amplitudes than typical of the 6-inch surrogates, though, and the side-scan sonar target in the vicinity appears to be associated with a 4-inch surrogate.

Table 11-2: Cable Route Mission Target Results from the 2017 Field Effort

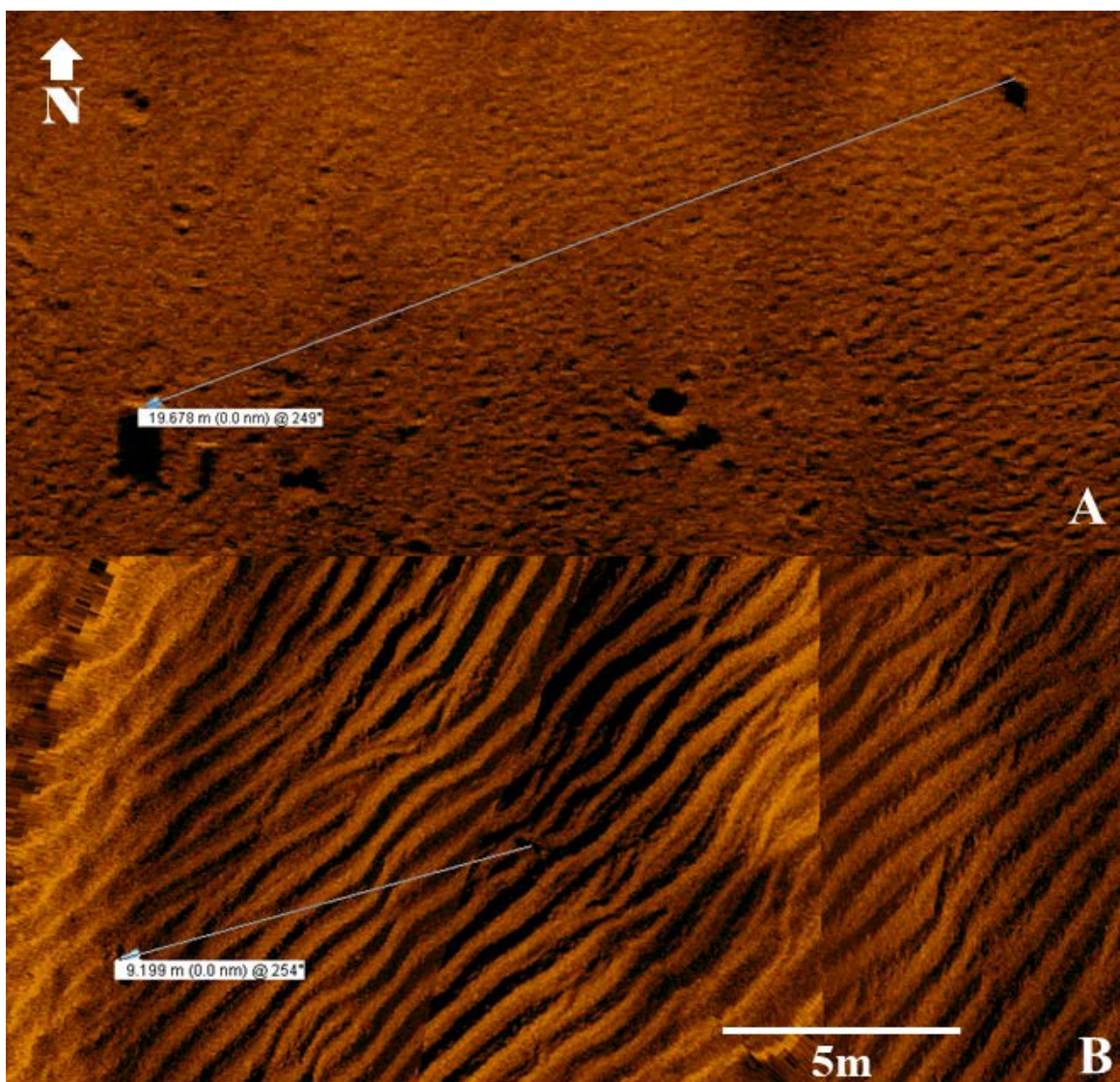
| Site | Depth (m) | Sediment Texture | 8-inch Proud | 8-inch Buried/ Obscured | 6-inch Proud | 6-inch Buried/ Obscured | 4-inch Proud | 4-inch Buried/ Obscured | 2-inch Proud | 2-inch Buried/ Obscured |
|---------------|-----------|------------------|--------------|----------------------------|--------------|----------------------------|--------------|----------------------------|--------------|----------------------------|
| Cable Route 1 | 22 | Fine | 0 | 0 | 1 | 2 | 1 | 1 | 0 | 1 |
| Cable Route 2 | 17 | Coarse | 1 | 0 | 1 | 1 | 0 | 1 | 0 | 1 |
| Cable Route 5 | 13 | Coarse | 0 | 0 | 2 | 0 | 1 | 1 | 0 | 0 |

Figure 11-12: Cable Route Mission Target Results from the 2017 Field Effort



With Cable Route 5, the results are split; for two of the four targets, mobility does not appear to have occurred. However, with one apparently buried 4-inch target, magnetics put it 5 m to the southwest. This is repeated with the southerly 6-inch surrogate, where magnetics put it 8 m to the SW. A questionable side-scan sonar target is also within the cluster magnetometer picks for this 6-inch surrogate, but it is unclear whether this actually the surrogate; there were a number of side-scan targets in Cable Route 5 with no associated magnetics, and it should be recalled that in the 2016 data, Cable Route 5 had a multitude of confusing targets that may have been biological in nature (see Section 10.3.3.2). That being said, unlike Cable Route 1, there is clear clustering of magnetic targets in both cases, indicating mobility likely occurred.

On Cable Route 2, while the 8-inch surrogate remained immobile and exposed, targets clearly identified in side-scan sonar and magnetometry as a 6-inch surrogate were found to be located 10 m WSW of the reported 2016 location. Given that the targets associated with the 8-inch surrogate are clustered around the reported 2016 location, indicated little if any navigational offset between missions, it cannot be conclusively ruled out that the 6-inch surrogate did not migrate. Further, reanalysis of the 2016 data set confirmed the location of the 6-inch surrogate; in multiple sonar passes, it appeared 20 m to the ENE of the 8-inch surrogate (Figure 11-13A). In the 2017 data set, it lies only 10 m to the ENE of the 8-inch surrogate (Figure 11-13B). While targets on Cable Route 5 may have become mobile, this appears to be the only conclusive case of mobility in the 2017 data set.

Figure 11-13: Comparison of Position and Orientation of Cable Route 2 Mobile Surrogate

11.4 Discussion

11.4.1 Sediment Transport and Morphodynamics

Five events with wave heights over 3 m occurred in the interim period between the 2016 and 2017 field efforts. This included the passing of Hurricane Hermine to the SE Between September 3 and 6, 2016, approximately 6 weeks after the 2016 field effort. Given estimates of near orbital velocities (Section 11.3.1), this storm was likely the first to cause significant sediment transport across the entire study area. During this event, storm waves approached from the ESE, rotating ENE as the hurricane moved out to sea (115° gradually shifting to 65°). In the following month, another two events passed through, generating similar magnitudes in orbital velocities, the first (September 29 to October 2) with waves approaching from the ENE shifting E (72° to 91°) and the second (October 9 to 10) from the SE shifting east (144° to 89°). Passing in late January 2017, a Nor'easter was the largest event in terms of near-bed orbital velocities during the interim period, with waves generated largely from the E (83° - 98°). The final event

occurred in mid-March (~30 days before the 2017 field campaign) and again, waves came out of the SE (130°-143°).

The review of the approaching wave direction is important when considering sediment transport and bedform morphology across the study area. As discussed in Section 11.3.2, boundary shifts in sediment distribution were evident, although a definitive direction could not be delineated. However, relict ripple bedforms on the seabed serve as a record of the last event with enough energy to generate ripple morphodynamics (DuVal, Trembanis and Skarke 2016, Voulgaris and Morin 2008). The wavelengths of the ripples scale to a fraction of the wave current orbital diameter, while the crests align orthogonal to the direction of the forcing (e.g., wave energy from the E will create ripple crests running N-S). In all of the mission sites with finer sediments, small-scale, truncated bedforms were generally aligned to the SE, or the direction of the March Nor'easter as it passed. Cable Route 2, although having coarser sediments, also showed larger wave orbital ripples oriented to the SE approaching waves. Furthermore, in Cable Route 5, heavily eroded ripples were present and also oriented to SE; however, more recent, small-scale ripples had formed over the top of the relict ripples and were oriented to the east, which suggest subsequent reworking of the relict ripples. Cable Route 5 is the shallowest site in the BOEM study area. The WAA backscatter also suggests that it has finer sediments than Cable Route 2 and Node 4, although coarser than other sites with fine sediments and with only small bedforms. As such, the newer ripples may have been formed by a small event that quickly followed the Nor'easter in March, which may have had just enough energy to form new ripples in the shallower, medium sized-sediments at Cable Route 5. Only Node 4, the deepest site with coarser sediments, deviated from this pattern. There, the ripples were aligned more easterly, suggesting the last ripple formation was associated with the January Nor'easter, not the subsequent storms.

The following morphodynamic inferences can be made from bedform morphology observed in the study area. First, the ripple morphology suggests that the last event to generate near-bed orbital currents with enough sustained energy to cause widespread sediment transport across the whole study area was the January 2017 Nor'easter. In effect, this storm 'reset' previously retained relict bedforms from the prior storms and left the entire study area in relict state reflecting the hydrodynamic conditions of the January 2017 Nor'easter. Afterwards, the March 2017 Nor'easter passed and modified much of the study area, although this storm did not have enough energy to completely reset the ripples in the deeper, coarser sediments, as seen in Node 4. This is supported in wave orbital velocity estimates at 25 m; the January Nor'easter topped 0.5 m/second velocities for 36 hours and 0.75 m/second velocities for 18 hours, peaking at 0.96 m/second during that period. On the other hand, the March Nor'easter topped 0.5 m/second velocities for only 21 hours and topped 0.75 m/second velocities for only 6 hours, peaking at only 0.79 m/second. Although peak velocities are important for ripple morphodynamics, ripples have been shown to form out of synchronization with rapidly changing conditions (e.g., (DuVal, Trembanis and Skarke 2016, Soulsby, Whitehouse and Marten 2012, Traykovski, Observations of wave orbital scale ripples and a non-equilibrium time dependent model 2007). Thus, for ripples to equilibrate to changing conditions, high-energy conditions must be sustained over long enough periods of time for ripple morphology to reflect the contemporary hydrodynamic conditions.

11.4.2 Fate of Surrogate MEC

The fate of the munitions surrogates at the BOEM study area are closely tied to the hydrodynamics, and consequential changes to morphology, that occurred during the interim

period. The characteristics of the sediment in which the surrogates lay also play a key role in the fate of the surrogates. As discussed in Section 11.3, most surrogates in finer sediments appear to have buried, while those in coarser sediments were more exposed. As noted, previous work was conducted on seabed mine burial, which can be used as analogues in discussing the apparent surrogate behavior at the BOEM study site. While there is ongoing research concerning MEC mobility and behavior, much of it is still preliminary, and much of the recent work builds off of previous mine burial data.

An important factor in the mine burial studies was the quantification and modeling of mine scour and burial. Much of this work was discussed in detail in journal articles by Trembanis et al., (2007), and Traykovski et al., (2007). The field data from the Traykovski et al., (2007) study was used by Trembanis et al., (2007) to inform and adapt existing scour models, such as those of Whitehouse, (1998) and Sumer et al. (1992). As noted before, areas with coarser sediment are more likely to form large-wave orbital ripples, in which objects may remain proud of the bed, but may be obscured, where finer sediment may not have bedforms, but objects may scour and bury. Traykovski et al. (2007) found that mines in fine sands would scour until the top of the mine was at the level of the surrounding seabed, and subsequently the scour pit would bury (fill in). Conversely, in coarse sediments, the mines would scour until the top of the mine presented similar hydrodynamic roughness to the surrounding ripple bedforms formed in the coarse sediments, or so that the height of the mines was roughly 1.3 times the equivalent to the height of the ripples. Using this information, Trembanis et al. (2007) incorporated Wiberg and Harris (1994) ripple height estimates into their model. Based on this work, predictions were made for scour and burial of the surrogates at the BOEM study area. The results, shown in Figures Figure 11-14 and Figure 11-15, are discussed below. Again, these serve as end-member predictions, at the shallowest and deepest parts of the study area, suggesting that scour and burial of surrogates within the study area would occur within these predicted ranges.

Figure 11-14: Scour and Burial Predictions for Surrogates at Shallow Sites by Sediment Type

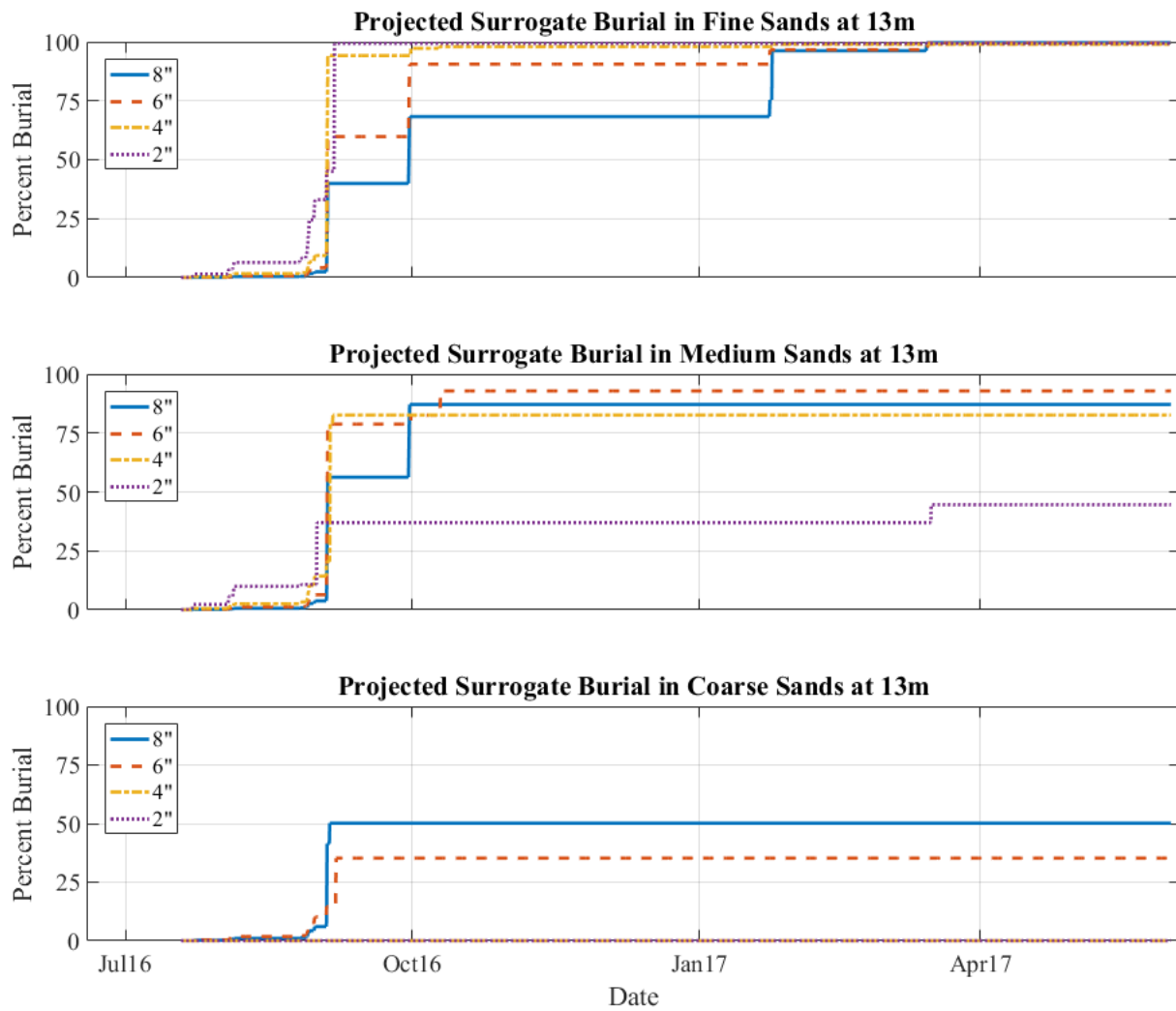
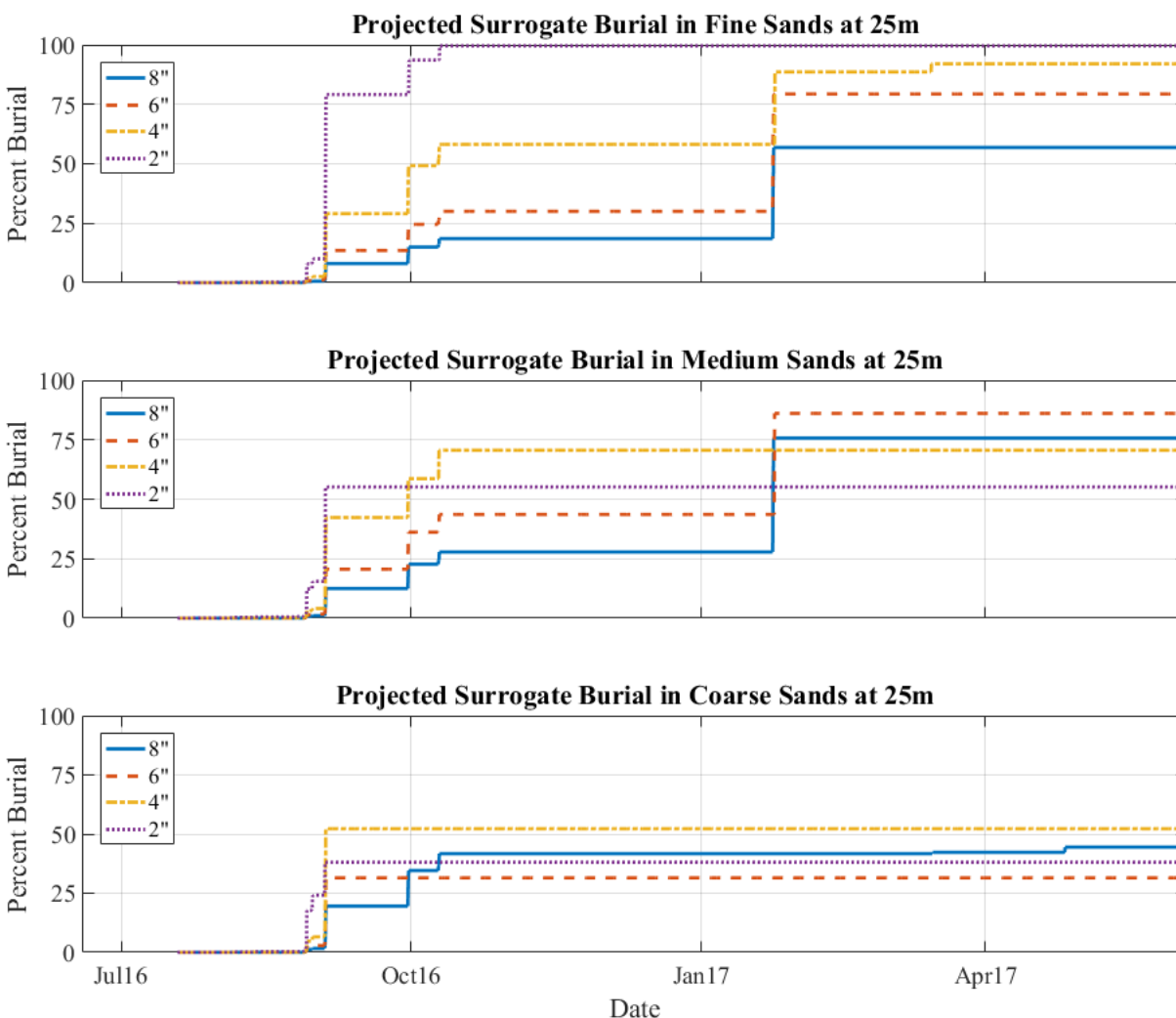


Figure 11-15: Scour and Burial Predictions for Surrogates at Deep Sites by Sediment Type



11.4.2.1 Exposed vs. Scour and Burial

The mine burial studies observed that objects within ripple bedform fields would only scour and bury until the top of the object was 1.3 times the height of the surrounding ripples (Traykovski, Richardson, et al. 2007). Given this, it is no surprise that all 8- and 6-inch (15 and 20 cm) surrogates were visible in Node 4, where the largest ripples were present and where predicted heights were as much as 15 cm ($15 \times 1.3 = 19\text{cm} \sim 8$ inches). The same result appears true in the shallower Cable Route 2 Site, where both an 8- and 6-inch surrogate are visible within a coarse sediment ripple field (with predicted ripple heights of approximately 10 cm). In Cable Route 5, where ripples were present but heavily eroded, three surrogates appear to be present in the side-scan sonar data, including two 6-inch surrogates and one 4-inch surrogate. In other sites, where finer sediments dominate, burial is expected.

Based on the scour model results, 2- and 4-inch surrogates in coarse sediments, shallow areas would undergo little, if any, burial by scour. This does not necessarily match observations, where no 4- or 2-inch surrogates were located in side-scan sonar data in areas with ripples. However, in flume studies by Voropayev et al., (2003), the authors noted that in conditions

where the ripple heights were greater than the diameter of an object, the object would be buried periodically by ripples migrating past the object. Thus, while the model does not predict scour and burial for these objects, it is possible that they were buried or obscured by relict ripple, and thus difficult or impossible to distinguish in side-scan sonar. The larger objects, on the other hand, likely underwent some scour and burial, but the total burial of the objects was impeded by the formation of large-wave orbital ripples. The models support this observation, with no more than 50% burial predicted with the 6- and 8-inch surrogates.

While the surrogates were expected to be partially exposed in the coarse sediments, burial was expected for surrogates in finer sediments. Despite this, there were a number of surrogates detectable by side-scan sonar in finer sediments. These were predominantly larger surrogates (8- and 6-inch), although one 4-inch surrogate was exposed in Cable Route 1. Cable Route 1, the shallowest site with finer sediment mapped in 2017, lies in about 22 m of water, while Node 1 Route and Node 3, also in finer sediments, lie in 25 m of water. In the model for finer sands in 25 m water depth suggest that the 8 and 6-inch surrogates would partially bury, but remain somewhat exposed, while the 4-inch surrogates would mostly bury. The model results for medium sands is largely the same. The direct observations are mixed: in Node 3, the sole 8-inch surrogate and one of five 6-inch surrogates were exposed, while in Node 1 Route, the sole 8-inch surrogate is buried and one of four 6-inch surrogates was exposed. The total percentage of burial for the exposed targets is difficult to determine, although in the case of the 8-inch in Node 3, it appears largely unburied. The remaining targets unaccounted for in side-scan sonar data, but present in magnetometry, suggest that burial occurred. Although the model does not suggest complete burial at 25 m, burial was complete enough to obscure them from side-scan sonar.

11.4.2.2 Mobility

Ongoing DoD SERDP studies (Traykovski, Continuous Monitoring of Mobility, Burial and Re-Exposure of Underwater Munitions in Energetic Near-Shore Environments, MR-2319 2017, Calantoni 2017, Puleo 2017) are addressing MEC mobility outside of the scope of this BOEM project. While object scour and burial has been extensively researched and modeled, mobility is less understood. In a recent journal article by Rennie et al., (2017), the authors parameterized the initiation of motion for cylinders, relating the “critical mobility parameter” to a ratio of the diameter of the object to bedform roughness. Flume tests on rigid bottoms produced mobility, although in sandy environments, the study found a contest between scour burial caused by the sediment being highly mobilized and the current forcing reaching the critical threshold for the objects to mobilize. In-field experiments, mobilization was observed in objects were the density of the object was closer to the density of sand (Traykovski, Continuous Monitoring of Mobility, Burial and Re-Exposure of Underwater Munitions in Energetic Near-Shore Environments, MR-2319 2017, Calantoni 2017). With the densities more reflective of real munitions, burial almost exclusively dominated.

The surrogates used in this study were not designed with a mobility study in mind. Rather, they reflected the materials suggested for geophysical system verification using ISOs (Environmental Security Technology Certification Program 2015b, 2009) to address the goals outlined for the primary 2016 in-field verification study. As described before, these were steel pipes cut to representative length with no end caps and no fill. Thus, sediment could, in theory, infill the surrogates and cause different behavior than the closed / solid surrogates used for previous mine burial and ongoing SERDP studies.

Therefore, the evidence of mobility in this study may not be a direct comparison to the parameterized mobility of the article by Rennie et al., (2017) or the observations by Traykovski (2017) and Calantoni (2017); the density of the surrogates used here will not be reflective of the surrogates used the aforementioned studies. However, data collected in this study suggests that at least one surrogate in Cable Route 2, and possibly an additional two surrogates in Cable Route 5, became mobilized. Table 11-3 defines the surrogate type, estimated distance and direction traveled, and shift in orientation for the three mobile surrogates. Most notable is the direction of travel for all three surrogates; all traveled to the WSW, within 12° bearing relative to each other. The direction of travel is reflective of the direction of storm waves indicated by the WaveWatch III hydrodynamic record: the WaveWatch III showed wave direction out of the ENE, E, and ESE during the various storms, or propagating to the WSW, W, or WNW. If mobility was to occur, it would be expected to travel in the direction of the storm wave propagation, which is supported by the observations in Table 11-3.

Table 11-3: Cable Route Mission Target Results from the 2017 Field Effort

| Site | Depth (m) | Sediment Texture | Bedforms / Seabed Texture | Surrogate Type | Direction Traveled (Compass) | Estimated Distance Traveled (m) | 2016 Orientation (Along Strike) | 2017 Orientation |
|---------------|-----------|------------------|---------------------------|----------------|------------------------------|---------------------------------|---------------------------------|------------------|
| Cable Route 2 | 17 | Coarse | Large Ripples | 6 | 252° | 10 | 305° (125°) | 290° (110°) |
| Cable Route 5 | 13 | Medium-Coarse | Eroded Ripples | 6 | 255° | 8 | 310° (130°) | 280° (100°) |
| Cable Route 5 | 13 | Medium-Coarse | Eroded Ripples | 4 | 240° | 5 | Not Discernable in Sonar | Buried |

The orientation of the surrogates prior to the storm events may have factored into the predisposition for the surrogates to become mobile versus local scour and burial. While a clear orientation cannot be estimated from the 4-inch surrogate at Cable Route 5, orientation along the long axis of both 6-inch surrogates were estimated before and after the storms. The orientation of the surrogates prior to the storms were >50° rotated relative to the direction of travel. Thus, the broad side of the surrogates were presented to the dominant direction of forcing during the storm events. After the storms, both 6-inch surrogates were rotated with long axis running WNW to ESE, or between 30° – 40° rotation relative to the direction of travel. Both 6-inch surrogates also appear to be oriented within 10° of each other after the storm. The final orientation of both are also orthogonal to the dominant direction of ripple formation (indicated by the orthogonal direction of the ripple crest orientation). This may indicate the instance or instances of mobility occurred previous to the last ripple formation event in mid-March 2017, where wave forcing came from the SE (130°-143°). If the orientation of the 6-inch surrogates at both Cable Routes 2 and 5 are largely orthogonal to the ripple formation, and thus the forcing direction, they would present less surface area for forcing, and may have not been mobile in that period.

In the case of Cable Route 2, the 8-inch surrogate at the site, while not mobile, also rotated relative to the surrogate's orientation in 2016 (Figure 11-13). The initial orientation was along 283° (103°). In the 2017 data, the orientation of the 8-inch surrogates is closer to 355° (175°). If the rotation occurred during the January 2017 storm, this orientation would line up with the dominant forcing direction during the January 2017 Nor'easter, and likely reflect the orientation of the ripple bedforms at the time. Indeed the orientation of the storm waves during the period of peak energy (January 23 - 24) ranged from (83° - 90°). This suggests the 8-inch surrogate rotated during the period of highest energy of the storm, aligning with the dominant wave forcing direction.

Both Cable Routes 2 and 5 were characterized by coarser sediments (although not as coarse in Cable Route 5 as in Cable Route 2) and large-wave orbital ripples, which may imply that the coarser sediments and associated larger ripple bedforms, play a factor in general object mobility. The apparent mobilization of all the objects detected in Node 4, which also has coarse sediment and large ripples, is considered suspect based on suspicions of navigational offset, as discussed in Section 11.3.4.1. Regardless, the potential for mobility in coarse sediment and/or ripple bedforms suggests further research is required on the topic. Some theoretical research and literature review on ripple bedform dynamics is ongoing as part of a SERDP study by Friedrichs (2017), and this topic has been tangentially discussed in laboratory tests for the mine burial studies and a SERDP study by Garcia (2017). Yet, no current field study focusing on MEC mobility in ripple bedforms is known to the authors at the time of this report.

11.4.3 Mission Design and IVS Performance Analysis

11.4.3.1 IVS Mission and Design

Design changes to the IVS proved beneficial during deployment, recovery and individual surrogate characterization in magnetometer missions. The design stretched the IVS from an overall length of 80 to 175 m. The increase of spacing between the objects from 6 to 15 m led to an increase of 30 to 75 m along the section containing surrogates. While this was intended to counter signal interference between surrogates, the increase in straight-line distance may have been expected to come with a slight decrease in navigational performance: AUVs running straight lines over greater distances have an increase in navigational drift. The distance increase was not much, however, and the results of the IVS missions suggest that this had no negative impact on navigational performance of the AUV. In fact, the surrogate locations derived from the AUV were overall less scattered in the 2017 missions than the 2016 mission (local mean radius ≤ 1.75 vs. ≤ 2.5 m). Although four less IVS missions were conducted in 2017, the improvement came with a design that in theory would reduce navigational performance. It is possible that by lengthening the IVS, and in turn the IVS mission transects, this allowed the AUV more time and distance to complete turns and align properly on transects thus improving both the overall navigational accuracy and the magnetometer discrimination ability.

The increase in spacing between the surrogates did improve the isolation of individual surrogates in the magnetometer data. The change in order of surrogates along the IVS was considered to facilitate deployment, but may have contributed to improved results by spacing the largest objects, with the largest magnetic signal, furthers apart. The placement of the 4-inch surrogates next to the 8-inch surrogates did make the former a somewhat more difficult to isolate, and the arrangement placed two 6-inch surrogates right next to each other, which resulted in some limited signal overlap (although still individually recognizable). This suggests that an additional

increase in spacing, perhaps from 15 to 20 m, may further improve the design for an IVS using surrogates of this size. As recommended in Section 10.4.2, if ISO sizes different from those used in this study are selected, further experimentation may be necessary. Regardless, the increase in length from the 2016 to 2017 IVS was found to facilitate deployment and recovery, while having no negative impact on AUV navigation, so an additional 25 meters across the IVS would not be expected to have a negative impact. The mission plan and IVS design used in this study did not experiment with methods to minimize AUV navigational drift, however, and further experimentation with IVS design or mission planning may better address the effects of navigational drift in future field efforts.

11.4.3.2 Mission Design on Magnetometer Performance

AUV missions were redesigned based on recommendations from the 2016 in-field verification study to improve magnetometer performance; this incorporated reductions in transect spacing from 8 to 4 m, and to run all missions with both N-S and E-W azimuthal orientations. The performance improvement is best exemplified by the number of magnetometer picks made in all Node 3 missions between 2016 and 2017. Table 11-4 compares the standard 2016 node mission results with the standard 2017 node mission results. The number of magnetometer picks from the 2016 2 m altitude mission with 8 m transect spacing, which was run with both N-S and E-W transects, was eight total picks; the number of magnetometer picks in the 2017 2 m altitude mission with 4 m transects spacing, also ran with both N-S and E-W, was 34 total picks. In other words, the number of picks increased over four-fold. This is logical when considering the transect grid. Spaced at 8 m transects, the area was effectively gridded at 8 x 8 m, or 64 m² per grid cell. Spaced at 4 m transects, the area was effectively gridded at 4 x 4 m, or only 16 m² per cell, a four-fold decrease in area. Curiously, the magnetometer picks did not differ greatly with increased altitude in the 2016 missions, although the 2017 mission altitude increase reduced the targets by nearly half.

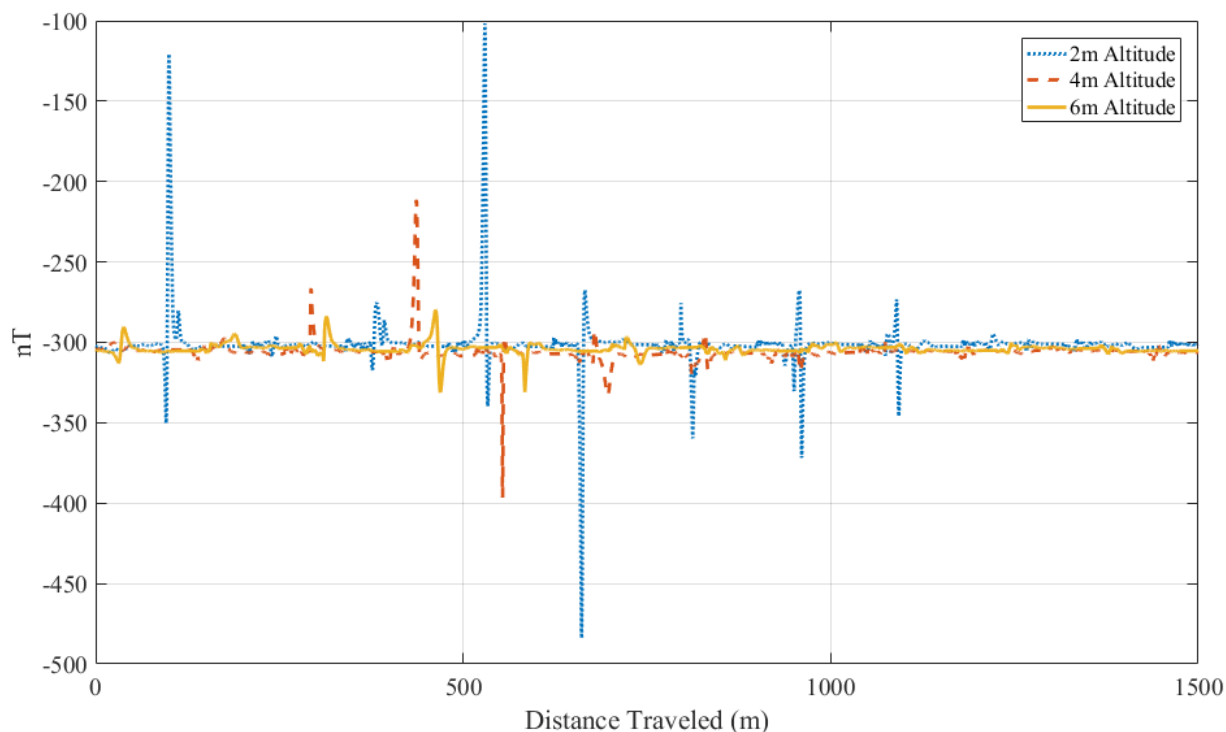
Table 11-4: Total Number of Magnetometer Picks during All Node 3 Missions

| Year | Altitude | Spacing | N-S | E-W | Total Magnetometer Picks |
|------|----------|---------|-----|-----|--------------------------|
| 2016 | 2 | 8 | Yes | Yes | 8 |
| 2016 | 2 | 4 | Yes | No | 8 |
| 2016 | 4 | 8 | Yes | Yes | 7 |
| 2016 | 4 | 4 | Yes | No | 7 |
| 2016 | 6 | 4 | Yes | No | 7 |
| 2017 | 2 | 4 | Yes | Yes | 34 |
| 2017 | 6 | 4 | Yes | Yes | 19 |

At the recommendation of BOEM, an additional 6 m altitude mission was conducted at Node 3 on April 14, 2017. Current guidelines suggest 6 m altitude, 30 m spaced transects for archaeological surveys at BOEM sites. A comparison of the results between the 2017 2 m altitude mission at 4 m transect spacing, the 2017 6 m altitude mission at 4 m transect spacing, and the 2016 4 m altitude mission at 4 m spacing are shown in Figure 11-16. Note that these missions were not equivalent in length or transect positioning; this serves only to demonstrate the amplitude of magnetometer detections by altitude for targets appearing in Node 3. The decrease in magnetic anomaly amplitude with increasing altitude is significant, given that the signal drop is a factor of a cube of the distance between the magnetometer sensor and the object. The

impacts of increased transect spacing from 4 to 8 m has been illustrated above as having significant influence on magnetometer detection numbers. Increasing transect spacing by double decreased detections by four-fold. Increasing the line spacing to 30 m would only exacerbate this, making objects the size of the 8-inch surrogate or smaller virtually impossible to detect effectively unless directly beneath the magnetometer.

Figure 11-16: Raw Magnetometer Data at Node 3 by Altitude



Note the anomaly locations do not reflect actual positioning.

11.4.3.3 Influence of Sediment Type and Bedforms on MEC Detection

In Section 11.4.3.1, attention was given on the influence of sediment type and bedforms on surrogate munition behavior. However, some discussion should address the effects of sediment type and bedforms on MEC detection. It is well demonstrated throughout this document that high-resolution side-scan sonar is an effective tool for surrogates exposed on an uncluttered seabed, and when combined with magnetometry (see Appendix D), it can become even more effective at distinguishing surrogates from non-ferrous objects. However, the results of the 2017 study suggest that after any period of time following energetic events, it is unlikely that MEC will be exposed and unobscured by bedforms. In fine sediments, where less obtrusive bedforms may be found, the probability of surrogate burial increases. In coarse sediment, where total burial is less likely, the probability of large bedforms obscuring the surrogates increases. In these conditions, side-scan sonar is no longer a singularly reliable tool for MEC detection. In the 2017 data set, side-scan sonar targets were outnumbered by magnetometer picks by 155 picks to 54 targets (versus the 251 side-scan sonar targets to 69 magnetometer picks in 2016). Of the 62 total surrogates deployed at the site (54 with known locations), only 17 were identified in side-scan sonar data in 2017; in 2016, 43 of 62 were identified in side-scan sonar data by the search team, and 54 of 62 were identified by the deployment team (as discussed in Section 10.3., not all

of the 62 deployed targets were reacquired by the deployment team). Thus, the impact of sediment type in which surrogates, or MEC, lies, will become a determining factor in the appropriate tools for detection, as will the size and type of MEC anticipated. Larger MEC than the surrogates used in this study will not be as susceptible to total burial or appear as obscured in ripple bedforms. Although surrogate detection by side-scan sonar was significantly hindered by burial and ripple bedforms in this study, this may not be representative of all cases. This case study reiterates the advantages in mission planning gained by conducting research on historical site usage (Section 3.0) and physical site properties (Section 2.0) prior to technology selection and implementation for MEC detection surveys.

This is not to suggest that burial is the end all fate for MEC in finer sediments, nor do ripple bedforms prevail in coarse sediments year around. In the mine burial studies, buried mine surrogates were at times partially unburied by energetic events, with reburial occurring as energy waned or in extended periods of low to moderate energy conditions (Traykovski, Richardson, et al. 2007, Trembanis, et al. 2007, Inman and Jenkins 2002). Likewise, large ripple bedforms were not present at the study site in July 2016. In sites where ripples are formed by episodic energetic events, periods of quiescent conditions often dominate. Under these conditions, relict ripples typically erode due to benthic organism activity and / or low to moderate hydrodynamic forcing (Soulsby, Whitehouse and Marten 2012, Balasubramanian, Voropayev and Fernando 2011, Hay 2006). Thus, not only do the physical characteristics of a site need to be considered when choosing the appropriate geophysical technologies and techniques, the timing of operations and the anticipated conditions of the seabed at a given time should be considered.

11.5 Conclusion

The 2017 field effort examined the fate of the munitions surrogates placed during the 2016 BOEM in-field verification study. The interim period between studies, spanning 255 days, was characterized by five separate storm events exceeding 3 m wave height and 0.5 m/s orbital velocities at portions of the site. While no direct *in situ* measurements were made, hydrodynamic conditions were estimated using NOAA WaveWatch III hindcasting data. A WAA was conducted, determining that site-wide sediment transport had occurred with shifts in sediment distribution within the site. AUV missions, redesigned based on the 2016 recommendations, found that the majority of surrogates in finer sediments underwent scour and burial, while surrogates in coarser sediment were exposed, but at times obscured by large-wave-orbital ripples. Observations of surrogate scour and burial compared well to models developed to predict seabed mine burial, although variations were observed. While not prevalent, at least one instance of surrogate mobility was confirmed, with two potential cases of mobility noted as well. All three cases occurred where large-wave-orbital ripples were present; suggesting that further research could better characterize the influence of coarse sediment or ripple bedforms on MEC mobility.

In addition to examining surrogate mobility, scour and burial, this study instituted and examined several of the recommendations forwarded by the 2016 in-field verification report. Increasing the spacing between the surrogates on the IVS was found to significantly improve individual target identification in IVS missions, while overall AUV navigational performance improved as well. Further, modifications to the IVS design were made that facilitated safe deployment and recovery. With AUV missions, decreasing the line spacing from 8 to 4 m, while running transects in both N-S and E-W directions significantly improved magnetometer detection rates.

Based on 2016 and 2017 mission data, increased altitude and increased spacing was not recommended for MEC detection or for objects of equivalent size; 2 m altitude missions conducted at 4 m line spacing provided the better probability for detection of 155 mm or smaller MEC than missions using greater altitude or transect spacing with the selected magnetometer. Further, sediment type and hydrodynamic conditions must be considered for the potential impact on MEC detection surveys and the geophysical technologies and techniques selected for MEC surveying. Future studies further characterizing the impacts of energetic events on MEC scour, mobility and burial, as well on the detectability of MEC in sites representative of the conditions found in BOEM offshore WEA's may aid in evaluating and managing MEC hazards.

Page Intentionally Left Blank.

12.0 References

- Alcocer, A., P. Oliveria, and A. Pascoa. 2006. "Underwater acoustic positioning systems based on buoys with GPS." *Proceedings from the Eighth European Conference on Underwater Acoustics*.
- ASV Global. 2016. *Products*. <http://asvglobal.com/products/>.
- Balasubramanian, S., S.I. Voropayev, and H.J.S. Fernando. 2011. "Heterogeneous sediment beds under weak oscillatory flow and turbulence: Ripples' transformation and decay." *Ocean Engineering* 38: 2281-2289.
- Balloch, R. 2010. "A New Generation of Sidescan Sonars." *International Ocean Systems*. Accessed January 2017. www.intoceansys.co.uk/articles-detail.php?iss=0000000015&acl=0000000109.
- Berhow, M. ed. 2015. *American Sea Coast Defenses: A Reference Guide, 3rd Edition*. McLean, VA: CDSG Press.
- Boesch, D.F. 1979. *Benthic ecological studies: macrobenthos. Chapter 6 in: Middle Atlantic outer continental shelf environmental studies. Final report*. Contract No. AA550-CT6062, Bureau of Land Management, 301.
- Breiner, S. 1999. "Application Manual for Portable Magnetometers." <ftp://geom.geometrics.com/pub/mag/literature/ampm-opt.pdf>.
- Bureau of Ocean Energy Management. 2012. "Commercial Wind Lease Issuance and Site Assessment Activities on the Atlantic Outer Continental Shelf Offshore New Jersey, Delaware, Maryland, and Virginia." Final Environmental Assessment. Report # BOEM 2012-003, U.S. Department of the Interior, 341. http://www.boem.gov/uploadedFiles/BOEM/Renewable_Energy_Program/Smart_from_the_Start/Mid-Atlantic_Final_EA_012012.pdf.
- . 2016. *Wind Planning Areas, Wind Energy Areas and Renewable Energy Leases*. <http://www.boem.gov/Renewable-Energy-GIS-Data/>.
- Butler, D. K. 2004. *Employing multiple geophysical sensors to enhance buried UXO "target recognition" capability*. U.S. Army Engineer Research and Development Center.
- Byrne, S., V. Schmidt, and O. Hengrenaes. 2015. "AUV-Acquired Bathymetry, Methods." *Sea Technology Vol 56, No 11* 17-22.
- Calantoni, J. 2017. *Long Time Series Measurements of Munitions Mobility in the Wave-Current Boundary Layer, MR-2320*. Accessed 2017. <https://www.serdp-estcp.org/Program-Areas/Munitions-Response/Underwater-Environments/MR-2320/MR-2320>.
- CALIBRE. 2016. *Project Management Plan. Unexploded Ordnance (UXO) Survey Methodology Investigation for Wind Energy Areas on the Atlantic Outer Continental Shelf*. Prepared for the U.S. Department of the Interior, Bureau of Safety and Environmental Enforcement. February.
- Camelli, R., B. Bingham, M. Jakuba, A. Duryea, R. LeBouvier, and M. Dock. 2009. "AUV sensors for real-time detection, localization, characterization, and monitoring of underwater munitions." *Marine Technology Society Journal* 43 (4): 76-84.

- Carton, G., J. C. King, and R. Bowers. 2012. "Munitions-related Technology demonstrations at Ordnance Reef (HI-06), Hawaii." *Marine Technology Society Journal* 46 (1): 63-82.
- Carton, G., K. Ciolfi, and M. Overfield. 2009. "Echoes of World War I: Chemical Warfare Materials on the Atlantic Coast." *Sea History*, December: pp. 14-18.
https://www.researchgate.net/publication/267395122_Echoes_of_World_War_I_Chemical_Warfare_Materials_on_the_Atlantic_Coast.
- Castelao, R., S. Glenn, and O. Schofield. 2010. "Temperature, salinity, and density variability in the central Middle Atlantic Bight." *J. Geophys. Res.* 115 (C10).
doi:10.1029/2009JC006082.
- Cecchetti, A. J. 2015. "USV Surveys Historic USS Arizona And USS Utah at Pearl Harbor." *Sea Technology*, February: 51-54.
- Christ, R. D., and R. L. Sr. Wernli. 2007. *The ROV manual, a user's guide for observation class remotely operated vehicles*. . Burlington: Elsevier.
- CIRIA. 2015. "Assessment and Management of Unexploded Ordnance (UXO) Risk in the Marine Environment, C754." London, UK, 165 pp.
- Coast Defense Study Group. 2013. *CDSG*. Accessed 2016. <http://cdsg.org/>.
- Cole, K.B., D.B. Carter, and T.K. Arndt. 2005. "Ensuring habitat considerations in beach and shoreline management along Delaware Bay – a bay wide perspective."
<http://el.erdc.usace.army.mil/workshops/05oct-dots/s8-Cole.pdf>.
- Dalyander, P.S., B. Butman, C.R. Sherwood, and R.P. Signell. 2012. "U.S. Geological Survey Sea Floor Stress and Sediment Mobility Database." U.S. Geological Survey data release.
<http://woodshole.er.usgs.gov/project-pages/mobility>.
- Delaware Department of Natural Resources and Environmental Control. 2011. "Delaware Water Quality Assessment Report."
http://iaspub.epa.gov/waters10/attains_index.control?p_area=DE.
- DuVal, C.B. 2014. "Hydrodynamic Variability and Bedform Dynamics at an Inner Shelf Artificial Reef. Master Thesis, University of Delaware, Newark, DE."
- DuVal, C.B., A.C. Trembanis, and A. Skarke. 2016. "Characterizing and Hindcasting Ripple Bedform Dynamics: Field Test Of Non-Equilibrium Models Utilizing A Fingerprint Algorithm." *Continental Shelf Research* 116: 103-155. doi:10.1016/j.csr.2015.12.015.
- EdgeTech. n.d. "9200 Littorial Mine Countermeasure Sonar (LMCS) System." Accessed January 1, 2017. <http://www.uvs.com.au/LiteratureRetrieve.aspx?ID=134537>.
- EdgeTech. 2005. *Application Note: Sidescan SONAR Beamwidth*. West Wareham, MA: EdgeTech.
- Edwards, M. H., R. Wilkins, C. Kelly, E. DeCarlo, K. MacDonald, S. Shjegstad, M. Van Woerkom, et al. 2012. "Methodologies for Surveying and Assessing Deep-water Munitions Disposal Sites." *Marine Technology Society Journal* 46 (1): 51-62.
<http://www.hummaproject.com/wp-content/uploads/2015/03/Edwards-final.pdf>.
- EIVA. n.d. *ScanFish III ROTV Technical Specifications*. <http://www.eiva.com/products/eiva-equipment/scanfish-iii-rotv/scanfish-rocio/technical-specifications>.

- Environmental Security Technology Certification Program. 2009. "Geophysical system verification: A physics-based alternative to geophysical prove-outs for munitions response." <https://www.serdp-estcp.org/content/download/7426/94837>.
- . 2010. "Deep Water Munitions Detection System, ESTCP Project MM-0739."
- . 2012. "Demonstration of the laser line scan system for UXO characterization." <https://serdp-estcp.org/index.php/Program-Areas/Munitions-Response/Underwater-Environments/MR-200911/MR-200911>.
- . 2015a. "Autonomous Underwater Munitions and Explosives of Concern Detection System, ESTCP Cost and Performance Report MR-201002." 37.
- . 2015b. *Final Report, Geophysical System Verification (GSV): A Physics-Based Alternative to Geophysical Prove-Outs for Munitions Response with Addendum*. SERDP/ESTCP Program Office, 74. <https://www.serdp-estcp.org/content/download/7426/94837/version/4/file/GSV+Final+Report+with+Addendum+%28V%29.pdf>.
- Friedrichs, C. 2017. *Simple Parameterized Models for Predicting Mobility, Burial and Re-Exposure of Underwater Munitions, MR-2224*. Accessed 2017. [https://www.serdp-estcp.org/Program-Areas/Munitions-Response/Underwater-Environments/MR-2224/MR-2224/\(language\)/eng-US](https://www.serdp-estcp.org/Program-Areas/Munitions-Response/Underwater-Environments/MR-2224/MR-2224/(language)/eng-US).
- Garcia, M. 2017. *Large-Scale Laboratory Experiments of Incipient Motion, Transport, and Fate of Underwater Munitions under Waves, Currents, and Combined Flows, MR-2410*. Accessed 2017. [https://www.serdp-estcp.org/Program-Areas/Munitions-Response/Underwater-Environments/MR-2410/\(language\)/eng-US](https://www.serdp-estcp.org/Program-Areas/Munitions-Response/Underwater-Environments/MR-2410/(language)/eng-US).
- Geometrics. n.d. "G-882 Marine Magnetometer." <http://www.geometrics.com/geometrics-products/geometrics-magnetometers/g-882-marine-magnetometer/>.
- Hansen, R. E. 2011. "Introduction to synthetic aperture sonar." In *Sonar Systems*, edited by Nikolai Kolev. INTECH.
- Harbor Defense Portal. 2015. *Fort Wiki*. Accessed 2016. www.fortwiki.com.
- Hartsfield, J.C. Jr. 2005. *Single Transponder Range Only Navigation Geometry (STRONG) Applied to REMUS Autonomous Under Water Vehicles*. Cambridge: Massachusetts Institute of Technology.
- Hay, A.E. 2006. "Biodegradation of wave-formed sand ripples during SAX04 (Sediment Acoustics Experiment 2004)." *J. Acoust. Soc. Am.* 120: 3097.
- HDR. 2013. *Former Seattle Naval Supply Depot Piers 90 & 91- Port of Seattle, Seattle, WA Formerly Used Defense Site #F10WA012501, Remedial Investigation Final Report*. Omaha, NE: USACE Omaha District.
- . 2014. *Supplemental Comprehensive Site Evaluation Phase II report for the Eglin AFB Legacy Bay Ranges, Final Report*. Omaha, NE: USACE Omaha District.
- Hoggarth, A., and K. Kenny. 2015. "Great Potential for SAS in Hydrography." *Hydro International*, March: 27-29.

- Inman, D.L., and S.A. Jenkins. 2002. *Scour and Burial of Bottom Mines: a Primer for Fleet Use. SIO Reference*. San Diego, La Jolla: Scripps Institution of Oceanography, University of California.
- iXBlue Inc. 2014. "PHINS Inertial Navigation System Technical Specifications." <https://www.ixblue.com/sites/default/files/downloads/ixblue-ps-phins-06-2014-web.pdf>.
- JW Fishers Mfg Inc. n.d. "Pulse 12 Boat Towed Metal Detector." http://www.jwfishers.com/datasheets/Pulse-12_16.pdf.
- Kaiser, M.J., and B. Snyder. 2011. "Offshore Wind Energy Installation and Decommissioning Cost Estimation in the U.S. Outer Continental Shelf." *Technology Assessment & Research Study 648*. U.S. Department of the Interior, Bureau of Ocean Energy Management. 340 pp. <http://www.bsee.gov/Technology-and-Research/Technology-Assessment-Programs/Reports/600-699/648AA/>.
- Kearfott Corp. n.d. "KI-4902S High Performance / Compact Card SEANAV INS/IMU Kit." http://auvac.org/uploads/manufacture_spec_sheet_pdf_nav/ki-4902_high_performance_inu.pdf.
- Keller, Bryan M., T. Hamilton, and S. Hird. 2015. "Low-Logistics AUV Pipeline Inspection." *Sea Technology* 37-41.
- Klein Associates, Inc. 2015. "System 5900, The Difference is in the Image." August. Accessed January 2017. http://www.l-3mps.com/klein/pdfs/S5900_FINAL_8_2015.pdf.
- Kraeutner, P.H., and J.S. Bird. 1997. "Principal components array processing for swath acoustic mapping." *OCEANS '97. MTS/IEEE Conference Proceedings*. Halifax, NS. Vol 2: 1246-1254. doi:10.1109/OCEANS.1997.624174.
- . 1999. "Beyond interferometry, resolving multiple angles-of-arrival in swath bathymetric imaging." *OCEANS '99 MTS/IEEE. Riding the Crest into the 21st Century*. Seattle: IEEE. 37-45.
- Kraken Sonar Systems, Inc. 2012. "Tomorrow's Sonar Today. AquaPix." Accessed January 2017. <http://www.krakensonar.com/images/pdf/AquaPix.Brochure.Nov2012.pdf>.
- . 2015a. "Kraken Announces KATFISH Sonar System." July 21. <http://www.krakensonar.com/en/investor/news/2015/69-kraken-announces-katfish-sonar-system>.
- . 2015b. "Vision is the Art of Seeing the Invisible." July. Accessed 2016. www.krakensonar.com/images/pdf/Kraken-July-2015-presentation.pdf.
- . 2016. *KRAKEN TO SUPPLY SONAR SYSTEM TO MAJOR ISRAELI DEFENCE CONTRACTOR*. February 23. <http://www.krakensonar.com/en/investor/news/2016/84-kraken-to-supply-sonar-system-to-major-israeli-defence-contractor>.
- Lentz, S.J. 2008. "Observations and a model of the mean circulation over the Middle Atlantic Bight continental shelf." *Journal of Physical Oceanography* Vol 38(6): 1203-1221.
- Marine Magnetics. 2016. "SeaSpy2." http://www.marinemagnetics.com/wordpress/wp-content/themes/marine/brochures/SeaSpy2_2016_lettersize_jp.pdf.

- Marine Technology Reporter. 2015. "Autonomy by (Software) Design." *Marine Technology Reporter*, October: 38-41.
- Martin, P., A. McDonald, and E. Munday. 2015. "Robust Data in Sensitive Enviroments." *Hydro International*, Nov-Dec: 24-27.
- Matsuda, T., T. Maki, T. Sakamaki, and T. Ura. 2013. "Toward wide seafloor surveys using multiple autonomous underwater vehicles." *Underwater Technlogy Symposium*. Tokyo: IEEE. 1-9.
- Mineral Management Service. 2007. "Programmatic Environmental Impact Statement for Alternative Energy Development and Production and Alternate Use of Facilities on the Outer Continental Shelf, Final." OCS EIS/EA MMS 2007-046., October.
<http://www.boem.gov/Renewable-Energy-Program/Regulatory-Information/Guide-To-EIS.aspx>.
- National Oceanic and Atmospheric Administration. 1926. "Nautical Chart 369, New York Harbor, Scale 1:40000." January. <https://historicalcharts.noaa.gov/historicals/search>.
- . 2001. *Underwater navigation*. In *Diving Manual, Diving for Science and Technology (4th ed.)*.
- . 2005. "Ahi Safety and Operations Manual V 1.5." November 23.
<ftp://ftp.soest.hawaii.edu/pibhmc/web/docs/AHI-Safety-Ops-Manual.pdf>.
- . 2016a. *Historical Map & Chart Collection*. Accessed 2016.
<http://www.historicalcharts.noaa.gov>.
- . 2016b. "Nautical Chart 13218, Martha's Vineyard to Block Island." *Electronic Navigation Charts*. Accessed 2016.
http://www.nauticalcharts.noaa.gov/mcd/enc/download_agreement.htm.
- . 2016c. *National Data Buoy Center*. May 10. <http://www.ndbc.noaa.gov/>.
- . 2016d. *U.S. Coastal Relief Model*. Accessed 2016.
<https://www.ngdc.noaa.gov/mgg/coastal/crm.html>.
- . 2016e. "Navagaion Chart 12300, Approaches to New York." *Electronic Navagation Charts*. Accessed 2016. http://www.nauticalcharts.noaa.gov/mcd/enc/download_agreement.htm.
- . 2016f. "Nautical Chart 13003, Cape Sable to Cape Hatteras." *Electronic Navagation Charts*. Accessed 2016. http://www.nauticalcharts.noaa.gov/mcd/enc/download_agreement.htm.
- . 2016g. "Nautical Chart 12208, Approaches to Chesepeake Bay." *Electronic Navagation Charts*. Accessed 2016.
http://www.nauticalcharts.noaa.gov/mcd/enc/download_agreement.htm.
- . 2016h. "Nautical Chart 12352, Shinnecock Bay to East Rockaway Inlet, South Coast of Long Island, 1:40,000 scale."
- . 2016i. *Multibeam Echo Sounders*. <http://www.nauticalcharts.noaa.gov/hsd/multibeam.html>.

- National Research Council. 1959. *Radioactive Waste Disposal Into Atlantic and Gulf Coastal Waters: A Report from a Working Group of the Committee on Oceanography*. Washington, DC: National Academy of Sciences--National Research Council, 37 pp.
- . 2015. *Sea Change: 2015-2025 Decadal Survey of Ocean Sciences*. Washington, DC: National Academies Press.
- Nautical Archaeology Society. 2009. *The NAS guide to principles and practice (2nd ed.)*. Boston, MA: Blackwell.
- Naval Research Laboratory. 2009. "EM61-MK2 Response of Three Munitions Surrogates, NRL/MR/6110-09-9183." Washington, DC. https://cluin.org/conf/itrc/uxoq_041310/MR_9183.pdf.
- Nordfjord, S. 2006. *Late Quaternary Geologic History of New Jersey Middle and Outer Continental Shelf*. Austin: University of Texas.
- Orca Maritime Inc. 2015. *Technology Demonstration Report for Underwater Survey Equipment in support of Explosive Remnants of War (ERW) Technical Survey Operations*. Geneva: Geneva International Centre for Humanitarian Demining. <http://www.gichd.org/resources/publications/detail/publication/a-guide-to-survey-and-clearance-of-underwater-explosive-ordnance/#.WA-RAXkVCEw>.
- Pfeiffer, F. 2012. "Changes in Properties of Explosives Due to Prolonged Seawater Exposure." *Marine Technology Society Journal* 46 (1): 102-110.
- Pratt, S. 1973. "Benthic fauna. In: Coastal and offshore environmental inventory, Cape Hatteras to Nantucket Shoals." *Univ. R.I., Mar. Pub. Ser.* Vol 2: 5-1 - 5-70.
- Puleo, J. 2017. *Quantification of Hydrodynamic Forcing and Burial, Exposure and Mobility of Munitions on the Beach Face, MR-2503*. Accessed 2017. [https://www.serdpestcp.org/Program-Areas/Munitions-Response/Underwater-Environments/MR-2503/\(language\)/eng-US](https://www.serdpestcp.org/Program-Areas/Munitions-Response/Underwater-Environments/MR-2503/(language)/eng-US).
- Raineault, N.A., A.C. Trembanis, D.C. Miller, and V. Capone. 2013. "Interannual changes in seafloor surficial geology at an artificial reef site on the inner continental shelf." *Continental Shelf Research* 58: 67-78.
- Rennie, S.E., A. Brandt, and C.T. Friedrichs. 2017. "Initiation of motion and scour burial of objects underwater." *Ocean Engineering* 131: 282-294.
- Robins, T.M. 1926. "U.S. Army Corps of Engineers." *Memo to Office of Supervisor of New York Harbor, Subject: Dumping Explosives At Sea, Southeast of Scotland Lightship*. August 20.
- Robinson, L. J., and O. Bjorkheim. 1989. "Interferometry; An Alternate Method In Sonar Mapping." *OCEANS '89. Proceedings*. Seattle: IEEE. 1134-1135.
- Schultz, G. M., J. Keranen, S. Billings, J. Foley, R. Fonda, and J. Hodgson. 2011. "Integrated methods for marine munitions site characterization: Technical approaches and recent site investigations." *Marine Technology Society Journal* 45 (6): 47-61.

- Schwartz, A., and E. Brandenburg. 2009. "An Overview of underwater technologies for operations involving underwater munitions." *Marine Technology Society Journal* 43 (4): 62-75.
- Secretary of War. 1944. "Danger Zone Regulations." *204.7 Atlantic Ocean in Vicinity of No Man's Land Island, Mass.; U.S. Navy Restricted Area*. January 8.
- Sonardyne. 2010. "Datasheet: Solstice Sidescan Sonar." April. Accessed January 2017. http://auvac.org/uploads/manufacturer_spec_sheet_pdf_sonar/sonardyne_Solstice%208200.pdf.
- . 2014. "C-Worker 6 set sail with GyroUSBL." *Baseline*, Spring: 6.
- Soulsby, R.L., R.J.S. Whitehouse, and K.V. Marten. 2012. "Prediction of time-evolving sand ripples in shelf seas." *Cont. Shelf Res.* 38: 47-62.
- Steimle, F.W., and C. Zetlin. 2000. "Reef habitats in the Middle Atlantic Bight: abundance, distribution, associated biological communities, and fishery resource use." *Mar. Fish. Rev.* Vol 62(2):24-42.
- Stevenson, D. 2004. *Characterization of the fishing practices and marine benthic ecosystems of the northeast U.S. shelf, and an evaluation of the potential effects of fishing on essential fish habitat*. Woods Hole, MA: U.S. Deptment of Commerce, National Oceanic and Atmospheric Administration, Northeast Fisheries Science Center. <http://purl.access.gpo.gov/GPO/LPS120183>.
- Strategic Environmental Research and Development Program. 2009. "Marine UXO characterization based n autonomous underwater vehicle (AUV) technology final technical report, MR-1631." <https://www.serdp-estcp.org/Program-Areas/Munitions-Response/Underwater-Environments/MR-1631>.
- Strategic Environmental Research and Development Program. 2013. "Detection of underwater UXOs in mud." <http://www.serdp-estcp.org/Program-Areas/Munitions-Response/Underwater-Environments/MR-2200/MR-2200>.
- Sumer, B.M., N. Christiansen, and J. Fredsøe. 1992. "Time scale of scour around a vertical pile" . *Proc. 2nd Int. Offshore Polar Eng. Conf.* San Francisco, CA. 308-315.
- Teledyne. 2013. "Workhouse Navigator, Doppler Velocity Log." http://rdinstruments.com/_documents/Brochures/navigator_datasheet_lr.pdf.
- The Nature Conservancy. 2016. "Northwest Atlantic Marine Ecological Risk Assessment." Accessed 5/6/2016. <http://maps.tnc.org/namera>.
- Thomson, D. 2005. "Acoustic Positioning Systems." http://www.ths.org.uk/documents/ths.org.uk/downloads/2005-04-05-hydrofest-3_acoustics.pdf.
- Traykovski, P. 2007. "Observations of wave orbital scale ripples and a non-equilibrium time dependent model." *Journal of Geophysical Research-Oceans* 112: C06026.
- Traykovski, P. 2017. *Continuous Monitoring of Mobility, Burial and Re-Exposure of Underwater Munitions in Energetic Near-Shore Environments, MR-2319*. Accessed

2017. [https://www.serdp-estcp.org/Program-Areas/Munitions-Response/Underwater-Environments/MR-2319/\(language\)/eng-US](https://www.serdp-estcp.org/Program-Areas/Munitions-Response/Underwater-Environments/MR-2319/(language)/eng-US).
- Traykovski, P., M.D. Richardson, L.A. Mayer, and J.D. Irish. 2007. "Mine burial experiments at the Martha's Vineyard Coastal Observatory." *IEEE Journal of Oceanic Engineering* 32(1): 150-166.
- Trembanis, A., C. DuVal, J. Beaudoin, V. Schmidt, D. Miller, and L. Mayer. 2013. "A detailed seabed signature from Hurricane Sandy revealed in bed forms and scour." *Geochem. Geophys. Geosyst.* 14 (10): 4334-4340.
- Trembanis, A.C., C.T. Friedrichs, M.D. Richardson, P. Traykovski, P.A. Howd, P.A. Elmore, and T.F. Wever. 2007. "Predicting seabed burial of cylinders by wave-induced scour: application to the sandy inner shelf off Florida and Massachusetts. IEEE Jo." *IEEE Journal of Oceanic Engineering* 32(1): 167-183.
- U.S. Air Force. 2014. "Military Munitions Response Program, Underwater Military Munitions Guidance."
- U.S. Army Corps of Engineers. 1994. "Ordnance and Explosive Waste, Archives Search Report, Findings for Assateague Island, Ocean City, Maryland, FUDS No. C03MD093001." June.
- . 1997. *Ordnance and Explosive Chemical Warfare Materials, Archives Search Report Findings, Fort Miles Military Reservation, FUDS Project C03DE006304*. St. Louis District.
- . 2006. "Final Military Munitions Remedial Investigation Report for the Former Fort Miles Military Reservation, Lewes, Delaware, Project C03DE006304." URS Corporation, September.
- . 2010. "Site Inspection Report for Delaware Target Areas, Sussex County, DE, FUDS Project No. C03DE006402."
- . 2013a. *Formerly Used Defense Sites Inventory*. Accessed 2016. www.fuds.mil.
- . 2013b. "Hydrographic Surveying. Engineering Pamphlet EM 1110-2-1003." http://www.publications.usace.army.mil/Portals/76/Publications/EngineerManuals/EM_1110-2-1003.pdf?ver=2014-01-06-155809-307.
- . 2014a. *Final Feasibility Study Report for Nantucket Beach, Former Nantucket Ordnance Site A.K.A. Tom Nevers Rocket Projectile Target; Tom Nevers Area, Formerly Used Defense Site Project D01MA045601, Aerial Rocket Range Target #1 Munitions Response Site*. New England District. Accessed 2016. <http://www.nae.usace.army.mil/Portals/74/docs/Topics/Nantucket/NantucketFinalFS.pdf>.
- . 2014b. "Preliminary Assessment, Cape Pogue Little Neck Bombing Target Site, Chappaquiddick Island, MA, FUDS # D01MA0595." <http://www.nae.usace.army.mil/Portals/74/docs/Topics/MarthasVineyard/CapePogue/CapePogueLittleNeckBTSiteFINAL-PARreport.pdf>.
- . 2015a. "Decision Document, Nantucket Beach, Former Nantucket Ordnance Site, A.K.A. Tom Nevers Rocket Projectile Target; Tom Nevers Area, FUDS Site # D01MA045601AND D01MA045602."

- <http://www.nae.usace.army.mil/Portals/74/docs/Topics/Nantucket/NantucketFinalDecisionDocument.pdf>.
- . 2015b. "Former Duck Target Facility Munitions Response Site, Remedial Investigation, Technical Project Planning Meeting 1." March 12.
http://www.townofkittyhawk.org/vertical/sites/%7B991BBDF3-791F-4435-80BA-FEB8F8D09BA4%7D/uploads/Appendix_B_-_Former_Duck_Target_Facility_Munitions_Response_Site.pdf.
- . 2015c. "Final Decision Document, Former Cape Poge Little Neck Bomb Target, Munitions Response Sites, Martha's Vineyard, MA." Accessed 2016.
<http://www.nae.usace.army.mil/Portals/74/docs/Topics/MarthasVineyard/CapePoge/CapePogeDecisionDoc.pdf>.
- . 2015d. *Final Feasibility Study, Tisbury Great Pond Munitions Response Area*. New England District.
<http://www.nae.usace.army.mil/Portals/74/docs/Topics/MarthasVineyard/Tisbury/TisburyFeasibilityStudy.pdf>.
- U.S. Army. 1944. "Supplement to the Harbor Defense Projects of New York."
- . 1945a. "Supplement to the Harbor Defense Project of The Delaware Bay."
- . 1945b. "Supplement to the Harbor Defense Project of Long Island Sound."
- . 1945c. "Supplement to the Harbor Defense Project of Narragansett Bay."
- . 2014. "Safety Risk Management." *Department of the Army Pamphlet 385-30*. December 2. 34 pp.
- U.S. Climate Data. 2016. *Climate Data for Lewes, DE*. Accessed May 5, 2016.
<http://www.usclimatedata.com/climate/lewes/delaware/united-states/usde0030>.
- U.S. Coast Guard. 1946. "(4163) Rhode Island - Narragansett Bay approach - Emergency bomb jettisoning area established." *Notice to Mariners*. July 20.
- U.S. Department of Commerce. 1947. "Restricted, Danger, and Anchorage Areas Information Supplementing United States Coast Pilots." January 1.
- . 1961. "United States Coast Pilot, Atlantic Coast." June 17.
- U.S. Environmental Protection Agency. 2006. *Guidance on Systematic Planning Using the Data Quality Objectives Process EPA QA/G-4 (EPA/240/B-06/001)*. USEPA, Quality System.
https://www.epa.gov/sites/production/files/documents/guidance_systematic_planning_dqo_process.pdf.
- U.S. Geological Survey and University of Colorado. 2005. "ATL_PRS: usSEABED PaRSed data for the entire U.S. Atlantic Coast." Accessed May 6, 2016.
http://pubs.usgs.gov/ds/2005/118/htmldocs/data_cata.htm. Last accessed 5/6/2016.
- U.S. Government Printing Office. 2016a. "33 CFR § 334.380 Atlantic Ocean south of entrance to Chesapeake Bay off Dam Neck, Virginia; naval firing range." *Code of Federal Regulations*. 547.
- . 2016b. "33 CFR § 334.390 Atlantic Ocean south of entrance to Chesapeake Bay; firing range." *Code of Federal Regulations*. 547-548.

- . 2016c. "33 CFR § 334.330 Atlantic Ocean and connecting waters in vicinity of Myrtle Island, Va.; Air Force practice bombing, rocket firing, and gunnery range." *Code of Federal Regulations*.
- U.S. Naval Air Station. 1945. "Ordnance Officer, Memo to Chief of the Bureau of Ordnance, Subject: Aircraft Bomb Fuzes Navy Type - Surveillance and Disposal of." March 14.
- U.S. Navy. 1919. "Log Book of the U.S.S. Elinor." February 1-28.
- . 1944a. "Practice Bombing Target Sites: U.S. Naval Air Station, Quonset Point, RI." May 26.
- . 1945a. "Memo from Commander Northern Group to Commandant U.S. Coast Guard. Subject: Request for Amendment of Restricted Areas for Gunfiring Ranges, Eastern Sea Frontier." March 17.
- . 1945b. "Bureau of Ordnance, Firing Range at Island Beach, New Jersey." February 8.
- . 1945c. "Commander Fifth Naval District, Status and Future Need for Targets in Naval Air Bases 5th Naval District." September 14.
- . 1946a. "Commander Fifth Naval District, Decontamination of Naval Facilities Declared Surplus." October 9.
- . 1946b. *Memo from Commander Eastern Sea Frontier Subject: Request for Retention of Danger and Caution Areas*. June 3.
- . 1946c. "Memo from Commander Eastern Sea Frontier Subject: Request for Retention of Danger and Caution Areas." April 30.
- . 1947a. "Compilation of Naval Air Targets, Gunnery and Bombing Areas. Office of the Chief of Naval Operations. 26 June."
- . 1947b. "Memo from Chief of Naval Operations to Commandant, Fifth Naval District, Subject: Regulations Governing Use of a Water Area off Cape Henry, VA." Bureau of Ordnance, October 30.
- . 1948. "Massachusetts, Nantucket Sound, Dangerous Area." *Index to Notices to Mariners Nos. 27 to 52, Inclusive*, Page 1842.
- . 1953. "Disposition of Sinkable Objects in Harbors and Approaches, Eastern Sea Frontier." December 10.
- . 1957. "Memo from Commandant Fifth Naval District, To Commander Eastern Sea Frontier, Subject: Live ammunition in approaches to Norfolk." October 16.
- . 1976. "Range Survey: No Man's Land Island, Naval Air Station, South Weymouth." January
- . 2008. *Marine Resources Assessment Update for the Virginia Capes Operating Area*. Department of the Navy, U.S. Fleet Forces Command, Norfolk, Virginia. Contract #N62470-02-D-9997, CTO 0056. Prepared by Geo-Marine, Inc., Hampton, Virginia.
- U.S. Navy at Cape Henlopen. 2016. *Submarines at the Cape: Friend and Foe*. Accessed May 2016. <http://www.navyatcapehenlopen.info/plussubmarinesatcape.html>.
- U-Boat Net. 2016. Accessed May 2016. <http://uboat.net/> and http://uboat.net/maps/us_east_coast.htm.

- University of Delaware. 2015. "R/V Hugh R. Sharp."
https://www.ceoe.udel.edu/File%20Library/Schools%20and%20Departments/School%20of%20Marine%20Science%20and%20Policy/Marine%20Operations/overview_2015_web.pdf.
- Voropayev, S.I., F.Y. Testik, H.J.S. Fernando, and D.L. Boyer. 2003. "Burial and scour around short cylinder under progressive shoaling wave." *Ocean Engineering* 30: 1647-1667.
- Voulgaris, G., and J.P. Morin. 2008. "A long-term real time sea bed morphology evolution system in the south Atlantic Bight." *Proceedings of the IEEE/OES/CMTC Ninth Working Conference on Current Measurement Technology, March 17-19, 2008*. Charleston, SC.
- War Department. 1920. "Water Transportation Division, Dumping Shells at Sea." May 15.
- Whitehouse, R. 1998. *Scour at Marine Structures, A Manual for Practical Applications*. London, UK: Thomas Telford.
- Wiberg, P.L., and C.K. Harris. 1994. "Ripple Geometry in Wave Dominated Environments." *Journal of Geophysical Research* 99(C4): 775-789.

Page Intentionally Left Blank.

Appendix A – In-Field Verification Trip Report

In-Field Testing and Methodology Verification Trip Report Bureau of Ocean Energy Management (BOEM) Unexploded Ordnance (UXO) Survey Methodology Investigation 10 August 2016

1. Introduction

In accordance with proposed efforts for BOEM’s UXO Survey Methodology Investigation, University of Delaware team members conducted an in-field verification of remote sensing technologies and methods for munitions and explosives of concern (MEC) detection selected from an intensive review of historical data, Wind Energy Area (WEA) physical site characteristics, and remote sensing technologies. Field work occurred over 12 July and from 18 to 28 July 2016 in the Delaware WEA. As outlined in the work plan, field work was conducted by two teams: a site preparatory team, and a search team. The preparatory team was tasked with surveying and identifying the field site, subsequently seeding the field site with munitions surrogates and placing the Instrument Verification Strip (IVS). The search team was tasked with testing the performance of the technologies and methods selected by the review process (see Technical Memorandum for Tasks 1 and 2) in their ability to positively locate and identify munitions surrogates and to evaluate methods for optimizing survey performance. Technologies selected for this task included: an dual-frequency 230/550 kHz EdgeTech 6205 phase-measuring bathymetric and side-scan sonar, and a Teledyne Gavia autonomous underwater vehicle (AUV) equipped with a selectable frequency 900/1800 kHz Marine Sonics side-scan sonar, Geometrics G880-AUV cesium vapor magnetometer, and 2 megapixel Point Grey color camera. Initial site selection and mapping took place on 12 July 2016. Site seeding with munitions surrogates and establishment of the IVS and preparation took place 18-19 July 2016. Search team operations were conducted from 20-28 July 2016. Daily operations are summarized below.

Day 1 – 12 July 2016

Objectives: Conduct surface vessel surveying of proposed field site with EdgeTech 6205 sonar. Surveying to include both 5 km “cable route” path and 2 x 2 km wind turbine box. Need to identify any large features or hazards that may complicate AUV operations.

Summary: Departed dock 0815 and proceeded to study area on *R/V Joanne Daiber*. After initial sonar calibration setup, surveying began on western end of proposed cable route and moved into the 2 x 2 km box. Surveying accomplished >200% coverage of dual-frequency 230/550 kHz side-scan sonar and >100% 550 kHz bathymetric of the entire survey. Complimentary conductivity-temperature-depth (CTD) and sound velocity profiles were collected at approximately 1 hour intervals. Surveying was completed within 6 hours. Returned to dock 1735.

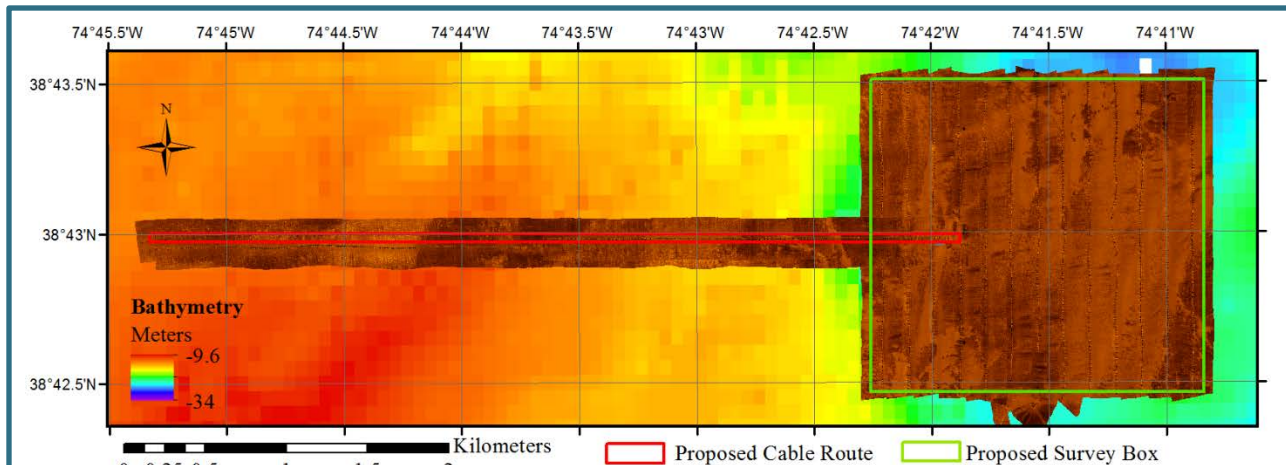


Figure 1: Side-scan sonar coverage of the cable route and 2 x 2 km survey box collected on 12 July 2016. Proposed survey areas were maintained for the remainder of the study.

Conclusions: Survey data showed no potential targets or obstructions to operations within the proposed field area. The area had low vessel traffic during survey operations. The proposed field site was finalized for seeding operations set to begin 18 July 2016.

Time on Water: 0815 – 1735

Personnel: Carter DuVal, deputy Principal Investigator (PI), Capt. Kevin Beam, and science team crew of Ken Haulsee, Alimjan Abla, and Peter Barron.

Data Collected: Bathymetry, Side-Scan Sonar, CTD

Day 2 – 18 July 2016

Objectives: Place IVS on site near the junction of cable route and planned AUV node survey box 2 along E-W orientation. Once in place, SCUBA divers, tracked from the surface by ultra-short baseline (USBL) navigation, will verify location and orientation of munition surrogates along the IVS. Divers will be recovered and taken back to shore, where munition surrogates for seeding the survey area will be loaded. *R/V Daiber* will return to the site and commence seeding of the western edge of the cable route as time allows.

Summary: Departed dock 0643 with SCUBA divers and IVS on board. Arrived onsite 0820 and commenced IVS placement. Difficulties with IVS placement resulted in SW-NE orientation and possibility of clumping of smaller munition surrogates at end of IVS. In preparation for SCUBA divers, surface buoy was attached to IVS, but buoy line became caught in *R/V Daiber's* starboard propeller. After unsuccessful attempts to free line, the buoy was cut and recovered. A second buoy was placed in the vicinity of the IVS. After anchoring, diver operations commenced 1027. Strong currents forced dive mission to be aborted at 1035. Divers were recovered. At 1100, surveying of IVS started. IVS was partially visible in data. Surveying ceased at 1125, and the

R/V Daiber departed site. Arrived dockside 1255 and commenced offload of SCUBA divers and equipment, and loaded one-half of surrogates. Departed dock by 1345 and proceeded to site. Marine weather conditions had deteriorated since the morning operations, and continued to worsen, forcing reduction in vessel speed. At 1447, the decision was made to return to port, as conditions had become too rough for safe deck operations. Instead, *R/V Daiber* returned to Delaware Bay and USBL tests were conducted to ensure USBL tracking of surrogates during deployment. Tests were successful. *R/V Daiber* returned to dock 1633.

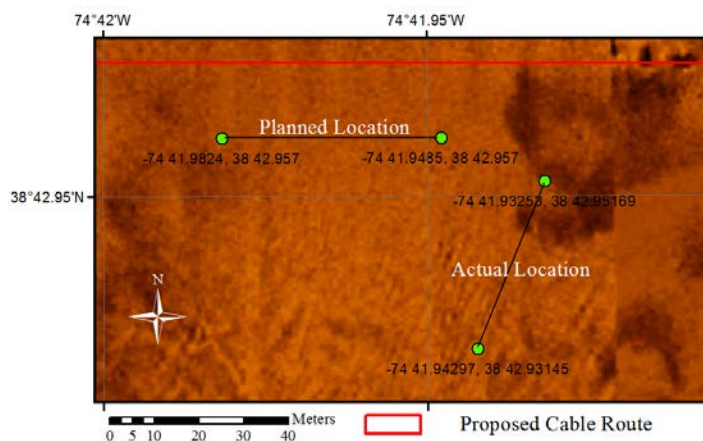


Figure 2: The IVS (left) was deployed in the vicinity of the planned location, but laid out in a NE-SW orientation instead of the planned E-W orientation. Verification from the AUV (see Day 5), indicated the IVS items were spaced and oriented appropriately.

Conclusions: The issues with the IVS require verification of exact location and proper surrogate alignment using the AUV. While the IVS appears to be laid out to its fullest extent, the surface survey could not fully resolve the surrogates along the IVS. This will likely have implication for the search team and their use of the 6205 to attempt to identify potential targets. The use of SCUBA divers was impeded by poor conditions on site. Regardless, the difficulties encountered suggest that SCUBA should be avoided for such operations in the future. Further, the decaying site conditions forced the *R/V Daiber* back to the more sheltered Delaware Bay, and surrogates seeding could not begin. This will require extra time dedicated to seed surrogates in the following days, although setup and verification of the USBL system will allow for immediate deployment.

Time on Water: 0643-1255, 1345-1633

Personnel: Carter DuVal, deputy PI, Capt. Kevin Beam, Dr. Mark Moline, diver, Hunter Brown, diver, and science team crew of Tim Pilegard, Drew Friedrichs, and Peter Barron.

Data Collected: Bathymetry, Side-Scan Sonar, CTD

Day 3 – 19 July 2016

Objectives: Start seeding munitions surrogates along the cable route. Surrogates will be placed in five groups within the cable route, each within a 1 km section of the cable route as stipulated in the work plan. If time allows, begin surrogate placement the 2 x 2 km survey box.

Summary: Remaining seeds were loaded onboard vessel starting 0700. By 0720, *R/V Daiber* departed dock for field site. *R/V Daiber* arrived on western end of cable route at 0845. CTD cast taken 0915 indicated a thermocline between 10 – 15 m water depths. Cable route seeding operations commenced 0934. USBL performance was satisfactory, and seeding progressed more rapidly than anticipated. Cable route seeding was concluded by 11:35, with all seeds successfully placed and positions recorded by USBL. At 1155, seeding was started within 2 x 2 km survey box. Issues with USBL performance were immediately apparent. A second CTD cast confirmed the presence of a sharp thermocline between 10-15 m water depths. USBL tracking was found to fail at depths below this thermocline. After several attempts, USBL tracking was abandoned, and seeds were marked by topside vessel location. Seeds were lowered directly below GPS antenna via rope and dropped once the rope was observed to have settled straight below the vessel. Seeding of all three groups was completed by 1440. In total, eight groupings of 62 total seeds were placed within the cable route and 2 x 2 km box. Surface sonar survey commenced 1505 to map in eight seeded areas. Mapping was completed by 1615, and vessel returned to dock by 1730.



Figure 3: Munitions surrogates (left) were initially lowered on a slack-line with USBL puck (right) attached. The USBL was abandoned for the later deployments due to complications from a strong thermocline. Vessel GPS was used to mark the remainder of the surrogate positions.

Conclusions: While seeding operations occurred more rapidly than anticipated, USBL performance was significantly hindered by a strong thermocline at greater depths. While vessel location was used to record the remaining surrogates, it is unlikely that these positions will be as accurate as the USBL aided locations, although within acceptable tolerances outlined by the work plan. USBL performance will hinder ROV navigation if used for visual target confirmation. The AUV may be a better solution for visual target confirmation by search team. CTD casts must be taken periodically throughout each day to account for the strong thermocline.

Time on Water: 0720-1730

Personnel: Carter DuVal, deputy PI, Capt. Kevin Beam, and science team crew of Tim Pilegard, Drew Friedrichs, Aviah Stillman, and Thaowan Giorno.

Data Collected: Bathymetry, Side-Scan Sonar, CTD, USBL Positioning

Day 4 – 20 July 2016

Objectives: Search team to begin surveying cable route and survey box with EdgeTech 6205 vessel-mounted sonar. Goal is to achieve 200% side-scan coverage and 100% bathymetric coverage of the search area. Team will process sonar and identify any potential targets for follow up by AUV survey.

Summary:

This was the first day for the search team and began at 0800 departing the dock in Lewes, DE. The search team arrived on station at 0932 and began with the deployment of the 6205 sonar pole and calibration sequence of the Coda F190R+. During the INS alignment period the team performed the first CTD cast for sound velocity profiling at 0940. Coda F190 Calibration was complete by 1013 at which point the team commenced to run the 5 km cable route. At the end of the cable route a time sync poor status message was noted coming from the EdgeTech laptop and this prompted a reboot of the EdgeTech computer and ultimately a restart of the Coda F190 to fully remove this error. Following completion of the 5 km cable route survey the team conducted another CTD cast for sound velocity profiling at 10:55. Next the search team commenced running the North-South survey lines to cover the 2 x 2 km survey box. CTD/Sound Velocity Profile casts were taken approximately every hour throughout the day. While continuously monitoring the live-feed of both high and low frequency sonar channel data coming in from the 6205 the team was unable to discern any targets of interest. The wide area swath survey did achieve full side-scan and bathymetry coverage and the resulting mosaics provide excellent bathymetric, geomorphic, and geological surface texture information about the site with clearly visible heterogeneity in sonar return apparent on the seabed throughout the search domain.

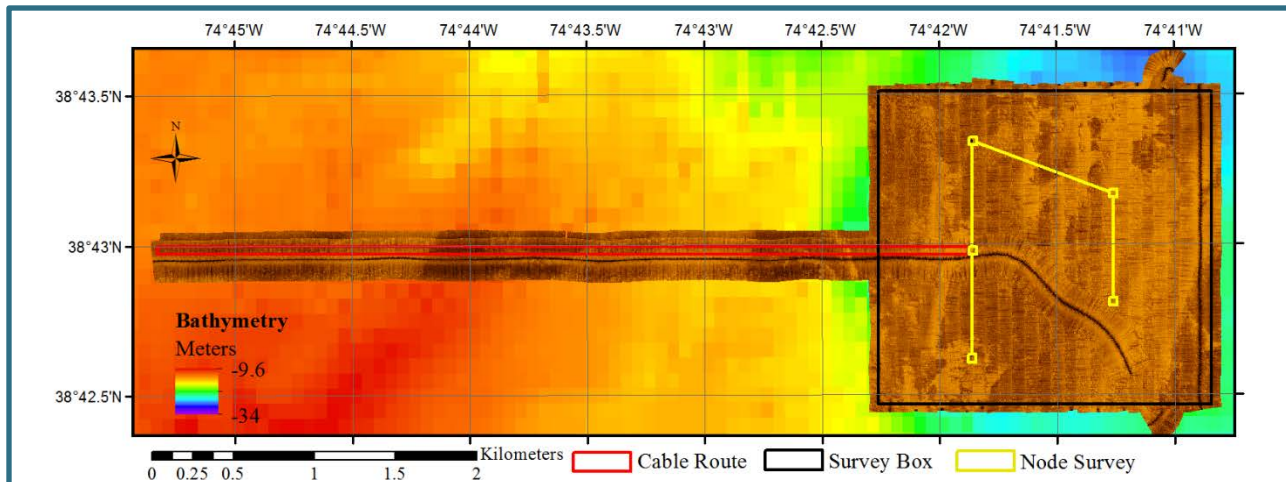


Figure 4: Side-scan sonar coverage of the cable route and 2 x 2 km survey box collected on 20 July 2016.

Conclusions: Sonar coverage goals were easily achieved. The time sync error message does not affect the sonar data visualization for targeting of seeds and the positioning and attitude metrics were never above threshold criteria still the team opted to restart the system just to be safe. However, no discernable targets of interest were identified by the team. Search team will conduct AUV mission to search for targets.

Time on Water: 0800 – 1630

Personnel: Dr. Art Trembanis PI, Capt. Kevin Beam and science team crew of Ken Haulsee, Dr. Doug Miller, Ellie Rothermel.

Data Collected: Bathymetry, Side-Scan Sonar, CTD

Day 5 – 21 July 2016

Objectives: Search Team will reacquire the IVS with the AUV and determine the specific location and strike. Once established, the AUV will fly the established IVS mission to evaluate for side-scan sonar and magnetometer performance. The search team will then begin surveying the monopile node locations specified by the seeding team. Monopile locations will be surveyed according the work plan, using high-resolution side-scan and magnetometry. At the end of the day, the IVS will be surveyed again.

Summary: Loaded AUV on board and departed dock 0730. Arrived on site 0900 and started preparations for AUV survey. Started first AUV IVS search mission 0934 and completed the mission at 1002. Located a portion of the IVS. Survey was adjusted accordingly and a second search mission was started 1013. AUV completed mission 1041. IVS was completely mapped. IVS lies along a 200° strike, and all objects were determined to be in the correct orientation. The IVS mission adapted and the AUV sent on the IVS mission at 1126. The mission was completed

at 1143. Due to proximity, the AUV was sent on a mission to map Node 2 and the cable route between Nodes 2 and 3. Node 2 mission started at 1155 and was completed at 1233. Preliminary sonar analysis indicated targets were present. The vehicle was then recovered and the battery replaced. The AUV was sent to run Node 3 and the cable route between Nodes 3 and 4 at 1328. The mission was completed at 1407. Preliminary sonar analysis indicated several potential targets. The AUV began the mission to map Node 4 and the cable route between Nodes 4 and 5 at 1417. The mission was completed at 1454. Preliminary results indicated several potential targets. The final mission was conducted over Node 5. The mission started at 1504 and was completed by 1533. Preliminary sonar analysis was inconclusive for targets. Due to time, the final IVS mission was scrapped. Returned to dock at 1720.

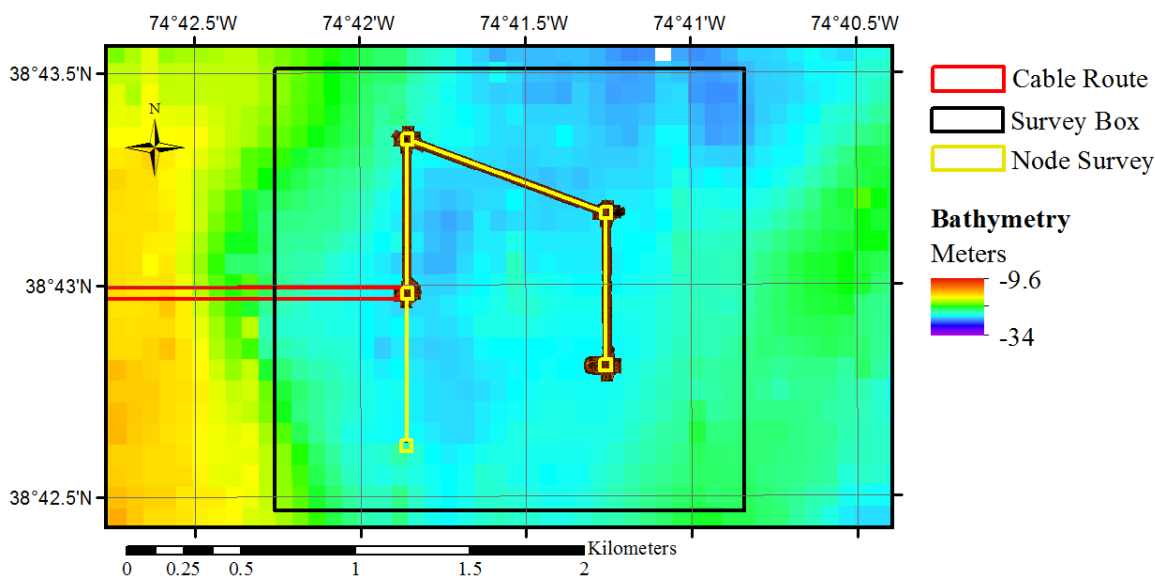


Figure 5: AUV side-scan sonar coverage of the Node surveys collected on 21 July 2016. Magnetometer coverage was collected concurrently.

Conclusions: The high-resolution from the side-scan was able to determine the IVS was deployed correctly. The position from the AUV, compared from the three morning missions over the IVS, suggested the AUV had a more accurate position for the IVS than determined from the deployment search. Preliminary magnetometer analysis from the IVS clearly indicated that the survey parameters were adequate to locate 8-inch and 155 mm surrogates. The scrapped IVS mission will be re-run with the same battery on the next mission.

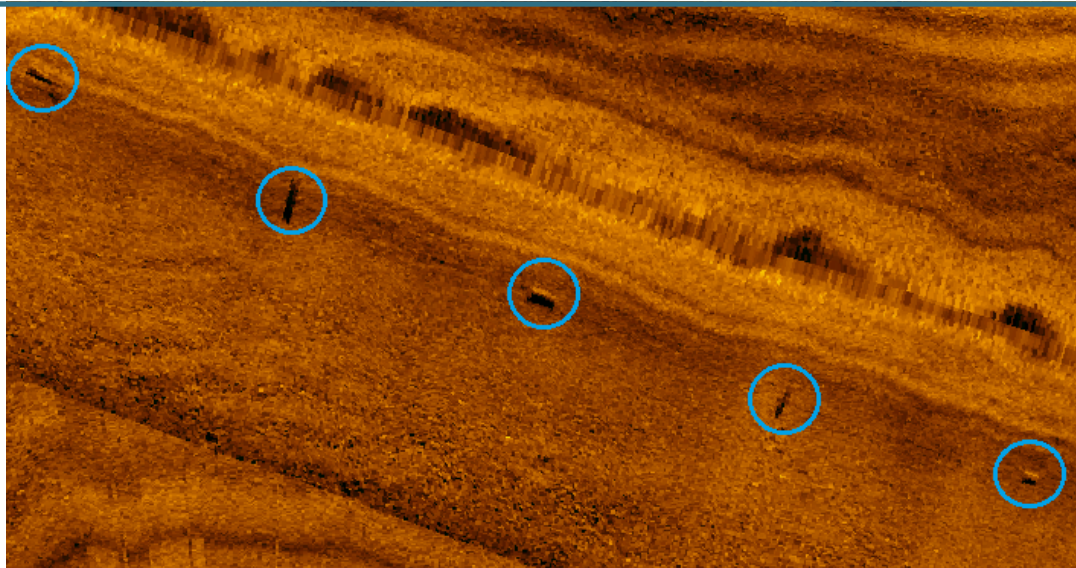


Figure 6: Side-scan sonar imagery of a portion of the IVS strip. The munitions surrogates are highlighted. Note the alternating orientation evident in the imagery.

Conditions for Friday, 22 July 2016 are questionable for AUV operations. Operations will resume Sunday, 24 July 2016.

Time on Water: 0730-1720

Personnel: Dr. Art Trembanis PI, Capt. Kevin Beam and science team crew of Ken Haulsee, Carter DuVal, Drew Friedrichs, and Ella Rothermel.

Data Collected: High-Resolution Side-Scan Sonar, Magnetometry, CTD

Day 6 – 24 July 2016

Objectives: Complete Node high-resolution side-scan and magnetometer survey missions. Repeat Node survey over area identified with magnetic and sonar surveys, testing variations in altitude and line spacing. If time, start mapping cable route.

Summary: Departed from dock 0800 and arrived on station at 0934. AUV ran IVS mission with battery used on previous day (mission from 1006-1023). After IVS mission, AUV was sent to complete node survey, covering Node 1 and the cable route between Nodes 1 and 2. Mission ran from 1044 – 1124. At 1150, started replicate missions over Node 3, which was determined by the search team to contain munition surrogates. The first Node 3 mission was flown at 4 m altitude (versus 2 m standard missions) with 8 m spacing to simulate 2 m surrogate burial for magnetometry. Mission was completed 1224. A second Node 3 mission (from 1232-1317) was flown at 4 m spacing with standard 2 m altitude. After completion of mission, AUV was recovered due to low battery, and battery was replaced. AUV was sent on first cable route mission at 1410 to collect high-resolution side-scan sonar and magnetometry. All cable route

missions will be conducted at 2 m altitude with 8 m line spacing. Mission was completed at 1558. AUV was sent on second IVS mission at 1606 to account for new battery. Mission was completed at 1624. AUV was recovered and *R/V Daiber* departed for dock. Arrived dockside at 1815.

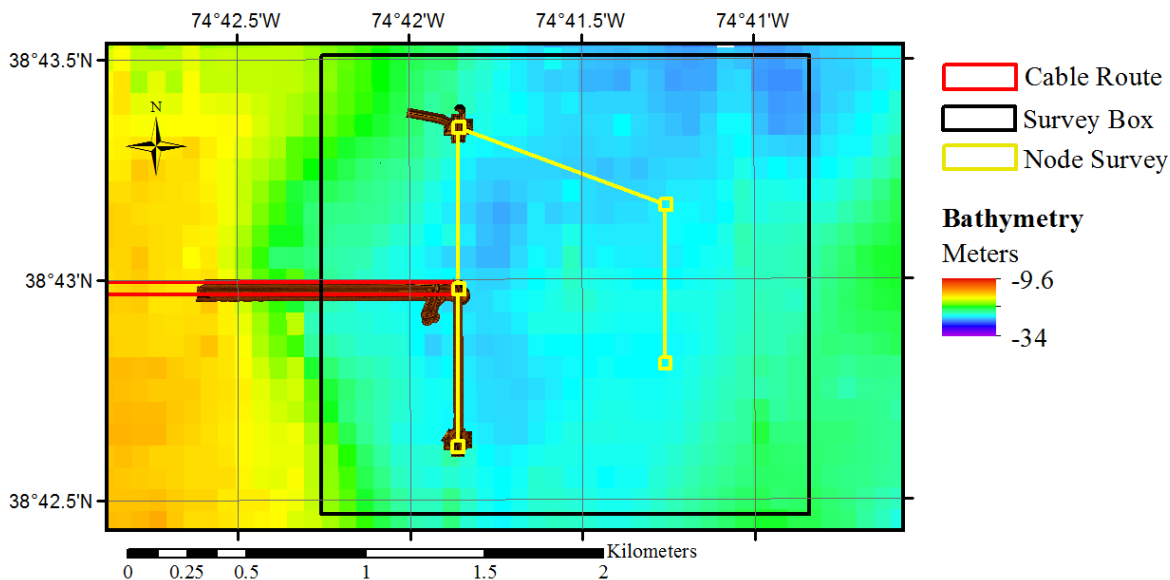


Figure 7: AUV side-scan sonar coverage of the node surveys collected on 24 July 2016. Magnetometer coverage was collected concurrently. Multiple surveys were conducted over Node 3 (NW corner) testing varying line spacing and AUV altitude.

Conclusions: Node 1 mission located potential targets in side-scan, although initial magnetometer results were inconclusive. Targets were noted in both magnetometer and side-scan sonar data for both Node 3 missions, indicating that magnetometer was able to detect some objects buried at depths of 2 m. Targets were also identified in side-scan sonar and magnetometer data for Cable Route 1 survey. No recommendations were made for the next day.

Time on Water: 0800-1815

Personnel: Dr. Art Trembanis PI, Capt. Kevin Beam and science team crew of Ken Haulsee, Carter DuVal, Tim Pilegard, and Alimjan Alba.

Data Collected: High-Resolution Side-Scan Sonar, Magnetometry, CTD

Day 7 – 25 July 2016

Objectives: Continue cable route surveys with AUV, collecting magnetometry and high-resolution side-scan sonar. At request of BOEM clients, two additional missions will be run over Node 3, testing performance of magnetometer at 4 m altitude with 4 m line spacing, and at 6 m altitude with 4 m line spacing. BOEM clients and project PI will be on board to observe.

Summary: Met BOEM clients and project PI at dock 0745. Departed dock 0805 for site. Arrived on site at 0940. Started initial IVS mission with AUV at 1012 and completed mission at 1028. AUV was sent on first of two Node 3 missions at 1051. AUV set to collect data at 4 m altitude and 4 m line spacing. Mission was completed at 1117. AUV was sent on second Node 3 mission at 1128. AUV set to collect data at 6 m altitude with 4 m line spacing. Mission was completed at 1158. AUV was recovered and battery replaced. AUV was redeployed at 1250 and sent on Cable Route 2 mission. Mission was completed at 1430. AUV was recovered and transported back to IVS to run final mission. IVS run was conducted from 1452 – 1505. Vehicle was recovered at 1512 and *R/V Daiber* departed for dock. Arrived dockside at 1650.

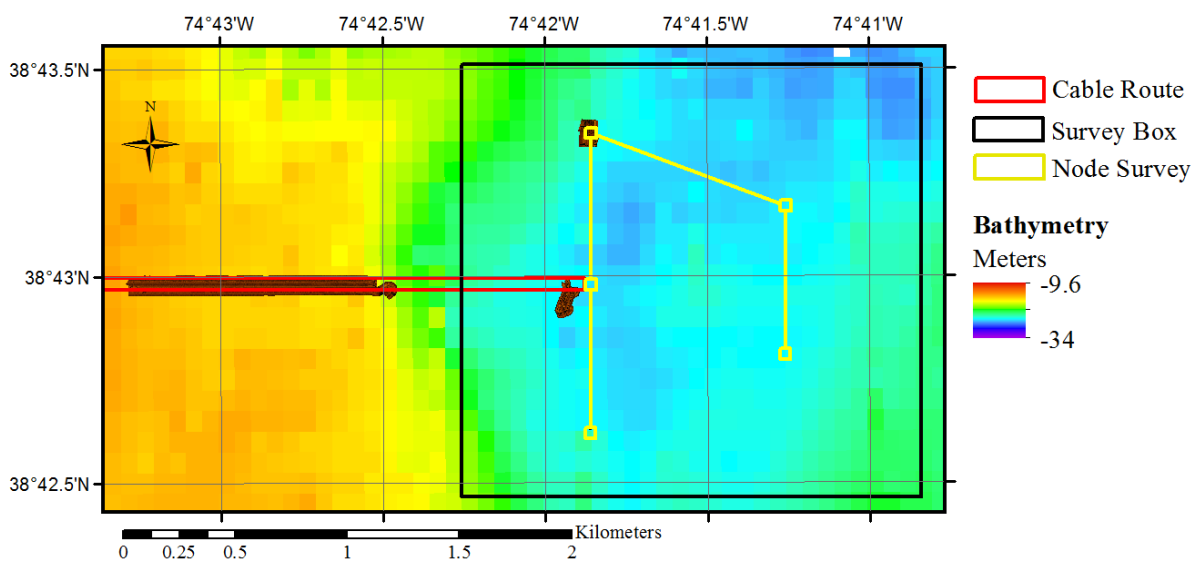


Figure 8: AUV side-scan sonar coverage of the node and cable route surveys collected on 25 July 2016. Magnetometer coverage was collected concurrently. Multiple surveys were conducted over Node 3 (NW corner) testing varying line spacing and AUV altitude.

Conclusions: Mission conducted successfully. Preliminary analysis suggests magnetometer still capable of detecting larger targets at 6 m altitude. Additional targets were identified from Cable Route 2 side-scan and magnetometer data. Cable Route missions will continue on the next work day.

Held discussions with BOEM client about performance of project and potential for follow-on project. Project would revisit the seeded areas several months after this field effort to see if munitions surrogates are still detectable. There is potential for transport and burial if storms occur over the area during the winter of 2016/2017. Team will follow up with the client regarding this potential study.

Time on Water: 0805-1650

Personnel: Dr. Art Trembanis PI, Capt. Kevin Beam and science team crew of Ken Haulsee, Carter DuVal, Drew Friedrichs, Alimjan Alba, Geoff Carton (CALIBRE), Jessica Stromberg (BOEM), and Jennifer Miller (BOEM).

Data Collected: High-Resolution Side-Scan Sonar, Magnetometry, CTD

Day 8 – 26 July 2016

Objectives: Continue to conduct cable route missions with AUV. If possible, complete cable route and begin AUV camera missions.

Summary: Departed dockside 0758. Arrived on station at 0930. Launched AUV and sent it on the first IVS mission at 0954. Mission was completed at 1008. AUV was recovered and transported to Cable Route 3 location. Vehicle was relaunched and sent on Cable Route 3 mission at 1057. AUV completed Cable Route 3 mission at 1229. AUV was sent on Cable Route 4 mission at 1247. Received aborted mission message from AUV at 1327 due to low battery; vehicle completed 2.5 lines of survey before mission aborted. AUV was recovered and the battery was replaced. Vehicle was relaunched and sent it on a mission to complete Cable Route 4 at 1419. The mission was completed at 1545. AUV was recovered once more and transported back to the IVS. AUV was sent on the final IVS mission at 1553, and it completed the mission at 1610. Vehicle was recovered and *R/V Daiber* departed site for dock at 1617. Arrived dockside at 1745.

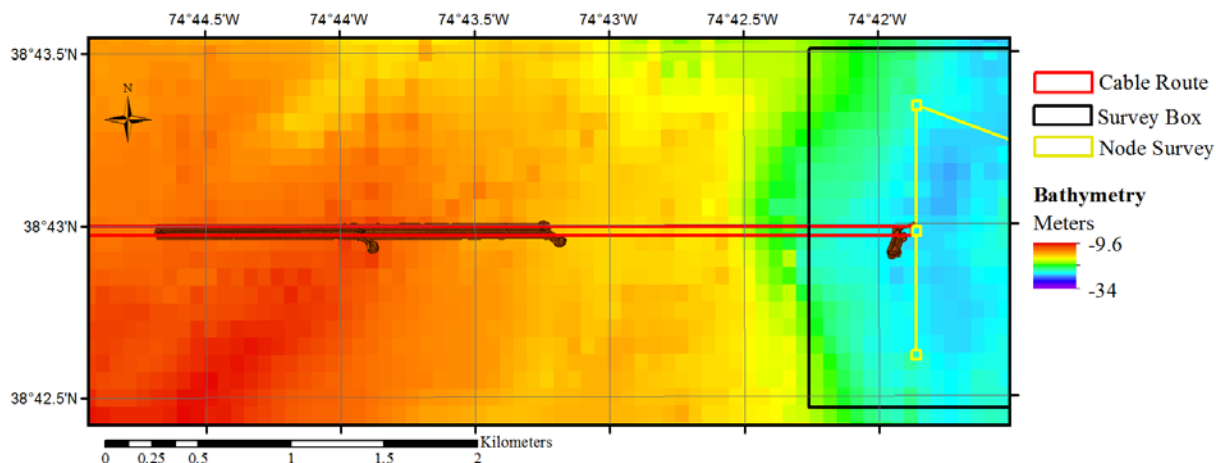


Figure 9: AUV side-scan sonar coverage of the cable route surveys collected on 26 July 2016. Magnetometer coverage was collected concurrently.

Conclusions: Despite the low battery abort on Cable Route 4 mission, the AUV was able to completely cover Cable Route 3 and 4 boxes. Magnetometer and side-scan sonar targets were identified within each survey. Due to time taken up by transporting vehicle back and forth to the IVS, as well as the delay caused by the aborted mission, we did not have time to conduct the final cable route mission. This will be completed on the next work day.

Time on Water: 0758-1745

Personnel: Dr. Art Trembanis PI, Capt. Kevin Beam and science team crew of Ken Haulsee, Carter DuVal, Drew Friedrichs, and Ella Rothermel.

Data Collected: High-Resolution Side-Scan Sonar, Magnetometry, CTD

Day 9 – 27 July 2016

Objectives: Complete final cable route mission and re-survey Node 1 and cable route between Nodes 1 and 2 to investigate potential side-scan targets further. Once completed, AUV camera missions will be conducted. AUV will collect images of Nodes 1 and 3.

Summary: Departed dock at 0803 and arrived on western end of cable route at 0912. AUV was launched and sent on final cable route survey at 0942. Mission was completed at 1155, arriving at surface nearly 40 minutes after anticipated return time. AUV was then taken to the IVS and sent on an IVS run at 1218, completing the mission at 1232. The AUV was recovered and the battery replaced. At 1311, the vehicle was relaunched and sent on a mission to investigate previously identified sonar targets in Node 1 and the cable route between Nodes 1 and 2. The vehicle completed the mission at 1356. The vehicle was then sent the final magnetometer IVS run at 1409. The mission was completed at 1425 and the vehicle was recovered for reconfiguration to camera missions. After configuration and ballasting, the AUV was sent to collect optical imagery and side-scan sonar data over the IVS at different altitudes at 1527. Mission was completed at 1545 and optical images reviewed to determine the best altitude. This was determined to be 2 meters. The vehicle was then sent on a mission to collect optical images and side-scan sonar in node at 1555. The mission was aborted due to low battery at 1630. The AUV was recovered, but not relaunched due to time. The *R/V Daiber* departed the study area and arrived dockside at 1818.

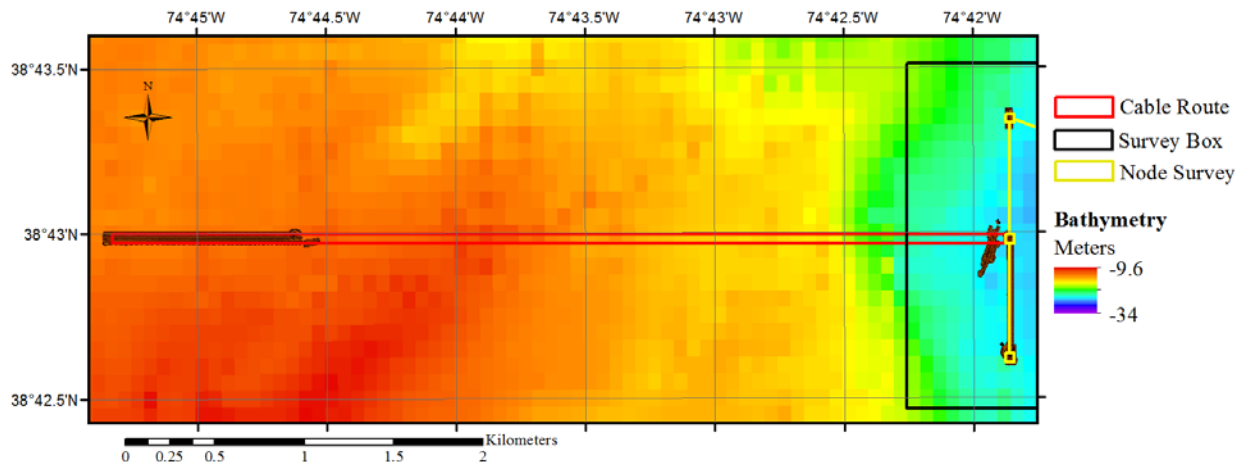


Figure 10: AUV side-scan sonar coverage of the node and cable route surveys collected on 27 July 2016. Magnetometer coverage was collected on cable route survey and Node 1. Camera surveys were conducted over the IVS and Nodes 3 (NW corner of Survey Box).

Conclusions: A review of mission logs indicated a strong current caused oscillations in AUV bottom tracking along first mission line of Cable Route 5, likely creating the 40 minute delay in return time. Data was reviewed and determined to be acceptable for target identification. The repeated survey of Node 1 and associated cable route determined that the sonar targets within Node 1 were likely not surrogates, although this will be verified with an AUV camera mission tomorrow. There was both magnetometer and side-scan targets identified from the cable route between Nodes 1 and 2. This will also be verified by AUV camera missions, and the Node 3 camera mission will be completed. The selection of 2 m altitude allowed for the best lighting of the seafloor, versus the 3 m, 2.5 m and 1.8 m (lowest possible with vehicle) altitudes tested. All remaining camera missions will be operated at 2 m altitude.

Time on Water: 0803-1818

Personnel: Dr. Art Trembanis PI, Capt. Kevin Beam and science team crew of Ken Haulsee, Carter DuVal, Peter Barron, Alex Maticcheri, and Hannah Rusch.

Data Collected: High-Resolution Side-Scan Sonar, Magnetometry, Photo, CTD

Day 10 – 28 July 2016

Objectives: Complete AUV camera mission over Node 3. Conduct additional AUV camera missions over Node 1 and Cable Route 1, and investigate potential targets between Nodes 1 and 2 with camera and high-resolution side-scan sonar. While the vehicle is on its final camera missions, recover the IVS.

Summary: Departed dock at 0640 and arrived on site at 0802. AUV was launched and sent on mission to survey Node 1, Node 2, and the cable route in between these nodes. The vehicle completed the mission at 0944. The AUV was then sent to run a camera and side-scan sonar mission over the IVS and to investigate targets identified within Cable Route 1. The vehicle aborted the mission due to low battery, while over Cable Route 1 targets. The vehicle was recovered at 1112 and the battery replaced. Relunched at 1529, the vehicle was sent to complete the investigating targets over Cable Route 1 and to complete the camera and side-scan sonar survey of Node 3 from the previous day. While on this mission, the *R/V Daiber* was repositioned to recover the IVS. The strip was grappled successfully at 1200, but attempts to recover the IVS were hampered by the weight and configuration of the strip. The recovery attempt was paused in order to recover the AUV, which completed its final mission at 1643. Once the AUV was recovered and stowed, attempts to recover the IVS resumed. After difficulty, two pieces from the IVS were recovered. However, during the recovery, the remainder of the IVS was lost. The decision was made to abort the recovery and to return to dock at 1330. Arrived dockside at 1500.

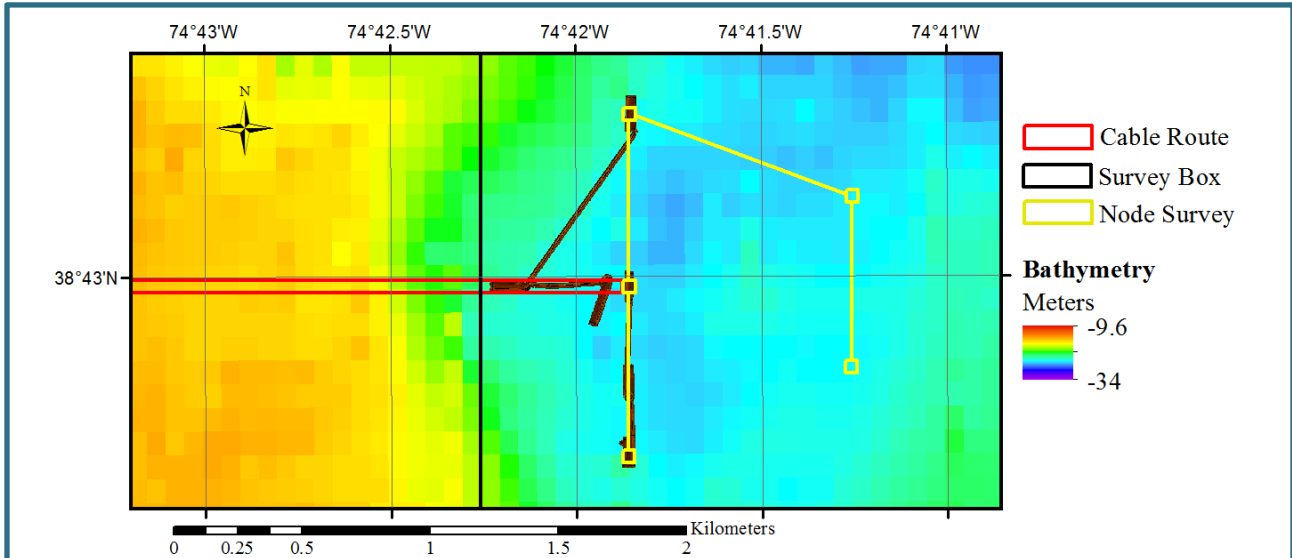


Figure 11: AUV side-scan sonar coverage of the node and cable route surveys collected on 28 July 2016. Camera surveys were conducted concurrently.

Conclusions: Targets were positively identified by camera imagery in Node 3, Cable Route 1 and the cable route between Nodes 1 and 2. However, the side-scan sonar targets within Node 1 were determined to be of geologic origin, having no associated magnetic signature and geological appearance in images. Heavy fog hampered locating and recovery of the AUV, and in the future, AUV mission may need to be suspended in similar conditions. Difficulties with the IVS recovery will lead to a redesign of IVSs in the future. While designed for proper orientation and spacing upon deployment, the location of the surrogates along the IVS line severely impeded the recovery attempts. Despite this, two of the six seeds from the IVS were recovered. This completed the in-field verification portion of the study.

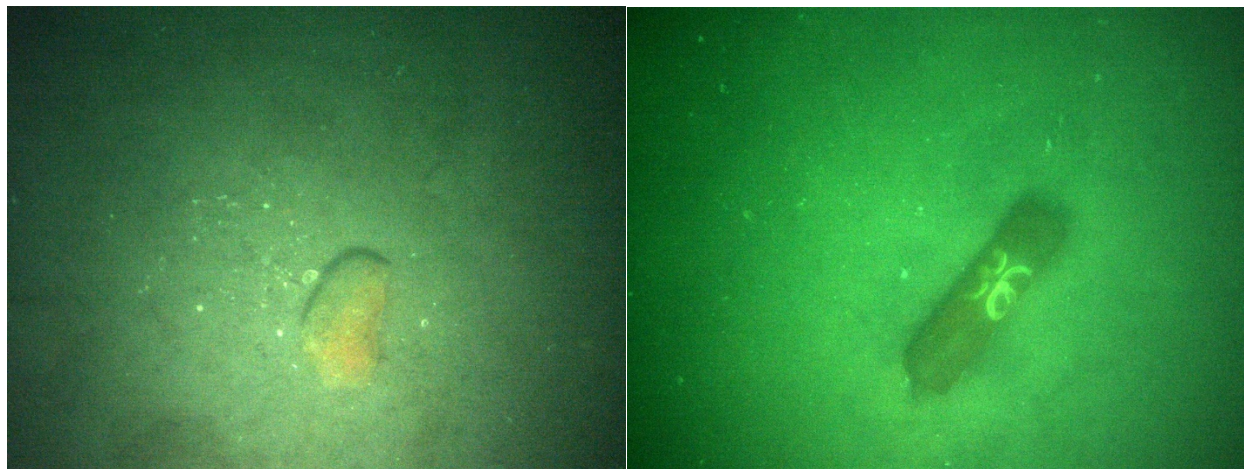


Figure 11: Imagery comparison of previously identified targets. The geologic target (left) had only a side-scan signature associated with it, while the surrogate (right), had both a side-scan sonar and magnetic signature.

Time on Water: 0640-1500

Personnel: Dr. Art Trembanis PI, Capt. Kevin Beam and science team crew of Ken Haulsee, Carter DuVal, Bryan Laboy, and Noah Engel.

Data Collected: High-Resolution Side-Scan Sonar, Photo, CTD

Project Participants

| <i>Shipboard Personnel</i> | <i>Role</i> | <i>Affiliation</i> |
|----------------------------|---|-----------------------------------|
| Alba, Alimjan | Graduate Student Observer | Middle East Technical University |
| Barron, Peter | NSF REU Intern | Carleton College |
| Beam, Kevin | Captain | University of Delaware |
| Brown, Hunter | SCUBA Diver | University of Delaware |
| Carton, Geoff | Observer | CALIBRE Systems |
| DuVal, Carter | Chief Scientist – Seeding Team | University of Delaware |
| Engel, Noah | Intern | U.S. Naval Academy |
| Friedrichs, Drew | Intern | Middlebury College |
| Giorno, Thaowan | NSF REU Intern | Beloit College |
| Haulsee, Kenny | Graduate Student Assistant – Search Team | University of Delaware |
| Laboy, Bryan | Intern | U.S. Naval Academy |
| Mataccheri, Alex | Intern | University of Delaware |
| Miller, Doug | Observer | University of Delaware |
| Miller, Jennifer | Observer | BOEM |
| Moline, Mark | SCUBA Diver | University of Delaware |
| Pilegard, Tim | Graduate Student Assistant – Seeding Team | University of Delaware |
| Rothermel, Ella | Intern | University of Delaware |
| Rusch, Hannah | Graduate Student Observer | University of Delaware |
| Stillman, Aviah | NSF REU Intern | University of Wisconsin - Madison |
| Stromberg, Jessica | Observer | BOEM |
| Trembanis, Art | Chief Scientist – Search Team | University of Delaware |

Page Intentionally Left Blank

Appendix B – Seed Descriptions and Location

Table B-1: Seed Sizes, and Locations

| Seed # | Type | Length (in) | Diameter (in) | Wall Thickness (in) | Weight (lbs) | Location |
|--------|--------|-------------|---------------|---------------------|--------------|---------------|
| 1 | 8" ISO | 36.25 | 8 | 0.36 | 85.5 | IVS |
| 2 | 8" ISO | 35.75 | 8 | 0.357 | 85.5 | IVS |
| 3 | 6" ISO | 24 | 6 | 0.295 | 35.5 | IVS |
| 4 | 6" ISO | 24.5 | 6 | 0.283 | 35.5 | IVS |
| 5 | 4" ISO | 12 | 4 | 0.262 | 10 | IVS |
| 6 | 4" ISO | 12.25 | 4 | 0.257 | 10 | IVS |
| 7 | 8" ISO | 34.5 | 7.5 | 0.278 | 48 | Cable Route 4 |
| 8 | 8" ISO | 34.5 | 7.5 | 0.27 | 47.5 | Node 4 |
| 9 | 8" ISO | 36.5 | 8 | 0.345 | 87 | Cable Route 2 |
| 10 | 8" ISO | 36.5 | 8 | 0.235 | 48.5 | Node 1 Route |
| 11 | 8" ISO | 36.5 | 8 | 0.342 | 87.5 | Node 3 |
| 12 | 6" ISO | 24 | 6 | 0.305 | 34 | Cable Route 5 |
| 13 | 6" ISO | 24 | 6 | 0.301 | 34 | Cable Route 3 |
| 14 | 6" ISO | 24 | 6 | 0.314 | 38.5 | Cable Route 3 |
| 15 | 6" ISO | 24 | 6 | 0.309 | 38.5 | Cable Route 4 |
| 16 | 6" ISO | 24 | 6 | 0.285 | 34.5 | Node 4 |
| 17 | 6" ISO | 24 | 6 | 0.28 | 35 | Node 4 |
| 18 | 6" ISO | 24 | 6 | 0.315 | 38.5 | Node 3 |
| 19 | 6" ISO | 24 | 6 | 0.256 | 32.5 | Node 3 |
| 20 | 6" ISO | 23.75 | 6 | 0.312 | 38 | Node 3 |
| 21 | 6" ISO | 23.75 | 6 | 0.355 | 38 | Cable Route 2 |
| 22 | 6" ISO | 24 | 6 | 0.29 | 37 | Cable Route 2 |
| 23 | 6" ISO | 24 | 6 | 0.275 | 35 | Cable Route 5 |
| 24 | 6" ISO | 24 | 6 | 0.275 | 33 | Cable Route 1 |
| 25 | 6" ISO | 24 | 6 | 0.308 | 37 | Cable Route 3 |
| 26 | 6" ISO | 24 | 6 | 0.282 | 33.5 | Cable Route 1 |
| 27 | 6" ISO | 24 | 6 | 0.316 | 38.5 | Node 1 Route |
| 28 | 6" ISO | 24 | 6 | 0.31 | 38.5 | Node 4 |
| 29 | 6" ISO | 24 | 6 | 0.317 | 38 | Node 1 Route |
| 30 | 6" ISO | 24 | 6 | 0.312 | 38 | Node 4 |
| 31 | 6" ISO | 23.75 | 6 | 0.295 | 37.5 | Node 4 |
| 32 | 6" ISO | 23.75 | 6 | 0.292 | 37 | Node 3 |
| 33 | 6" ISO | 23.75 | 6 | 0.271 | 34.5 | Node 1 Route |
| 34 | 6" ISO | 24 | 6 | 0.204 | 25 | Node 4 |
| 35 | 6" ISO | 24 | 6 | 0.203 | 24.5 | Cable Route 1 |
| 36 | 6" ISO | 24 | 6 | 0.203 | 25 | Node 3 |

| Seed # | Type | Length (in) | Diameter (in) | Wall Thickness (in) | Weight (lbs) | Location |
|--------|--------|-------------|---------------|---------------------|--------------|---------------|
| 37 | 6" ISO | 22.5 | 6 | 0.31 | 35.5 | Node 1 Route |
| 38 | 4" ISO | 12 | 4 | 0.259 | 11 | Node 3 |
| 39 | 4" ISO | 12 | 4 | 0.25 | 11 | Cable Route 3 |
| 40 | 4" ISO | 12 | 4 | 0.247 | 11 | Node 4 |
| 41 | 4" ISO | 12.25 | 4 | 0.252 | 11 | Node 4 |
| 42 | 4" ISO | 12 | 4 | 0.254 | 11 | Node 4 |
| 43 | 4" ISO | 12 | 4 | 0.246 | 10.5 | Node 3 |
| 44 | 4" ISO | 12 | 4 | 0.255 | 11 | Node 3 |
| 45 | 4" ISO | 12 | 4 | 0.256 | 11 | Cable Route 1 |
| 46 | 4" ISO | 12 | 4 | 0.259 | 11 | Cable Route 3 |
| 47 | 4" ISO | 11.75 | 4 | 0.251 | 10.5 | Node 3 |
| 48 | 4" ISO | 11.75 | 4 | 0.255 | 11 | Cable Route 2 |
| 49 | 4" ISO | 12 | 4 | 0.255 | 11 | Cable Route 5 |
| 50 | 4" ISO | 12 | 4 | 0.237 | 10 | Cable Route 5 |
| 51 | 4" ISO | 12 | 4 | 0.233 | 10 | Cable Route 4 |
| 52 | 4" ISO | 11.75 | 4 | 0.238 | 9.5 | Node 1 Route |
| 53 | 4" ISO | 12 | 4 | 0.236 | 10 | Cable Route 1 |
| 54 | 4" ISO | 12 | 3.5 | 0.23 | 8.5 | Cable Route 4 |
| 55 | 4" ISO | 11.75 | 3.5 | 0.224 | 8.5 | Cable Route 3 |
| 56 | 4" ISO | 12 | 3.5 | 0.225 | 8.5 | Node 1 Route |
| 57 | 4" ISO | 11.75 | 3.5 | 0.222 | 8.5 | Node 1 Route |
| 58 | 2" ISO | 7.75 | 2 | 0.125 | 1.5 | Node 3 |
| 59 | 2" ISO | 7.75 | 2 | 0.119 | 1.5 | Cable Route 1 |
| 60 | 2" ISO | 7.75 | 2 | 0.114 | 1.5 | Cable Route 5 |
| 61 | 2" ISO | 7.75 | 2 | 0.12 | 1.5 | Cable Route 4 |
| 62 | 2" ISO | 8 | 2 | 0.118 | 1.5 | Node 1 Route |
| 63 | 2" ISO | 8 | 2 | 0.123 | 1.5 | Node 3 |
| 64 | 2" ISO | 7.75 | 2 | 0.114 | 1.5 | Cable Route 2 |
| 65 | 2" ISO | 8 | 2 | 0.12 | 1.5 | Node 1 Route |
| 66 | 2" ISO | 7.75 | 2 | 0.115 | 1.5 | Node 4 |
| 67 | 2" ISO | 7.75 | 2 | 0.121 | 1.5 | Node 1 Route |
| 68 | 2" ISO | 8 | 2 | 0.112 | 1.5 | Node 4 |

Note: Seeds are sized for similarity to specific munitions. For example, the 8-inch seed is similar in diameter and length to an 8-inch projectile, the 6-inch seed is similar in length and diameter to a 155 mm projectile, and the 4-inch seed is similar in length and diameter to a 105 mm projectile.

Appendix C – Target Selection, Positioning and Size Estimation

The results discussed in this appendix refer to the rawest of data points, specifically, whether or not a surrogate was located each time it appeared in the data, and not focused on whether or not a target was detected and identified overall within a mission (as discussed in Section 10.0). Since almost all of the targets were either imaged in side-scan sonar or detected by the magnetometer two or more times, the number of targets are greater than the number of actual surrogates. This analysis is more indicative of sensor and user performance than overall mission design performance. For instance, a target may only be detectable by the sensor, or detected by the user, 50% of the times it falls within data coverage (e.g., two out of four sonar transects), but still be counted as properly located and identified in the overall mission results.

C.1. Target Selection

Targets selected by the detection team that were positively identified as surrogates by the seeding team were characterized as a “true positive.” A true positive was indicated for any target, not solely those within the 5 m navigational constraint used for the field effort, which is discussed in Section 10.3.2.2. Those targets that were identified, but were not surrogates were labeled “false positives.” Lastly, those targets not located were labeled “false negatives.” Total false negatives were calculated by the number of side-scan sonar or magnetometer transects in which the target could possibly be located (e.g., individual sonar files covering the surrogate positions). Again, it must be noted that these rates consider that multiple targets may be identified for only one individual surrogate on the seafloor should there be multiple instances of the surrogate in the data.

C.1.1 Magnetometer Target Selection

Target identification from magnetometer data alone is outlined in Table C-1. Standard node missions were significantly more successful in locating targets than cable missions (53.66% true positive rate vs. 26.47%). Further, false-positive rates were significantly higher in cable missions (20.59% vs. 4.88%). Variations in node mission spacing and altitude did not significantly alter detection rate (54.72 %), although no false positives were observed. False negative rates were largely consistent throughout standard node missions, varied height and spacing node missions, and cable route missions (41.46 – 52.94%).

Table C-1: Target Identification Results by Mission and Mission Type for Magnetometer Data Along-track

| Region | Altitude (meters) | Spacing (meters) | True Positive | False-Positive | False Negative |
|--|-------------------|------------------|---------------|----------------|----------------|
| Node Survey | | | | | |
| Node 1 Route | 2 | 8 | 2 | 0 | 5 |
| Node 3 | 2 | 8 | 7 | 1 | 8 |
| Node 4 | 2 | 8 | 13 | 1 | 4 |
| Subtotal | | | 22 | 2 | 17 |
| Percentage | | | 53.66% | 4.88% | 41.46% |
| Cable Route Survey | | | | | |
| Cable Route 1 | 2 | 8 | 1 | 1 | 6 |
| Cable Route 2 | 2 | 8 | 2 | 1 | 3 |
| Cable Route 3 | 2 | 8 | 3 | 1 | 3 |
| Cable Route 4 | 2 | 8 | 3 | 0 | 2 |
| Cable Route 5 | 2 | 8 | 0 | 4 | 4 |
| Subtotal | | | 9 | 7 | 18 |
| Percentage | | | 26.47% | 20.59% | 52.94% |
| Combined Results for Node and Cable Route Surveys Conducted at 2 m Altitude and 8 m Spacing | | | | | |
| Total Standard Mission | | | 31 | 9 | 35 |
| Percentage | | | 41.33% | 12.00% | 46.67% |
| Node 3 Survey Varied Altitude and Spacing | | | | | |
| Node 3 | 2 | 4 | 8 | 0 | 6 |
| Node 3 | 4 | 8 | 7 | 0 | 4 |
| Node 3 | 4 | 4 | 7 | 0 | 6 |
| Node 3 | 6 | 8 | 7 | 0 | 8 |
| Subtotal | | | 29 | 0 | 24 |
| Percentage | | | 54.72% | 0.00% | 45.28% |
| Combined Results for All Surveys | | | | | |
| Total | | | 60 | 9 | 59 |
| Percentage | | | 46.88% | 7.03% | 46.09% |

C.1.2 Side-Scan Sonar Identification

Target identification from side-scan sonar aided by magnetometer picks is outlined in Table C-2. Standard node missions were significantly more successful in locating targets than cable missions (85.51% true positive rate vs. 56.34%), as observed from targets picked by magnetometer alone. Additionally, false-positive rates were once again significantly higher in cable missions versus node missions (23.94% vs. 1.45%). Variations in node mission spacing and altitude significantly decreased detection rate (44.20%) versus standard node mission configurations, while false positives increased (9.42%). False negative rates were lower in side-scan sonar than magnetometer alone for standard node missions, and cable route missions (13.04% and 19.72% respectively). False negative rates for varied height and spacing node missions were more consistent with results for targets identified from magnetometer alone (46.38% for side scan sonar vs. 45.28% for magnetometer).

Table C-2: Target Identification Results by Mission and Mission Type for Side-scan Sonar Data

| Region | Altitude (meters) | Spacing (meters) | True Positive | False Positive | False Negative |
|--|-------------------|------------------|---------------|----------------|----------------|
| Node Survey | | | | | |
| Node 1 Route | 2 | 8 | 35 | 1 | 0 |
| Node 3 | 2 | 8 | 45 | 0 | 6 |
| Node 4 | 2 | 8 | 38 | 1 | 12 |
| Subtotal | | | 118 | 2 | 18 |
| Percentage | | | 85.51% | 1.45% | 13.04% |
| Cable Route Survey | | | | | |
| Cable Route 1 | 2 | 8 | 8 | 3 | 5 |
| Cable Route 2 | 2 | 8 | 11 | 2 | 4 |
| Cable Route 3 | 2 | 8 | 8 | 2 | 3 |
| Cable Route 4 | 2 | 8 | 9 | 4 | 0 |
| Cable Route 5 | 2 | 8 | 4 | 6 | 2 |
| Subtotal | | | 40 | 17 | 14 |
| Percentage | | | 56.34% | 23.94% | 19.72% |
| Combined Results for Node and Cable Route Surveys Conducted at 2 m Altitude and 8 m Spacing | | | | | |
| Total Standard Mission | | | 158 | 19 | 32 |
| Percentage | | | 75.60% | 9.09% | 15.31% |
| Node 3 Survey Varied Altitude and Spacing | | | | | |
| Node 3 | 2 | 4 | 24 | 5 | 18 |
| Node 3 | 4 | 8 | 20 | 3 | 6 |
| Node 3 | 4 | 4 | 9 | 3 | 25 |
| Node 3 | 6 | 8 | 8 | 2 | 15 |
| Subtotal | | | 61 | 13 | 64 |
| Percentage | | | 44.20% | 9.42% | 46.38% |
| Combined Results for All Surveys | | | | | |
| Total | | | 219 | 32 | 96 |
| Percentage | | | 63.11% | 9.22% | 27.67% |

C.2. Surrogate Positioning and Size Estimation

The success criteria for surrogate positioning required that targets fall within a 5 m radius of the known surrogate positions. This was calculated by building 5 m buffer rings using the ESRI ArcGIS “Buffer” tool for each target position. Target positions within the 5 m rings were given attributes reflecting the known target, including target identity and size. Size estimates given by the detection team for the targets within the 5 m buffer were then compared to the recorded surrogate sizes. Totals for both correct and incorrect sizes were tabulated, with the latter further defined by those targets that were identified as larger or smaller than the actual surrogate sizes.

C.2.1 Magnetometer Positioning and Size Estimation

Positioning and size estimations from magnetometer alone is outlined in Table C-3. Standard node missions were significantly more successful in positioning than cable missions (70.83% vs. 37.5%). Target positioning improved to 93.10% in varied spacing and altitude node missions.

Size estimation was best in standard node missions (58.82%), decreasing slightly in varied spacing and altitude node missions (51.85%) and more significantly in cable routes (33.33%); in three of five cable route missions, no correct surrogate sizes were estimated. Of the false size estimations, the majority of estimates were larger only in varied node missions (76.92%), whereas both standard node and cable route mission estimates skewed smaller (85.71% and 75% respectively).

Table C-3: Positioning and Size Estimate Results by Mission and Mission Type for Magnetometer Data Alone

| Region | Altitude (meters) | Spacing (meters) | Total True Positives | Total w/in 5m Buffer | Correct Size | False Size | Larger | Smaller |
|--|-------------------|------------------|----------------------|----------------------|--------------|------------|-----------|-----------|
| Node Survey | | | | | | | | |
| Node 1 Route | 2 | 8 | 2 | 1 | 1 | 0 | 0 | 0 |
| Node 3 | 2 | 8 | 9 | 6 | 3 | 3 | 1 | 2 |
| Node 4 | 2 | 8 | 13 | 10 | 6 | 4 | 0 | 4 |
| Subtotal | | | 24 | 17 | 10 | 7 | 1 | 6 |
| Percentage | | | | 70.83% | 58.82% | 41.18% | 14.29% | 85.71% |
| Cable Route Survey | | | | | | | | |
| Cable Route 1 | 2 | 8 | 2 | 0 | 0 | 0 | 0 | 0 |
| Cable Route 2 | 2 | 8 | 3 | 2 | 1 | 1 | 0 | 1 |
| Cable Route 3 | 2 | 8 | 4 | 2 | 1 | 1 | 1 | 0 |
| Cable Route 4 | 2 | 8 | 3 | 2 | 0 | 2 | 0 | 2 |
| Cable Route 5 | 2 | 8 | 4 | 0 | 0 | 0 | 0 | 0 |
| Subtotal | | | 16 | 6 | 2 | 4 | 1 | 3 |
| Percentage | | | | 37.50% | 33.33% | 66.67% | 25.00% | 75.00% |
| Combined Results for Node and Cable Route Surveys Conducted at 2 m Altitude and 8 m Spacing | | | | | | | | |
| Total Standard Mission | | | 40 | 23 | 12 | 11 | 2 | 9 |
| Percentage | | | | 57.50% | 52.17% | 47.83% | 18.18% | 81.82% |
| Node 3 Survey Varied Altitude and Spacing | | | | | | | | |
| Node 3 | 2 | 4 | 8 | 8 | 4 | 4 | 1 | 3 |
| Node 3 | 4 | 8 | 7 | 6 | 3 | 3 | 3 | 0 |
| Node 3 | 4 | 4 | 7 | 6 | 3 | 3 | 3 | 0 |
| Node 3 | 6 | 8 | 7 | 7 | 4 | 3 | 3 | 0 |
| Subtotal | | | 29 | 27 | 14 | 13 | 10 | 3 |
| Percentage | | | | 93.10% | 51.85% | 48.15% | 76.92% | 23.08% |
| Combined Results for All Surveys | | | | | | | | |
| Total | | | 69 | 50 | 26 | 24 | 12 | 12 |
| Percentage | | | | 72.46% | 52.00% | 48.00% | 50.00% | 50.00% |

C.2.2 Side-Scan Sonar Positioning and Size Estimation

Positioning and size estimations from side-scan sonar is outlined in Table C-4. Standard node missions were once again more successful in positioning than cable missions (92.5% vs. 58.62%). In contrast to magnetometer picks, target positioning decreased slightly in varied

spacing and altitude node missions (86.49%) as compared to standard node missions. However, size estimations were best in varied node missions (56.25%), decreasing slightly in cable route missions (47.06 %) and standard node missions (42.34%). No missions had zero correct surrogate sizes estimated. Of the false size estimations, the majority of estimates were once again larger only in varied node missions (57.14%), whereas both standard node and cable route mission estimates skewed smaller (54.69% and 83.33% respectively).

Table C-4: Positioning and Size Estimate Results by Mission and Mission Type for Side-scan Sonar

| Region | Altitude (meters) | Spacing (meters) | Total True Positives | Total w/in 5m Buffer | Correct Size | False Size | Larger | Smaller |
|--|-------------------|------------------|----------------------|----------------------|--------------|------------|-----------|-----------|
| Node Survey | | | | | | | | |
| Node 1 Route | 2 | 8 | 36 | 32 | 10 | 22 | 3 | 19 |
| Node 3 | 2 | 8 | 45 | 42 | 18 | 24 | 17 | 7 |
| Node 4 | 2 | 8 | 39 | 37 | 19 | 18 | 9 | 9 |
| Subtotal | | | 120 | 111 | 47 | 64 | 29 | 35 |
| Percentage | | | | 92.50% | 42.34% | 57.66% | 45.31% | 54.69% |
| Cable Route Survey | | | | | | | | |
| Cable Route 1 | 2 | 8 | 11 | 5 | 4 | 1 | 0 | 1 |
| Cable Route 2 | 2 | 8 | 13 | 11 | 5 | 6 | 0 | 6 |
| Cable Route 3 | 2 | 8 | 10 | 5 | 2 | 3 | 1 | 2 |
| Cable Route 4 | 2 | 8 | 14 | 9 | 3 | 6 | 1 | 5 |
| Cable Route 5 | 2 | 8 | 10 | 4 | 2 | 2 | 1 | 1 |
| Subtotal | | | 58 | 34 | 16 | 18 | 3 | 15 |
| Percentage | | | | 58.62% | 47.06% | 52.94% | 16.67% | 83.33% |
| Combined Results for Node and Cable Route Surveys Conducted at 2 m Altitude and 8 m Spacing | | | | | | | | |
| Total Standard Mission | | | 178 | 145 | 63 | 82 | 32 | 50 |
| Percentage | | | | 81.46% | 43.45% | 56.55% | 39.02% | 60.98% |
| Node 3 Survey Varied Altitude and Spacing | | | | | | | | |
| Node 3 | 2 | 4 | 29 | 24 | 14 | 10 | 4 | 6 |
| Node 3 | 4 | 8 | 23 | 21 | 11 | 10 | 7 | 3 |
| Node 3 | 4 | 4 | 12 | 10 | 7 | 3 | 2 | 1 |
| Node 3 | 6 | 8 | 10 | 9 | 4 | 5 | 3 | 2 |
| Subtotal | | | 74 | 64 | 36 | 28 | 16 | 12 |
| Percentage | | | | 86.49% | 56.25% | 43.75% | 57.14% | 42.86% |
| Combined Results for All Surveys | | | | | | | | |
| Total | | | 252 | 209 | 99 | 110 | 48 | 62 |
| Percentage | | | | 82.94% | 47.37% | 52.63% | 43.64% | 56.36% |

Page Intentionally Left Blank.

Appendix D – Combined Magnetometer and Side-scan Reanalysis

Detection team target selection focused on magnetometer and side-scan data to identify and select targets. While both were used to identify targets in the side-scan, the primary size estimation was conducted using these two resources separately. Subsequent to the detection team analysis, the data was reanalyzed by combining the two data sets and merging their properties to estimate size. This was achieved through ESRI ArcGIS Spatial Join tool. Size estimates were derived by a weighted average biased to magnetometer size. For instance, if the side-scan sonar size estimated a 4-inch surrogate, but the magnetometer estimated a 6-inch surrogate, the non-weighted average would be 5-inch, which is not a surrogate size used. Instead, the weighted average would select a 6-inch, which was the magnetometer estimation. Further, each magnetometer pick was only added to side-scan sonar targets within 5 m of that magnetometer pick, so as not to bias size estimation of other side-scan sonar targets in close proximity that were associated with another magnetometer pick. The threshold for correctly positioned targets was selected by the study to be all targets within a 5 m radius of the known seed positions. Anything beyond that threshold was counted as improperly positioned, since such a reported position would make it difficult to relocate the actual surrogate. The results of the reanalysis are shown in Table D-1. Comparisons between side-scan alone, magnetometer alone, and reanalysis are drawn in Table D-2.

The Spatial Join combined magnetometer to side-scan sonar positions, so changes in the total number of targets within the 5 m buffer was negligible. With regards to size estimates, improvements were shown across many of the missions. Node missions improved from 47 to 64 surrogates correctly identified, as compared to side-scan sizing alone, and from 10 to 64 over magnetometer sizing alone. Improvements over side-scan in cable routes were actually negligible, with both side-scan and combined sensor analysis correctly identifying 16 surrogates. However, the combined analysis improved cable routes greatly over magnetometer alone, with a 2 to 16 improvement in the correct identification of surrogates overall. In variable height and spacing missions (discussed more in Section 10.3.3), improvement was more varied in comparison to side-scan alone, but overall improvement was seen (from 36 to 39 surrogates correctly identified). Again, the combined method was significantly improved over magnetometer alone (from 14 to 39 surrogates correctly identified).

This reanalysis tested weighting the average to either side-scan or magnetometer for size estimation. The latter method showed significantly more improvement, although this may only be the case for this particular study. Regardless, the combined method approach demonstrates that the use of multiple sensors for target identification and size estimation is not strictly additive, but in some cases, is vastly improved over the performance of one sensor alone. This supports the use of multi-sensor platforms for MEC detection.

Table D-1: Combined Magnetometer and Side-scan Reanalysis for Target Size Identification

| Region | Altitude (meters) | Spacing (meters) | Total True Positives | Total w/in 5m Buffer | Correct Size | False Size | Larger | Smaller |
|--|-------------------|------------------|----------------------|----------------------|--------------|------------|-----------|-----------|
| Node Survey | | | | | | | | |
| Node 1 Route | 2 | 8 | 35 | 32 | 14 | 18 | 1 | 17 |
| Node 3 | 2 | 8 | 45 | 42 | 23 | 19 | 12 | 7 |
| Node 4 | 2 | 8 | 39 | 37 | 27 | 10 | 0 | 10 |
| Subtotal | | | 119 | 111 | 64 | 47 | 13 | 34 |
| Percentage | | | | 93.28% | 57.66% | 42.34% | 27.66% | 72.34% |
| Cable Route Survey | | | | | | | | |
| Cable Route 1 | 2 | 8 | 11 | 5 | 4 | 1 | 0 | 1 |
| Cable Route 2 | 2 | 8 | 13 | 11 | 4 | 7 | 2 | 5 |
| Cable Route 3 | 2 | 8 | 10 | 5 | 3 | 2 | 1 | 1 |
| Cable Route 4 | 2 | 8 | 14 | 9 | 3 | 6 | 0 | 6 |
| Cable Route 5 | 2 | 8 | 10 | 4 | 2 | 2 | 1 | 1 |
| Subtotal | | | 58 | 34 | 16 | 18 | 4 | 14 |
| Percentage | | | | 58.62% | 47.06% | 52.94% | 22.22% | 77.78% |
| Combined Results for Node and Cable Route Surveys Conducted at 2 m Altitude and 8 m Spacing | | | | | | | | |
| Total Standard Mission | | | 177 | 145 | 80 | 65 | 17 | 48 |
| Percentage | | | | 81.92% | 55.17% | 44.83% | 26.15% | 73.85% |
| Node 3 Survey Varied Altitude and Spacing | | | | | | | | |
| Node 3 | 2 | 4 | 29 | 24 | 17 | 7 | 4 | 3 |
| Node 3 | 4 | 8 | 23 | 21 | 10 | 11 | 10 | 1 |
| Node 3 | 4 | 4 | 12 | 10 | 6 | 4 | 4 | 0 |
| Node 3 | 6 | 8 | 10 | 9 | 6 | 4 | 3 | 1 |
| Subtotal | | | 74 | 64 | 39 | 26 | 21 | 5 |
| Percentage | | | | 86.49% | 60.94% | 40.63% | 80.77% | 19.23% |
| Combined Results for All Surveys | | | | | | | | |
| Total | | | 251 | 86.49% | 60.94% | 40.63% | 80.77% | 19.23% |
| Percentage | | | | 209 | 119 | 91 | 38 | 53 |

Table D-2: Comparison of Results between Side-scan Sonar, Magnetometry and Combined Reanalysis Target Size Estimation

| Region | Altitude (meters) | Spacing (meters) | Correct Size | | |
|--|-------------------|------------------|----------------------|--------------------|---------------------|
| | | | Sidescan Sonar Alone | Magnetometer Alone | Combined Reanalysis |
| Node Survey | | | | | |
| Node 1 Route | 2 | 8 | 10 | 1 | 14 |
| Node 3 | 2 | 8 | 18 | 3 | 23 |
| Node 4 | 2 | 8 | 19 | 6 | 27 |
| Subtotal | | | 47 | 10 | 64 |
| Cable Route Survey | | | | | |
| Cable Route 1 | 2 | 8 | 4 | 0 | 4 |
| Cable Route 2 | 2 | 8 | 5 | 1 | 4 |
| Cable Route 3 | 2 | 8 | 2 | 1 | 3 |
| Cable Route 4 | 2 | 8 | 3 | 0 | 3 |
| Cable Route 5 | 2 | 8 | 2 | 0 | 2 |
| Subtotal | | | 16 | 2 | 16 |
| Combined Results for Node and Cable Route Surveys Conducted at 2 m Altitude and 8 m Spacing | | | | | |
| Total Standard Mission | | | 63 | 12 | 80 |
| Node 3 Survey Varied Altitude and Spacing | | | | | |
| Node 3 | 2 | 4 | 14 | 4 | 17 |
| Node 3 | 4 | 8 | 11 | 3 | 10 |
| Node 3 | 4 | 4 | 7 | 3 | 6 |
| Node 3 | 6 | 8 | 4 | 4 | 6 |
| Subtotal | | | 36 | 14 | 39 |
| Combined Results for All Surveys | | | | | |
| Total | | | 99 | 26 | 119 |

Page Intentionally Left Blank.

Appendix E – Post-Storm Season Assessment Trip Report

Trip Report
Post-Storm Season Assessment of Surrogate Mobility
and Field Methodology Examination
Bureau of Ocean Energy Management (BOEM) Unexploded Ordnance (UXO)
Survey Methodology Investigation
10 - 14 April 2017

1. Introduction

In July 2016, 62 surrogate munitions were strategically placed within the Delaware wind energy area as part of an in-field verification of technologies and methodologies for the detection of munitions and explosives of concern. During the study, 54 of the 62 surrogate munitions (Industry Standard Objects or ISOs) were reacquired and locations verified using the University of Delaware's Teledyne Gavia autonomous underwater vehicle (AUV) equipped with a selectable frequency 900/1800 kHz Marine Sonics side-scan sonar, Geometrics G880-AUV cesium vapor magnetometer, and 2 megapixel Point Grey color camera (refer to Sections 9.0 and 10.0 of the BOEM In-field Testing and Methodology Verification Munitions and Explosives of Concern Survey Methodology Investigation for Wind Energy Areas of the Atlantic OCS Report). Instrument verification determined the navigational and sensor precision of the AUV on repeated passes to be within 2.5 meters (m), thus establishing an estimated accuracy of the reported surrogate locations within 2.5 m of the actual surrogate locations. In the winter following the in-field verification, several events with significant wave energy occurred, which had the potential to bury or mobilize the surrogates. Using the baseline locations established during the July 2016 in-field verification, a post-storm season field effort used the same technologies as the in-field verification to reacquire and establish whether burial or mobility of the surrogates occurred.

Operational plans incorporated re-conducting a wide area assessment (WAA) of the entire field area (Figure 1), which consisted of a 2 x 2 kilometer (km) box and 5 x 0.05 km cable route, to establish whether large scale alteration to seabed morphology occurred. Surveying was conducted with a vessel mounted dual frequency 230/550 kHz Edgetech 6205 phase measuring bathymetric and side-scan sonar. Subsequently, targeted AUV missions were conducted over selected areas where surrogate munitions were placed in July 2016. These sites were prioritized to include sites representative of the different sediment types, bathymetric slope and depth, and surrogates present throughout the field area. An instrument verification strip (IVS), modified based on recommendations developed from the 2016 field operations (Section 10.4.1 of BOEM In-field Verification Report), was placed on site and mapped with the AUV twice daily. Field work was conducted from 10 – 14 April 2017. Daily operations are summarized below.

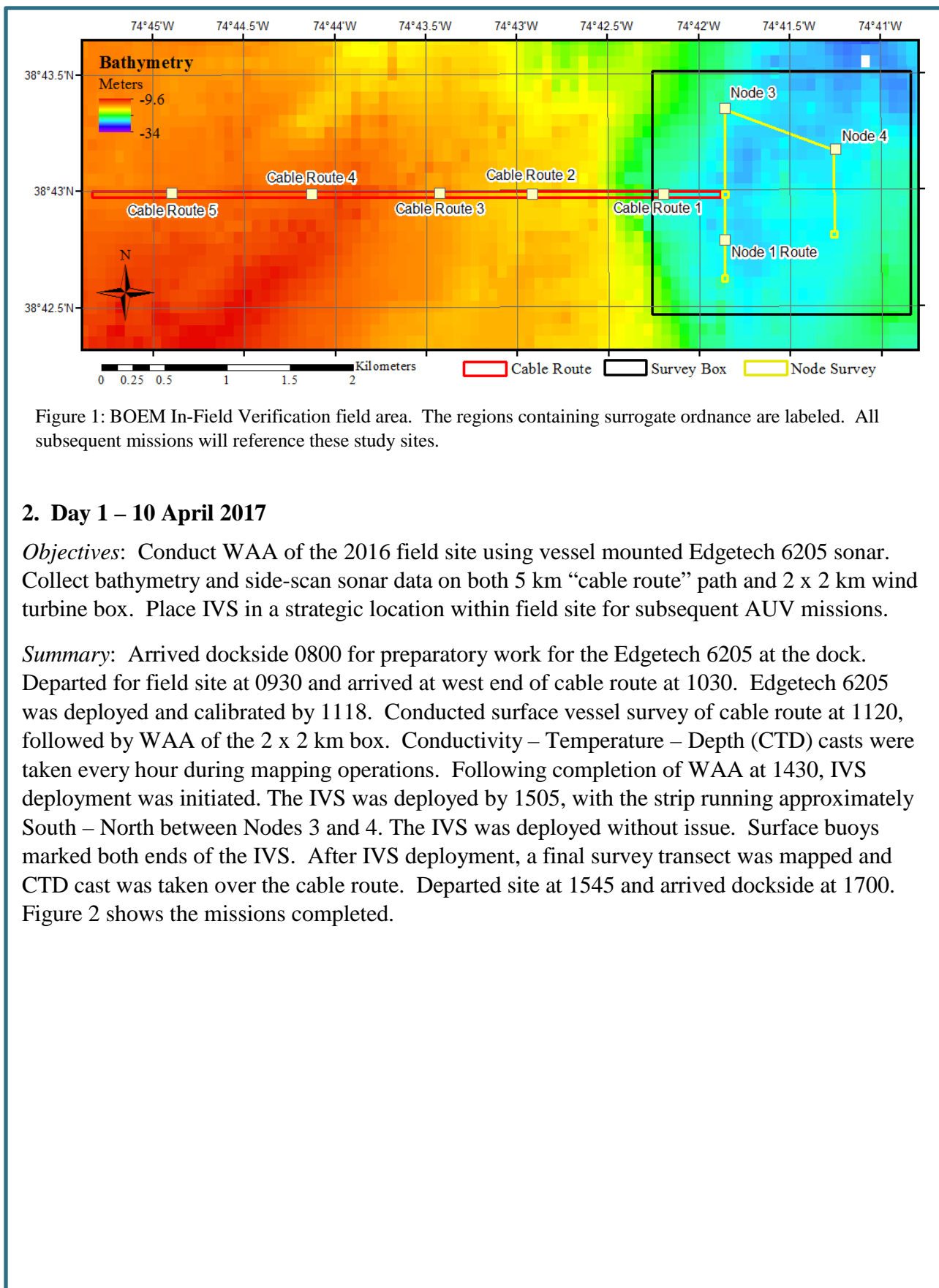


Figure 1: BOEM In-Field Verification field area. The regions containing surrogate ordnance are labeled. All subsequent missions will reference these study sites.

2. Day 1 – 10 April 2017

Objectives: Conduct WAA of the 2016 field site using vessel mounted Edgetech 6205 sonar. Collect bathymetry and side-scan sonar data on both 5 km “cable route” path and 2 x 2 km wind turbine box. Place IVS in a strategic location within field site for subsequent AUV missions.

Summary: Arrived dockside 0800 for preparatory work for the Edgetech 6205 at the dock. Departed for field site at 0930 and arrived at west end of cable route at 1030. Edgetech 6205 was deployed and calibrated by 1118. Conducted surface vessel survey of cable route at 1120, followed by WAA of the 2 x 2 km box. Conductivity – Temperature – Depth (CTD) casts were taken every hour during mapping operations. Following completion of WAA at 1430, IVS deployment was initiated. The IVS was deployed by 1505, with the strip running approximately South – North between Nodes 3 and 4. The IVS was deployed without issue. Surface buoys marked both ends of the IVS. After IVS deployment, a final survey transect was mapped and CTD cast was taken over the cable route. Departed site at 1545 and arrived dockside at 1700. Figure 2 shows the missions completed.

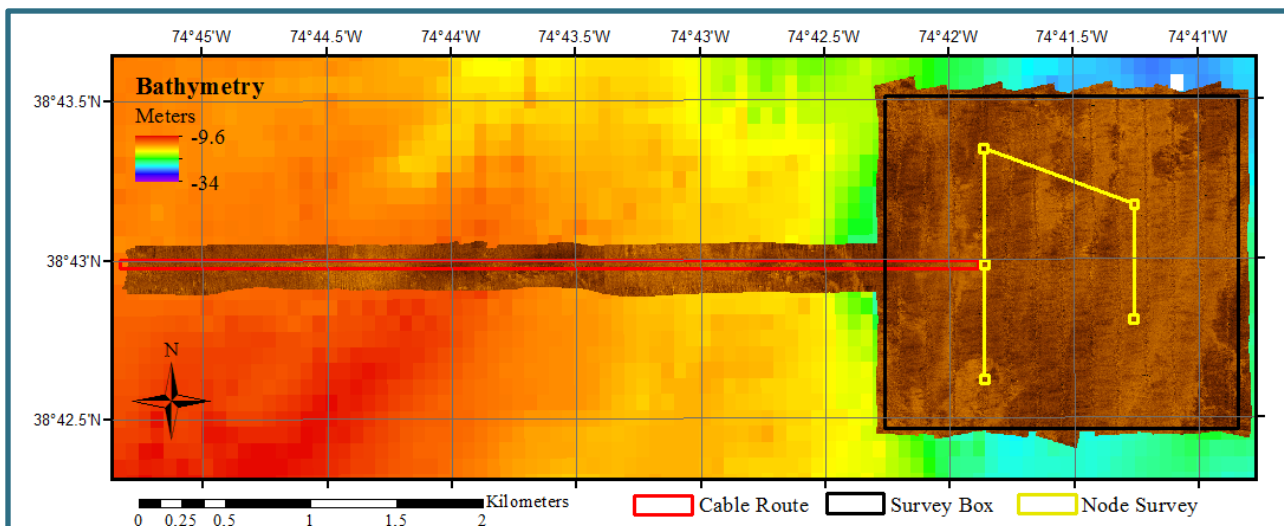


Figure 2: Side-scan sonar coverage of the cable route and 2 x 2 km survey box collected on 10 April 2017. Field area and survey boxes from the 2016 field campaign are illustrated.

Conclusions: Preliminary analysis of sonar data suggests many small scale morphological expressions (i.e., ripples) at the site were in a relict state from energetic conditions during the winter season. These features were not present in the July 2016 field effort. Boundary shifts of sorted bedforms appear to have occurred, although further analysis is required to determine extent and direction. CTD casts showed that the field site was fairly well mixed, unlike conditions during field work the previous summer. The IVS was placed between Nodes 3 and 4, allowing for strategic access to the IVS during missions. A new IVS design incorporated wider spacing between ISOs than the 2016 design (from 6 to 15 m) to reduce the likelihood of signal overlap. Further, the design incorporated removable ISOs, which were placed in a different configuration to ensure safer deployment (Figure 3). Surface buoys were placed to allow for quicker reacquisition during AUV deployment and to simplify recovery.

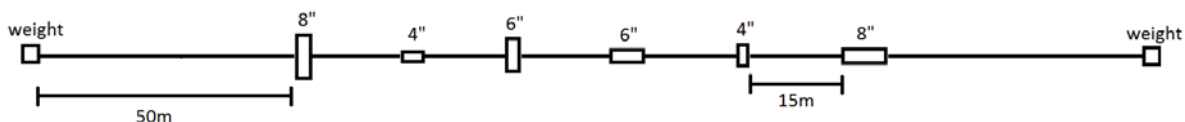


Figure 3: The new IVS design spaced the ISOs further out than the 2016 IVS, spacing them 15 m apart. Further, the heaviest ISOs were placed at opposite ends of the strip, and longer lead-in lines were made to facilitate easier and safer deployment and recovery.

Time on Water: 0930 - 1700

Personnel: Art Trembanis, Principal Investigator (PI), Carter DuVal, deputy PI, Kenny Haulsee, Tim Pilegard, Andrew Caldwell, Caitlyn Stockwell, Annie Daw, and Kevin Beam, CAPT.

Data Collected: Bathymetry, Side-Scan Sonar, CTD

3. Day 2 – 11 April 2017

Objectives: Due to poor weather conditions, the backup plan, involving sensor calibration in the Delaware Bay, was initiated. Conduct patch testing of Edgetech 6205 for bathymetric production, and calibration of the AUV magnetometer to account for vehicle noise with new batteries.

Summary: Depart dock 0800 for patch test site in Delaware Bay. Arrived at site by 0815 and began inertial measurement unit (IMU) calibration for the Edgetech 6205. Calibration completed 0845, began patch test for pitch, yaw, and latency. Completed first stage at 0935, took CTD cast. Transited to site for roll patch test; started patch test at 1028 and completed by 1037. Collected another CTD cast and departed for dock. Arrived dockside at 1100, loaded AUV equipment and reconfigured vessel for AUV operations. Departed dock for AUV calibration site at 1245. Arrived at calibration site 1300. Ballasted AUV on site for magnetometer configuration. Launched AUV at 1400 for first calibration mission. Due to strong currents, mission was aborted twice. AUV was recovered and moved to better position. Deployed AUV and sent on mission at 1508. AUV completed first calibration mission at 1522. Recovered AUV and swapped battery. Launched AUV and sent on final calibration mission at 1620. AUV completed mission at 1633. AUV was recovered and *R/V Daiber* departed for dockside. Arrived dockside at 1655.

Conclusions: Conditions on site were too rough for AUV field operations (sea state 3-5 feet, winds 15 – 20 knots with gust to 25 knots). Instead, the calmer conditions in the Delaware Bay (seas 1-2 feet, winds 10 – 15 knots) allowed for necessary calibration of the AUV magnetometer to new batteries being used on the vehicle, as well as patch testing the Edgetech 6205 to correct for physical positional offsets on the sonar for bathymetric surface production. Patch test was conducted without issue. Strong currents presented issues initially for AUV missions. Strategic deployment of the AUV up-current of the mission site compensated for issue. Calibration missions were successful. Figure 4 illustrates the improvement of the compensated data versus uncalibrated data from the first calibration mission.

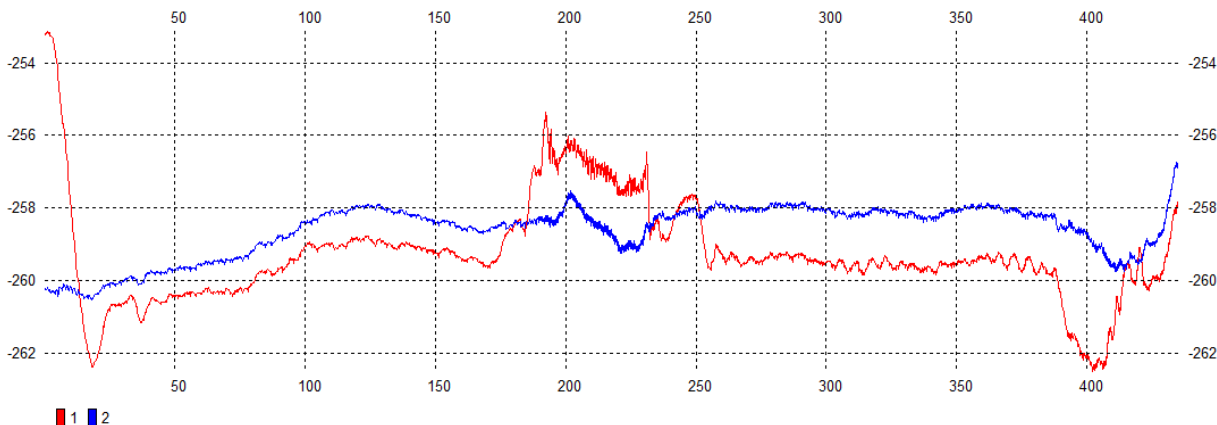


Figure 4: AUV magnetometer data from the calibration run. Uncalibrated data (red) is compensated for AUV battery discharge and vehicle noise (blue) to reduce overall noise and improve object detection.

Time on Water: 0800 – 1100, 1245-1645

Personnel: Art Trembanis, PI, Carter DuVal, deputy PI, Tim Pilegard, Alimjan Alba, Kevin Beam, CAPT.

Data Collected: Magnetometry, Side-Scan Sonar, CTD

4. Day 3 – 12 April 2017

Objectives: Reacquire the IVS with the AUV and determine the specific location and strike. Once established, the AUV will run IVS missions for each battery on the vehicle. Survey will follow, starting with the monopile node locations prioritized by team; Node 3 and Node 4 highest priority. Monopile locations will be surveyed with high-resolution side-scan and magnetometry. Missions will expand 20 m beyond the 40 x 40 m nodes to account for the potential of surrogate mobility. Figure 5 shows the missions completed.

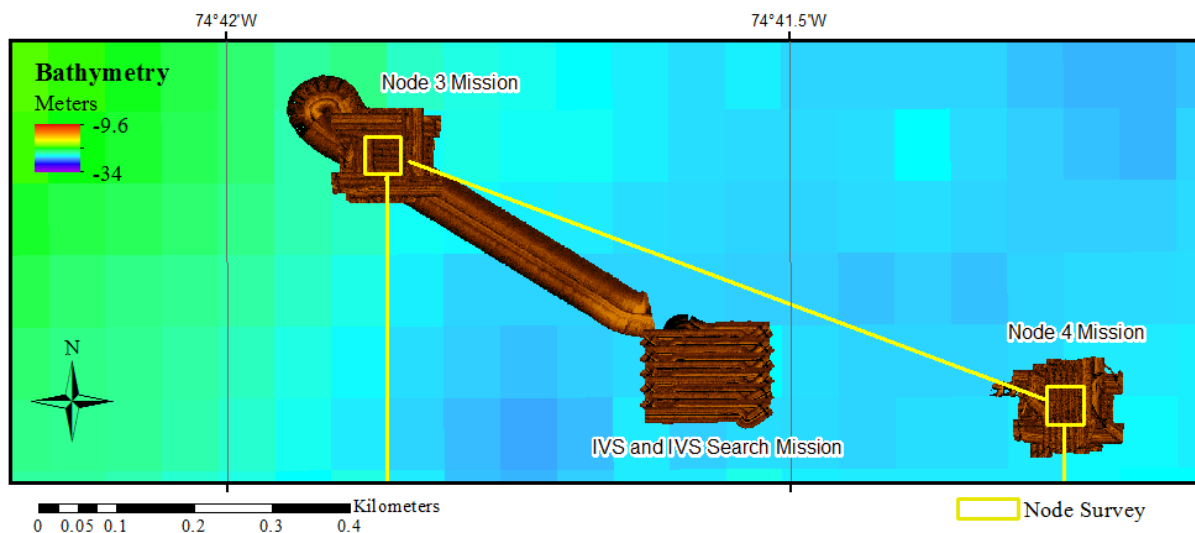


Figure 5: AUV side-scan sonar coverage from 12 April 2017. IVS (center) is located between Node 3 (left) and Node 4 (right). Magnetometer and side-scan sonar data was collected simultaneously.

Summary: Departed dock 0845. Arrived on site 1030 and began AUV calibration. First AUV mission commenced at 1130 to acquire the exact position of the IVS and the mission was completed at 1205. While post processing the AUV sonar data from the first mission to determine the final IVS position, the AUV was sent on a mission to run Node 3 at 1209. The mission was completed at 1336. AUV maneuvered and surfaced, it was then sent on a standard IVS mission. IVS mission completed at 1422. AUV was then recovered and the battery replaced. The AUV was then sent to run IVS mission for new battery at 1513. This second IVS mission was completed at 1528. AUV immediately sent to map Node 4 at 1532. The mission was completed at 1720. Recovered AUV departed for dock at 1730. Arrived dockside 1850.

Conclusions: Surface buoys allowed for rapid relocation of IVS, improving efficiency. The new IVS design still allowed for ideal orientation of the ISOs on seafloor. Ripple bedforms, not present in the July 2016 field operations, were present at Node 3 and Node 4. In Node 4, the ripples made it particularly difficult to identify objects. This is illustrated in Figure 6. While magnetic signatures reflective of the ISOs were located within the 2016 Node boundaries, preliminary magnetics analysis found that no ferrous objects were present beyond the initial 40 x 40 m boundary of the nodes, suggesting surrogate mobility was limited, if occurring at all. Difficulty in locating targets in side-scan sonar data suggest partial burial occurred. Further analysis is required.

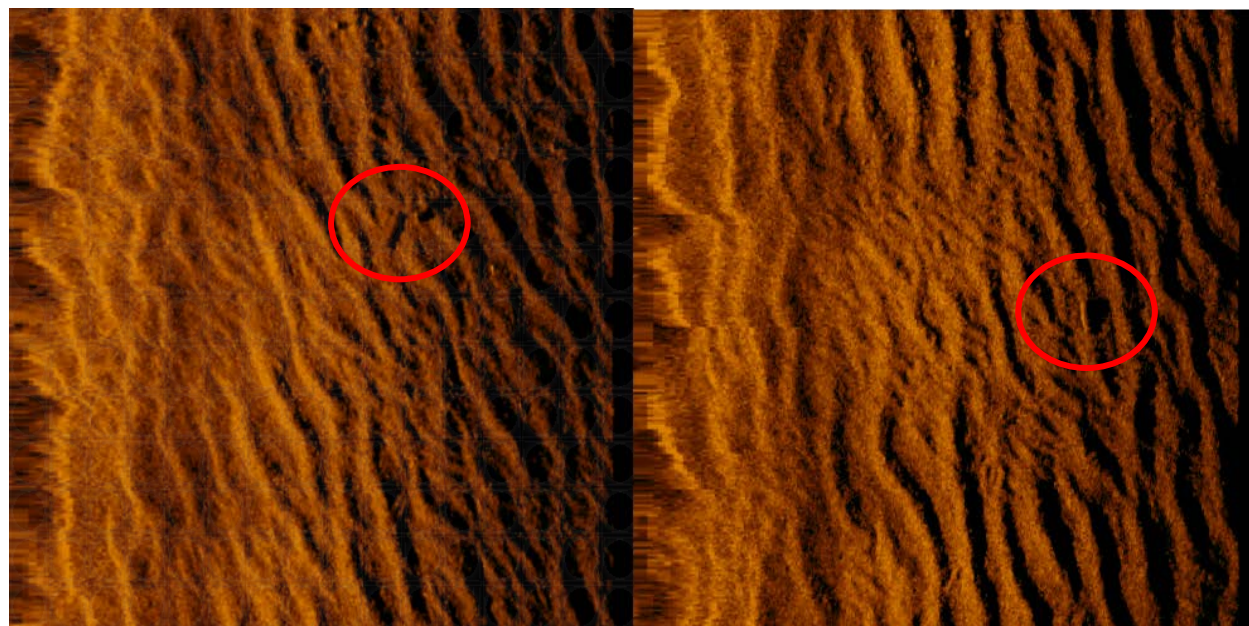


Figure 6: AUV side-scan sonar coverage from Node 4 collected 12 April 2017. Note the surrogate munitions appear similar in expression to ripple crests.

Time on Water: 0845 - 1850

Personnel: Art Trembanis, PI, Carter DuVal, deputy PI, Kevin Beam, CAPT, Emily Ruhl, Cody Cribb, and Kaliopi Bousses.

Data Collected: Magnetometry, Side-Scan Sonar, CTD

5. Day 4 – 13 April 2017

Objectives: Continue AUV survey side-scan sonar and magnetometry. Map Node 1 Route and cable routes (1, 2, and 5) that were prioritized by site conditions and surrogate types (see introduction for more detail).

Summary: Departed dock at 0915 and arrived at site 1025. Sent AUV on first IVS mission at 1056 and completed IVS mission at 1111. Recovered and positioned AUV for Node 1 Route

mission. Sent AUV on Node 1 Route mission at 1127. Mission completed at 1258. AUV again recovered and positioned for Cable Route 1 mission. AUV sent on mission at 1314 and mission completed at 1415. AUV was recovered and battery swapped. After the IMU calibration, vehicle was sent on IVS mission for new battery. The IVS mission was started at 1456 and completed at 1511. AUV was recovered and positioned for Cable Route 2 mission. The Cable Route 2 mission was started at 1529 and completed at 1632. AUV was once again recovered and positioned for the final mission of the day at Cable Route 5. AUV was sent on the Cable Route 5 mission at 1652 and the mission was completed at 1756. AUV was recovered. Departed field site and arrived dockside at 1915. Figure 7 shows the missions completed.

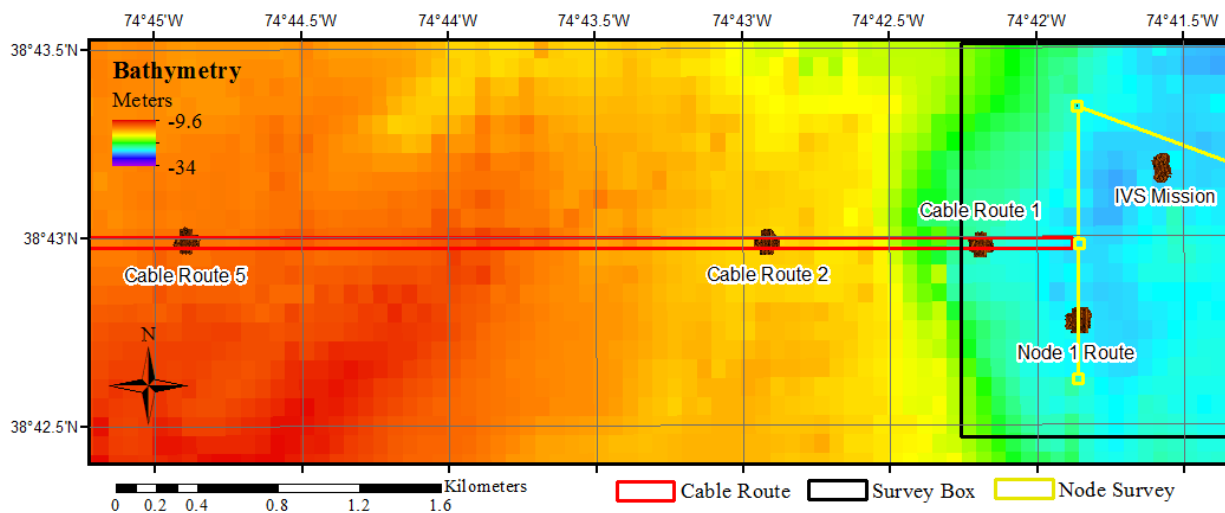


Figure 7: AUV side-scan sonar coverage from 13 April 2017. Note IVS (twice), Node 1 Route, and Cable Routes 1, 2 and 5 were surveyed. Magnetometer data was collected simultaneously.

Conclusions: Preliminary analysis of magnetometer data from Nodes 3 and 4 and Node 1 Route suggested little if any surrogate mobility occurred, and subsequent missions were reduced to 2016 boundaries. This reduced mission time and allowed for completion of all three priority cable route missions. Cable routes were prioritized by surrogate types within each site, sediment type, and bathymetric relief. Each cable route selected was characterized by different combinations of these variables (e.g., coarse versus fine sands, no slope versus slope, shallower versus deep) to be representative of the whole field area.

Time on Water: 0915 - 1915

Personnel: Art Trembanis, PI, Carter DuVal, deputy PI, Kevin Beam, CAPT, Bonnie Ram, Jennifer Draher (BOEM), Geoff Carton (CALIBRE), and Maria Spadaro.

Data Collected: Magnetometry, Side-Scan Sonar, CTD

6. Day 5 – 14 April 2017

Objectives: Re-survey Node 3 at 6 m altitude to test magnetometer detection threshold. Reconfigure AUV for camera surveying and photomosaic Node 3. Recover IVS strip.

Summary: Departed for site at 0750 and arrived on site at 0910. Sent AUV on IVS mission at 0944. IVS mission complete at 0955. AUV immediately sent on Node 3 mission run at 6 m altitude. While the AUV ran the Node 3 mission, the IVS was recovered. The IVS recovery took 30 minutes. The AUV completed the Node 3 mission at 1109. The AUV was recovered and reconfigured for camera mission. After reconfiguration and ballasting, the AUV was sent on Node 3 camera mission at 1210. The camera mission was completed at 1253 and the AUV was recovered. Departed for dock 1300 and arrived dockside at 1415. De-mobilized equipment dockside. Figure 8 shows the missions completed.

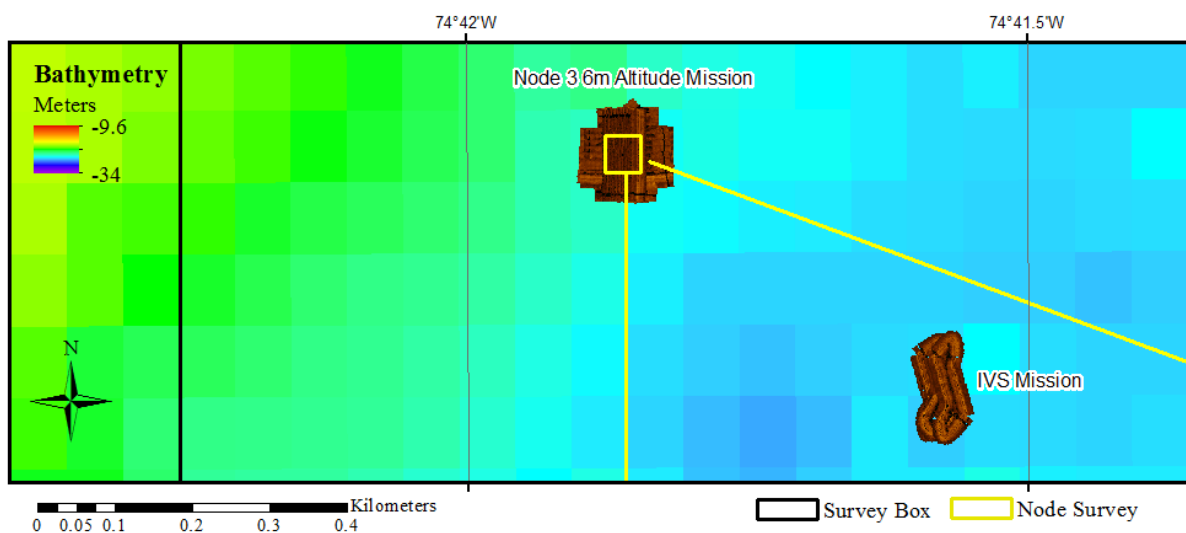


Figure 8: AUV side-scan sonar coverage from 14 April 2017.

Conclusions: Preliminary analysis of the 6 m altitude missions suggest similar magnetometer results to the 2016 mission. The new design of the IVS allowed for its simple and safe recovery. Reconfiguring the AUV required time to re-ballast the vehicle. Different surface conditions (colder temperatures) meant ballasting used in 2016 did not work with vehicle, and more time was required to find ideal ballasting. The AUV operated without issue during the camera mission, but the camera did not work despite passing the on deck pre-operational testing. Further analysis is required to identify the root cause of this failure. Due to time constraints for demobilizing equipment on the *R/V Daiber*, and low priority of camera mission, no further mission was conducted.

Time on Water: 0750 - 1415

Personnel: Art Trembanis, PI, Carter DuVal, deputy PI, Kevin Beam, CAPT, Pete Hesson, Jack Sypher and Sophie Taylor.

Data Collected: Magnetometry, Side-Scan Sonar, CTD



Department of the Interior (DOI)

The Department of the Interior protects and manages the Nation's natural resources and cultural heritage; provides scientific and other information about those resources; and honors the Nation's trust responsibilities or special commitments to American Indians, Alaska Natives, and affiliated island communities.



Bureau of Ocean Energy Management (BOEM)

The mission of the Bureau of Ocean Energy Management is to manage development of U.S. Outer Continental Shelf energy and mineral resources in an environmentally and economically responsible way.

BOEM Environmental Studies Program

The mission of the Environmental Studies Program is to provide the information needed to predict, assess, and manage impacts from offshore energy and marine mineral exploration, development, and production activities on human, marine, and coastal environments. The proposal, selection, research, review, collaboration, production, and dissemination of each of BOEM's Environmental Studies follows the DOI Code of Scientific and Scholarly Conduct, in support of a culture of scientific and professional integrity, as set out in the DOI Departmental Manual (305 DM 3).